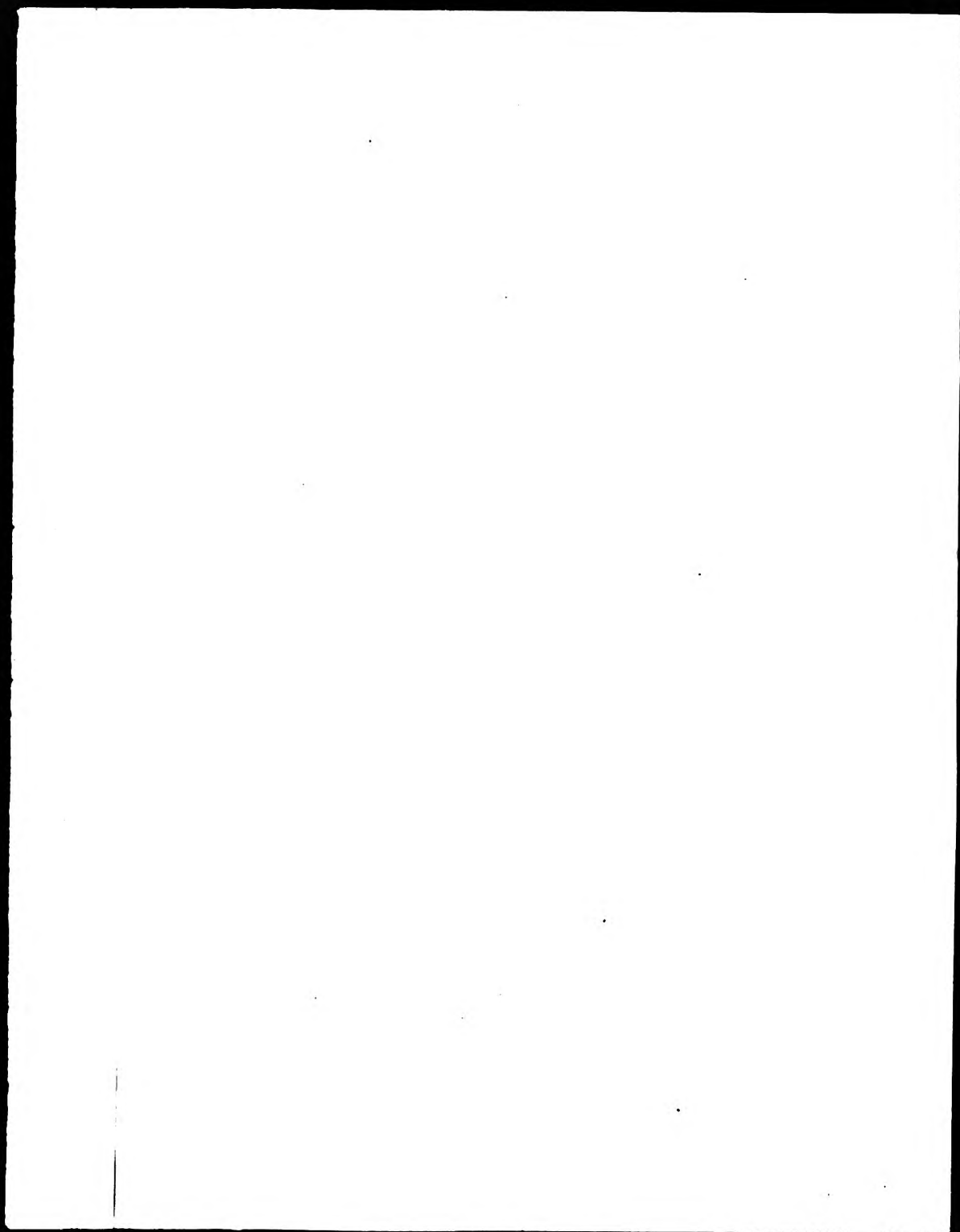


This PDF was created from the British Library's microfilm copy of the original thesis. As such the images are greyscale and no colour was captured.

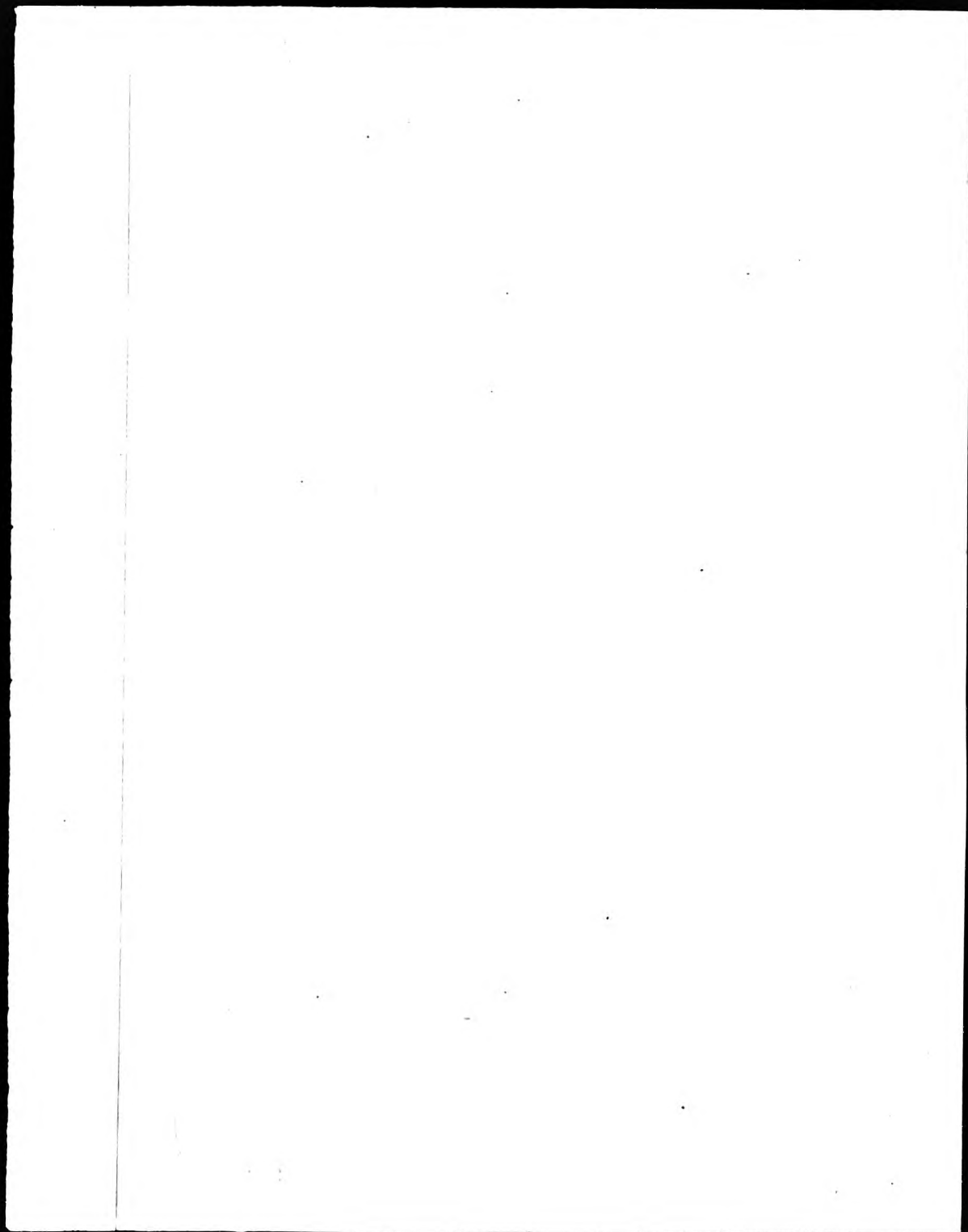
Due to the scanning process, an area greater than the page area is recorded and extraneous details can be captured.

This is the best available copy



DX

91543



THE BRITISH LIBRARY DOCUMENT SUPPLY CENTRE

TITLE THE COLOURING, SEALING AND ABRASION RESISTANCE
OF ANODIC OXIDE COATINGS

AUTHOR MARILYN SMITH

INSTITUTION
and DATE
City of London Polytechnic
CNA A 1990

Attention is drawn to the fact that the copyright of this thesis rests with its author.

This copy of the thesis has been supplied on condition that anyone who consults it is understood to recognise that its copyright rests with its author and that no information derived from it may be published without the author's prior written consent.

THE BRITISH LIBRARY
DOCUMENT SUPPLY CENTRE
Boston Spa, Wetherby
West Yorkshire
United Kingdom

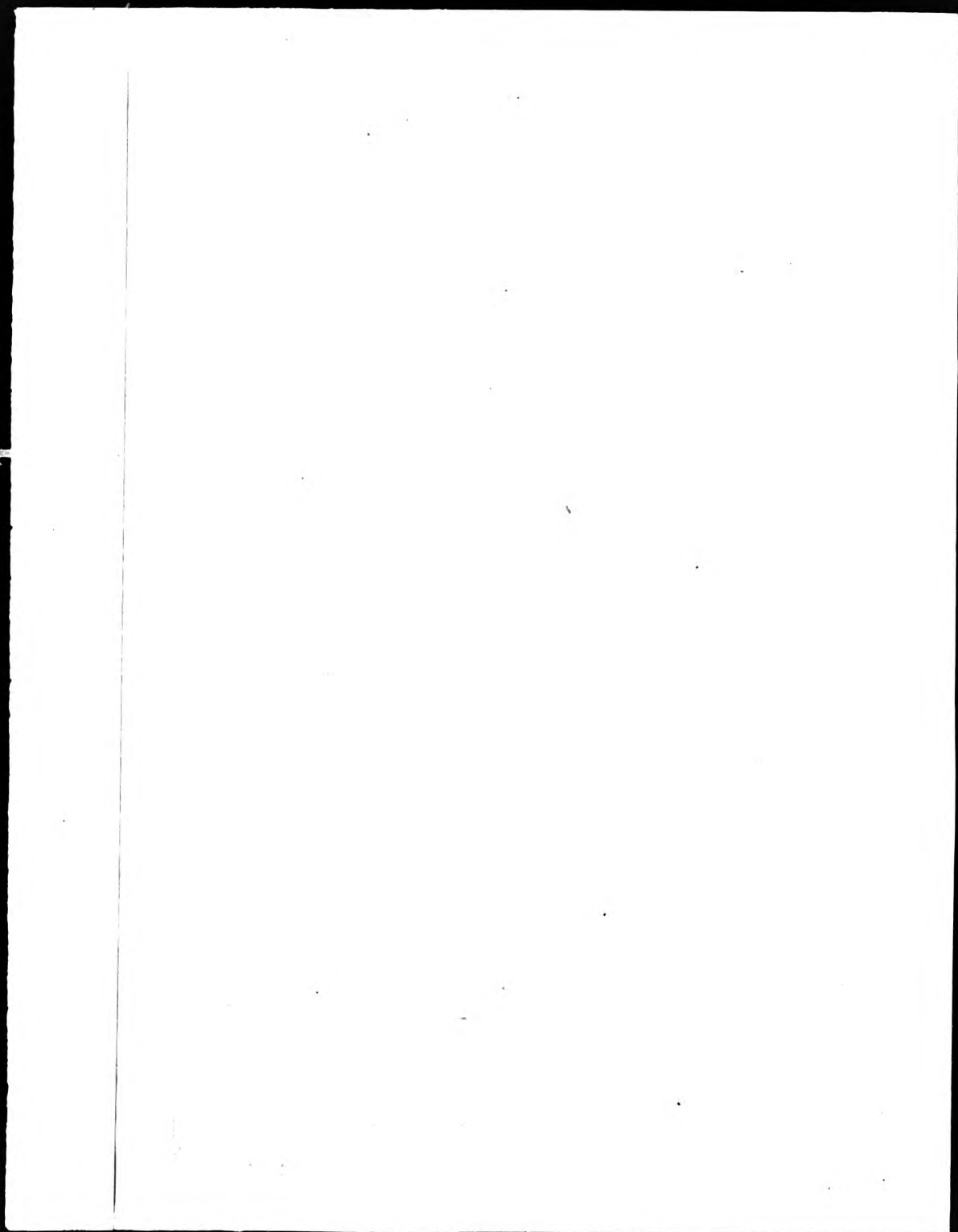
1	2	3	4	5	6
cms.					

20

REDUCTION X

CNA A

8



THE COLOURING, SEALING AND ABRASION RESISTANCE
OF ANODIC OXIDE COATINGS

MARILYN SMITH

A thesis submitted in partial fulfilment of the
requirements of the Council for National Academic Awards
for the degree of Doctor of Philosophy

June 1990

Department of Metallurgy and Materials Engineering
City of London Polytechnic

BEST COPY
AVAILABLE

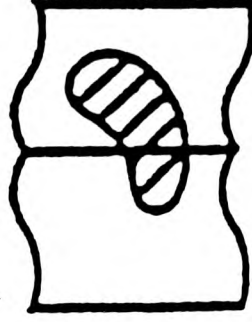


TABLE OF CONTENTS

<u>CHAPTER 1</u>		PAGE
Introduction		1
 <u>CHAPTER 2 LITERATURE SURVEY</u>		
2.1	Anodising Alloys, Jigs and Pretreatments	10
2.1.1	Anodising Alloys	10
2.1.2	Jigs	11
2.1.3	Pretreatments	11
2.2	Anodising Aluminium and Its Alloys	15
2.2.1	Introduction	15
2.2.2	Porous Film Growth From Acidic Solutions	18
2.2.3	Barrier Films	22
2.2.4	Porous Films	25
2.2.5	Alternating Current (A.c.) Anodising	47
2.3	Methods of Colouring the Anodic Film	48
2.3.1	Introduction	48
2.3.2	Absorptive and Adsorptive Dyeing	51
2.3.3	Integral Colour Anodising	56
2.3.4	Electrolytic Colouring	61
2.3.5	Interference Colouring	71
2.3.6	Combinations of Two Finishing Systems	75
2.3.7	Colorimetry	78
2.4	Sealing	85
2.4.1	Introduction to Sealing	85
2.4.2	Hydrothermal Sealing Mechanisms	87
2.4.3	Practical Aspects of Sealing	93
2.4.4	Steam Sealing	96

2.4.5	Sealing Bloom	97
2.4.6	Sealing Bath Additives	102
2.4.7	Dichromate and Other Sealing Solutions	104
2.4.8	Impregnation of the Anodic Oxide Film	106
2.5	Sealing Smut, Weathering Bloom and Pitting of the Anodic Oxide Film	107
2.5.1	Introduction	
2.5.2	Assessment Tests	110
2.5.3	Acid Immersion Tests	119
2.5.4	Abrasion Resistance	122
2.5.5	Resistance to Degradation of the Anodic Film	130
2.5.6	Weathering	132
2.5.7	Effects of Impregnation on Anodic Film Degradation	138
<u>CHAPTER 3 EXPERIMENTAL SECTION</u>		
3.1	Preparation and Pretreatment of Specimens	141
3.1.1	Specimen Preparation	141
3.1.2	Specimen Pretreatments	141
3.2	Anodising	142
3.2.1	The Anodising Bath	142
3.2.2	The Anodising Process	142
3.3	Colouring	145
3.3.1	Inorganic Dyeing	145
3.3.2	Electrolytic Colouring	146
3.3.3	Hull Cell Test	148
3.4	Sealing	149
3.5	Assessment Tests	150
3.5.1	Thickness Measurements by the Eddy Current	

	Principle	150
3.5.2	Gravimetric Method for Thickness	
	Determination by Stripping	150
3.5.3	Admittance Measurements	151
3.5.4	Dye Spot Test	156
3.5.5	Phosphoric-Chromic Acid Test	156
3.5.6	Acidified Sulphite Test	157
3.5.7	Bleach Test	157
3.5.8	Total Reflectance	158
3.5.9	Abrasion Resistance	160
3.5.10	Abrasive Wheel Test Apparatus Used as a Microtome	163
3.6	Sulphur Dioxide Experiments	163
3.6.1	Sulphur Dioxide Test	163
3.6.2	Quantitative Analysis of Sulphur Dioxide Gas During Ambient Temperature Experiments	166
CHAPTER 4 RESULTS		
4.1	The Admittance Drift Test	168
4.2	The Nitric Acid Predip	175
4.3	Improved Admittance Drift Test	179
4.4	Thickness and Weight Loss Due to Nitric Acid Immersion	185
4.5	Sealing with 'Alcoa 482'	187
4.6	Long Term Cold Sealing	190
4.7	Sulphur Dioxide Test	192
4.8	Sealing Bloom	202
4.9	The Weathering of Unsealed, Partially Sealed and Fully Sealed Anodised Panels	207
4.10	Linear Regression of $Y_t(25^\circ\text{C})$ Against	

	Thickness for Natural Panels	213
4.11	Linear Regression of $Y_t(25^\circ\text{C})$ Against Thickness for Coloured Panels	215
4.12	Results Using Standard Colouring Solution	220
4.13	Analysis of Tin	226
4.13.1	X-Ray Diffraction Analysis	226
4.13.2	Powder Diffraction Analysis	227
4.14	The Effect of Elevated Temperatures During Anodising, Soaking and Colouring	227
4.15	The Effects of Using 'Tribrite' in the Tin Colouring Solution	234
4.15.1	Experiments Using Optimum Amounts of 'Tribrite'	256
4.15.2	Colorimetry	264
4.15.3	Stannous Tin Content of the Colouring Baths	264
<u>CHAPTER 5 DISCUSSION OF RESULTS</u>		
5.1	The Nitric Acid Predip	266
5.2	33% Nitric Acid Admittance Drift Test	268
5.3	Concentrated Nitric Acid Admittance Drift Test	271
5.4	A Proposed Mechanism for Sealing in Nickel Acetate Solutions	273
5.5	A Proposed Mechanism for Long Term Cold Sealing	278
5.5.1	The $Y-\delta$ Profile Method on Films Sealed in Boiling 'Alcoa 482'	283
5.6	Weathering	285
5.7	Sulphur Dioxide Tests	290
5.7.1	Sealing Bloom	293

5.8	Analysis of the Gradients of Yt(25°C) Against Thickness Found by Linear Regression for Natural Coloured Films	295
5.9	Electrolytic Colouring (Electrocolouring)	297
5.9.1	Theory of the Gradient Found by Linear Regression of Admittance Against Thickness for Electrocoloured Films	304
5.9.2	Flaws and Defects	308
5.10	Elevated Anodising, Soaking and Colouring Temperatures	309
5.11	The Role of 'Tribrite' in Electrolytic Colouring	315
5.11.1	Colorimetry	320
5.11.2	The Effects of 'Tribrite' on the Gradients of Admittance Against Thickness Found by Linear Regression	321

CHAPTER 6 CONCLUSIONS

6.1	Nitric Acid Predip	323
6.2	33% Nitric Acid Admittance Drift Test	323
6.3	Nickel Acetate Sealing	324
6.4	Long term Cold Immersion	325
6.5	Outdoor Exposure of Anodised Films	326
6.6	Sulphur Dioxide Test	328
6.7	Sealing Bloom	328
6.8	The Significance of the Gradients of the Graph of Yt(25°C) Against Thickness as Found by the Linear Regression Method	329
6.9	Electrocoloured Oxide Films	330
6.10	The Effects of Anodising, Soaking and	

	Colouring at Elevated Temperatures	333
6.11	The Effects of Using 'Tribrite' in the Electrolytic Colouring Solution	335
<u>CHAPTER 7 FUTURE WORK</u>		
7.1	The Admittance Drift Test (\dot{Y})	338
7.2	The Admittance-Abrasion ($Y-\dot{\xi}$) Profile	338
7.3	The Abrasive Wheel Test	339
7.4	The Use of Addition Agents During Electrolytic Colouring of Anodic Oxide Films	339
	<u>REFERENCES</u>	341

LIST OF TABLES, GRAPHS AND FIGURES

	PAGE
Figures 1 and 2	19
Figure 3	23
Figure 4	27
Figures 5 and 6	31
Figures 7 and 8	42
Figures 9, 10 and 11	49
Figures 12a and 12b	50
Figures 13 and 14	67
Figure 15	73
Figures 16 and 17	81
Figure 18	84
Figures 19 and 20	91
Figure 21	101
Figures 22 and 23	116
Figure 24	143
Tables 13 and 15	144
Figures 25 and 26	147
Figure 27	159
Figures 28 and 29	164
Figure 30	167
Graphs 1a and 1b	171
Graphs 1c and 2	172
Tables 18 and 20	174
Table 21	177
Graphs 3 and 4	178
Table 22	181
Graphs 5a and 5b	183

Graphs 5c and 6	184
Table 23	186
Graphs 7 and 8	189
Graphs 9 and 10	193
Table 26	196
Table 27	197
Table 28	198
Table 29	199
Table 30	206
Graphs 11a and 11b	209
Graphs 12 and 13	214
Graphs 14a and 15a	217
Graphs 14b and 15b	218
Graphs 16a and 16b	221
Graphs 17 and 18	223
Graphs 19 and 20	224
Graphs 21 and 22	225
Table 32	229
Table 33	230
Graphs 23 and 24	231
Table 34	232
Graphs 25 and 26	235
Graphs 27a and 27b	238
Figure 31	239
Figure 32	240
Figure 33	241
Figure 34	242
Figure 35	243
Figure 36	244

Figure 37	245
Figure 38	246
Figures 39 and 40	247
Figures 41 and 42	248
Figure 43	249
Graphs 28 and 29a	250
Graphs 29b and 29c	253
Graphs 30 and 31	255
Graphs 32 and 33	257
Table 35	258
Graphs 34 and 35	262
Graphs 36 and 37	263

ACKNOWLEDGEMENTS

I would like to thank my supervisor Dr. M. Clarke for all his help, advice and invaluable support, and Mr. P. G. Sheasby of Alcan International Ltd. for his additional assistance. My gratitude is also extended to the teaching staff and technicians of the Department of Metallurgy and Materials Engineering.

ABSTRACT

The service performance of anodised aluminium in architecture is dependent upon the control of the anodising, colouring and sealing processes. The quality of the anodic oxide film is determined by assessment tests. The use of a nitric acid 'predip' on soft films was shown to dissolve a soft outer layer. A new admittance test was devised in which the 'drift', \dot{Y} , was measured using 33% nitric acid. This test threw light on the sealing quality of films exposed to the environment and those sealed in nickel salt solutions. Well-sealed, hard films gave a \dot{Y} value of 0.1 to 0.2. A sealing mechanism for nickel acetate solutions is proposed in which ageing of a Ni-Al complex is thought to play a significant role. The admittance-abrasion ($Y-\delta$) profile was used to supplement other test data. An accelerated sulphur dioxide test was investigated, the optimum conditions for which were 40°C for 6 hours. The presence of a sealing bloom was determined by a simple go/no go three paper abrasion test. The assumption is made that $Y_t(25^\circ\text{C}) = a + bt$ and linear regression has been used to find b . It has been found that for batches having a range of thicknesses but a common sealing time, the linear relation is a reasonable assumption when the gradient is $<+10$. The admittance values of electrocoloured tin black films have been found to be anomalous. The gradients are negative due to the presence of tin in the pores. Linear regression has been used to obtain an average value of b over the whole thickness range, which gives information as to the degree of sealing. Colouring and soaking in sulphuric acid at elevated temperatures (before sealing) reduces the abrasion resistance. The abrasive wheel test was also used to show the depth of tin within the pores. The use of the addition agent 'Tribrite' in tin colouring solutions suppresses the outward, whiskery growth of tin in the pores.

CHAPTER 1

INTRODUCTION

During the early part of this century processes were developed which took advantage of the fact that a protective oxide coat could be grown on aluminium artificially by anodic electrolysis, the natural film having been removed before anodising. Bengough and Stuart (1) introduced the first commercial process for chromic acid anodising in the United Kingdom, while the oxalic acid process was revealed in Japan by Setoh and Miyata (2). In the same period electrolysis in sulphuric acid was found to produce a good anodic oxide coat. This was first patented in this country in 1927 and is the most widely used process for architectural anodising, bright trim anodising and hard anodising.

Over the last 50 years the basic anodising processes have changed very little. The excellent properties exhibited by anodised aluminium (architectural and decorative uses, the ability to be coloured, the very good resistance to deterioration, and the strength shown by such a lightweight metal), has promoted research in order to keep pace with the demands for novel, attractive and economic products.

The popularity of coloured anodised aluminium for architectural uses has increased over the past 20 years. The three main methods for colouring are absorptive dyeing, integral colouring and electrolytic colouring. The trend has been to move away from the first method and towards the

latter methods. However, electrolytic colouring is not a recent advance since the first patent was issued in 1936 to Caboni (3), although commercial exploitation did not occur until after 1960.

This research is concerned with the use of anodising for the long term protection of aluminium alloys used in external architectural applications. Reference is made to the British Standard Specifications as outlined in Table 15 of the Experimental section, page 144.

The life expectancy of any external architectural component is 25 to 40 years. Thickness, colouring and sealing must achieve a minimum quality for the anodic oxide coating to perform well in service. Many of the anodising, colouring and sealing processes are adequate for internal environments only and other uses where decorative properties are more important than protection. In these cases the life expectancy is 10 to 15 years even though the thicknesses may be 5µm or less. As well as serving as protection in architecture or for decoration, another application is as a pretreatment for other processes such as painting, organic finishing, and electrodeposition. Specific properties of the coatings such as the porous nature, hardness and wear resistance, electrical and thermal insulation, are of value for specialised applications. Table 1 gives the minimum thicknesses of anodic oxide coatings for specific service conditions (B.S. 1615:1987).

Table 1

Grade	Minimum Average Thickness (μm)	Service Conditions
AA25	25	Aggressive environments; permanent external architectural applications.
AA20	20	
AA15	15	Outdoor architectural use when cleaned frequently; arduous indoor conditions.
AA10	10	Special outdoor use with frequent cleaning e.g., decorative car trim; indoor use.
AA5	5	
AA3	3	Reflectors and as a paint base.
AA1	1	

The extensive use of anodised aluminium has created a need for guidelines for the anodiser and the purchaser. In the United Kingdom these are the British Standards. Other industrial countries have similar, but not identical specifications, and there is also the series of International Organisation for Standardisation documents. Both series specify certain requirements for clear and coloured anodic oxide coatings for external architectural use. However they do not cover minimum plant requirements

and as a result of discussions between the European Wrought Aluminium Association (E.W.A.A.) and the European Anodisers Association (E.U.R.A.S.) the Qualanod labelling scheme was launched (4). Recommendations published in 1969 by the E.W.A.A. were very similar to the standard specifications, but also included these minimum plant requirements for sulphuric acid anodising, which set out the needs for the operation of each process step. However, they did not include a class above 20 μ m film thickness. No production criteria were drawn up for other processes, but it was suggested that the finished product should pass the same tests as sulphuric acid anodising. Electrolytic colour anodising has shown anomalous results for some tests and attention is drawn to this since caution is needed in interpreting the results. Each country has its own national Qualanod organisation which is responsible for issuing Qualanod licences. The specification outlines the rules for granting the licence and subsequent quality inspections. Independent inspections are carried out at plants to ensure adequate product quality which is assurance for both anodiser and purchaser. The Qualanod scheme gives the guarantee that the work is done by specific processes under controlled conditions. The scheme allows minimum average thicknesses of 15, 20 and 25 μ m for external applications and the choice of thickness class depends upon the relevant national standards. Routine examination of the anodising plant facilities and testing procedures of the finished architectural products are carried out at least twice a year.

Prior to standards being implemented research must be carried out to ensure that all stages of the processes together with the testing techniques are reliable and valid.

The aim of this investigation was to examine existing processes and test techniques with a view to modifying and improving them in order to extend the information they provide about coating quality. Quality test problems had arisen directly from anomalous results which were obtained in the course of recent large anodising contracts, particularly where new processes were applied which did not seem amenable to existing test methods, and where variations in thickness and thickness-related properties had been found. The distributions of these properties present practical problems in specifying, testing, inspecting and for the performance, since specifications are based on laboratory work with minimal thickness variation. Subsequent colouring and sealing processes are contingent on thickness and all processes are operated assuming no thickness distribution exists in process loads passing through the plant. Therefore the consequences and nature of these distributions also warranted investigation.

The objectives of this thesis were studied by carrying out systematic investigations of the problems arising from the testing and industrial uses of anodic oxide coatings for architectural purposes.

1. Kape's test (B.S.6161:Part 4:1981) uses a 10 minute

predip in nitric acid before immersion in the acidified sulphite solution. A number of points had arisen from this 'predip'. European films used the absence of a large loss to 'prove' films were hard. In conjunction with the abrasive wheel test, the effect of nitric acid on various types of anodic oxide coatings was investigated. Whether nitric acid itself has a role in softening films as distinct from affecting films already softened by other agents was determined.

2. Earlier work led to the idea of the admittance drift test, \dot{Y} . The use of an alternative electrolyte, nitric acid is proposed and the admittance test method modified to record any 'drift' in the admittance with time. Similarly, the measurement of the admittance before and after the application of the nitric acid is proposed. The best technique is investigated to develop a convenient non-destructive test. This could be applied as

i) an alternative test for the electrolytic colouring problem when $Yt(25^\circ C)$ is greater than $500/t$ (μS), where t is the thickness of the coating.

ii) an alternative test for weathered films where $Yt(25^\circ C)$ is less than $500/t$ (μS).

iii) an alternative test for 'Alcoa 482' and impregnated films. Does the 'ageing' of impregnated films affect the drift result?

iv) a useful test for unsealed films subject to long term cold immersion.

3. In industry it had been found that the degree of sealing of individual samples from one batch varied due to a range of thicknesses being sealed for the same time. The validation of the gradient b in $Y_t(25^\circ\text{C}) = a + bt$ as a criterion of good sealing in this case was investigated.

4. The admittance test is used to assess the quality of sealed anodic oxide coatings and is the only non-destructive test available for acceptance inspection. For a hydrothermally sealed film the value shall not be greater than $500/t$ (μS) (B.S.1615:1987). However, it is noted in the specification that "this test may give anomalous results with some electrolytically coloured anodised aluminium." The extension of the use of b [from $Y_t(25^\circ\text{C}) = a + bt$] to anomalous cases of electrolytically coloured coatings (dark colours and especially tin-coloured films) was studied where $Y_t(25^\circ\text{C})$ was greater than $500/t$ (μS) even when anodic oxide coatings are well-sealed. Hence, was b still valid?

5. A converse situation of objective 4 arises for unsealed anodic oxide coatings which have been exposed to the weather. They often appear to be sealed [$Y_t(25^\circ\text{C})$ is less than $500/t$ (μS)] although they fail the Kape or Phosphoric acid/Chromic acid tests. Is b still a useful criterion for sealing in this case?

6. With industrial films electrolytically coloured black in tin solutions b was found to be large and negative. Did

this indicate well-sealed anodic oxide coatings but with tin filling more than 50% of the pore length? Did b continue to have a useful connection with the question of the degree of sealing of batches having a range of thickness but a common sealing time? Comparison of commercial electrolytically coloured black films with those produced having a deliberate range of thickness will be made to assess if the average linear gradient over the range is a reasonable assumption. Could colorimetry provide additional information on the colouring processes?

7. How critical is the control of the acid tin bath temperature? It had been found that tin electrolytically coloured films processed in Italy were very soft. Although the anodising was carried out at 18°C, during the summer the room temperature would be in excess of 30°C. The application of the abrasive wheel test may elucidate the problem as it can be used to provide a depth profile of the film. This may reveal the position of the tin in the pores.

8. A very simple go/no go abrasion test is proposed to supplement information provided by the abrasive wheel test.

9. An hypothesis exists that the outward growth tendency of tin plating baths was a cause of the tin growing up the pores, compared with nickel and cobalt deposits which remain at the base of the pores. An addition agent called 'Tribrite' is known to cause lateral growth in the electrodeposits of tin in preference to whiskery growth and

so could this agent be beneficial to the tin electrolyte colouring bath?

10. The specification for assessing sealing quality does not include unsealed or impregnated coatings. The use of nickel salts in hydrothermal sealing is thought to 'block' the pores. Anomalous results of the Phosphoric acid/Chromic acid and admittance tests for short sealing times in 'Alcoa 482' nickel seal have been reported. An industrial plant using only the Phosphoric acid/Chromic acid test thought they had discovered how to seal in 10 - 15sec/ μm , but $Y_t(25^\circ\text{C})$ was greater than 5000 and b was greater than +30. Which result should be accepted? Similar results were achieved during an undergraduate project. The cause of this problem was investigated. If sealing by a form of impregnation is a slower, more extended process than hydrothermal sealing, then the the procedure to record the admittance within 48 hours is called into dispute.

11. The sulphur dioxide test in B.S.1615:Appendix H:1972 is no longer in the revised 1987 edition. Could the very simple sulphur dioxide test developed for gold be adapted to assess the degree of sealing of anodic oxide coatings? A gas test for sealing is useful for complex extrusion profiles which may present difficulties for acid weight loss tests. The evaluation of the 'bloom' may detect incorrect process conditions, for example.

CHAPTER 2

LITERATURE SURVEY

2.1 Anodising Alloys, Jigs and Pretreatments

2.1.1 Anodising Alloys

Alloy choice is of crucial importance when deciding upon the finish of the anodised surface. Composition and purity of the alloy can influence the appearance and colour, reflectivity, abrasion and corrosion resistance, and anodic film thickness. The range of alloys is varied; the main alloying elements are silicon (Si), magnesium (Mg), copper (Cu), iron (Fe), manganese (Mn), zinc (Zn), chromium (Cr), titanium (Ti) and nickel (Ni) (5). Aluminium can be formed as sheet, extrusion, forgings and castings and this too is a deciding factor when choosing the alloy. Many alloys have been developed, mainly for hardness, strength and ability to be heat treated. Only a few are suitable for sulphuric acid anodising; mainly high purity alloys with Mg, Si and Mn. Alloys with Cu, Zn and Cr are not suitable. Chromic acid will treat the widest range, including Cu alloys, but it is used only for protection and cannot easily give coloured films. Integral colour anodising needs special alloys according to the colour required. Oxalic acid gives a different range of colours to the other electrolytes.

2.1.2 Jigs

The components to be anodised are fitted into jigs or racks (6). This is not only for holding them securely but also to form the electrical contact between the component and the current supply. Jigging is very important and requires careful forethought for ease of use in service. Jigs must be well maintained to prolong their life and to ensure good electrical contact since poor connections create problems during anodising. The assembly of the components on the jigs is significant. Contact areas must be on non-significant surfaces. Hollows and crevices create traps for air and solutions, and the 'drag-out' (carrying over one solution to another) results in contamination of other solutions and the rinse tank, unnecessary loss of solutions and necessitates more rigorous effluent control.

2.1.3 Pretreatments

Pretreatment of aluminium is required before anodising to remove surface inhomogeneities, scratches and surface contaminants. In doing so, pretreatments give characteristic surface topographies to the metal. This influences the type of anodic oxide film subsequently formed during anodising. The usual pretreatments are degreasing, etching and desmutting. If the surface of the metal carries much oil or grease, the bulk must be removed by vapour or emulsion degreasing. More vigorous cleaning (7), where heavy lubricants and the oxide scale are to be removed is performed by liquid cleaners, usually

alkali-based at temperatures of 65 to 70°C. The absence of a hydrophobic surface film is indicated by the 'water break test'. The water forms a continuous film on the surface and does not break up into droplets. The cleaning solution has a surfactant to facilitate degreasing and little foam is produced. It does not contain silicates as these attack the surface.

Mechanical polishing is performed manually or automatically to give a smooth, blemish-free surface. This is achieved under the influence of high local temperatures and pressure, producing a flowed amorphous surface. Manual polishing is required to remove deep scratches and to produce a mirrored surface. However, at the microscopic level an irregular surface remains. Matt finishes are obtained by sand and vapour blasting. Grinding, banding and brushing (8) give finishes with a directional texture.

Electropolishing requires an applied potential to facilitate smoothing of the surface. This removes abrasive marks and scratches, and occurs when high points are selectively dissolved. Boundaries of the cellular structure have ridges giving a scalloped appearance. Depressions are protected by the impedance of the electrical current by formation of a viscous layer (8). Electropolishing solutions are based on phosphoric acid.

Electrobrightening is a less intense process than electropolishing. Less metal is removed due to the more superficial nature of the surface deformations. The original 'Alzak' electrobrightening process (8) was based on a 2.5% solution of hydrofluoroboric acid at 30°C. The

'Brytal' process (8) superceded the former, and is still used today for super and high purity aluminium. It consists of 60g/l anhydrous trisodium phosphate and 200g/l anhydrous sodium carbonate at 80 to 90°C.

Companies doing bright anodising polish mechanically first and follow this with electro- or chemical polishing. Mechanical polishing is much more effective at smoothing but leaves abrasives embedded in the metal. Electro- and chemical polishing gives a final brilliant clean surface. Chemical polishing is caused by the oxidising agents in the solution. This proceeds because there is an electrochemical potential difference between microscopic anodic and cathodic regions on the surface.

The original chemical polishing process was based on 60 to 75% by volume phosphoric acid and 25 to 40% by volume sulphuric acid (8). A white film of aluminium phosphate remains after immersion which can be removed in 1% chromic acid solution. The most important solutions for chemical polishing are known as 'Phosbrite' (trade name of Albright and Wilson Ltd.) solutions. The basic solution composition is phosphoric acid, nitric acid, sulphuric acid, boric acid, copper salts, wetting agents and anti-fuming agents, at a temperature of 95 to 105°C. After this treatment a desmutting solution of nitric or chromic acid is used to remove the copper impurities which have dissolved out of the alloy. These impurities are deposited on the metal ridges of the boundaries of the cellular structure (9) which act as the cathodic regions. The anodic regions are between the boundaries.

Alkaline etches are based on caustic soda liquor 50% by weight (7). They are long-life systems in which the aluminium content quickly reaches equilibrium. Acid etches (8) contain hydrofluoric acid and nitric acid mixtures or the former acid only. Acid FPL etch contains sodium dichromate and sulphuric acid. The drag-out is balanced by the dissolution of the aluminium. Etches are relatively cheap and can be stored in bulk. However, they are very important since the surface texture is determined by the etch, and a variety exist which give specific finishes. The components to be etched must be flawless since etching emphasises any defects. Both alkaline and acid FPL etches (9) produce scalloped surfaces. In acid fluoride etches there is preferential attack at grain boundaries.

Smut, which forms on the surface after etching, consists of undissolved metals other than aluminium. Desmutting removes these and also neutralises any alkali. Proprietary solutions have become popular, although nitric acid is still used.

All pretreatments give peaks and troughs on the metal substrate often producing a scalloped texture. Metal ridges are preferentially located at the boundaries of the scallops and, as in chemical polishing, are often local segregations of metallic impurities. Desmutting does not always successfully remove all impurities, and with second phase material, both can be left protruding from the surface. Similarly, very small concentrations of impurities (even in 99.99% pure aluminium) may be enhanced by pretreatments giving metal segregates, zone formation or

intermetallic compounds (10).

Rinsing is carried out between all process steps to clean the components and prevent contamination between solutions.

2.2 Anodising Aluminium and Its Alloys

2.2.1 Introduction

Aluminium is anodised using electrolytes which are in two categories; those which produce porous films and those giving barrier films. Below are some electrolytes of each type and the conditions under which they produce anodic oxide films. Operating conditions vary within these ranges, and standard procedures are found in the literature (11).

Porous Films

Hard anodising:

H_2SO_4 , 15-35% wt., -5 to +5°C, 2.5-15A/dm², 40-100V (8).

CrO_3 , 2-15%wt., usually 3%wt., 40°C, 0.3A/dm² or 10%wt.,

54°C, 1.2A/dm² (8).

Other processes:

$(COOH)_2$, 3-5%, 15 to 35°C, 1-3A/dm², 30-60V d.c. or 40-60V a.c. (8).

H_3PO_4 , 25-30%, 25°C, 1-2A/dm², 30-60V (8).

Sulphosalicylic acid, 40-100g/l, plus 30-60g/l H_2SO_4 , 30°C, 2.5-3.5A/dm², 80V (8).

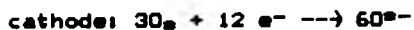
Barrier Films

$B(OH)_3$, 4%, plus 0.05-0.5% borax, 70 to 100°C, 0.5-1.0A/dm², 50-750V (8).

Tartaric acid, 3% plus NH_4OH , 2A/dm² (8).

Ammonium pentaborate 5%wt., 1A/dm², 25°C (12).

Upon the application of an electric potential to the cell [which consists of the electrolyte, anode (aluminium) and cathode (usually lead)], the surface of the anode is converted into oxide. This oxide film adheres strongly to the metal, altering its physical and chemical properties. During anodising with direct current (d.c.), hydrogen gas is liberated at the cathode and the aluminium combines with water to form the oxide, with very little evolution of oxygen:



The porous films have more widespread applications than barrier films. The main difference between the two types is the degree of solubility of the film in the electrolyte. Porous films are sparingly soluble and pore growth competes with other processes occurring on the metal surface. The actual structure is known as a 'duplex' structure, having a barrier layer adjacent to the

metal and a porous layer extending outwards from this thin layer. The appearance of the resultant oxide film and its associated properties are dependent upon the anodising conditions and aluminium alloy used. Oxide films with different properties can be produced by changing these variables. Some anodising variables can be altered to give undesirable properties to the oxide film.

Porous film growth proceeds as for barrier film growth, but growth is accompanied by dissolution of the film. Pores are formed within the oxide which extend to the barrier layer. Film growth slows as film thickness increases. Film thickness attains a constant value when the rate of film growth equals the rate of film dissolution. Maximum film thickness is dependent upon the electrolyte, its ability to dissolve the film and the operating conditions. Film growth is favoured by high current densities (c.d.), low electrolyte temperature and low acid concentration. Dissolution is favoured by low current densities, high anodising temperature and high acid concentration. The film grows from 'within' the oxide at the metal/oxide interface. The outer surface of the oxide is more prone to dissolution than the metal/oxide interface. For every $3\mu\text{m}$ of coating formed, the metal surface retreats approximately $2\mu\text{m}$ and the exterior surface advances about $1\mu\text{m}$. The voltage increases linearly and after passing through a maximum, establishing the barrier layer, the voltage decreases to a relatively constant value. The thickness of the barrier layer is directly proportional to the forming voltage which is not the case

for the porous layer.

The barrier film is almost non-conducting. Film growth continues until resistance of the film prevents current from reaching the anode. These films are extremely thin and dielectrically compact. The electrolytes used exert no solvent action on the oxide and voltage increases linearly with time, until a maximum is reached beyond which dielectric breakdown occurs. If the voltage is not allowed to reach the breakdown value, the current decreases to a very low value called the leakage current (13). After a short time film growth ceases and the limiting thickness is much smaller than can be achieved with porous films.

There is a fine dividing line between porous and non-porous films. Small changes in conditions can bring about significant variations in structure. Generally the maximum thickness of barrier films is $1\mu\text{m}$ and porous films can attain hundreds of microns in thickness (13).

2.2.2 Porous Film Growth From Acidic Solutions

Figs 1 and 2 show a schematic current density-time curve at constant voltage, and typical voltage-time curve at constant current density, respectively. Both graphs show an initial non-steady state region followed by a steady state region of constant current density or voltage accordingly. During the non-steady state periods non-uniform growth occurs accompanied by pore development. The porous anodic film thickens coulombically in the steady-state period (14).

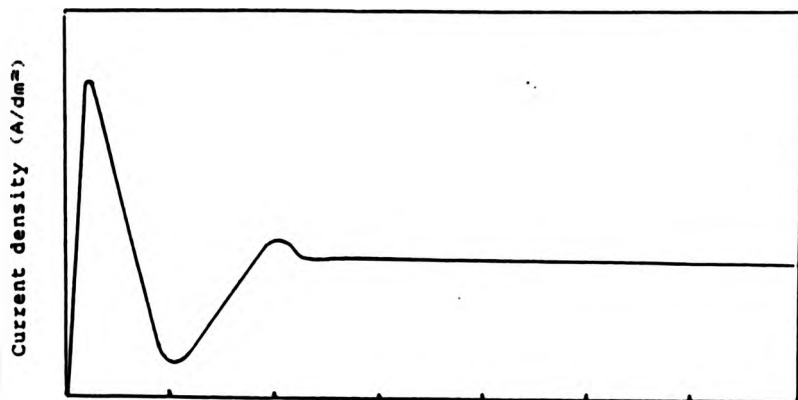


Fig. 1 (14)

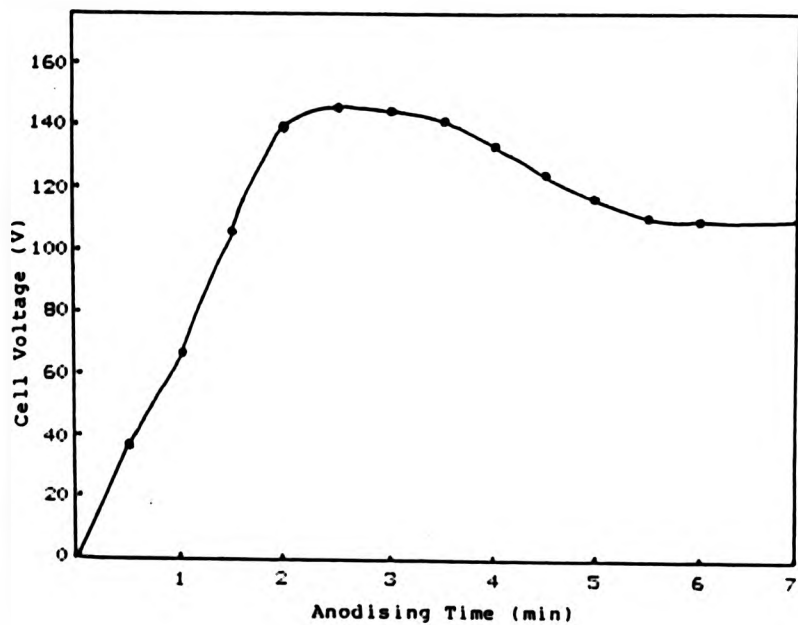


Fig. 2 (14)

The current density, i , is related to the field strength, V/d across the barrier layer of thickness d by the expressions:

$$i = A \exp(BV/d) \quad (2.1)$$

where A and B are temperature-dependent parameters (constants). This expression shows that the anodic film parameters are directly dependent upon the formation voltage and the current density, which itself governs the rate of film formation. Although the discussion of the above graphs implies that any desired thickness could be achieved, in reality a voltage maximum is reached for all acids, and this maximum is often accompanied by electrical breakdown of the film.

The applied voltage largely determines the structure of the film; barrier layer thickness, cell wall thickness, cell diameter and pore diameter. However, particular films may be formed by changing anodising parameters as shown in Table 2.

Barrier and porous film dimensions vary according to the electrolyte and conditions used. O'Sullivan and Wood (15) made direct measurements from photomicrographs of films formed in phosphoric acid. It was found that the cell wall thickness was always $0.71 \times$ barrier layer thickness. Barrier layer nm/V ratio was 1.04 and cell diameter nm/V ratio was 2.77.

Table 2

Variable	Effect on Anodic Film
Temperature	Files become softer as temperature rises.
Acid concentration	As above, as concentration rises.
Current Density	Rate of film formation increases giving a denser coating (risk of burning) as c.d. rises. Pores enlarge.
Anodising Time	Film thickness increases with time, (limiting thickness may be reached), films may soften.

It can be shown that

$$p = c - 2 \times 0.71d \quad (2.2)$$

where p is the pore diameter,

c is the cell diameter,

d is the barrier layer thickness.

If $c = 2.77V$

and $d = 1.04V$,

expressed in nanometres (where
 V is formation voltage)

then $p = 1.29V$

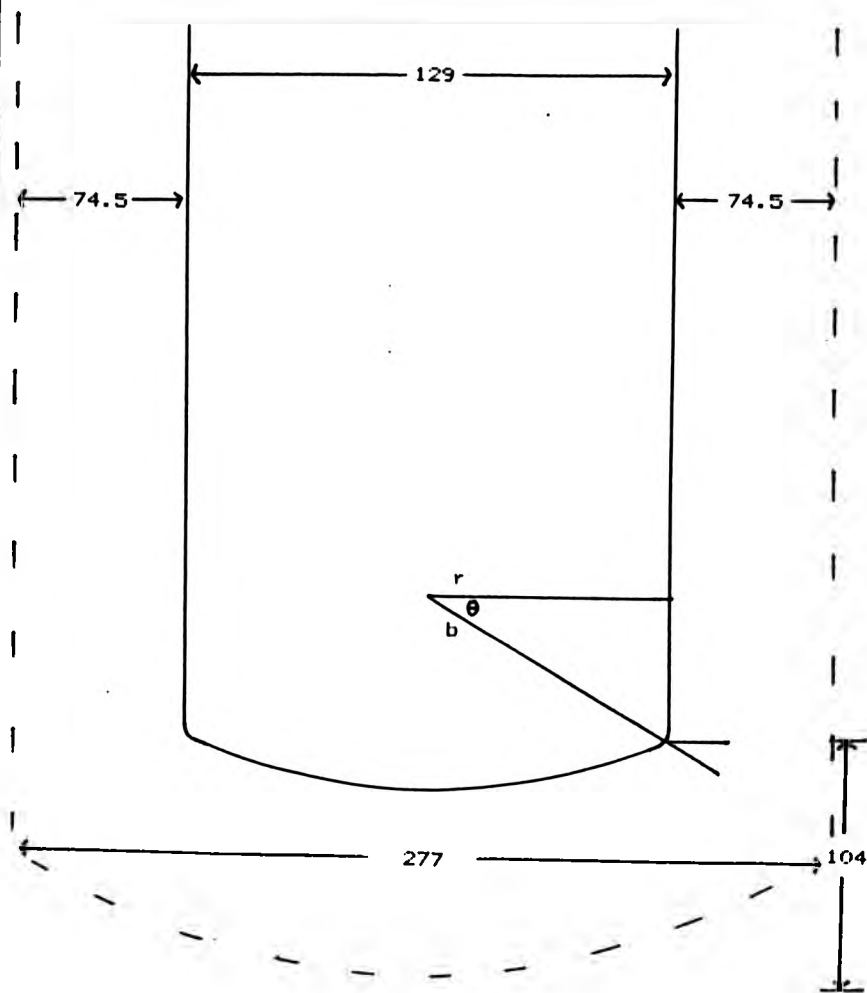
If both cell and pore radii of curvature were the same,
 θ in Fig.3 is given by $\cos^{-1}0.71$. The oxide cell was formed
at 100V.

2.2.3 Barrier Films

A brief discussion of barrier films is necessary
in preparation for a discussion of porous layer growth in
dissolving electrolytes because some fundamental factors
are crucial to both processes.

In the early days it appeared as if barrier films
had no definite structure due to their small size and the
difficulty in obtaining high resolution on an electron
microscope. They were thought to be either 'amorphous' or
microcrystalline $\gamma\text{-Al}_2\text{O}_3$ or $\gamma'\text{-Al}_2\text{O}_3$. On later examination
when techniques had progressed, some workers found a fine
structure when films were formed above 100V. They (16)
proposed a structure in which crystalline islands were
within the amorphous film.

Franklin (17) studied barrier films for use as



where r is pore diameter,

b is radius of curvature of pore base,

θ is \cos^{-1}

units are in nanometres

Fig. 3 (15)

electrolytic capacitors. When using a boric acid-borax electrolyte he showed that there was an hexagonal cellular structure. The cells differed in degree of hydration and crystallinity, but were composed of an outer region of γ' - Al_2O_3 with an amorphous centre. The diameter of the cell was shown to be proportional to the applied voltage. The thickness was also governed by the voltage and approximated to 1.4nm/V for solutions with little or no solvent action. It was found to be 1.15nm/V for barrier layer films formed under porous anodic conditions.

Ionic conduction in these films could be by metal cations, acid anions, oxygen ions, hydroxide ions, protons or a combination of some of them. It was not clear whether the ions move through the film under the influence of the field, making jumps in the amorphous structure, or became trapped after moving several lattice spacings. Similarly, movement could occur within the crystalline or amorphous regions.

It is now thought that two simultaneous processes occur in barrier layer formation:

1. New oxide is formed at the metal/oxide interface. Growth occurs due to the migration of Al^{3+} , O^{2-} and OH^- ions through the existing film.
2. At the film/electrolyte interface a solid film forms by dissolution/precipitation or dissolution/deposition under field mechanisms and/or solid state mechanisms.

The film formed by either mechanism is dependent upon the fate of Al^{3+} ions ejected initially at the film/solution interface. Whether these ions contribute to solid film growth at the film/solution interface depends on their efficiency of precipitation/deposition (18).

2.2.4 Porous Films

Many authors have proposed mechanisms for barrier layer growth, pore initiation and growth, and the inter-relationships between the basis metal and the barrier and porous layers.

The first model to be proposed for porous oxide growth in acid electrolytes (sulphuric, chromic and oxalic acids) was that of Keller, Hunter and Robinson (19). Their work was based on observations from electron micrographs. The mechanism of barrier layer growth was not put forward, but that it was formed rapidly and completely once the leakage current was reached. The thickness of this layer, which was non-porous, was found to be $1.4nm/V$, being a function of the applied voltage. The model proposed that the porous oxide layer extended from a thin compact and scalloped barrier layer, which was adjacent to the metal. Close-packed hexagonal cells, with a star-shaped cross-sectional central pore, extended through the porous layer from the oxide/solution interface almost to the barrier layer. Single rows of cells formed along the sides of subgrain boundaries of the aluminium due to lower resistance from the 'open-structured' oxide. Each of these

cells was initiated by the solvent action of the electrolyte at a specific point. Current flowed through the thinned area causing more oxide dissolution due to resistance heating of the electrolyte. The hexagonal shape of the cell was due to geometric (steric) factors, since each individual cell had six near neighbours. A continuous oxide film resulted because the pillars of metal trapped between the hexagonal array maintained electrical contact which converted them into oxide, Fig.4 . The thickness of the oxide wall increased linearly with voltage, as shown by a straight line on the graph of cell size against forming voltage, while the pore diameter remained constant. The difference between cell size and thickness of oxide comprising two sides of cell wall, was a constant value i.e. the pore diameter, which was found to be 12nm by extrapolation to zero forming voltage. Other dimensions could be established. Cell size formed at any voltage could be calculated from the equation (19):

$$C = 2WE + P \quad (2.3)$$

where C is cell size,

W is wall thickness (nm/V)

E is the forming voltage,

P is the pore diameter.

The diameter of the cell was approximately twice the barrier layer thickness, which was proportional to linear forming voltage. The rate of cell wall formation was 1nm/V.

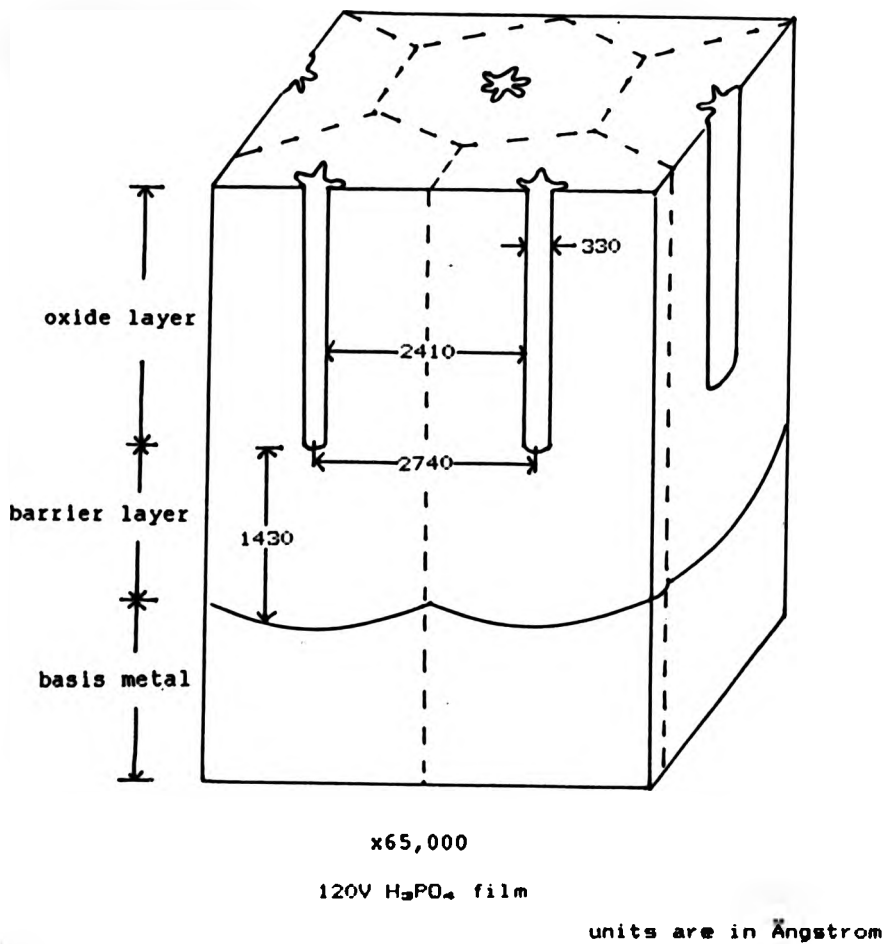


Fig. 4 (19)

The pores were independent of voltage, but dependent upon electrolyte composition and conditions; the electrolyte exerting solvent action along the pore walls. Concentration and temperature had only a limited effect on the pore size.

This 'idealised' model had some short comings which subsequent workers attempted to correct. However, this classic work has been the corner-stone from which subsequent ideas have been formulated. In 1959 Hoar and Mott (20) showed that it was not simply the solvent action of the electrolyte (sulphuric and chromic acid) which was competing with film growth, but that the dissolution was field-assisted at the base of the pores. This kept the barrier layer film thickness constant, and simultaneously oxide ions passed through the film from the pore bases, the base being the point of initiation, so that the whole film grew thicker. It followed that film dissolution rates at the pore bases increased at higher formation current densities, when the film thickened faster. The transfer of oxide ions was achieved because protons present at the pore bases formed hydroxyl ions with the oxide ions. These hydroxyl ions required less energy to move through the film than the oxide ions due to their smaller single charge. Under the influence of the high field these ions were pulled through the film from the electrolyte, and neutralized the aluminium ions at the metal/oxide interface. This resulted in oxide formation with the release of protons back to the electrolyte. Conversely, the aluminium ions neutralized the oxide ions and the barrier layer thickness was kept constant. The neutralization of

the aluminium ions at the metal/film interface caused the bottom of the pore to approach closer to the metal, allowing oxide ions to be spread over a larger area i.e. the metal surface rather than the pore base. This was another factor in keeping the barrier layer thickness constant. Pores were initiated by lowering the surface potential barrier of the proton and pore growth occurred at thick regions of the developing film (21). Pores were not found to be perpendicular to the basis metal, but inclined to each other when formed on concave and convex surfaces (9).

Hoar and Mott (20) gave a more detailed account of the mechanism of dissolution and growth than that of Keller et al (19), but it was not until 1970 when O'Sullivan and Wood (15) showed the main discrepancy to be that pore diameter was not independent of formation voltage. Barrier layer thickness, cell diameter, as well as pore diameter were all proportional to the forming voltage. Fundamentally, the model of Keller et al (19) was confirmed. The barrier layer thickness (rather than the porous layer) was formed by the steady state between oxide growth and field-assisted oxide dissolution. Pore and cell diameters and barrier layer thickness were influenced by geometric factors, and dissolution may have been aided by local heating effects. The regularity in pore and cell sizes, and the hexagonal packing were found, but not to the same extent as predicted Keller et al (19). New discoveries by O'Sullivan and Wood (15) and Wood and O'Sullivan (22), which were the measurement of the barrier layer thickness

for the first time, and this together with pore and cell dimensions were thought to be influenced by hydrogen-bonding and anion incorporation. It was found that pores often did not extend through the whole film but merged, branched or terminated occasionally. This was a consequence of the mechanism of pore initiation whereby locally thickened oxide regions merged and the current was concentrated into thin areas. No evidence was found for the star-shaped pores, nor for pore widening along the pore length. Chemical dissolution played a small part in widening the 'mouths' of pores producing 'trumpet-shaped' pores. Aggressive electrolytes caused pore widening and film collapse upon drying, whereas non-aggressive electrolytes produced thick barrier layers next to which formed large pores. Wood and O'Sullivan (22) found that low pH gave porous films, and as pH was raised towards neutrality, the importance of pitting by metal dissolution became greater. The main indication of field-assisted oxide dissolution was that dissolution at pore bases occurred faster at $80\text{A}/\text{dm}^2$ than at $10\text{A}/\text{dm}^2$. O'Sullivan and Wood (15) gave a model of field-assisted oxide dissolution, Fig.5. When a field was applied the Al-O bonds were polarized and the oxide ions were drawn towards the growing oxide while aluminium ions were pushed into the electrolyte Fig.5b. The aluminium ions were solvated by water molecules and the oxide ions were removed by H_3O^+ ions Fig.5c and 5d. Fig.6 shows a representation of a pore and the direction of the lines of force of the field. This also represents the least resistant path for current to flow. The field was greater

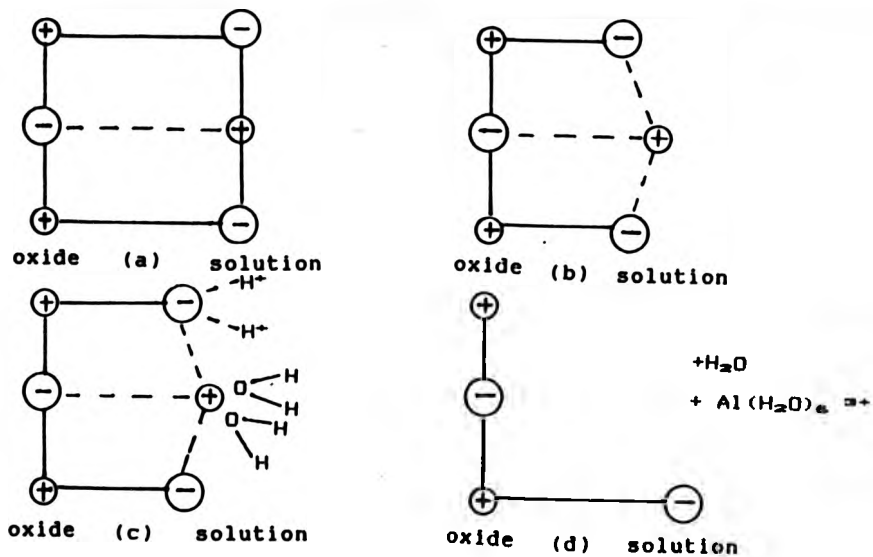


Fig. 5 (15)

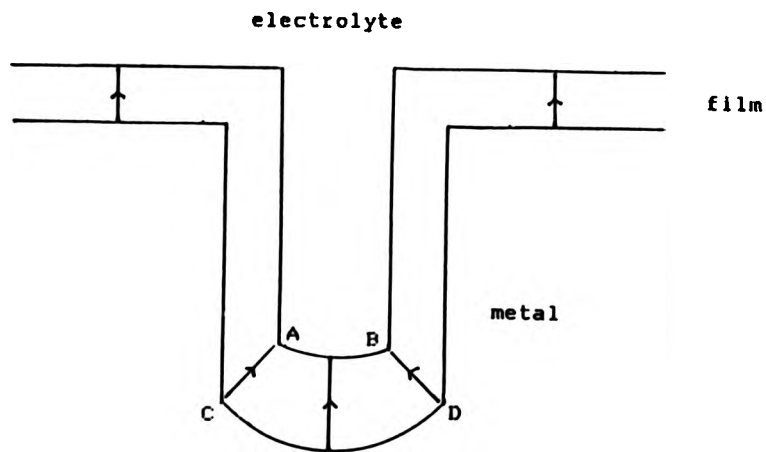


Fig. 6 (15)

at AB than at CD and this helped the dissolution at the oxide/solution interface, while the average field between AB and CD controlled film growth. Therefore upon pore initiation, dissolution was greater than oxide growth. If the radius of curvature of the pore base increased too much, the field across AB decreased and the pore ceased to grow. Oxide growth under the average field across the barrier layer, oxide dissolution under the local field at the oxide/electrolyte interface, the pore diameter and pore base radius of curvature were finely balanced under set conditions. This theory puts forward the suggestion that there is a larger proportion of hydroxide ions and acid anions at the oxide/electrolyte interface than at the oxide/metal interface. The amount of anions is influenced by their size, charge and ease of discharge at the oxide/electrolyte interface. Conversely, there are more aluminium ions at the oxide/metal interface than at the oxide/electrolyte interface. It is presumed that hydroxide ions form O^{2-} ions, as well as protons which move out of the oxide under the field. The potential energy of the ion is changed due to interaction by the field, with the result that the ion moves in the direction of the field. Other protons and hydroxide ions within the oxide layer may be held by hydrogen-bonding. However, hydroxide ions water molecules and acid anions all compete to enter the film. The hydroxide and oxide ions within the film may have resulted from the water or acid anions. There is a fundamental flaw with this 'hydroxide' theory. In acid solutions, at pH 0 the concentration is only 1×10^{-14}

g ion/l. In a monolayer of water molecules residing next to the aluminium surface the quantity of OH⁻ ions is:

$$[\text{OH}^-] = 1 \times 10^{-14} \times 1000x$$

where x is the amount of OH⁻ ions.

Now, if the current density is 200A/m², then

the discharge is $\frac{200 \times 1}{96500} \times 3$ OH⁻ per second

Time to discharge all OH⁻ in a monolayer x, is

$$\frac{1 \times 10^{-14} x \times 1 \times 10^3}{200} \text{ sec}$$

$$= 5 \times 10^{-18} \text{ sec}$$

If dissociation of the H-OH bond is considered to be represented by doubling the bond length from 1×10^{-10} to 1×10^{-9} m i.e a distance of 1×10^{-9} m, then

$$\text{velocity} = \frac{1 \times 10^{-9}}{5 \times 10^{-18}}$$

$$= 5000 \text{ms}^{-1}$$

This would be too fast to sustain the rate of $200\text{A}/\text{m}^2$.

Csokan (23) also discounted some of the Keller et al (19) assumptions. The electrolyte at the base of the pore could not have been heated by Joule heating because this would have resulted in enlarged pore bases. Keller et al (19) assumed that the surface structure at the metal/film interface was determined by initial current, and was not influenced by later changes. The converse of this was true. It was thought that the external oxide layer was electrically insulating and it was via the electrolyte that ionic conduction of current and material transport could occur. This could not have been true because it would not explain how the walls of the cells thickened. According to Keller et al (19) the density of pores on the surface were in a uniform distribution, but Csokan found that the distribution was irregular. The coincidence of chemical dissolution along the electrical lines of force during pore formation had no founding.

So, some of the Keller et al assumptions were shown to be incorrect and alternative explanations given over a decade later. However, soon after the Keller paper, in 1961, Murphy and Michelson (24) proposed a model which introduced colloidal chemistry as an explanation for oxide film growth in sulphuric, phosphoric or oxalic acid. The main features were that a gel-like matrix formed consisting of two types of oxides which made up the outer porous region. An hydrous oxide was formed by hydration, hydrogen-bonding and proton migration which surrounded a

relatively anhydrous oxide. The hydrous portion contained anions and water molecules, while embedded in the matrix were the anhydrous sub-microcrystallites. An important structural feature of this model, although purely speculative, was that the hydrous oxide formed 'internal surfaces' and via these, oxygen-containing species were brought to the barrier layer, so that film growth occurred at the barrier layer/oxide interface. Aluminium ions migrated from the metal to the barrier layer where they formed the anhydrous oxide by combining with oxide ions. The oxide ions were provided by hydroxide ions and water molecules with the resultant release of protons. The supply of hydroxide ions is doubtful as discussed previously. Another important point was that the anodising field assisted proton migration leading to hydrogen-bonding and subsequently assisting current conduction. If current paths converged, for example at defect sites, the oxide was dissolved by the heated acid producing less dense areas and these areas ultimately became pores. Pore formation was not considered to be a condition of oxide growth. Pores were found to be orientated at an angle or normal to the metal surface. Upon proposing that hydrogen-bonding, anion incorporation in internal surfaces and local variations of oxide solubility were governing oxide film formation, Murphy and Michelson considered that electrolyte type and the chemical nature of the oxide were the important factors. Later (25) both Murphy and Michelson expounded upon their original work. The barrier layer grew by Al^{3+} ions moving under the field and reacting in the outer

regions with OH^- ions to form alumina. The barrier layer contained anhydrous alumina but discrete particles of disordered hydrogen-bonded areas formed, and the degree of hydration increased with distance from the metal. The protons and hydroxide ions moved in opposite directions at high rates and the barrier layer thickness was determined by the dehydrating and hydrating rates. The thickness of the barrier was proportional to the voltage. The microcrystallites were close-packed and were not readily available to the electrolyte. Consequently, as the severity of the anodising conditions increased, the intercrystalline regions became more 'open'. However, the involvement of hydroxide ions must be doubted.

At about the same time as the above model Ginsberg and Wefers (26) described the oxide structure as fibrous. They claimed to have isolated individual fibres whose optical structures were a result of a growth process. The fibres had only a short range order and were composed of an amorphous outer coat, with hydroxide ions and electrolyte anions at an inner 'active' surface of the hollow fibrous tubes. These tubes were separated by hydroxide ions also. Both sulphuric and oxalic acids were used but no conclusions were reached about the binding of the anions, except that they constituted part of the film. No optical structure was found within the fibres and it was suggested that the reactions took place either by ion exchange or by the ions moving as a 'liquid'. The electrolyte penetrated to the metal/film interface via the active surface and by attack of the barrier layer at the

base of the growing fibre. With thickening around the point of attack, the film increased in size. The fibres were orientated normal to the aluminium. The curved fibre base was formed due to a two-zone structure and was dependent upon the size and arrangement of aluminium, oxygen and sulphur ions.

The two models proposed after that of Keller et al (19), were the electric field-assisted dissolution by Hoar and Mott, and a structural model based on a hydrogen-bonded matrix of oxide, anions and water, by Murphy and Michelson. The model of Ginsberg and Wefers is an intermediate between these two. Others have followed with similar explanations based on these models (21, 27, 28, 31, 32).

Siejka and Ortega (27) proposed a more complex model of pore formation by ionic currents: $I_{O_{2-}}$ is the transfer of oxygenated anions from solution (sulphuric acid) to the metal/oxide interface, I_{Al} is the transfer of aluminium ions through the base layer and passing directly into solution, $I_{O_{2-}}^*$ is the transfer of ions generated by field-assisted decomposition of the oxide, $I_{O_{2-}}^-$ is the transfer by cations to solution, $I_{O_{2-}}^+$ is the transfer of anions to the metal/oxide interface, I_{Al} is the total interfacial transfer current of cations passing into solution, where

$$I_{Al} = I_{Al} + I_{O_{2-}}^*$$

An O^{2-} tracing technique was used in which the barrier

layer was formed from an O^{18} labelled solution and further anodising was carried out in a non-labelled electrolyte. It was found that the O^{18} content of the barrier layer, after reanodising, was redistributed to the outer portion of the porous layer, and that the O^{18} changes were not due to oxygen losses. It was suggested that migration of oxygen vacancies through 'easy paths' caused porous oxide growth. The oxide was formed at the oxide/metal interface from the oxygen at the base of the pores as well as oxygen from the solution. As the pores formed, the O^{18} displaced by them was found just below the O^{18} enriched layer. Siejka and Ortega proposed that a barrier layer sub-structure was present which resulted in the O^{18} transferring to the outer regions during growth. It was found that SO_4^{2-} anion incorporation was probably due to the fact that the interatomic distances between the oxygen atoms in both Al_2O_3 and the SO_4^{2-} ion were the same. Cations moved via an interstitial position. Two mechanisms were proposed for the movement of oxide ions originating from oxide decomposition, I_{ox} . They varied only in the mode of oxygen migration. They are the interstitial theory (Hoar and Mott) and vacancy motion through 'easy paths' (Siejka and Ortega).

In 1978 Thompson, Furneaux, Wood, Richardson and Goode (28) extended the field-assisted dissolution theory to include direct loss of Al^{3+} ions into solution, as proposed previously (27). By using phosphoric acid it was shown that no phosphate anion incorporation occurred for 25 to 35% of the barrier layer from the metal/oxide interface.

They considered that two simultaneous processes proceeded: relatively pure alumina was formed near the metal/oxide interface due to ionic migration of the mobile ions Al^{3+} , OH^- and O^{2-} , and microcrystalline anion-containing material occurred at the oxide/solution interface by deposition. Some Al^{3+} ions were incorporated here in the growing oxide while others formed hydrated ions in solution. The film was assumed to be solid at the inner layer and gel-like at the outer layer. The solid oxide formed from a colloidal hydrated oxide by deprotonation of the hydrated Al^{3+} ion.



There was preferential thickening of the oxide above metal ridges (topographical features) and at cell boundaries. The ridges were flattened as the oxide thickened locally. With subsequent anodising, pores were formed in preferential cells giving a scalloped metal surface. These cells were shown to be hexagonal by electron microscopy.

Another investigation which may be compared with the Hoar and Mott model is that by Parkhutik (21). Acid anion incorporation was proposed again, along with pore initiation. Sulphuric, oxalic and phosphoric acids were used to investigate acid anion participation which was studied by Auger Electron Spectroscopy (AES) and ion etching. In this model the space-charge of the anions played an important part of porous film formation. Oxide dissolution proceeded due to a proton-assisted mechanism whereby the potential barrier of the oxide/electrolyte interface was

decreased. At the moment of pore initiation, the anion concentration reached saturation point and anions moved into the oxide. As the oxide grew, the anion maximum spread, although distribution was not uniform. An anion maximum was buried in the oxide, although as in reference 28, anion incorporation was confined to the outer regions of the oxide film. Sulphur was found to be present as SO_4^{2-} . Similarly, $\text{C}_2\text{O}_4^{2-}$ and PO_4^{3-} were found for oxalic and phosphoric acid respectively. However, the PO_4^{3-} anion exhibited some special features. After prolonged electron irradiation the bivalent phosphorus ion was indicated; a reduction reaction. PO_4^{3-} anion distribution differed from those of SO_4^{2-} and $\text{C}_2\text{O}_4^{2-}$. There was no phosphorus maximum buried in the oxide for thick oxides but anion distribution was located at the oxide/electrolyte interface. This was due to the anion size and structure giving it a low mobility. [As early as 1958 Plumb (29) showed the phosphorus was incorporated into the oxide, but suggested the form was P_2O_5 .] Pores were initiated at thin regions of the barrier oxide, unlike thick region initiation postulated by Hoar and Mott. It has been found (30) that for films with a large cell size, growth occurs preferentially above ridges on the basis metal. Ridges could be described as flaws, and there will be highly localised stress development in the film growth above them. The consequent high current density will produce a crack/heal process in the oxide. High points on the oxide form and the metal ridges are flattened as the barrier layer between ridges is thickened. Eventually the high

current density moves to the thinner areas, since these then attain lower resistance than the ridges. Pore development and scalloping of the basis metal occurs at these thin areas.

O'Sullivan, Hockey and Wood (31) gave evidence for a gel-like matrix of anhydrous and hydrated regions similar to that of Murphy and Michelson (24). They showed by infra-red spectroscopy (I.R.) that a freshly prepared film contained molecular water which was removed upon evacuation. It was shown that on the exterior of crystallites were hydroxyl groups or ions. Both the molecular water and hydroxyl groups were within the intercrystallite regions since it was found that deuterium exchange took place here. If the groups were bound within the crystallites there would be no exchange. Thus the matrix was described as an amorphous 'open array' of anhydrous crystallites, interspersed with hydrous intercrystallite regions.

Xu, Thompson and Wood (32) described the oxide film in terms of cell boundary bands and extended the theory of microcrystallites by suggesting that the inner layer of porous oxide was compact and did not contain anion species. The outer regions were open and contaminated by PO_4^{3-} ions. By means of exposure to an electron beam in an electron microscope, the film material was analysed and was shown to contain decreasing amounts of phosphorus from the pore wall, Fig.7(a), towards the cell boundary band, Fig.7(c). The cell boundary band itself contained no significant amount of phosphorus. Similarly, the amount of

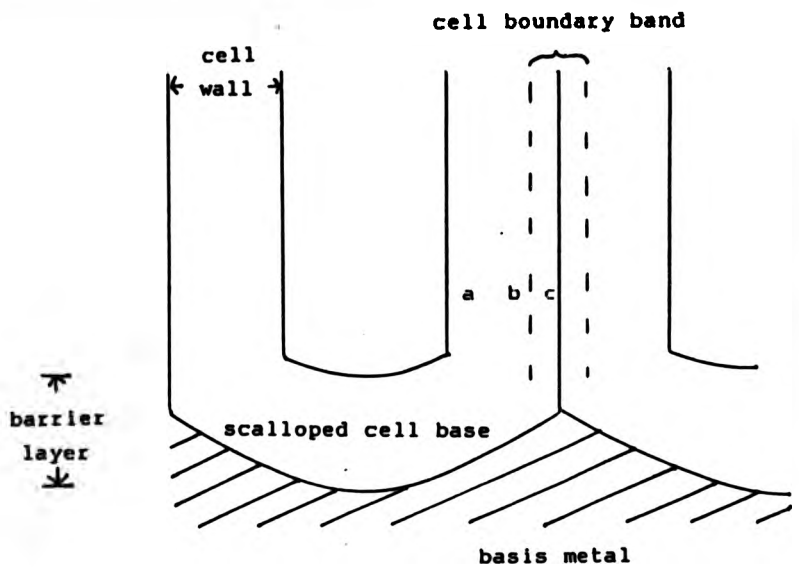
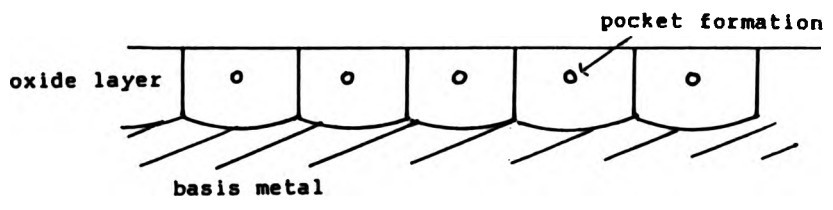
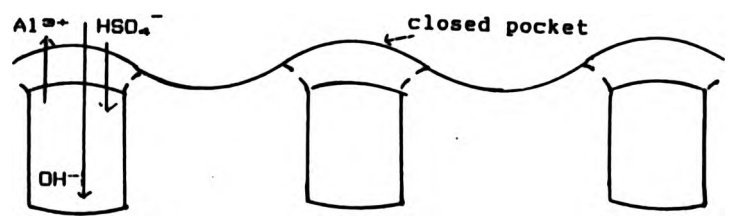


Fig. 7



(a)



(b)

Fig. 8 (35)

anion species extending from the film/solution interface decreased towards the metal/film interface. It was suggested that the difference in texture between the pore walls and cell boundary bands was shown up more under the electron beam due to the intercrystallite regions decomposing. This resulted in a relatively large internal surface to reveal the phosphorus content. Electron microscopy and allied techniques in high vacua and high fields are said by some critics to result in artefacts. The diffraction pattern observed may be that of the features which were heated and changed during analysis.

Other models have been proposed which describe factors that have formerly been given secondary importance or which are totally new concepts. These include: dissolution by local Joule heating effects (33), a nucleation model (34) and a colloidal model containing pockets (35).

Leach and Neufeld (33) showed that oxide solubility was the main factor in porous oxide growth and that films could show typical barrier or porous structures according to the temperature of the electrolyte. The electrical and optical properties of films formed at high current densities were different from those formed at low current densities. These differences were probably due to high fields or temperatures, and not a result of changes in pore structure. The increased local temperature caused greater dissolution of the cells which in turn increased the current through the pores. Barrier films differed from porous films only in the rate of thickening at constant

applied voltage. Pores developed in barrier films when current was allowed to decay to a relatively low value. At 50°C a distinct current minimum occurred. It was found that the final current was higher at 50°C than at 25°C. No pores were observed if current decay was omitted. Pore dimensions were not only a function of electrolyte composition and field conditions but also a function of time. Thus all barrier films would show some porous growth if the voltage was kept constant for a sufficient length of time.

Csokan (34) used cine film to record the process of anodic oxidation and concluded that it occurred by a nucleation mechanism of which there were several stages. The first stage was an initial (induction) period during which 'clusters' of aluminium-oxide or aluminium-oxygen formed at energetically favourable points. The second stage was a period of nucleation. Nuclei of primary aluminium oxide formed in concentric circles, although the growth was not uniform. Subsequent nuclei appeared and the surface was very rapidly covered with an oxide film. This formed the barrier layer which reached a limiting thickness in electrolytes with no solvent power. Upon anodising in electrolytes with dissolving power, secondary oxidation formed on the edges of the primary nuclei. The final structure was a surface covered by 'rosettes' which themselves were made up of textured 'terraces'. The final stage was pore formation. This resulted from ion and electron diffusion as well as proton transfer. Pores were formed irregularly by the solvent action of the electrolyte at specific areas due to the non-uniform secondary oxide

structure. The oxide grew normal to the metal/oxide interface, but lamellar growth was also found parallel to the basis metal. This was said to be due to different potential differences over the surface which caused interlamellar current conductance until the potential differences equalised.

The last paper did not give an explanation for the formation of the pores themselves. Heber (35) proposed a mechanism which described 'pockets' as preceding pore development within a colloid. The theory of Murphy and Michelson (24) was based on colloid chemistry but it was described in terms of a matrix of two layers and no discussion was given about interface relationships. Heber proposed that in an aqueous solution a colloidal layer of aluminium hydroxide formed at the electrolyte/metal interface, if conditions were favourable Fig.8a. If the aluminium was an anodically polarised electrode, any oxide layer must be partially colloidal. As anodising proceeded more colloid was formed. Two alternative mechanisms were given for the formation of 'closed pockets', Fig.8b. The first described a foam of hydroxide covered droplets which would reduce the surface tension of the liquid and accumulate at the interface. Each pocket would be covered by an hydroxide skin. The other explanation was that whirls of incoming hydroxide ions would react with a 'boundary layer' to form a colloid. Each pocket would be closed by a dynamic boundary layer. Pockets grew due to increasing inner pressure of ions. Each pocket would reach equilibrium horizontally, in a manner similar to the equalising of

potential differences as described by Csokan (34). The growth stopped and the covers were dissolved by accumulation of charge on them. This corresponded to the deceleration on the voltage-time curve, Fig.2. Pores formed in a non-solidified colloid. Solidification occurred because the aluminium hydroxide hydrosol coagulated in the presence of the sulphate ion, amongst others. Once the pocket cover was dissolved, field-assisted oxide dissolution took place as described by others.

By using X-ray photoelectron spectroscopy (XPS), Treverton and Davies (36) found that there were two types of sulphur species present in the oxide layer. These were sulphate and sulphide ions. It was concluded that the different species could be accounted for in two ways. One theory was that oxide formed at the metal/oxide interface and sulphates present there could have been in the correct environment to form sulphides upon etching. The other theory was that hydrated alumina was formed by Al^{3+} ions entering the solution and reacting with water at the solution/oxide interface. The sulphate ions may have helped in a reprecipitation process or be residues of coagulation of $Al(OH)_3$ as described by Heber. Since sulphides are isoelectronic with oxide ions it may be possible that the sulphides replaced the oxide ions. This may account for the fact that the sulphates are found in a higher proportion within the anodic films than any other anion.

2.2.5 Alternating Current (A.c.) Anodising

It would first appear that a.c. anodising has an advantage over d.c. anodising in that two loads of work can be anodised during the anodic half-cycles. However, on the alternate cathodic half-cycle a different electrolytic mechanism occurs. Sulphuric acid is cathodically reduced to sulphur and its compounds, both of which are incorporated into the film, and H_2S is given off. This is the main drawback of a.c. anodising (37). Sulphides may combine with alloy metals to produce integral colours. Recent work has been performed on the addition of oxidising agents to counteract the sulphur compounds. The oxidant depolarised the cathodic half-cycle reaction of H_2 evolution, so eliminating SO_4^{2-} reduction (38). It was found that by adding ferric salts, particularly the chloride, a reducer, thick coatings were produced where earlier investigations had only formed thin coatings of 6 to 8 μm . It was of interest that, despite the cathodic production of sulphur, it was only detected in the outer regions of the oxide, and no iron was detected within the film. Current investigations (30) are under way to find out how important the sulphate-sulphide reaction is as an inhibitor in film growth and whether the $Fe^{3+}-Fe^{2+}$ redox reaction is an anode reaction which may produce an oxidant internally. Ferrous or ferric sulphate and ferrous oxalate are also used, and are favoured over ferric chloride since it is known that chlorides undermine corrosion performance. As well as reducers, neutral modifiers such as Na_2SO_4 have been used.

The Keller et al (19) model gave a good fundamental basis from which a greater understanding of porous anodic oxide growth has developed. With advances in technology, research has substantiated or disproved hypotheses. Caution is still needed, however, in interpreting data and applying it to the different theories.

2.3 Methods of Colouring the Anodic Film

2.3.1 Introduction

It was discovered in the first days of anodising with the Bengough and Stuart process (1) that alizarine dyes could produce many colours. Other dyeing processes have been developed which exploit the porous nature of the anodic oxide film. Once anodised aluminium had become established as a popular material for use in architecture demand grew for coloured finishes as opposed to the shades of grey available from sulphuric acid anodising, or pale yellow from oxalic acid anodising. Aesthetics became increasingly important.

The different colouring methods can be distinguished by the type of colouring component and its position within the oxide film; absorptive dyeing Fig.9, integral colour anodising Fig.10, and electrolytic colouring Fig.11 (interference colouring Fig.12 a and b). Over the last 10 to 15 years there has been a move away from the first two methods and electrolytic colouring,

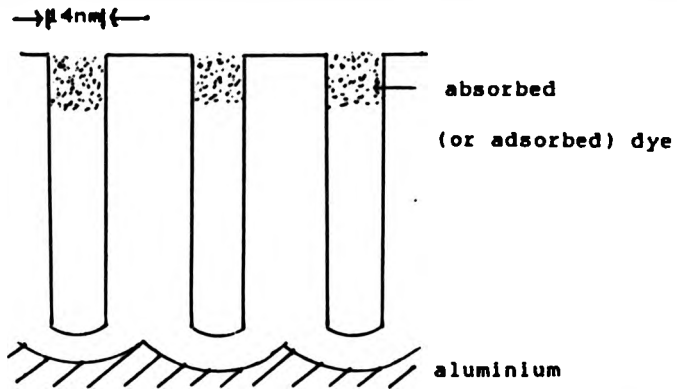


Fig. 9

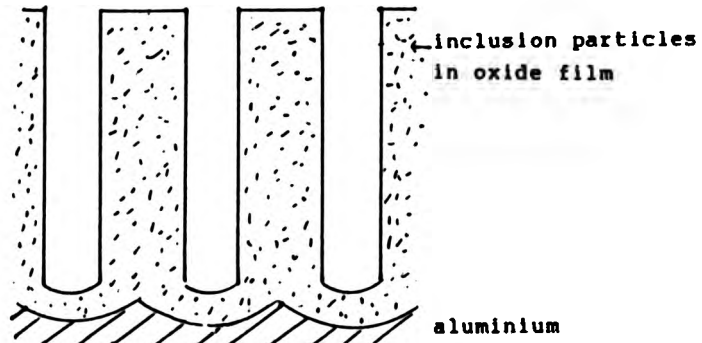


Fig. 10

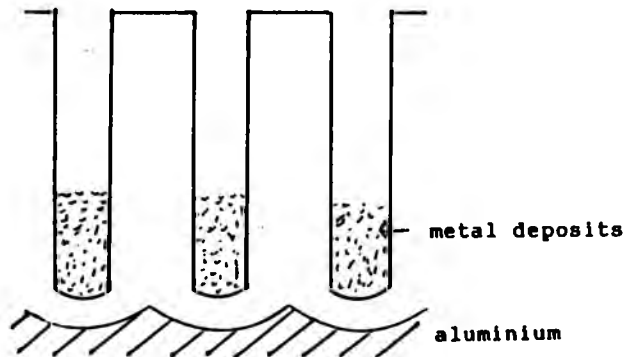


Fig. 11

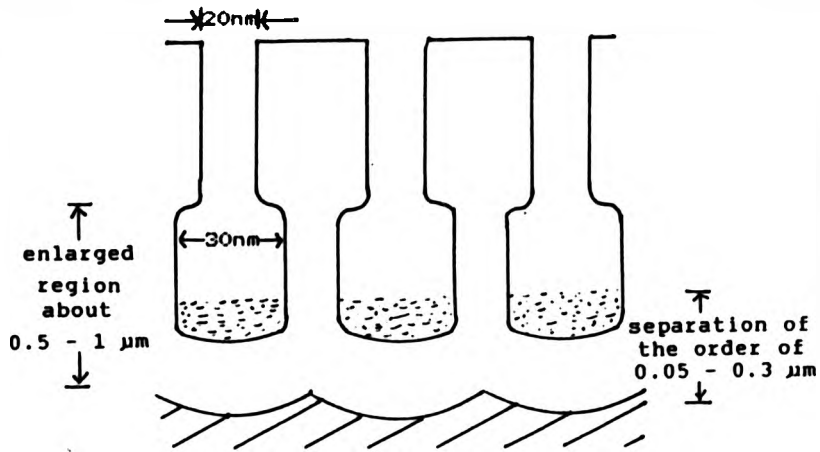


Fig. 12a (63)

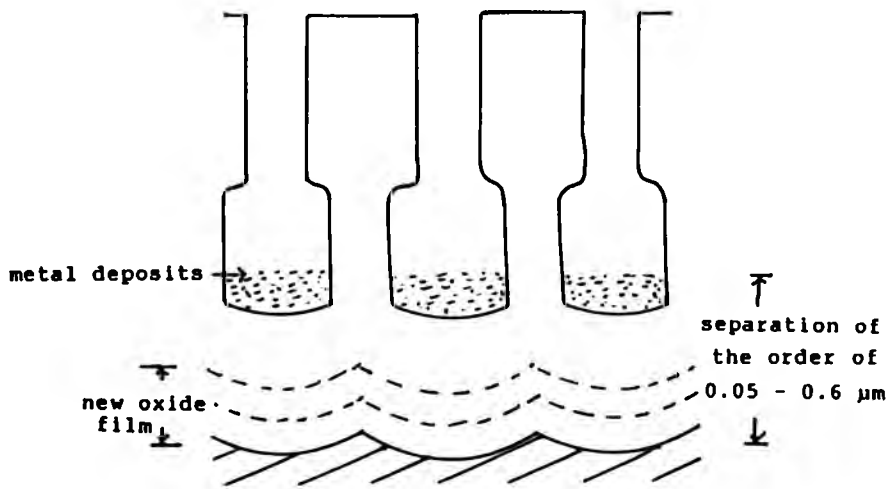


Fig. 12b (63)

(together with interference colouring) has become the dominant procedure. This can be attributed to improvements in uniformity and reproducibility of colour, corrosion resistance, ease of use and lower cost. Electrolytic colouring produces shades of gold, bronze, black, grey and red but commercial pressure has prompted technical application into discovering more varied colours. Integral colouring gives a broader range of colours than electrolytic colouring but interference colouring provides the spectral colours now demanded. Sometimes particular interference finishes do not give the high standard of weather resistance required. Most spectral colours can be obtained by the conventional absorptive dyeing techniques, but the light fastness can be poor compared to interference colouring for long term architectural uses. Thick anodic films (25 - 30 μ m) and strict control of anodising and sealing conditions are required. Dyeing is adequate for internal uses where light fastness is less critical.

2.3.2 Absorptive and Adsorptive Dyeing

The porous structure of anodised aluminium allows it to be coloured by absorption or adsorption of dyes into the pores. This is achieved by inorganic pigments or organic dyestuffs respectively, Fig.9.

There are two main methods for the application of inorganic colouring; immersing the oxide into a solution of a heavy metal salt which hydrolyses to give the pigment, and the double decomposition method in which the oxide is

immersed in one solution, rinsed and immersed in a second solution. The two solutions react within the pores to form a precipitate. The most notable process for the immersion method is the use of ferric ammonium oxalate (39) which gives a yellow/gold colour resulting from the deposition of iron oxide, Table 3. Another immersion method is the combination of cobalt acetate and potassium permanganate which gives a gold/bronze colour. It can be said that this is a double decomposition method also, Table 4.

The amount of pigment precipitated will depend on the absorption and diffusion of small cations and anions into the pores. This diffusion will depend on the surface charge with respect to a given solution (42).

When colouring with organic dyestuffs, the oxide film is immersed in the dye for a period of time at a selected temperature. The thickness must be at least 25 μ m. No mixtures of dyestuffs are used, only proprietary preparations. Unlike inorganic dyeing, the organic dyes are thought to react with the oxide layer and are adsorbed into the film (43). If the oxide film is treated with acid prior to dyeing, the acid anions on the surface are replaced by the anions of the dyestuff. It was envisaged that the oxide surface was dissolved or etched by the acid which caused an increase in surface area and increased the amount of dye on the external surface. The dye diffused into the pores which was thought to be the rate-determining step. If the surface is subject to dissolution, pore widening must occur which may affect corrosion resistance.

Table 3 (40)

Compound	Concentration (g/l)	pH	Temperature (°C)	Time (min)
FeNH ₄ (COO) ₂	10(light)	5.5	50	2
	25(dark)	±0.5		
Co(CH ₃ COO) ₂	50	-	50	2
+KMnO ₄	30	-	30	2

Examples of the double decomposition method are given in Table 4, (41).

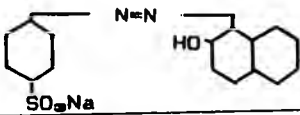
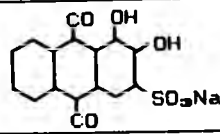
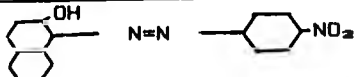
Table 4

Colour	Reaction
Red-brown	$2\text{CuSO}_4 + [\text{Fe}(\text{CN})_6]\text{K}_4 \rightarrow [\text{Fe}(\text{CN})_6]\text{Cu}_2 + 2\text{K}_2\text{SO}_4$
Brown	$2\text{AgNO}_3 + \text{K}_2\text{Cr}_2\text{O}_7 \rightarrow \text{Ag}_2\text{Cr}_2\text{O}_7 + 2\text{KNO}_3$
Dark brown	$\text{Pb}(\text{CH}_3\text{COO})_2 + (\text{NH}_4)_2\text{S} \rightarrow \text{PbS} + 2\text{NH}_4(\text{CH}_3\text{COO})$
Yellow	$\text{Pb}(\text{CH}_3\text{COO})_2 + \text{K}_2\text{CrO}_4 \rightarrow \text{PbCrO}_4 + 2\text{K}(\text{CH}_3\text{COO})$
White	$\text{Pb}(\text{CH}_3\text{COO})_2 + \text{Na}_2\text{SO}_4 \rightarrow \text{PbSO}_4 + 2\text{Na}(\text{CH}_3\text{COO})$
Blue	$2\text{Fe}_2(\text{SO}_4)_3 + 3[\text{Fe}(\text{CN})_6]\text{K}_4 \rightarrow [\text{Fe}(\text{CN})_6]_2\text{Fe}_4 + 6\text{K}_2\text{SO}_4$
Black	$\text{Co}(\text{CH}_3\text{COO})_2 + \text{Na}_2\text{S} \rightarrow \text{CoS} + 2\text{Na}(\text{CH}_3\text{COO})$

Dyestuffs may be aqueous or solvent-based. Aqueous dyes are either adsorbed onto the oxide by anions

such as the sulphonate group forming covalent bonds with the aluminium ions, or by chelation where a hydrogen or metal atom is held between two atoms of a single molecule i.e. the oxide lattice, or by the coupling of diazonium salts ($ArH + Ar'N_2 + X^-$ where Ar is the aromatic group and X^- a halide) to form azo dyes of the formula $Ar-N=N-Ar'$. Table 5 gives some examples.

Table 5

Fixation mechanism	Dye	Structural Formula
Adsorption by covalent bonding	Orange II	
Chelation	Alizarin Red	
Diazotisation	Para Red	

Non-aqueous-based dyes can be used in solution in benzene, toluene, acetone, ethanol, chlorinated benzenes or substituted naphthalenes. It was claimed that these dyes have better heat and light fastness than aqueous-based dyes and that adsorption is immediate. Care is needed when using these dyes due to the hazardous nature of the solvents.

Operating conditions for both inorganic and organic dyeing must be carefully controlled. Temperature, time, concentration, pH and film thickness affect the

colour. The temperature must not exceed 80°C otherwise sealing may occur, preventing incorporation of the dye. It should be kept within $\pm 1^\circ\text{C}$ of the operating temperature and the pH within ± 0.5 ; the most common range is 5.5 to 7.0. Concentration also varies, but the more concentrated the solution, the darker the colour. Cold dyeing is slower and easier to control. Mains water should be avoided as calcium and magnesium form insoluble compounds with the dyestuffs. The solutions and work loads should be kept free from dirt and grease as these impair the colouring ability. Slow agitation gives uniformity of colour. Rinsing times are also critical. Generally inorganic pigments have better light and heat fastness than organic dyes.

Recently a spray dyeing technique has been developed for organic dyes which is proving very economical (44). Operating at the same concentration, time and temperature as conventional immersion dyeing, anodised films are mounted in an enclosed chamber and the organic dye is sprayed from different directions. The excess dye drains off and is recycled. The quality of the finishes has been good, but the apparatus must be designed to accommodate different shapes and the solution must not accumulate in intricate parts. This could cause uneven dyeing and drag-out of the dye. The disadvantage is the large capital cost. The advantages are numerous.

2.3.3 Integral Colour Anodising

The oxalic acid process (45), first used in Japan in 1923, can be considered to be one form of integral colour anodising. Alternating current or a combination of alternating and direct current was used and hard anodic coatings were produced which varied in colour from yellow to bronze. The colour was the least important aspect at that time and was not controlled very well because the process was not fully understood. In the 1950's interest grew in colours other than grey which were provided by this process.

Alcoa patented the 'Duranodic 300' process. The main constituent was sulphophthalic acid electrolyte. The Alcoa headquarters in Pittsburgh, USA was one of the first buildings to be clad in integrally anodised aluminium using a silicon alloy, although the colour remained grey. The Duranodic process is still used today.

A similar process is 'Kalcolor' which was developed at the end of the 1950's (45). 5-sulphosalicylic acid was used and golds, bronzes and brown, as well as grey were produced Table 6. This process was the corner-stone of integral colour anodising, but is no longer used.

The basis of the method is the incorporation of particles into the growing oxide film, Fig.10. It is the use of organic acid electrolytes which is peculiar to this process. A small quantity of sulphuric acid is essential since the organic acid alone gives a barrier film. The sulphuric acid can be replaced by a metal sulphate. The

alloy composition also affects the colour and is a major consideration. Generally grey colours are produced by silicon alloys while yellow/gold colours are formed on chromium alloys. Current density, voltage, temperature and time are strictly controlled. The aluminium content must be kept within 1.5 to 3g/l of solution and a cation exchange resin is used to remove the excess aluminium. The oxalic acid/organic acid/sulphuric acid mixtures tolerate less aluminium than do the sulphonated aromatic acids.

Table 6

'Kalcolor' Composition	
Sulphosalicylic acid	60 - 100g/l
Sulphuric acid	5g/l
Temperature	25°C
Current density and voltage	2.5 - 3A/dm ² , up to 70V
'Duranodic' is very similar to 'Kalcolor' except 100g/l sulphophthalic acid replaces sulphosalicylic acid.	

Integral colour anodising gives harder and more abrasion resistant coatings than sulphuric acid anodising, due to the use of high voltages. High current densities and voltages make the process more expensive. Higher heat out-put requires efficient cooling systems. Colour control is also critical. This process has been popular and has had much success, although colours are restricted.

Sulphuric acid is well known for giving hard

transparent coatings, but it can also produce coloured films by altering the conditions (46). Hard coatings are formed by reducing the ability of the electrolyte to attack the film and this is achieved by reducing the temperature. However, the voltage must be raised in order to maintain the current density. Coloured films can also be produced by reducing the sulphuric acid concentration. These conditions are not practical, however.

The integral colour process can be regarded as anodising in low concentrations of sulphuric acid, or the sulphuric acid can be said to be modified by sulphonation i.e. XSO_3H where X is the aromatic acid group. Sulphonation makes these groups more suitable for anodising by increasing the solubility and conductivity. Organic acids incorporating the carboxylate group are also used, but sulphate is present. Organic acids used are: maleic, succinic, citric, cresolsulphonic, tartaric, formic, sulphanthranilic. There should not be too great a difference between the anodising strengths of the mixed acids (47). The concentrations of the acids should be inversely proportional to their anodising strengths.

A third electrolyte may be incorporated and this is called a 'bridging' electrolyte. It is usually of intermediate strength, since if a weak and a strong electrolyte are used together, the anodising takes place as if only the stronger acid were present. For example, weak tartaric acid and strong sulphuric acid are mixed with the intermediate oxalic acid.

Research has been carried out on anodising in

organic acids only. Perhaps the best known electrolyte is oxalic acid. This gives good polished finishes unlike other integral colour anodising which tends to roughen the metal/oxide interface. All organic acid electrolytes are sensitive to chloride contamination which causes pitting of the film. Kape (48) gave a detailed account of films formed in various organic acids. It was concluded that anodic film formation was achieved in di- and tribasic acids, but not so readily in monobasic acids. Pitting tended to be the predominant process for the latter acids. The factor which determines whether film formation or pitting occurs is the strength of the acid i.e. degree of ionisation. The strength influences the thickness and colour of the films.

Alloy composition (49) also influences colour as well as quality of the film, and this together with electrolyte composition must be carefully controlled. As the anodic film thickens, the colouring effect increases. The alloying composition can be made up of prime elements or intermetallic particles. Their solubility in the electrolyte is another consideration as is the size and distribution of the particles. Iron, manganese, nickel and silicon are insoluble and cause coloration. Although magnesium and zinc are distributed uniformly, the anodic film is clear. Copper causes coloration after ageing. Table 7 gives the colours produced with the 'Kalcolor' process. In the case of the KE45 alloy, the alloying elements produce Al-Fe-Si constituents with copper or manganese replacing the iron (50). They are insoluble in the electrolyte and give the film its colour.

Table 7

Extrusion	Colour
HE9	Bronze
HE20	Black
or HE30	Grey/black
KE45 (HE9-type with 0.2% Cu and Mn)	Dark bronze

Despite the many variables and processes available, the range of colours is limited, leaving the architect to choose between many anodising systems which give basically the same colours.

The precise mechanism of film colouring is unsure and there has been little investigation into this. A number of theories exist (51), including aluminium particles or alloying constituents dispersed in the film; a reaction similar to the Kolbe reaction, where anions embedded in the film are polymerised; colour dispersion of carbon-containing compounds within the film (reduction or decomposition of organic acids); colour by reduction products of sulphur. The colour must be related to pore and cell dimensions since colours are voltage dependent. The colours are produced by the scattering of incident light caused by these particles and therefore depth of shade depends solely on film thickness. It is likely that the mechanism proceeds by a combination of the above theories,

but alloying constituents have a major role to play.

Tajima, Baba, Mori and Shimura (52) used super purity 99.99% aluminium specimens. They showed that the electrolyte anions also played an important role in the formation of the film with respect to structure and colour. By using resistivity measurements they showed that at higher current densities and with increasing thickness, more anions were incorporated into the film. This resulted in a less than perfect structure. The resistivity was unchanged with changing thickness when additions of organic acids were made to either sulphuric or malonic acid. The organic acids had little effect on the resistivity and it was the dominant anions which influenced the colour. Infra-red spectroscopy confirmed the theory that anions were incorporated into the film. From electron micrographs the authors thought that the cells had transparent centres while the other 'circle' was colour. As the thickness increased the colour spread over the whole surface. From this the authors indicated that the material between the cells gave rise to the colour. However, the 'transparent' centres were simply the cell pore which reflected white light in the microscope.

2.3.4 Electrolytic Colouring

The process of electrolytic colouring is simple. Aluminium is anodised in a conventional sulphuric acid electrolyte, rinsed, and transferred to an electrolyte containing metallic salts. Sinusoidal a.c. supply is

applied and metallic particles are deposited irreversibly at the metal/oxide interface i.e. the pore base, during the cathodic half cycle, Fig.11. Other waveforms have been tried with some degree of success. Counter-electrodes can be made of either the same metal as the salt solution, or graphite, stainless steel or lead.

The main advantage of this process over integral colour anodising is that it is significantly cheaper. The desired colour can be achieved regardless of the thickness, although 'over-colouring' must be avoided; the colouring process is separate from anodising allowing colouring to be controlled independently; the basis metal does affect the colour but much less so than with integral colouring; low voltages and currents are used. A range of gold, bronze and black colours similar to integral colours are produced when nickel, tin or cobalt salts are used, or combinations of these. Copper-based electrolytes give red and black finishes, but the latter colour is not used in the UK due to doubts about light fastness and corrosion resistance. Generally, electrolytic coloured films have similar properties to 'natural' sulphuric acid films, since the colouring components are deposited at the base of the pores and do not affect surface phenomena such as light fastness, Fig.11.

In 1936 Caboni (53) disclosed a method of colouring anodically formed films by electrolytic techniques. He used copper, nickel or silver salts and an a.c. supply. Electrolytic colouring was made commercially feasible by Asada in Japan during the 1960's, and in 1966

the Alcan company obtained the world rights for the process outside Japan. 'Alcan' produced the well known 'Anolok' colour range using first a nickel salt solution and later cobalt salts. Today electrolytic colouring is widespread in the architectural anodising industry, and much research has been carried out to improve the techniques. The precise mechanisms involved and problems encountered are still under scrutiny, and investigation into these forms part of this thesis.

Nickel-based electrolytes (54) are still widely used in Japan although use elsewhere is less common. They are cheaper than tin or cobalt electrolytes but black finishes can be difficult to obtain. They have low colour throwing power i.e. the variation in colour between high and low current densities, and are sensitive to contaminants such as sodium. These problems can be resolved by adding salts such as magnesium sulphate, aluminium sulphate and sulphonc acids. Nickel and cobalt finishes give good abrasion resistance and light fastness, and compare well with 'natural' sulphuric acid films. Corrosion resistance is good also.

Cobalt-based electrolytes are the most expensive, but bronze and black finishes can be produced. The colour throwing power is good and cobalt solutions are less sensitive to contaminants than nickel-based electrolytes. Cobalt-based electrolytes are stable and loss is due to drag-out and electrolytic deposition only.

Tin-based electrolytes are of intermediate cost, and claims have been made that they give good colour

uniformity and fast colouring rates. However, there has been recent concern over the quality of dark bronze and black finishes which have been investigated in this thesis. Sensitivity to contaminants is fairly low; only nitrates and chlorides have an effect at concentrations of 1g/l or more. Colour throwing power is high. The stannous compounds precipitate and do not redissolve. These components no longer perform any useful function. In order to reduce loss by oxidation, stabilising agents are added such as phenol sulphonic acid, cresol sulphonic acid or sulphophthalic acid. Doubts have been cast over the abrasion resistance and corrosion resistance of tin-coloured finishes, although there is little difference between the light fastness of tin, cobalt and nickel finishes. There is low pitting resistance for dark bronze and black tin finishes, even when the thickness is 25 μ m, although light bronzes fair well.

Copper-based finishes give doubtful performance qualities. Pink and maroon shades are obtained, as well as black, but the light fastness compares only with colouring in dyestuffs. Black copper finishes have low pitting resistance despite the good light fastness.

Generally, solutions of the sulphates are used for colouring with nickel, cobalt, tin and copper. The former two metals operate at a pH of 3.5 to 5.5. Boric acid is added as a buffering agent and ammonium sulphate is added to increase conductivity. Typical concentrations are given in Table B.

Table B (66)

Colouring Solution	Composition (g/l)
1. Boric acid	25
Cobalt sulphate	20
Ammonium sulphate	15
2. Boric acid	30
Nickel sulphate	30
Ammonium sulphate	15
3. Copper sulphate	20
Sulphuric acid	7
4. Stannous sulphate	20
Sulphuric acid	20
Phenol sulphonic acid	20

Tin and copper electrolytes operate at the low pH range of 1 to 1.5. Colouring is carried out at ambient temperatures, current density ranges from 0.2 to 0.8A/dm² and a voltage of 5 to 25V. Colouring may be carried out for a fixed time at various voltages or vice versa. A fixed voltage is the more common procedure. In order to maintain consistent colouring, the voltage should be increased to the optimum at the same rate for each load.

Colour is dependent upon the length of colouring time and hence the amount of metal deposited. In the early

days it was thought that metal oxides were deposited (55), but it now seems certain that the deposits are metallic in nature (56). Tin electrolytes give a light champagne colour at 1min colouring time, bronze after 5min and black after 10min. Similarly, length of time varies the colours for the other electrolytes. The colour is caused by light scattering of the metallic particles. Dark bronze and black tin finishes, and black copper finishes do not perform well in corrosion and abrasion tests due to the distribution of the metal in the pores. Scanning electron micrographs of cobalt and tin black finishes, Figs.13 and 14, show the position of the metal. Tin approaches the surface and has an irregular distribution. Cobalt is more compact and regular. For light to mid-bronze colours the difference is not as pronounced, although tin deposits tend to converge in places. X-ray energy dispersive analysis has been used to show the metal 'rods' and deposit-free regions between converging rods (57). The differences in metal distribution are thought to account for the differing film properties such as corrosion resistance. Where metal extends to the outer surface of the film, pitting occurs (58). These are areas of locally high conductivity, and corrosive media, such as that used in the acidified salt spray test, promote pit formation. Sheasby and Cooke (53) found no effect on abrasion results with a high tin content.

High admittance values have been found (53) for dark colours, and this was due to the combination of the high conductivity of the metal deposits and their position. Consequently, these films are more difficult to seal than

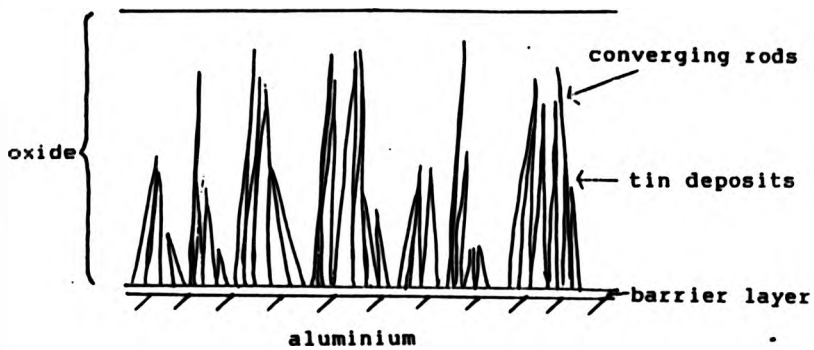


Fig. 13

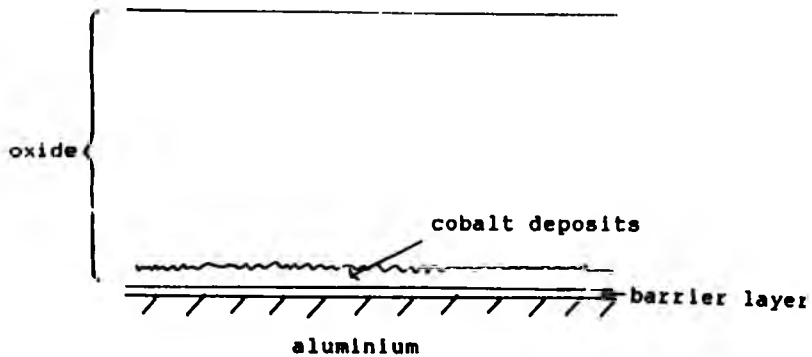


Fig. 14

films with metal confined to the pore bases. Furneaux (58) suggested that these potential pitting sites are dependent upon film thickness, but did not explain why. Presumably he referred to thick cobalt-containing films and implied that thin films would be susceptible to pitting if coloured for long periods. This 'over-colouring' has been found (59) to occur more in tin than cobalt finishes. Extended colouring times do not change the colour (although the tin may appear at the surface, imparting a grey colour), but film admittance continues to increase. Furneaux (58) has reported that it was possible to over-colour cobalt films when a non-uniform distribution was present. Depending on the metal ion and/or pH of the solution, differing amount of deposits are required to produce the black colour.

The pH affects the barrier layer during the a.c. treatment (58). It has been found that, for acidic electrolytes, processes involved in colouring are influenced by the magnitudes of the effective anodising and colouring voltages.

Doughty et al (60) showed that during a.c. anodising in acidic solutions (pH 1), the thickness of the barrier layer was determined by the applied voltage and was 1.1 nmV^{-1} , at peak voltage. When using sulphuric acid reanodising occurred beneath the original barrier layer (formed in oxalic acid) after a recovery period. It was suggested that there were three stages during electrolytic colouring. During the recovery period field-assisted dissolution proceeded until the barrier layer decreased to a value governed by the colouring voltage, when it was

lower than the forming voltage. Reanodising then took place. During the recovery period, new incipient pores formed, since dissolution and acid anion penetration predominated over oxidation, and barrier layer thinning occurred locally. This was due to the low field across the barrier layer and current was concentrated at certain areas, probably at pores whose bases had flaws. When colouring voltage was higher than the forming voltage, deposition occurred immediately and simultaneously barrier layer thickening took place. Metal oxidation was favoured by the field distribution across the original barrier layer (58).

The second stage was deposition of metal in the original pores during the cathodic half-cycle. Electronic conduction across the barrier layer was thought to occur by means of flaws which bridged the 'insulating' barrier layer between the porous film and the metal substrate. Alternatively, conduction may occur by electron tunneling or solid-state conduction.

Reanodising occurred on the anodic half-cycle. However, reanodising and deposition may interfere with each other since migration of solution species could be inhibited by the metal deposits (58). Doughty et al (60) gave evidence for the absence of acid anions in the reanodised layer, suggesting that these species were too large to pass the deposited metal. Similarly, solvated aluminium ions cannot pass out of the oxide layer. This assumes that the metal completely fills the pore diameter (33nm) and no spaces exist which are large enough to allow

solution species through. (Ionic radii of Sn^{4+} is 70 - 95pm, OH^- is 118 - 123pm and Al^{3+} is 53 - 67.5pm.)

No alterations of the barrier layer were thought to occur in neutral pH solutions (58), but Tachihara et al (61) showed that when the colouring voltage was higher than the forming voltage, barrier layer thickening occurred, as in acidic solutions. No significant thinning occurred due to the absence of an acidic medium. It was found that interfacial impedance of a.c. coloured films (using nickel sulphate and boric acid mixture) was larger than that of uncoloured films. They concluded that this was due to the new barrier layer growth. However, this information must not be confused with films coloured in tin baths, in which impedance values are lower than uncoloured films. The nickel-containing films were only coloured for 120sec. It was suggested that impedance values may be different for longer colouring times. The experiment was designed to show the presence of the new barrier and not the effect of the deposited metal.

A problem encountered in electrolytic colouring is spalling of the film from the basis metal; where the oxide coating flakes away. This can occur with all electrolytes. It had been found (59) that high colouring voltages or increasing the voltage too fast at the beginning of the colouring treatment, resulted in spalling. It tends to occur at lower voltages in nickel and cobalt electrolytes than in the more acidic ones. Spalling is possibly due to hydrogen evolution which competes with metal deposition on the cathodic half-cycle. Alternatively,

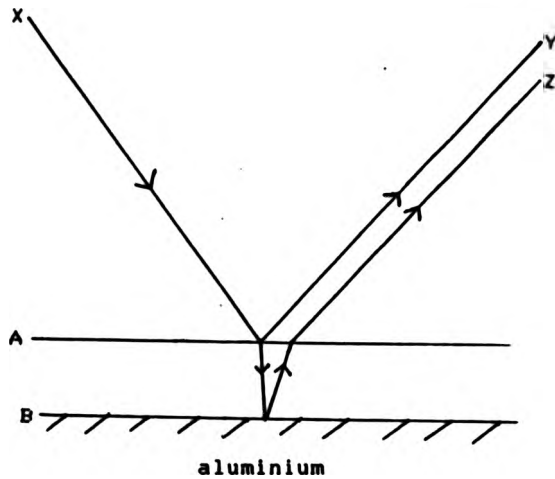
reanodising may form a less mechanically sound film beneath the original barrier layer. Balasubramanian and Shenoi (62) reviewed the use of chemical additions and pH control to limit the risk of spalling. Using counter-electrodes of the same metal as that to be deposited has proved beneficial. Double anodising was discussed which is covered in the next section.

2.3.5 Interference Colouring

Optical interference is the most recent advance in colouring anodised aluminium. The advantages over electrolytic colouring are that different colours can be obtained from one solution, and the amount of metal deposited is much less Fig.12. The drawback is that an intermediate stage is required between conventional anodising and colouring. This involves a second anodising stage where phosphoric acid is used to alter the pore dimensions in order to facilitate the formation of interference colours. Typical phosphoric acid concentration is 100 to 150g/l. This is used at 15 to 35°C for 2 to 10min at 10 to 40V. A.c. and d.c. conditions or a combination of them can be used. Conventional metal salt solutions of nickel, cobalt or tin are used for the electrolytic colouring stage. Instead of bronze shades, grey-blue, green-grey, yellow and reddish-purple are produced.

Anodising in phosphoric acid is the most important step in interference colouring (63). The pore bases are enlarged, Fig.12. Other electrolytes were found

to give similar results, but phosphoric acid was the most convenient. Sheasby et al (63) found that a deposit size of 29nm was required before interference effects were seen. The original pore size was found to be 14.6nm, Fig.9, smaller than the final pore size which was slightly enlarged throughout its pore length, approximately 20nm. The authors concluded that enlargement was greatest at the bottom $1\mu\text{m}$ and was caused by dissolution. Figs 12 and 9 show the difference in the size of the pores after phosphoric acid anodising and conventional sulphuric acid anodising respectively. These figures show the positions of the deposits. In interference colouring the deposits are confined to the pore bases. This creates a 'thin layer' effect. The distance between the deposited metal surface and the aluminium/oxide interface should be of the order of the wavelength of light. These two surfaces cause reflection and refraction, Fig.15. As more metal is deposited the distance between the two surfaces increases, changing the interference colours. Conventional bronzes are formed when the metal extends into the narrow part of the pore. Even if separation between the two surfaces was appropriate in electrolytic colouring, the deposit diameter would be too small to give interference colours. Not all pores are enlarged in the intermediate stage and bronze overtones may be detected. This bronzing effect increases as colouring proceeds. The authors also showed by electron microscopy that deposits in conventional electrocoloured films were very irregular in height, whereas those of interference films were compact and regular (63).



where X is beam of incidence light,
 Y and Z are reflected beams,
 A is surface of deposited metal,
 B is surface of aluminium substrate.

Constructive interference occurs at $n\lambda$
 when n is an odd integer and λ
 is the wavelength of light.

Destructive interference occurs when
 the optical path difference is $\frac{n\lambda}{2}$

Fig. 15

It was discovered (63) that brighter colours were produced in acidic colouring electrolytes. This was caused by film growth beneath the metal deposit layer Fig.12b. This was achieved during the electrolytic stage or in a post-colouring stage. By using an electrolyte of pH <2.5 for the former process, it was found that after a certain period of time, metal deposition ceased and anodising beneath the deposit layer began. However, conditions were critical to achieve this. As the depth of new oxide film was increased the whole spectrum of interference colours were produced; from blue through to red. Co-deposits of cobalt and nickel were found to be more acid resistant than single metal deposition. Transferring the coloured films to a post-anodising solution of sulphosalicylic acid, containing no colouring components, showed the new oxide growth.

Large scale laboratory tests have provided good colour reproducibility and uniformity for blue-grey interference finishes, and several buildings have architectural components coloured by this process (64).

The properties of these finishes are similar to electrolytically coloured films but they are not so abrasion resistant due to chemical dissolution during phosphoric acid anodising. Careful control is needed to enlarge the pores sufficiently but not to undermine the anodic film.

2.3.5 Combinations of Two Finishing Systems

The positions of the colouring components in the anodic oxide film are shown in Figs.9, 10 and 11. The distribution is different for each method and hence absorptive (or adsorptive) dyeing can be combined with integral or electrolytic colouring.

The electron microprobe has been used (44) to show the positions of the colouring components in the combination method of electrolytic/dye colouring. Speiser (44) concluded that electrolytic colouring does not obstruct dye absorption and the properties of the two processes remained independent. The author states that over dyeing with tin during the electrocolouring stage does not alter the amount of metal deposited, but others have shown that tin can extend to the outer surface of the oxide film (58, 59). This would inhibit absorption of dyestuffs. 'Over dyeing' would imply that a black colour was produced and subsequent absorptive dyeing would be redundant. Only light to mid bronzes would benefit from dyeing. The anodising and electrolytic colouring stages are carried out in accordance with BS1615:1987 and BS3987:1974. The dyeing step is carried out according to the 'Sandodal' system (44). A number of buildings have been built with architectural components coloured by the combination process 'Sandolor' (44), which performs well, although a Sandolor blue system installed 7 years ago is beginning to fade.

The quality of the sealed film was found to be the same as absorptive dyed finishes. Corrosion resistance

and weather resistance were unaffected by the underlying metal. Light fastness was found to be better than dyed films because light is not reflected from the basis metal. It is absorbed by the electrolytic layer and fading occurs only from the light incident directly on the external surface. There is no 'back reflection' which normally fades the dye from 'inside' the oxide film.

The disadvantage of this combination process is that although only one tank is required for the electrolytic stage, a number of tanks are required to hold the dyes. Alternatively the dyestuff may be applied by the spraying technique. The combination process must be carefully controlled to attain reproducible finishes. Caution is needed during the rinse between electrolytic and dyeing, since contamination of the latter bath by the metal salt would impair the dyeing ability.

By virtue of the colour component distribution, dyeing followed by electrolytic colouring is generally not possible. 'Sanodal Blue G' or 'Turquoise PLW' (44) may be used before electrolytic colouring, but these are affected by the acidity of the electrolytic colouring electrolyte.

Integrally coloured films have the colouring component included in the oxide film itself, leaving the pores open for adsorptive dyeing. Due to the difficulty in obtaining consistent thickness of $25\mu\text{m}$, there were differences in adsorption of dyestuffs and therefore light fastness. To overcome this the anodising temperature was varied in order to achieve consistent thicknesses (65). However, light/weather fastness tests showed losses of 5 to

25% of organic dye which were acceptable and corresponded to external weathering of approximately 10 years. Admittance values for integral/dyed coatings compared well with natural integral coatings, showing that the dye did not affect sealing quality. The chromic acid/phosphoric acid weight loss test showed results within the weight loss limit. There was no difference in corrosion tests between dyed integral colours and natural integral colours. It was found that the amount of dye adsorbed decreased with increased intensity of the integral colour. This was due to varying the anodising temperature and voltage in order to maintain a thickness of 25 μ m. As integral colours became darker, the number of pores per surface unit area and pore volume decreased. Integral/dyeing systems are based on the E.U.R.A.S. specifications. Various shades of gold and bronze with yellow, red, blue and turquoise overtones can be produced. These are not as bright as conventional adsorptive dyeing methods.

The disadvantages of this combination process are that the coating must be kept to a constant thickness in order to achieve reproducible results; different integral colour finishes have different dye adsorptive capacities and this too must be taken into account. The range of colours is almost identical to the electrolytic/ adsorptive dyeing systems, and as far as is known, the integral/dyed system has not been used commercially. The advantage is that only two stages are involved.

2.3.7 Colorimetry

The colour of pigmented anodic oxide films in most production plants is matched by eye. Not only is the visual appearance dependent upon the actual colour, but also on the texture of the finished surface and on the type of illuminant used. The eye is more versatile than any instrument because of its sensitivity to geometric factors such as rolling direction or die-lines, and etched or patterned surfaces. The consistency of these geometric factors is as important as the control of the colouring technique itself. However, evaluations by eye are subjective and variable with changes in viewing conditions and from observer to observer. Instruments are less flexible than the eye but they provide numerical quantities which are more repeatable and usually may be correlated with visual evaluations.

Instruments may be grouped into two categories: those which measure chromatic attributes, i.e. colour, and those defining geometric attributes, i.e. texture, gloss etc.(67). The former is due to selective absorption while the latter refers to the manner in which the incident light is distributed in various directions. Secondly instruments may give physical or psychophysical evaluations. Spectrophotometers are physical analysis instruments, while colorimeters are psychophysical analysis instruments which give measurements that correlate with the human eye-brain impressions. Every instrument incorporates both chromatic and geometric factors to some extent, but

for that which measures colour, spectral properties are the most important.

Metals with diffusing metal oxides such as anodised aluminium are considered as opaque objects where colour is seen by diffuse reflection. An instrument which may be used to measure the colour of such a surface is the Sheen Miniature Colorimeter. This has a light source, a place for the object to be observed and a photoelectric light receiver. A collimated beam, which has been passed through a narrow band colour filter, falls on the surface at an angle of incidence of 45° . Any specularly reflected light is absorbed on the black wall of the colour head. A photoelectric cell, with an area considerably larger than the illuminated area, is placed normal to the surface, and detects light diffused over a range of angles on either side of the normal. The main components of light diffused in the directions in which coloured finishes are observed by eye are measured, but those at low glancing angles are not. The reflectance of the instrument is calibrated against black velvet (0% reflectance) and a block of white magnesium carbonate (100% reflectance). The reflectance of the panel is measured at six wavelengths using six C.I.E. (Commission Internationale de L'eclairage) colour filters: $660\mu\text{m}$ (red), $610\mu\text{m}$ (orange), $570\mu\text{m}$ (yellow), $520\mu\text{m}$ (green), $480\mu\text{m}$ (blue), $450\mu\text{m}$ (violet). The instrument is calibrated after each reading, for each colour. The factors which affect the appearance of anodised aluminium on which the anodic oxide is coloured are more complex than those affecting painted surfaces. This is because the coloured

anodic oxide is transparent, and both its own surface and that of the metal beneath diffuse light which contributes to the appearance. The metal surface is almost always anisotropic, which causes the appearance to vary quite markedly with the directions of incidence of light and that from which the surface is viewed.

Both sheet and extruded alloys, when etched, develop textures whose appearance differs with direction. The limits of high and low reflectivity are usually found in the directions parallel to and normal to the directions in which sheet was rolled, or extruded alloys passed through the die. Both gloss and colour reflectances vary between limits corresponding to the incidence of illumination parallel to and normal to the rolling or extrusion directions. The simplest characterisation of anodised aluminium therefore requires two measurements to be made at each wavelength, parallel to, and normal to the texture axes of the metal.

The colour can be represented as a graph of percentage reflectance against wavelength; the spectral reflectivity curve. It can also be characterised by numerical values, the chromaticity co-ordinates, and can be presented in terms of the C.I.E. colour triangle, Fig. 16 (6B). The co-ordinates are evaluated from equations involving the reflectivities at $660\mu\text{m}$, $520\mu\text{m}$ and $480\mu\text{m}$, the X, Y, Z tristimulus values. [A spectrophotometer measures the percentage reflectance from the object only, while a colorimeter takes into account the illuminant and observer also. The readings given by a colorimeter are actually the

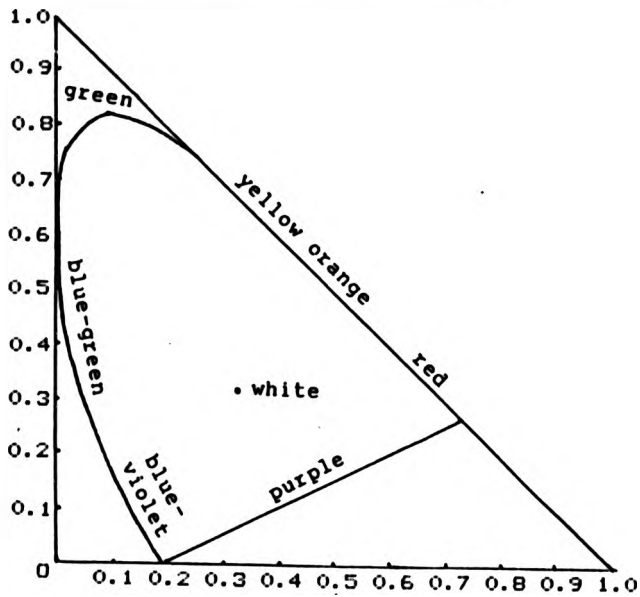


Fig. 16 (68)

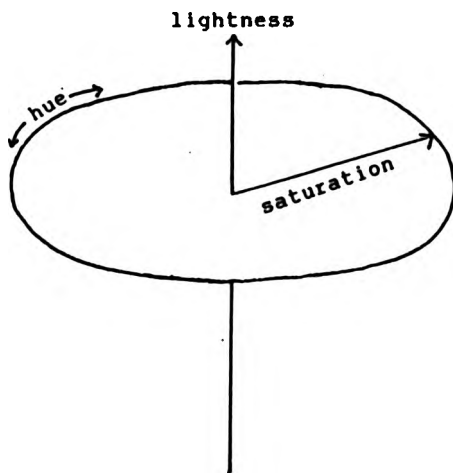


Fig. 17

X, Y, Z integrals. A spectral curve can be plotted from the colorimeter values since it is the same shape as that produced by readings taken from a spectrophotometer, except that the values are evaluated in different ways (67).]

Colour can be considered to be a vector whose components are lightness, hue and saturation, Fig.17 (67). The hue is usually referred to as the colour. Saturation is where colours of the same hue differ in the depth of colour. While the tristimulus value Y correlates with lightness or the luminance, X and Z do not correlate with hue, saturation, or any visually meaningful attribute of colour appearance. Chromaticity co-ordinates are defined as:

$$x = \frac{X}{X + Y + Z} \quad y = \frac{Y}{X + Y + Z} \quad z = \frac{Z}{X + Y + Z}$$

Alone x, y and z do not correlate with any attribute of colour, but when incorporated into the C.I.E colour triangle the relationships of the co-ordinates are established.

The colour triangle is not uniform in the spacing of colours; the relative sizes of differences between colours on the diagram do not correspond to the sizes of the differences sensed by the eye. Therefore attempts have been made to develop uniform colour scales on which measured values of colour were more easily related to visual attributes of colour. The C.I.E. L,a,b (opponent-colours) colour solid is one such uniform scale

(67). This is derived from the tristimulus values. L is lightness, a is redness-greenness and b is yellowness-blueness. L,a,b can be regarded as combining to form a vector in rectangular co-ordinates. Two different colours may have the difference expressed as ΔE from the equation:

$$\Delta E = \sqrt{(\Delta L)^2 + (\Delta a)^2 + (\Delta b)^2}$$

This is the difference between $L_0 a_0 b_0$ and $L_1 a_1 b_1$ in Fig. 18 i.e. $\Delta L \Delta a \Delta b$ is the difference between the co-ordinates of each of the two points. This gives only the size of the difference and not the direction or nature of the difference from the reference colour. Hence it is more advantageous to record L, a, b and ΔE values in order to assess colour difference in a 3-dimensional representation, Fig.18 (67).

The C.I.E. Y, x, y scale can be applied to all stimuli, but the C.I.E. L, a, b scale is used for opaque diffuse objects. All scales are based on visual units of colour perception and relate to perceived colour and colour differences. Two colours that can be differentiated visually can be represented quantitatively by the measured value difference. If all production stages, including colour quality control are under strict processing conditions, the anodised coating will not only look good initially, but withstand many years of service although fading may occur in certain circumstances.

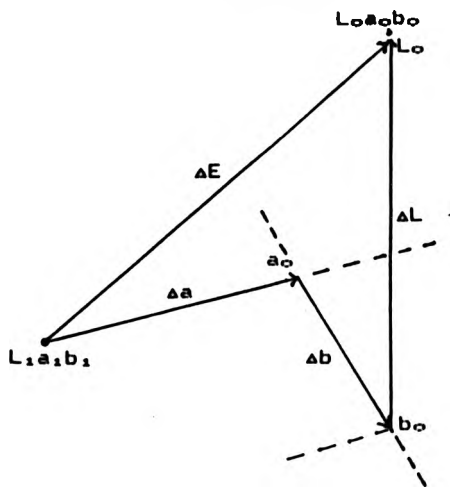


Fig. 18 (67)

2.4 Sealing

2.4.1 Introduction to Sealing

The porous nature of anodised aluminium allows it to be coloured by a number of processes. If no further treatments are used after colouring there remains the propensity for media to penetrate the pores. If the media are corrosive the oxide film will be undermined. The need arises to block or close the pores in order to minimise corrosion and to halt the potential degradation of colouring components. Generally, it has been observed that the longer anodised films are left exposed to the atmosphere, the more difficult it becomes to colour them. This was attributed to an irreversible reaction between the oxide and water vapour in the air, resulting in a decreased porosity. It was suggested that the anhydrous oxide became hydrated to form boehmite crystals, $AlO.OH$ or $Al_2O_3.H_2O$. This process is accelerated at high temperatures i.e. immersion in solutions above $90^\circ C$ or suspension over steam.



At lower temperatures another crystalline form, bayerite, is produced, $Al(OH)_3$ or $Al_2O_3.3H_2O$, which does not seal the pores as well as boehmite.



Sealing is carried out in deionised or demineralised water to minimise the deleterious effects of calcium and magnesium, silicates and phosphates. The exact mechanism of sealing has been the subject of much debate. With improved analytical techniques in recent years, experimental evidence has thrown more light on the mechanisms involved.

Sealing is also performed in water containing chemical additives such as nickel salts (acetate, sulphate or nitrate), ammonium acetate, triethanolamine, dichromate solutions and sodium silicate. In nickel salt sealing the mechanisms are different from those of hydrothermal sealing, although hydration still occurs with high temperatures. The additives augment the sealing process by forming 'plugs' inside the pores. Dichromate sealing is also a combination of two processes; the absorption of chromate ions plus hydration. Sodium silicate is the least used solution. It also seals by forming plugs of aluminium silicate, but it is known that the presence of silicate inhibits hydration. This renders the process less attractive than the other pore plugging solutions.

Cold sealing or impregnation processes are currently under development and investigation, but they are a more recent advance and there is little public information on the pore closure mechanisms or performance in service. Many operate below 60°C and hydration is unlikely to occur to any significant extent. Pore plugging takes place by precipitation of salts.

Another form of sealing is 'physical' sealing where coatings such as oils, waxes or lacquers are applied

to the oxide film. There is no chemical participation of these substances i.e. they do not react with the oxide but impart a superficial layer on the surface. They may also 'impregnate' the pores. These and other organic sealants are used only for specialised purposes; where surface phenomena are more important than the inherent properties of the oxide layer. Waxes and oils are often applied after sealing as a temporary barrier to alkaline media used during building construction.

2.4.2 Hydrothermal Sealing Mechanisms

The simplest explanation for the sealing mechanism is the hydration of alumina Al_2O_3 , to give boehmite $AlO.OH$. This compound closes the pore due to the volume expansion within them. But the mechanism is more complex than this and a number of theories exist.

Bernard and Randall (69) suggested that the hydrated product formed, when aluminium metal reacted with boiling water, was the same as that formed on barrier layers in boiling water. The rate of hydration of the oxide film and the rate of formation of the product on aluminium were similar. They concluded that the mechanisms must be the same. The assumptions were only based on rates and X-ray diffraction patterns which were similar in both cases. It is fair to say that although a compound similar to boehmite was found in both instances, which has since been proved, the mechanisms of formation were not substantiated.

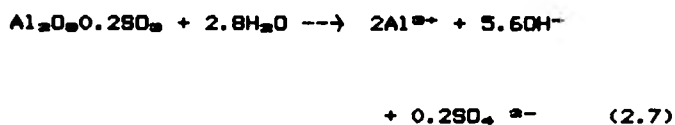
Ginsberg and Wefers (70) examined films formed on aluminium by water and steam. They called the products 'hydroxide films' since nomenclature had not been well defined. Only a small proportion of film material was crystalline, and this was found to be bayerite when aluminium was reacted with pressurised steam below 150°C. Above this temperature boehmite was formed. The admission by the authors that only a small amount of hydrated material was crystalline suggested that some other amorphous compound dominated the hydrated layer. In a subsequent paper Ginsberg and Wefers (71) described needle-shaped crystallites which grew normal to the 'fibre bundles' of the anodic oxide. These bundles consisted of γ -boehmite which grew inwards from the surface. This formed due to movement of hydroxyl ions through the lattice under a field. The field was caused by the diffusion of hydrogen ions through the film. Spooner and Forsyth (72) showed by means of X-ray spectroscopy that sealing proceeded inwards. Although a boehmite structure was formed, it was not identical to $Al_2O_3 \cdot H_2O$ and had previously (69) been found to contain stoichiometrically more water.

In 1969 O'Sullivan, Hockey and Wood (73) studied unsealed and sealed films by infra-red spectroscopy. They too concluded that although the boehmite was found for films examined at ambient temperatures, no positive identification of all hydrated species could be made. It was not possible to calculate the precise amount of molecular water retained within the films, although this had been estimated previously (72). The stretching

vibration of water enhanced one particular absorption band, and this was the characteristic band of boehmite and bayerite. These crystals were in the minority since this absorption band changed little. Crystal growth tended to occur mainly at the pore mouths and although the evidence showed that after a sealing time of 24 hours, the whole pore had been sealed, the material was of an undefined form. Initially a 'plug' formed at the surface, but eventually the whole pore sealed by agglomeration of the amorphous anhydrous alumina crystallites. Deuteron exchange of the accessible hydroxyl groups was progressively retarded as sealing proceeded, indicating that these groups had become 'locked' in the structure. Electron micrographs (74) clearly showed the changes which occurred to the porous structure. As sealing progressed the more difficult it became to define the pore walls as they became filled with precipitated sealing material.

Pseudoboehmite was proposed by Vedder and Vermilyea (75) to be the crystalline material. This has the formula $Al_2O_3 \cdot nH_2O$ where n is between 1.5 and 2.5. It is like boehmite but with an excess of crystalline water. These molecules were chemically bound to the large surface area of the crystallites.

Wefers (76) described a detailed mechanism for sealing in which water penetrated the pores and pore walls, and dissolved the oxide, liberating the anion SO_4^{2-} from sulphuric acid films. Reprecipitation occurred forming pseudoboehmite which crystallised and sealed the pore mouths. The equation for this reaction is:



The mobilization of the SO_4^{2-} ions by dissolution decreased the pH at the oxide/liquid interface and hydrated aluminium oxide reprecipitated on the pore walls and at the pore mouths. This ion exchange mechanism was not applicable to oxides formed in solutions such as chromic acid where the anion content was low (77). Chromate or dichromate ions were not as readily absorbed by the film as sulphate ions, and it was thought that the chromium was incorporated as dichromate rather than chromate ions which accounted for the small amount. It was at the oxide/liquid interface that protons, set free by hydrolysis of the alumina, were removed by diffusion. Fig. 19 (78) shows how this occurred, releasing water in a condensation reaction at a later stage of the process. Initially, a solid formed rapidly at the surface of the film. The hydrated alumina first precipitated as a hydroxide gel and as the pH decreased, crystalline boehmite formed. Condensation gradually slowed to leave small crystallites which contained excess amounts of bound water. Some of the condensed water progressed inwards down the pores which continued to seal inwardly. A 'glaze' layer (78), also known as an intermediate layer, was formed just beneath the exterior surface of the oxide, Fig. 20 (78). Some of the reprecipitated hydrated alumina diffused through to the surface and formed a sealing smut.

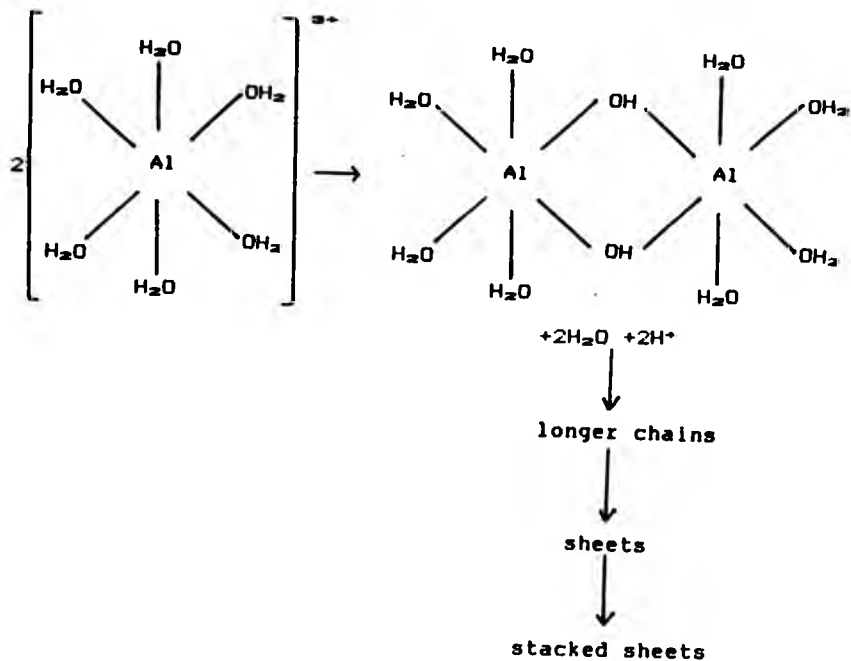


Fig. 19 (78)

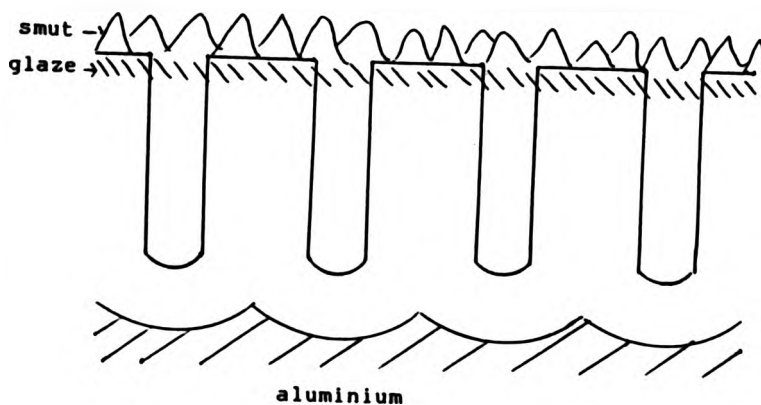


Fig. 20 (78)

This was in a different form to that of the glaze layer and was found above it on the exterior of the oxide layer, Fig. 20. It was concluded that the amount of water taken up was one pore volume before this protective glaze layer formed. Subsequently, water had to diffuse through this layer. This can therefore be described as a diffusion mechanism rather than an ion exchange mechanism. The thickness of the glaze layer increased with sealing time at a rate that increased with solution temperature and decreasing acidity. Under certain conditions it was found that the glaze layer could penetrate to the basis metal. However, under normal sealing times it was usually $<1\mu\text{m}$ thick.

The most recent theory is by Thompson and Wood (79). They described a dissolution/precipitation process which is comparable to that of Wefers (76). Thompson and Wood found that the hydrated alumina within the pores did not exhibit well defined crystallinity, while that formed on the outer surface did, giving a 'needle-like' structure. The glaze layer, of undefined morphology, developed beneath these surface crystallites. Large particles agglomerated by the dissolution/precipitation process in preference to small ones over a period of time. This is now known to be the ageing process. The hydroxyl ion content increased because the molecular water was trapped beneath the forming solid. The microcrystallite surfaces played a role in forming these hydroxyl ions. Acid anions were intrinsic in the sealing process and sealing occurred at different rates for films formed in different acids.

2.4.3 Practical Aspects of Sealing

Operating considerations for water sealing must be carefully followed. All work must be rinsed thoroughly before sealing to avoid contaminating the seal bath since contaminants affect the sealing quality. Ideally there should be two rinsing stages followed by a soak time. Sealing tanks may have lids or floating polypropylene spheres to reduce evaporation. The tanks should be insulated to avoid heat loss. The sealing solution is agitated by means of its convection currents.

The ideal sealing temperature is between 98 to 100°C. Below 90°C the sealing rate is reduced, and at 95°C the sealing tests may be passed but the rate of sealing is slower than at 98°C. Specialised thermostats are required to maintain the temperature just below 100°C since this gives the most efficient use of energy. The introduction of large amounts of metal reduces the temperature locally and this must be accounted for in the bath heat input.

The longer the work is sealed, the less weight loss there is in sealing assessment tests. The sealing is adequate if the weight loss is less than 2g/m² using the Kape test or 3g/m² using the phosphoric acid/chromic acid test. In the United Kingdom a sealing time of 2min/μm is considered to be adequate. Elsewhere 3 or 4min/μm are required. The important factor is that the work should pass the acceptance tests. Oversealing (sealing for long periods) has no advantage over adequate times and is inefficient. Although admittance test values may be

favourable for long sealing times, it is at the expense of weather resistance of the film due to increased softness. It is known that unsealed films have a higher abrasion resistance than sealed films.

The pH of the sealing solution is important and a range between 5.5 and 7.0 can be recommended. Two common ranges are 5.6 to 5.8 and 6.4 to 6.6 (80). If the pH exceeds a value of 7.0 the coating may be attacked by the sealing solution, and below 5.4 the sealing quality is poor. Sealing solutions tend to become acid in use due to the drag-in of anodising electrolytes. This may be counteracted by additions of ammonia or caustic soda. It is advisable to buffer the sealing bath against pH changes by adding 1g/l ammonium acetate. If the pH should rise, it can be corrected by adding acetic acid.

As with dyeing, mains water should be avoided since it contains impurities. The demineralised water may become contaminated and the effect of these impurities has been reviewed (81). Table 9 gives some common contaminants. However, different testing methods define different tolerances. The silica tolerance is so low that it must be kept in check. It has been found to be pH dependent and the largest effects occur below < pH 6.0. Admittance tests fail to detect poor sealing due to the presence of silica or phosphate ions. Phosphate is also known to inhibit sealing. Films grown in phosphoric acid have inherent phosphate ions and despite having large pores (compared to sulphuric acid films), which might be expected to hydrate more readily, these films seal only after prolonged

treatments (B2). These species inhibit sealing because they form strong bonds with the surfaces of the pore walls. Dissolution of the oxide and incorporated anions is therefore more difficult and reprecipitation is inhibited.

Table 9 (B1)

Contaminant	Maximum tolerance mg/l
PO_4^{3-}	5
SiO_2	10
F^- (Although NaF has been found	5
Cl^- to be harmless at 50mg/l, and Cl^- at 400mg/l.)	100
Cu^{2+} } Fe^{2+} }	detrimental to sealing
Ca^{2+} (It has been found that refluxing with $CaCO_3$ deteriorated the solution.)	

Crazing of the anodic film is an unwanted side effect which occurs due to a difference in the coefficient of thermal expansion between the metal and the oxide. This can be avoided by heating the work by holding it over a small amount of steam before immersing in the sealing solution. Crazing can be reduced if the aluminium is etched to produce a rough surface. This breaks up the stresses in the film, as does a fine particle distribution.

2.4.4 Steam Sealing

Sealing in steam, often at high pressures is an alternative to sealing in boiling water. The advantage is that steam and vapour are unlikely to contain contaminants such as calcium or silicates. The condensed steam is in effect distilled water. The disadvantages are that it is difficult to operate and expensive. Large batches of work are needed to fill the steam chamber in order to make the process efficient. An inverted chamber is required to prevent loss of steam upon removal of the work. The chamber must be air-tight to ensure a positive pressure of steam. Additives or pH monitoring and/or adjustments are very difficult to make. As the steam condenses on the work it may cause streaking of dyed films, although bleeding occurs less. Rinsing the work is essential since any trapped solution would not be diluted to the same extent as in a volume of water; the trapped solutions would be washed away slowly, possibly affecting the surfaces with which they came into contact.

Generally, steam sealing is as good as water sealing and the choice is based on cost and operating efficiency. The best operating conditions are that the steam must be damp and at a positive pressure to give a temperature of 110°C (83).

Vapour sealing (84) uses 50/50 water and, either trichloroethylene or perchloroethylene and has been used in a vapour degreasing-type of operation. This operates at below 100°C.

2.4.5 Sealing Bloom

Sealing bloom or smut is a loose, precipitated powder found on the exterior of the porous oxide and is formed by hydrated alumina diffusing to the surface during hydrothermal sealing, Fig. 20 (78). It is the order of wavelength thickness and differs from the sealed oxide since it dissolves in acid and is not abrasion resistant. It appears as a white iridescent coating; not to be confused with the bloom formed from weathering. The bloom is considered a nuisance, particularly on coloured finishes. The smut is not touch-resistant and picks up dirt and grease easily. There are two solutions to this problem: removal and prevention. Originally the bloom was removed by buffing with pumice powder, or a wax emulsion was applied to mask it. Due to the degradation of these waxes with time, the bloom reappeared later. Buffing is very labour intensive, and although waxing is quicker, it too takes considerable manpower. Another method of removal is by dipping in 30%/vol nitric acid at 20 to 30°C for 10min (85). It should be ensured that the work is well sealed (indicated by the formation of the bloom!) so that the acid does not attack the film.

The bloom can be prevented by stopping the sealing reaction just before the bloom forms. This practice must be approached with caution because the absence of bloom may mean inferior sealing. The most common form of prevention is to include additives in the sealing solution.

These inhibit bloom formation but must be carefully controlled since if the levels rise, they may also inhibit the sealing reaction itself.

Nickel acetate was one of the first solutions to be used which facilitated easier removal of the bloom. The porous coating is sealed with nickel hydroxide which still forms a bloom, but this is more easily dissolved in nitric acid (86) than the bloom formed in water. This process was modified further to include dispersing agents which reduced the amount of nickel hydroxide and boehmite deposits, but did not eliminate them totally.

Another approach was to use organic chemicals which completely prevented smut formation. The difficulty with this was that the sealing reaction and smut formation result from the same chemical reaction. The chemicals must be specifically tailored to prevent formation of bloom on the surface while allowing boehmite formation within the pores.

Although phosphate is known to inhibit the sealing reaction, it can be used as a smut preventative in concentrations of 3 to 10 parts per million (ppm) (87). The concentration must be monitored carefully. Phosphoric acid is also used (86), but some phosphate is always present and the concentration limits are soon reached. Polyhydroxycarboxylates give a better finish than phosphoric acid, and these together with phosphonates are the most widely used additives at present (86). Polyhydroxycarboxylates have low sensitivities to metal ions and acids, and give the clearest surface finish.

Two other classes of organic compounds used are polycarboxylates and polyhydroxys. The former class is precipitated by acids and heavy metal ions, but they give good dye spot test results. Polyhydroxys also perform well in this test, but they are thermally unstable, and tend to foam (85).

Additive concentrations are usually 1 to 2ml/l or g/l, and solution temperature, pH and sealing time are the same as for conventional sealing. Anti-smut additives have stringent characteristics. They must not affect the performance of the sealing solution, even when the concentration is inadvertently high. There must be no discoloration of the film during sealing or weathering. They must be soluble in water and leave no residues on the surface of the oxide. They must not make the sealing solution sensitive to metal ions such as aluminium, calcium, tin, nickel or cobalt, and they must be thermally stable. The anti-smut additives must not affect the results of sealing tests, particularly the admittance test, dye spot test and weight loss test. The first is governed by the filled pore and so any additive which affects sealing as a whole will give poor results. The latter two tests are not only governed by the filled pores but also by surface phenomena. Therefore if an additive prevents bloom by attaching itself to the surface, then this will affect the dye spot test. It is necessary to perform as many tests as possible in view of these facts. It follows that the anti-smut additive must be restricted to the surface of the oxide film so as not to modify the pore filling material.

This can be controlled by increasing the molecular size so that it cannot enter the pores. Gohausen and Shoener (86) proposed that smut is actually suppressed rather than masked by the additives. They put forward the theory of the 'threshold effect'. The additive, in very small non-stoichiometric concentrations, prevents the formation of crystalline compounds. This is shown in Fig. 21 (86), where the anti-smut agent is adsorbed onto the growth centres of the crystal nuclei and prevents further growth. Obviously, the anti-smut agent must fit correctly in order to prevent crystal growth, and therefore different agents will give different degrees of smut prevention. These agents act immediately at the start of smut growth, and so are only needed in small amounts. It can be seen that these additives affect the surface phenomena and react with the dye stain molecules to give various results for different additives.

It is difficult to apply additives to steam seals since it is only condensed water which comes into contact with the oxide surface. A pre-seal may be used where the work is immersed in a solution containing an anti-smut agent. It is subsequently sealed in steam. The smut preventative may be washed off by the condensing steam to leave a patchy surface.

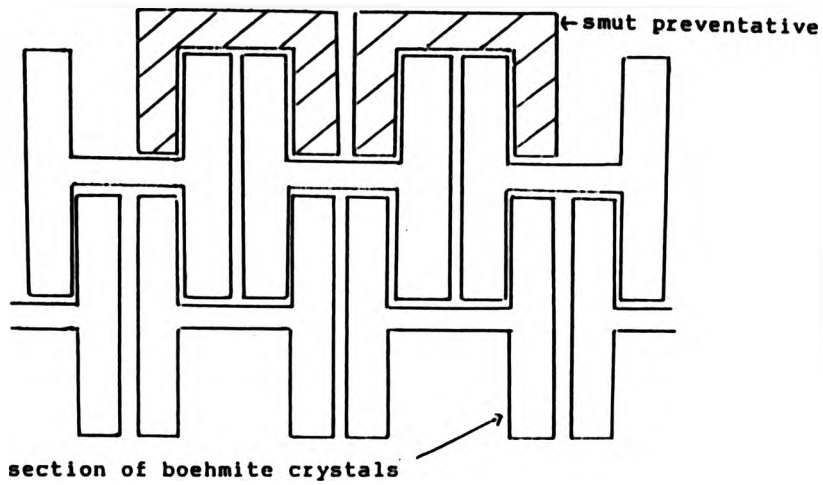


Fig. 21 (86)
schematic representation

2.4.6 Sealing Bath Additives

These additives augment the hydration reaction by co-precipitation of metal salts in the pores. The most common sealing solution is that containing nickel salts, usually the acetate. Nickel hydroxide is co-precipitated along with the hydration reaction to 'plug' the pores. Hoar and Wood (88) suggested that the pores closed by successive stages of inward movement of sealing material. The pore mouth was also closed. The mechanism proposed was an 'advanced proton' model for the transport of OH^- ions and other anions through the oxide. The H^+ ion moves readily between O^{2-} ions and after formation of OH^- ions in the surface layer, the OH^- ions thermally dissociate and H^+ ions move by thermal diffusion into the second O^{2-} layer. This movement of protons attracts anions such as OH^- ions present in the nickel acetate solution. This is caused by a high electrostatic field. This high field stops thermal diffusion of OH^- ions.

Nickel acetate can also be used in conjunction with cobalt acetate. Typical concentrations and conditions are given in Table 10.

Table 10

Nickel acetate	5-5.8g/l	15 to 20 min, 70 - 90°C, pH 5 - 6 (optimum).
Cobalt acetate	1.0g/l	
Boric acid	8-8.4g/l	

The boric acid acts as a buffer. Nickel acetate can either be used as a pre-seal solution followed by immersion in boiling water, or used near to the boiling point itself, usually containing smut inhibitors. Control of smut inhibitors is necessary since the nickel hydroxide bloom becomes heavy if left unchecked. Smut inhibitors may act by the 'threshold effect' or they may act as dispersants for the hydroxide or be more specific than this (89).

Advantages of nickel salt seals are that they are less sensitive to bath contaminants than deionised water. Phosphate and silicate are precipitated as insoluble nickel salts, and are rendered harmless to the sealing mechanism. The precipitated nickel hydroxide inhibits staining, increases the resistance to alkaline media and increases the lightfastness of some dyes. Certain dyes, Golden Orange RLW, Orange GL, Red GLW and Red RLW are less lightfast and tend to bleed in the solution. Those which do benefit are Bordeaux RL, Bronze G and Black LL (90). The precipitation of the salts prevents bleeding and they may also react with the nickel and/or cobalt to form a new metal complex. The dye can be said to be 'fixed' by the seal.

Generally coatings sealed by these methods show inferior corrosion-resistance compared to water sealed coatings. Bloom can appear on long term exposure as a result of weathering combined with the re-emergence of hydroxide deposits (91).

More nickel salt solution is retained in the pores of films which have been anodised at high temperatures. This is due to the 'funnel' shape of the

pores created by the greater acid dissolution of the exterior surface at the high temperatures.

2.4.7 Dichromate and Other Sealing Solutions

Corrosion resistance of anodised aluminium can be improved by sealing in a solution of chromate/dichromate. Typical concentrations for highest corrosion resistance are given in Table 11.

Table 11 (92 and 94)

Sodium dichromate	70 - 100g/l	
Sodium carbonate	18g/l	2 to 4 min or
or Sodium hydroxide	13g/l	up to 10 min.
pH	6.3 - 7.4	
Temperature not less than	96°C	
Potassium dichromate	15g/l	
Sodium carbonate	4g/l	2 to 4 min or
or Sodium hydroxide	3g/l	up to 10 min.
pH	6.5 - 7.5	
Temperature	90 - 95°C	

As with nickel salt seals the mechanism of sealing includes incorporation of metal ions and hydration. Chromate is absorbed at low pH and the hydration process which closes the pores and traps the CrO_4^{2-} ions occurs at an optimum pH greater than 6.0. With increasing pH the chromium uptake decreases while pore closure increases. Chromium uptake is greater at the pore mouths and is due to slower pore closure at low pH allowing more solution to enter the pores. It was noted by Hoar and Wood (88) that the initially slow sealing rate of dichromate solution increased with time, probably due to chromate exchanging with O^{2-} in the film. This increased the pH. For reduced chromate consumption the concentrations in Table 11 are used.

The corrosion resistance is a function of the hydration reaction and the resistance of the absorbed chromate to leaching. The type of exposure to the atmosphere is more important than the pH is to the degree of leaching. The absorbed chromate gives the film a distinct yellow coloration, and this limits the use of this process to work where colour is of little importance.

An important addition to deionised water is ammonium acetate. This acts as a buffer and does not alter the hydration mechanism. It buffers the solution against pH fluctuations which can be caused by drag-in of acid. It has been found (93) that this solution is slightly more tolerant of phosphate and silicate than pure deionised water.

2.4.8 Impregnation of the Anodic Oxide Film

The mechanism involves 'pore plugging' rather than hydration. This is due to the low temperatures used. Water does play an important part in a condensation or 'ageing' process at ambient temperatures which is a post-treatment reaction. Both aqueous and alcohol-water solutions are used which contain silica or fluorides which are precipitated out to plug the pores. Sacchi (95) described the impregnation mechanism. The 'plug', at the mouth of the pore, forms more slowly than that formed during high temperature hydrothermal sealing. During the latter process, once the pore mouth has been closed, the remainder of the pore is sealed by a 'condensation' mechanism with a reduction of free energy. Partially sealed films become well sealed upon ageing. This is more pronounced in nickel salt sealed films. The presence of nickel prevents the deleterious effects of contaminants. If the mouths were to remain open for longer, the sealing inside the pore would be more complete. This is the aim of impregnation. Admittance tests are not passed until a few hours after impregnation. This result improves after days and weeks. This is an analogous situation to partially sealed hydrothermal films. Hoar and Wood (88) showed by impedance measurements that a short plug of semi-solid material probably formed. The absence of a sufficient surface plug allows a high conductance and lower electrical capacity. This allows the ageing process to proceed and eventually the film becomes well sealed. The disadvantage

of impregnation is that sealing quality cannot be checked immediately after sealing. Good admittance test results have been achieved immediately after production by accelerating the ageing process by means of a hot water treatment, but this negates the supposed advantage of 'cold sealing' of saving energy.

2.5 Sealing Smut, Weathering Bloom and Pitting of the Anodic Oxide Film

2.5.1 Introduction

Sealing smut, or bloom, is a fairly soft, powdery precipitate (by comparison with the normal film) which is formed on the surface of the oxide during sealing. This bloom is reprecipitated hydrated alumina (boehmite), which diffuses to the coating surface. Once removed by abrasive cleaning with pumice, sealing bloom does not return, and the coated article is ready to be used in architectural construction. Providing the oxide film quality meets certain specifications, then it should perform well for many years, with appropriate periodic cleaning. However, if the specifications have not been met or the anodising process conditions are not correct, the work may suffer various forms of deterioration. A disfiguring bloom may form which is different to that formed during sealing. It cannot be permanently removed by cleaning. Initially, cleaning may improve the appearance, but the bloom often

returns. This bloom is the result of physical degradation of the structure of the film caused by weathering and chemical attack. The most significant factors which influence the resistance to deterioration are the sealing quality, the anodic oxide coating thickness and the abrasion resistance.

Weathering bloom, also known as 'chalking', (96) can be described as cracking and flaking of the surface of the film. It is associated with chemical attack by acidic or alkaline media. In the environment it is usually caused by sulphur dioxide gas which forms sulphurous acid in solution. The basis metal is not affected by this form of degradation. The effects of weathering can have other adverse consequences on the anodic film: iridescence, irregular bloom within the film rather than 'chalk' on the surface, and pitting corrosion. Coloured films can come under attack. Bloom or iridescence can affect the colour. Fading of dyes is accelerated by inadequate sealing.

Iridescence can be seen most clearly on dark coloured films, but it can be observed also on 'natural' colours. It is caused by interference effects within thin layers of translucent bloom. This initial stage of weathering is often a precursor to the more obvious bloom. The iridescence can be removed by cleaning although this is very expensive.

International Standards only recognise two forms of superficial weathering: 'chalking', which is a powdery surface deposit, and 'weathering bloom', which is a whitening of the film caused by mild chemical attack.

However, Furneaux (97) distinguished four different types of degradation due to outdoor exposure, and ascertained whether particular anodising and sealing methods influenced the type of degradation observed.

1. 'Chalking' was found to occur on 'soft' films which had been produced in aggressive electrolytes, or anodised at high temperatures, or where work was immersed in the electrolyte for long periods. Chalking was caused by flaking of the oxide film and was bound up with a water loss-gain cycle which may have affected the intermediate layer. This layer has been found to be thicker than $5\mu\text{m}$ in soft films, whereas normally it is less than $1\mu\text{m}$.

2. Weathering bloom (not that caused by chalking) was associated with poor sealing. Gross surface etching occurred where cell boundaries had been preferentially attacked producing thin surface layers of different refractive indices. This gave heavy bloom, while light matting was associated with attack of the cellular structure. Both types of weathering probably occur after the iridescent layer, or regions susceptible to resmutting, have been lost.

3. 'Resmutting' occurred during weathering when an anti-smut agent was used during sealing. This agent decreased the formation of sealing smut. Any smut which formed was easier to remove. It was thought that no intermediate layer was formed when additives have been

used. It was concluded that resmutting was a surface etching together with some precipitation of basic aluminium sulphate. This attack was thought to be localised because anti-smut additives inhibit sealing at the pore mouths. Similarly, when additives have not been used, resmutting can occur once the iridescent layer has been weathered away.

4. Iridescence occurred on well-sealed films when cleaning had not been sufficient to remove the sealing smut and the intermediate layer. It was the latter layer which caused the interference effects.

The last form of attack is pitting corrosion (96). This is not as dependent upon sealing quality as upon alloy type and film thickness. Pitting is a very localised form of attack, usually associated with defect sites such as flaws in the basis metal. Pitting declines with an increase in the purity of the aluminium and is associated with intermetallic constituents. It is a long-term form of degradation and although a film may be well sealed, pitting can eventually undermine the oxide coat.

2.5.2 Assessments Tests

The need to prevent deterioration of the appearance of the finish of the anodic oxide is of the utmost importance. Mill finished aluminium is sufficiently corrosion resistant for buildings but soon looks unattractive. The cost of anodising or painting is entirely

to retain a good appearance, hence any loss of aesthetics is a fault even when corrosion is not serious. To ensure a good appearance, every aspect of anodising must be considered: alloy composition and microstructure, surface topography, pretreatments, anodising process variables, colouring and sealing processes together with coating properties, fabrication and installation, and environmental conditions. Each of the conditions of any of these stages may be changed to impart a different affect on the oxide film. Changes may be advantageous or detrimental, and it is the skill of the anodiser to achieve the optimum conditions for the film that is required.

Anodic oxide film properties need to be assessed in routine production control to maintain standards laid down. This is done by assessment tests, which indicate how the anodic film will perform 'in service'. Performance can be judged from these tests in most cases, but information from short term 'accelerated corrosion tests' and long term exposure tests completes the picture. The accelerated tests are devised in order to speed up the effects of weathering and corrosive environments. In this way observations of resistance to deterioration can be made over a manageable period of time. Long term exposure 'in the field' is the only genuine way to monitor performance. Assessment tests and short term tests are compared to the performance in service.

Two of the most significant factors in architectural anodising are the sealing quality and abrasion resistance which together give some indication of

the aesthetic durability. Other properties which are important are anodic film thickness, light fastness and u.v. light fastness (for coloured films), optical and electrical properties. Generally, optical properties such as specular and total reflectivity and image clarity, and electrical properties such as breakdown voltage and dielectric strength are important in uses for anodised aluminium other than in architecture. Light fastness is usually only applicable to coloured films (section 2.3). Degradation of coloured architectural components can still be regarded as poor aesthetics since the original architecture is changed by it. Fading may be due to surface degradation and must be prevented. Anodic film thickness is very important in architectural applications. Up to 10 μ m thickness is used for decorative applications where appearance rather than corrosion resistance is the prime factor. Thicknesses less than 10 μ m are adequate for internal use. United Kingdom specifications for external applications (ISO2064:1980, BS1615:1987 and BS3987:1974) require a thickness of 25 μ m. Anodising dulls bright finishes and as the thickness is increased, the coatings lose their specularity. This is usually unimportant in architecture since a matt, etched finish is the norm. The emphasis is on maximum protection to preserve the aesthetic appearance. Very thick films (>50 μ m) are used in engineering because of their hardness and abrasion resistance. Unsealed components of high thickness are used for high wear conditions. Colouring processes in architectural anodising do not normally affect the film

thickness. Dyes require a film of at least 15µm in thickness to be properly absorbed. Thickness is irrelevant to electrolytic and interference colouring. Integrally coloured films depend upon coating thickness.

Film thickness, sealing quality, abrasion resistance, corrosion resistance and weathering are all inter-related as each is a function of the anodic oxide coat. Each function can be assessed separately by different tests. The true picture is assimilated from information derived from all the functions involved.

Measurement of film thickness is straightforward and has been described in the Experimental section, as have a number of other tests for sealing quality. The quality control tests are the dye spot test (ISO2143:1981 and BS6161:Part 5:1982) and the admittance test (ISO2931:1983 and BS6161:Part 6:1984). These are non-destructive tests. Other tests are used for referee purposes and where the former two are not suitable. These are the nitric acid pretreatment followed by immersion in acidified sodium sulphite solution or in sodium acetate/acetic acid solution (ISO2932:1981 and BS6161:Part 4:1981). Also immersion in chromic acid/phosphoric acid solution (ISO3210:1983 and BS6161:Part 3:1984). These are destructive tests. All the above tests examine different aspects of the anodic film. The dye spot test examines the sealing quality at the surface of the film in one specific area. It measures the sorptive properties of the film surface. Admittance measurements are dependent upon film thickness and sealing quality for a defined area. This test measures the

impedance properties between the basis metal and the electrolyte on the surface (and within the pores). (However, 1KHz a.c. is used and the resistance is high even without sealing because of the barrier layer.) The immersion tests measure the chemical resistance of the film where general surface attack is assessed.

The requirement of these tests is a minimum sealing quality, rather than different degrees of sealing. Sealing gives the film a good chemical resistance which is observed when it passes the above tests. The admittance test does not indicate the presence of contaminants or excess anti-smut agents. Dye spot tests (98) rely on the absorption of a dye into the open pores of the oxide film. This is a surface phenomenon. The first solution sensitizes the surface. The second solution is a dye which is absorbed by unsealed or poorly sealed films. No dye absorption occurs with well sealed films since the pores are blocked by boehmite. This is a quick and simple test but is prone to subjective evaluation of the intensity of the dyed spot. It cannot be used with dark coloured films and is less sensitive to seal quality with nickel or cobalt sealing solutions. Anti-smut agents can give misleading results. The test can be used 'on site' and on the production line, and can be applied to non-significant surfaces.

The effects of sealing can be studied by a.c.-bridge measurements of the electrical impedance of the film during sealing over a wide range of frequencies (99). Impedance for an anodic film is related to the combined values of resistance and capacitance, which is dependent on

frequency. The thickness, structure, composition, method of formation and type and extent of sealing affect the ability of the film to pass a very low voltage alternating current when in contact with an electrolyte over a specified area.

Hoar and Wood (88) measured impedance characteristics of films during sealing using a series-resistance-capacitance balancing arm in an a.c. bridge. The analogues comprising of resistance, R and capacitance, C , which represent the anodic film are given in Figs. 22 and 23 (88). Wernick, Pinner and Sheasby (100) noted that the values of R and C were not specifically related to any physical feature of the films and no supposition was made concerning any electrical analogue. It was only an analogy of how the film could be represented by an electrical circuit. The individual components could not be measured, but they represented the functions of the barrier layer, pore etc. By observing the difference in values between unsealed, partially sealed and well sealed films, it could be inferred from a knowledge of the mechanistic models, how each component, and the whole film, was affected by the changes brought about by sealing. When the a.c. bridge was balanced over a wide range of frequencies for one set of components, then a parallel had been established between the network of components and the film. This parallel was clearly demonstrated by Hoar and Wood (88) who described Fig 22 as an unsealed film, and Fig 23 as a partially sealed film. By using resistance-capacitance balancing arm in the a.c. bridge, estimates of the components of the complex impedance were

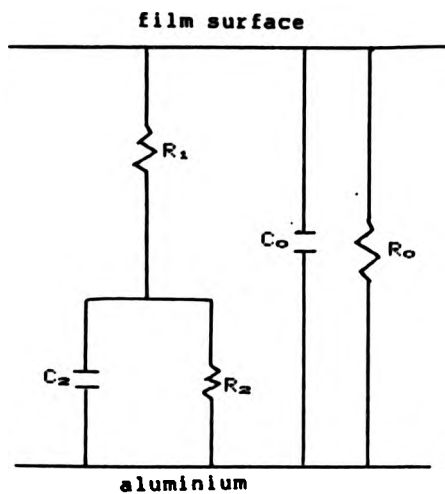


Fig. 22 (88)

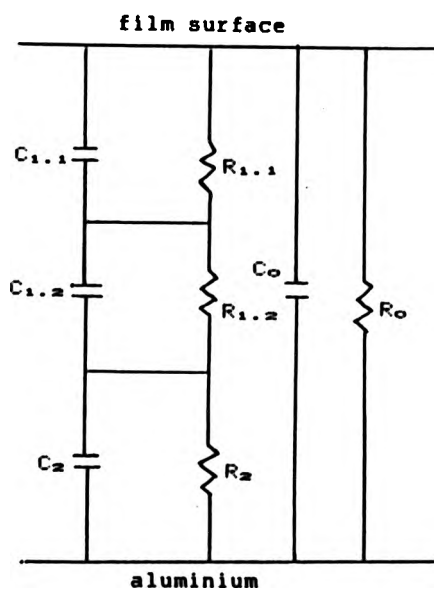


Fig. 23 (88)

found. When films were sealed in nickel acetate solution the pore resistance increased. A substantial part of R_1 was concentrated as $R_{1.1}$ which was interpreted as a short 'plug' of semi-solid material. This had a higher resistance than the electrolyte. Across the length of the 'plug' was a moderately high capacitance $C_{1.1}$. The 'plug' retained a substantial amount of water and the high dielectric constant would have contributed to the large capacitance. Prolonged sealing increased the pore resistance. $C_{1.1}$ and $C_{1.2}$ were reduced due to the decrease in the diameter of the main pore length. The 'plug' also increased in solidity probably reducing the effect of the high dielectric constant of water. The barrier layer capacitance C_2 was reduced which corresponded to an increase in the thickness of this layer. However, since a.c. as well as d.c. causes aluminium to be anodised, the prolonged application of a.c. to unsealed and partly sealed films may change the film being studied.

The reciprocal of impedance, $1/Z$, is the admittance and is a more useful term to use. The operating details are given in the Experimental section (3.5.3). The admittance readings are satisfactory over the range 5 to 30 μ m in thickness. The method of measurement commercially is not the same as the a.c. bridge technique. Commercial instruments give a value for the admittance directly, and a single frequency of 1000Hz is standard. These instruments are useful in production control. They are very useful alone but can give even more information when combined with other tests. Electrolytically coloured films have given

anomalous results which are discussed in a later section (4.9). The effects of contaminants such as silicates and phosphates are not detected and anomalous results can also be obtained with some sealing additives. The apparatus can be used 'on-site' and on the production lines on any flat surface.

Wood and Marron (101) used a.c. impedance measurements together with electron probe microanalysis to investigate the sealing properties of various solutions at different stages of sealing. Nickel-containing and chromium-containing solutions were used, and impedance measurements were made as soon as possible after entry into the solution. This method was not as sensitive to the initial stages of sealing as readings taken at ambient temperatures after sealing. The conclusions drawn were confirmed: the increase in R_s with time was a measure of pore closure, ageing continued for very long periods after removal from the solution, pores closed in depth but with pore plugging near the surface the most significant factor. After an initial stage where the sealing solution ions rapidly penetrated the pores to form a gel, particularly at the pore mouths, the second stage caused a solidification of the gel. The impedance increased, and the transfer of hydrating species was reduced. The solidification continued in the third stage, presumably by the 'advanced proton' mechanism (88). It was impedance measurements which monitored the gel changes. The impedance increased with solidification.

Impedance measurements are also influenced by

film thinning and the dielectric constant of the electrolyte, as well as species such as nickel and chromium ions which become trapped within the pores. For nickel solutions with low concentrations the impedance would be higher for a given extent of pore closure. There would be a lower sealing rate and a slow pore closure would be given by a high absorption of nickel. All chromium solutions showed an induction period before impedance increased significantly. In a subsequent paper, Wood and Marron (101) showed that the impedance became less the higher the film formation temperature. The film was more porous and CrO_4^{2-} ions were absorbed for a longer period of time. pH was kept low so hydration was slower. The impedance was also lower because of the large cross-sectional area of the pores. It was also suggested that prolonged sealing may be detrimental to the film.

2.5.3 Acid Immersion Tests

The minimum sealing quality is assessed by the chemical resistance of anodic oxide films in certain solutions. These are destructive tests and are generally used for referee purposes in cases of dispute. A representative sample must be taken from the production line for analysis. The test cannot be used 'on-site'. The tests give a quantitative evaluation of the degree of sealing by weight loss measurements over a fixed period of immersion. There is no dissolution of the basis metal.

The acidified sulphite test (Kape test) uses a

fresh solution (BS6161:Part 4:1981 and ISO2932:1981). There is a 10min predip in 50% nitric acid. The weight loss at this stage may give useful information; for example a weight loss over $1\text{g}/\text{dm}^2$ often suggests inadequate film quality. The specimen is then immersed in the test solution and the weight loss per unit area calculated. The maximum weight loss for adequate sealing is $2\text{g}/\text{dm}^2$. The acidified sulphite test is a controlled laboratory experiment designed to create a corrosive environment similar to that found in service. Sulphur dioxide is produced in solution.

The chromic acid/phosphoric acid test is another immersion test (ISO3210:1984 and BS6161:Part 3:1984). This solution is reusable until 0.1m^2 of anodised surface has been treated per litre of solution. The nitric acid predip is not specified but the BSI committee is considering introducing it in a future revision. Chromic acid/phosphoric acid is slightly more aggressive than the Kape test, and a maximum weight loss of $3\text{g}/\text{dm}^2$ is acceptable.

Furneau and Wood (102) assessed the effect of acid immersion on unsealed, partially sealed and well sealed anodic films. It is known that the nitric acid predip 'sensitizes' the film surface. Unsealed and partly sealed films lost the surface and intermediate layers during the predip, which does not occur in other solutions. This 'sensitizing' of the film surface indicates that the surface sealing products are undermined. Dissolution occurs readily in the sulphite solution. However, when a well sealed film was subjected to the predip, not all the

intermediate layer was removed. A slightly acidic pH, caused by the presence of sulphite and sulphate ions, influenced the aluminium oxide/water reaction and the solute or dispersed aluminium-containing phases were precipitated on the film surface. Initial pathways opened up by the nitric acid healed over due to the precipitation, and the admittance readings were found to decrease. Other acids did not undermine the surface crystals due to the nature of the acid anions and the degree to which they interacted with the solute or dispersed aluminium-containing phases. Compared with phosphoric acid/chromic acid solution, nitric acid attacked unsealed and partially sealed films less rapidly, possibly due to the low temperature. The chromic acid/phosphoric acid test attacked the coating fairly uniformly; slow dissolution of the surface crystals followed by more rapid dissolution of the intermediate layer. Unsealed films were rapidly dissolved because the film was unprotected and the solution temperatures were high. It was shown that the surface topography of the basis metal influenced the attack of immersion solutions on poorly sealed films. Sites for preferential attack were possibly ridges or depressions, and the composition of these may have varied the susceptibility to attack.

The precursor to acid immersion tests were the absorption of dyes and coloured chemicals, and the subsequent qualitative and quantitative estimate of those chemicals. In 1960 Hoar and Wood (103) proposed a colorimetric method of estimating the degree of sealing. A

post-sealing treatment was applied where the film was immersed in potassium dichromate solution at 95°C, dissolved in sodium hydroxide and the chromate content determined by diphenylcarbazide. The results were compared to those obtained by a.c. impedance and weight increase measurements. It was found that unsealed films absorbed the coloured chemicals. The longer the films were sealed, the less the chemicals were absorbed, but the influence of the film thickness, sealing solution, concentration of dichromate, pH and temperature on chromium uptake was important. It is well known that dichromate is a sealant itself (section 2.4.7) and its use at 95°C as a post-sealant must be in serious doubt. This is in effect a second sealing treatment, and no assumptions can be made upon the content of chromate as found by the diphenylcarbazide method. This test was not pursued further.

2.5.4 Abrasion Resistance

Abrasion resistance and hardness of anodic coatings are very important for engineering applications since wear resistance and strength are the main properties required. Due to the effects of degradation and weathering of architectural anodic finishes, the measurement of abrasion resistance has become increasingly significant, especially with respect to sealing quality and coating thickness.

Abrasion resistance and hardness are two separate properties, and it is only the former which plays a

significant role in architectural anodising. In order to distinguish between the two properties, an explanation of each is given. Hardness (104) can be measured only for materials which undergo plastic deformation, and allow an indentation to form. A hardness value is calculated from the known load applied and the measurements of the indentation. Elastomers recover as soon as the load is removed, while hard, brittle materials like glass, fracture at a critical load rather than deform. The anodised metal is composed of a hard oxide coating on a soft substrate, and any load applied will affect the aluminium. The hardness figure represents a combined value of the oxide coating and the substrate; the latter actually suffers the majority of the indentation, which ruptures under the applied load. To avoid the effect of the soft substrate, a normal micro-hardness indenter (105) is used which makes a series of indentations on a cross-section of the film, using very low loads e.g. 15 or 50g. This method is only used for hard anodic films and those greater than 25 μ m in thickness. The hardness at various positions throughout the film can be tested in this way. This method is not influenced by the basis metal and therefore the 'hardness' of the anodic film is measured.

Abrasion resistance should be a measure of the resistance to an abrasive medium. This can be interpreted as a wear resistance rather than resistance to deformation at a specific point. A conventional method is the jet abrasive test. This is quoted in terms of the mass of silicon carbide per micron of coating required to penetrate

the film. The Schuh and Kern abrasive jet method was adopted in BS1615:1972 and is now included in ISO8252:1987 and BS6161:Part 10:1987. The abrasive and air supplied to the apparatus must be dry. The values obtained are comparative only and depend upon the particular apparatus used. Other jet tests give different results on the same test sample due to experimental variation of the apparatus. It has been found that dyed, pigmented or impregnated coatings may be assessed, where admittance values are untrustworthy (106).

A more recent advance is the abrasive wheel test (section 3.5.9). This method is becoming increasingly widespread in its use and is the subject of a draft international standard (ISO DP8251) and is included in BS6161:Part 9:1987. This method is not subject to variations associated with the jet abrasion test; the abrasive paper is standard and varies little, whereas, by virtue of the jet test using a particulate abrasive under pressure, variations have been found (107). These were associated with the abrasive, the apparatus, the rates used and the water content in the air and silicon carbide. The abrasive wheel method (105) uses a load of 400 gram force (gf) and 400 double strokes (ds). The film thickness loss (or weight loss) from the abraded area as a function of the number of double strokes used, is the measure of the degree of abrasion. This can be quoted in terms of wear resistance: the number of double strokes per micron of wear; or the abrasion resistance which is the thickness loss per 100 double strokes. The wear index (mass or

thickness) is given as

$$\text{wear index} = \frac{\text{loss (mass or thickness) of sample}}{\text{loss (mass or thickness) of standard}} \quad (2.8)$$

20°C, H₂SO₄ film

for a specified number of double strokes. This method can give a 'profile' of an oxide coating showing changes in hardness throughout the film as it is abraded away. Information about production and/or degradation may be revealed, for example soft layers within the film. A standard film is used for comparative purposes only. The disadvantage of this method is that it requires a test sample from the production line and cannot be used on-site. The process is also time consuming to set up and often upto 200 samples are required for quality assurance.

The need arose for a simple non-destructive abrasion test which could be used 'on-site' on non-significant surfaces. Clarke (108) has devised a simple abrasion test for the control of quality of anodic films. Using glass, garnet and silicon carbide abrasive papers in turn, anodised films can be divided into classes which indicate the propensity to 'chalk' in service. The test is based upon the principle that one material is only scratched by another which is harder. This is Mohs' principle. If the abrasive is harder than the oxide, film dust is picked up by the paper. The abrasive can be felt to 'bite' into the film, abrading it. If a film is harder than the abrasive then no chalk-like dust appears. The abrasive

paper merely burnishes the film. The loss of thickness, if any, is measured by the eddy current method. The three divisions of anodic film given by glass, garnet and silicon carbide paper are as follows:

1. Films scratched by glass paper are too soft for external applications.
2. Films scratched by garnet and silicon carbide but not glass paper are those produced by correct sulphuric acid anodising procedures, and dyed correctly by any of the standard processes.
3. Those films scratched by silicon carbide paper only are those produced by correctly operated integral colour anodising procedures, those formed in oxalic acid, sulphuric acid films formed below 5°C (hard anodising), films produced by normal sulphuric acid anodising but not hydrothermally sealed.

Clarke (108) made between 13 and 200 tests on individual members of numerous samples drawn from production batches. The Acceptance Quality Level (AQL) used in acceptance testing is 1%. This is because not all members have the same abrasion resistance and there will be slight variations. If more than 1% of the members of a batch are scratched by glass, then they are put in the glass category. If less than 1% then they are in the garnet category. Similarly if more than 1% are scratched by garnet, they are in the garnet category and if less than 1%, they are in the silicon carbide category.

Table 12 (108) shows natural and coloured films

Table 12

Loss in thickness (micrometres) caused by the abrasive wheel test, 400 double-strokes, 400 g, with silicon carbide (ISO DP6251), garnet, and glass papers, compared with the results of the three paper test.

Rank	Film Type and Colour	Abrasive Wheel Loss (micrometres)			Three Paper Scratched by:
		SIC	GARNET	GLASS	
1	Oxalic acid, black	2.2	1.7	0.4	SIC
2	Integral colour, bronze	3.3	1.5	0.3	SIC
3	Integral colour, bronze	3.5	0.7	- 2.8	SIC
4	Sulphuric, unsealed, natural	4.4	1.5	0.6	SIC
5	Integral colour, bronze	5.0	2.2	- 0.6	GARNET
6	Sulphuric, electrocolour, black	6.1	—	—	GARNET
7	Sulphuric, combination, red	6.6	5.0	0.9	GARNET
8	Sulphuric, natural	7.6	7.4	0.1	GARNET
9	Sulphuric, natural	7.9	5.5	1.5	GARNET
10	Sulphuric, Prussian blue	8.9	7.0	1.8	GARNET
11	Sulphuric, natural	9.4	8.1	1.4	GARNET
12	Sulphuric, electrocolour, black	9.6	9.2	5.9	GLASS
13	Sulphuric, electrocolour, black	12.5	7.1	6.6	GLASS
14	Sulphuric, dyed bronze	20.1	17.3	15.1	GLASS

Note: negative values in the GLASS column represent thickness gain.

abrasive wheel test (apparatus manufactured by the Suga Instrument Company) using glass, garnet and silicon carbide papers, and the three paper test. The hardness boundaries between the three abrasives are defined in terms of this abrasive wheel test. The tests were repeated with garnet paper and glass paper to provide a comparison with the silicon carbide paper. The conclusion was that the softer abrasive papers removed the film almost as fast as silicon carbide if the film was soft, but they removed almost nothing when the film was harder. Some materials such as very hard matt anodic films increase in thickness after the glass paper test because they pick up burnished glass from the paper during the test.

A major distinction between the abrasive wheel test and the three paper test is that the latter can detect a film which possesses a soft outer layer of 1 to 2µm in thickness. This occurs under certain production processes.

It can be removed by cleaning to leave the underlying hard film. The soft layer is revealed by dust on the glass paper. If a fresh area of glass paper is used on the same wear track a second or third time, no dust appears, indicating the outer layer has been removed. A check with the eddy current meter confirms this and the resistance of the 'bite' is no longer felt. If the film was soft throughout, repeated glass paper tests would continue to show the dust, and the abrasive wheel test would show unsatisfactory results.

These are comparative tests. The thickness loss varies for the abrasive wheel test with the load and number of double strokes. If an anodic film is rough or uneven, the abrasive wheel test removes more film from high spots. The three paper test is not affected in this way. The degree of pressure exerted does not affect the result since if a film is harder than the abrasive, no amount of pressure will scratch it. If a film is of sufficient quality, the small test area will not be subjected to degradation since the film thickness loss is negligible by virtue of the nature of the test i.e. a poor quality film scratched by abrasives will not reach the minimum requirements and hence will not perform well in service.

If the three paper test is to be used in conjunction with the abrasive wheel test, careful interpretation is required of both test results. The thickness wear resistance ($\mu\text{m}/100\text{ds}$) gives a good indication as to the film quality. In commercial anodising limits must be set to allow for a percentage variation. In

this case an upper limit of 1.4 for the thickness wear index (glass paper) has been suggested on a defined percentage, since variations do occur in production. It has been proposed that an AQL (B.S.1615:1987, Appendix E) of 1% above the thickness wear index of 1.4 (109) ensures that poor quality work is rejected. If the three paper test is used in conjunction with the abrasive wheel test as a go/no go test, better quality control could be achieved. 100% compliance with a specification requires 100% inspection which is often impractical when there are more than 100 items. If a number of random samples from a batch are tested by the go/no go test and are found to be acceptable, and if those same samples are tested by the abrasive wheel method, the batch as a whole may be accepted upon a specified percentage of samples which are below a specified wear index value. If one or two samples, which have not been tested are outside the acceptance limits and do chalk in service, then it is not unduly costly to replace them.

Abrasion resistance tests are becoming more important as a means to predict performance in service, since they are sensitive guides to factors which have an influence on weathering behaviour. At the same time information about the anodising and sealing conditions may be revealed. By using these tests to supplement existing assessment tests, a much clearer picture of the history and future performance can be formed.

The abrasion resistance is influenced by the anodising and sealing variables. Low sealing temperatures increase abrasion resistance, whereas most other tests show

inferior film quality under these conditions. It has been found (110) that abrasion resistance is decreased by higher anodising temperatures. Oxalic acid additions compensate for the effects of high anodising temperature. The duration of anodising also influences the abrasion resistance; long anodising times decrease it. Electrolytes with high concentrations also decrease the abrasion resistance. Sealing lowers the abrasion resistance to 50 to 70% of the unsealed value. Similarly ageing reduces the resistance due to slow hydration. Smut inhibitors do not affect abrasion resistance. A higher anodising current density increases the abrasion resistance although it has been reported (111) that constant results were obtained when varying the current density and the concentration at a constant temperature of 18°C. Abrasion resistance is increased by increasing the homogeneity of the alloy. Especially highly alloyed material reacts with more sensitivity to changes in the anodising conditions. It has been found that abrasion resistance is not influenced by adsorptive dyeing nor by electrolytic colouring (111). Elevated temperatures used in the two-stage electrolytic colouring can reduce abrasion resistance.

2.5.5 Resistance to Degradation of the Anodic Film

The acid immersion tests can be interpreted in terms of the sealing quality of an anodic film. Corrosion tests measure the resistance to pitting corrosion in a corrosive medium. They are separate from the former tests

since sealing quality has less influence on pitting than does the film thickness or alloy used. However sealing quality is important in preventing staining.

Anodised aluminium exhibits good resistance to corrosive environments and hence the acetic acid salt spray test (ISO3769:1976 and B.S.5466:Part 2:1977) and copper-accelerated acetic acid salt spray test (CASS Test ISO3770:1976 and BS5466:Part 3:1977) were devised to reflect this (112). Caution is needed in interpreting the results. Their correlation with service performance gives the best indication of corrosion resistance. The tests simulate the effects of the environment, but at an accelerated rate. In order to pass the tests there should be no pitting of the specimens. The CASS test is now used for thick coatings. A rating for frequency of pitting is allowed from 0 to 10, where 10 indicates no pitting. The specimen area is divided into specific squares and the corrosion frequency is the ratio of squares with corrosion pits expressed as a percentage of the total number of squares. The CASS test is useful for distinguishing good and bad films. This is not a sealing test and fails to discriminate between sealed and unsealed films. However, parallels must be drawn with long term exposure since unsealed coatings, after a period of time, appear to seal to some extent. Experiments (113) have shown that the CASS test could have a sealing effect. Various workers found that during accelerated tests the films underwent a pore closure reaction which resembled the sealing process itself. Strazzi (113) used the CASS test as a starting

point for a more selective corrosion test to distinguish between sealed and unsealed films. Lower temperatures were used so as to reduce the 'sealing' effect. The CASS test was changed by the addition of sodium metabisulphite which liberated sulphur dioxide. A similar modification to the CASS test has been used in Japan (112). It too combines sulphur dioxide gas with the CASS test and the authors claim that it relates better to atmospheric corrosion than the unmodified CASS test. However, others (114) have favoured the CASS test results. These modified tests are not widely used, and careful monitoring of all parameters involved is needed to assess the optimum conditions which give the most accurate results.

2.5.6 Weathering

The simplification of corrosion conditions, and the acceleration of corrosion rates in the interests of short term results, renders corrosion tests unreliable to an extent such that long term exposure tests are still needed. A major factor affecting corrosion resistance is the environment to which an anodic film is exposed. Comparative tests have been performed in rural, marine and industrial sites. The last environment has been shown to be the most severe on anodised aluminium. By virtue of its location, the industrial atmosphere is polluted with dirt and acidic components such as sulphur dioxide. The severity is compounded by wet weather (especially in the UK) leading to corrosive solutions.

Clarke and Leeds (115) adapted a test first devised by Britton and Clarke which was used originally to measure the porosity of coatings of gold and platinum metals on substrates of copper and its alloys, nickel and silver. It has since been applied as an accelerated corrosion test for oxide films. Similarly the Kape test is intended to provide conditions where sulphur dioxide is present. The sulphur dioxide test in BS1615:1972 has disappeared from the 1987 edition, because it was taken from BS1224 originally, and dropped from this too. When BS1224 discarded it the test lapsed. For BS1615 it is still felt that a sulphur dioxide test would be useful but there is none at present. In an enclosed chamber moist air is used containing 0.5 to 2.0% (vol) sulphur dioxide. The temperature is $25 \pm 2^\circ\text{C}$. This can be classed as a sealing test since poorly sealed films produce a white bloom after exposure. The test sets out to produce an environment similar to that which is experienced on industrial sites, although dirt accumulation is not present.

Industrial sites are the most aggressive towards anodised aluminium compared to rural and marine sites. It has been found (105) that a marine site on Hayling Island is similar to a rural site at Banbury. Sheasby (116) investigated a number of factors affecting pitting corrosion by exposing anodised aluminium at a selection of sites. Anodised panels were produced by standard sulphuric acid anodising. In an industrial environment the accumulation of dirt had a significant bearing on corrosion since pitting occurred due to condensation of moisture at

dirt deposits. Sulphur dioxide dissolved in this water and attacked the anodic film at weak points. It was found that a high rate of dirt deposition, combined with wet weather produced more corrosion than at a site with higher levels of sulphur dioxide but less dirt deposition.

The position of anodised aluminium components on a building has an effect on film degradation. Sheltered components tend to show more pitting than those which are 'washed' by rain. The amount of exposure is equally important. For these reasons the sulphur dioxide humidity test may not correctly simulate the natural environment. Areas which are protected from sunlight and rain accumulate more dirt, and condensation does not dry as quickly. This was confirmed by panels exposed at 45° facing due south in which the underside was subjected to greater pitting attack. This also occurred at an earlier stage than on the exposed face (116). These results show the need for maintenance cleaning. Anodised aluminium in marine and rural sites need less frequent cleaning than that in industrial sites. Cleaning prolongs the life of anodised aluminium. Water and a mild detergent applied with a nylon brush is adequate. Harsh abrasives and chemical cleaners should be avoided. Organic solvents remove grease or sticky materials.

Once blooming and pitting have taken place they cannot be permanently removed by cleaning, although the progress of corrosion may be halted if caught in the early stages. Once a pit forms, it acts as a trap for more dirt, so perpetuating the process. Pits eventually 'stifle' and

the amount of corrosion that occurs reaches a limiting or 'threshold' value. Prevention is the best policy, since if cleaning is carried out after blooming or pitting is detected, then harsher methods are required which may themselves shorten the life of the anodic film.

Other factors affecting corrosion performance described by Sheasby (116) are:-

1. Alloy used,
2. Pretreatments,
3. Film thickness,
4. Anodising conditions,
5. Quality of sealing,
6. Post sealing treatments.

1. The alloy composition influences blooming and pitting. If commercial purity aluminium is taken as a standard, the addition of copper, manganese or silicon decreases pitting resistance while magnesium increases it. High silicon alloys and Al-Zn-Mg alloys are particularly prone to bloom formation, but regular cleaning reduces this.

2. Pretreatments do not affect bloom formation, but do have a bearing on pitting. Smooth finishes have less tendency to pitting than rough ones. Conversely, if bloom does appear, it is more obtrusive on the smooth surface than when light is diffused by a matt surface. Etching decreases the pitting resistance while mechanically or electrochemically brightened aluminium has an increased pitting resistance. This is because rough surfaces retain more dirt and moisture. Defects or flaws increase the incidence of

pitting for the same reasons. Thickness is lower at these sites giving an uneven surface. Finger print corrosion of the substrate promotes pitting.

3. Anodic film thickness is the most important factor affecting pitting resistance. Generally the thicker the film, the greater the pitting resistance, but although the number of pits is fewer, individual pits tend to be larger. Films thicker than $30\mu\text{m}$ have a lower resistance to pitting than thinner films because the anodising time is long, unless higher current densities are used. Due to this longer time in the electrolyte, the abrasion resistance is lowered and the film is said to be 'soft', and more porous i.e. the pores are larger. It is more difficult to seal and the combined affects of all these factors lowers the pitting resistance.

4. Anodising conditions used are very important. Temperature and electrolyte concentration, if too high, give soft films. However, it was found (116) that raising the temperature from 15 to 21 to 25°C increased the pitting resistance in certain alloys containing intermetallic particles. This must be viewed with caution since high anodising temperatures are known to produce soft films.

5. Sealing quality has little effect on pitting resistance, but is a determining factor in bloom formation (section 2.5). The effects of 'crazing' were discussed in section 2.4.3. If it does occur then pitting will take place preferentially along the craze lines. The problem is made worse with very thick films ($>30\mu\text{m}$) and particularly where the pretreatment has formed a smooth surface. Crazing is

reduced on films which have been etched or have fine particle distribution. These break up stresses in the film.

6. Lacquering or waxing the film protects it from attack by wet mortar, plaster and cement. Wax is usually removed once the anodised aluminium has been erected. Lacquer was applied widely 20 to 25 years ago. It was supposed that it would weather and be detached, but in practice some remained for long periods in a semi-detached condition. Lacquer was abandoned in favour of low tack tape or a sprayed rubber solution which formed a pliable film. More recently, a thin film of 2 μ m of acrylic lacquer has been applied as an aqueous emulsion (rather than the 10 to 20 μ m film in organic solvent of 20 years ago). This is cleaned off fairly early in the life of the coating. There is little experience of the effectiveness of this approach to date.

The performance of dyed anodic coatings depends on the nature of the dyestuff used, the amount of dye absorbed and the quality of sealing. Integral colour films and electrolytically coloured films, (bronze, grey, blue-grey or black) tend to have adequate resistance to the detrimental effects of weathering, and have good colour-fastness. Electrocolouring with copper fades and reduces the durability of the film. Black electrolytic finishes produced with tin have reduced resistance if the tin extends up the pores.

Witt and Jahnke (117) monitored specimen panels over a period of time which included periods of exposure and periods of storage. Results of weathering these films

in an industrial atmosphere showed that they remained essentially unchanged or even improved. This result has never been reported elsewhere and is dubious.

In conclusion, accelerated tests have shown reasonable correlation with exposure tests. Tests providing information about pitting rather than blooming are harder to evaluate. They are based on visual inspection, and not on quantitative measurements such as weight loss, although the rating for the frequency of pitting has been discussed. Pitting is independent of blooming, and a film prone to blooming may have a good resistance to pitting and vice versa.

2.5.7 Effects of Impregnation on Anodic Film Degradation

Due to the relatively recent introduction of impregnation of anodic oxide films, there has been little information on long term exposure performance. The 'Fox 33' cold sealing process was the first sold in the UK. Acid immersion tests may be less suitable for evaluating impregnated films (118). Others (113) have found that the phosphoric acid/chromic acid test and the dye spot test give valid results. It is well known that ageing of impregnated films markedly increases the 'sealing' quality. The length of time between production and testing was not recorded (113). The only comparison to be found is that both impregnated and hydrothermally sealed films were tested at the same time after production. Ageing was not taken into account. Weight loss results were found "to be

within the limits stipulated" for 'sealed' films. However, the main purpose of the communication was to evaluate the corrosion resistance of impregnated films by modifying the CASS test in order that it did not produce a sealing effect on the films. It was concluded that this modified test gave useful information on the "quality of fixation" and on corrosion resistance.

It has been demonstrated (119), by using admittance values and weight loss results in the phosphoric acid/chromic acid test that ageing does have a significant role in the process of impregnation. Weight loss measurements and admittance values were found to decrease with time, whereas conventional hydrothermally sealed films remained constant over periods of days, but over periods of months both films showed decreased admittance. These authors also wished to know the subsequent corrosion resistance of impregnated films in the light of the assessment test results. They recognised the existence of the ageing process. They concluded that impregnation gave better protection against blooming after an ageing period of 15 days than did conventional hydrothermally sealing. However, this did not automatically mean that impregnated films also gave better protection against pitting. The CASS test was considered not to give useful information on pitting since the degree of sealing does not have a particularly large influence compared to film thickness. Therefore it was assumed that such tests would not reveal any substantial difference between impregnated and hydrothermally sealed films. The effect of ageing of

impregnated films on the propensity to pitting is slower than in the case of blooming, compared to hot water sealing. Thus a certain period of ageing is required in order to reach the same resistance to blooming as a conventionally sealed film, but a much longer ageing time is needed in order to attain the same pitting resistance.

It is clear from these two conflicting accounts (113 and 119) that much more research is needed and long term exposure tests will be the ultimate test for impregnated films. Research (120) has shown obvious pitting after an exposure of 4 years, which indicates these seals may not give the same protection as hydrothermal sealing. However, the advantages of impregnation become evident after long ageing periods and this may have some bearing on how pitting resistance is studied.

CHAPTER 3

EXPERIMENTAL SECTION

3.1 Preparation and Pretreatment of Specimens

3.1.1 Specimen Preparation

The aluminium alloy used in this investigation was rolled sheet aluminium, grade 1200 (B.S.1470), formerly designated S1C, the percentage chemical composition of which is Al 99.0, Cu 0.05, Si+Fe 0.6, Mn 0.05, Zn 0.1, Ti 0.05, other impurities 0.15%. The specimens used were flat panels measuring 100x150 millimetres (mm) (standard size), 100x75mm and 50x75mm. A small hole was made in the corner with a punch which designated the 'top' of the panel, and identification marks stamped along the shorter edge designated the 'bottom'. The latter also signified the 'front' while the 'back' had no markings.

3.1.2 Specimen Pretreatments

The panels were degreased in trichloroethylene vapour and wiped over with tissue soaked in acetone. They were fitted into jigs made of alloy 6063 (B.S.1474), formerly designated HE9, the percentage chemical composition of which is Cu 0.1, Mg 0.45-0.9, Si 0.2-0.6, Fe 0.35, Mn, Zn, Cr, and Ti 0.1% each, the remaining percentage being Al. Each jig was shaped to hold one or two panels which rested on notches on the jig. The panels were held securely by the tension of the jig imparted by the springy alloy. All jigs had been etched for 1 minute(min)

in 4 - 10% sodium hydroxide at 70°C and the notches filed. The panels were etched for between 30 seconds(sec) and 2min, immediately rinsed, and desmutted for 5sec in 50%/vol. nitric acid at ambient temperature. After a final rinse the jigs were clamped firmly in the anodising bath. The panels were not allowed to dry between pretreatment stages. Rinsing between all steps, including anodising, colouring and sealing is essential to ensure the best results and minimise contamination between baths.

3.2 Anodising

3.2.1 The Anodising Bath

Anodic oxidation of aluminium was carried out in 165 grams per litre (g/l) sulphuric acid in a 60 litre (l) plastic tank as illustrated in Fig.24. The electrolyte was agitated by compressed air and the temperature was maintained at 20°C by means of cooling coils. A 50 Watt immersion heater was used to raise the bath temperature for elevated temperature anodising, while liquid nitrogen was poured into a clamped stainless steel beaker in order to lower the temperature. During either of these procedures the cooling water was omitted but agitation was maintained.

3.2.2 The Anodising Process

The anodic oxide coating can be formed either by maintaining a constant current density (c.d.) and altering the anodising time, or vice versa. The values in Table 13 refer to a single standard panel. If the size and/or

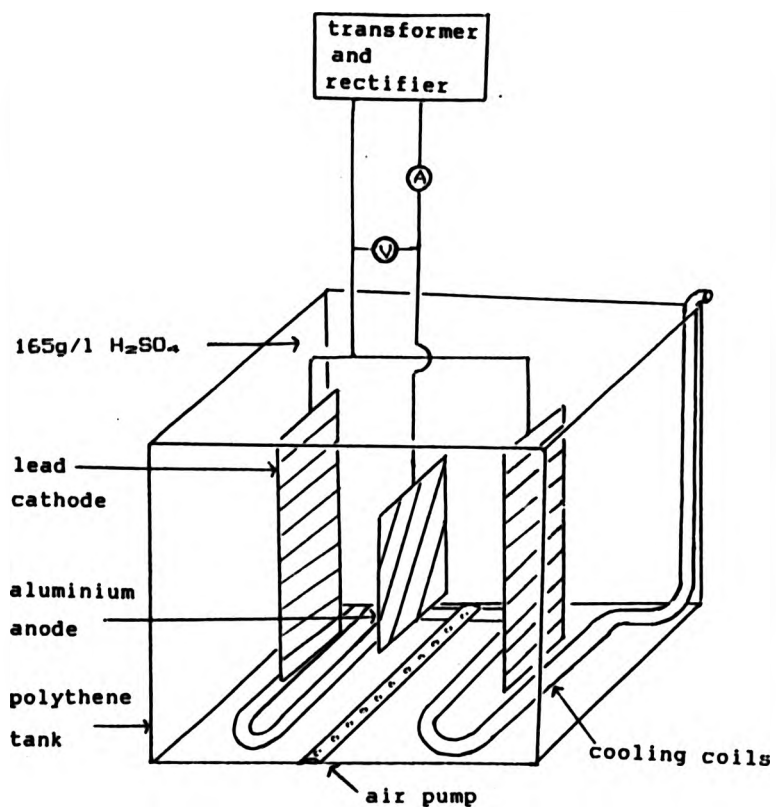


Fig. 24

Table 13

Current density (A/dm ²)	Current (A)	Thickness (µm)	Theoretical Time(min)	Actual Time (min)
1.8	5.4	10	18	23
"	"	15	27	35
"	"	20	36	46
"	"	25	45	60
0.54	1.6	10	-	-
0.81	2.4	15	-	-
1.08	3.3	20	-	-
1.8	5.4	25	-	-

Table 15

Section	Reference
3.5.1	B.S.5411:Part 3:1984 B.S.3987:Appendix B:1974
3.5.2	B.S.6161:Part 1:1984
3.5.3	B.S.6161:Part 6:1984
3.5.4	B.S.6161:Part 5:1982
3.5.5	B.S.6161:Part 3:1984
3.5.6	B.S.6161:Part 4:1981
3.5.8	B.S.6161:Part 11:1985
3.5.9	B.S.6161:Part 9:1987

quantity of panels is altered, then the current is similarly altered.

The equations used to calculate the values are:

$$\text{c.d.} = \frac{\text{thickness} \times 323}{\text{time}} \quad (3.1)$$

$$\text{current} = \text{c.d.} \times \text{area of panel} \quad (3.2)$$

To achieve the target thickness for constant anodising current density it was found to be necessary to increase the theoretical anodising time by 33%. The anodising voltage was in the range of 17-21 volts (V). Panels were anodised to produce anodic films nominally 25µm in thickness, unless otherwise stated.

3.3 Colouring

The anodic oxide film was coloured by two methods: inorganic dyeing and electrolytic colouring.

3.3.1 Inorganic Dyeing

In this investigation anodised panels were dyed by the 'double dip' method. The panel was immersed consecutively in two solutions with rinsing between immersions. The two combinations of solutions used were: 50g/l cobalt acetate and 30g/l potassium permanganate; 30g/l potassium ferrocyanide and 50g/l ferric sulphate. The former pair gave a range of colours from pale gold to bronze, and the latter gave varying shades of blue. The

colours resulted from the reaction of the two compounds to form an inorganic pigment.

Gold colour:



Blue colour:



Best results were obtained when the solutions were heated to 50°C (KMnO₄ at 30°C). The depth of colour was increased by repeating the procedures.

3.3.2 Electrolytic Colouring

Panels were anodised in 165g/l sulphuric acid, rinsed and coloured in a metal salt solution by means of an alternating current (a.c.). The basic colouring solution used was composed of 20g/l sulphuric acid, 20g/l stannous sulphate and 20g/l phenol sulphonic acid, at a pH of 1. The freshly prepared solution was left to stand for 24 hours before being decanted to remove the basic stannic sulphate which accumulates as a result of oxidation of the stannous sulphate. Phenol sulphonic acid was added in order to stabilise the solution with respect to this oxidation. When not in use the solutions were bottled to prevent unnecessary oxidation. The c.d used was 0.5A/dm² at a ^{p.d.} current density of 12V. During the first minute of treatment the voltage rose smoothly to approximately 1A/dm², but gradually decreased to a steady value of

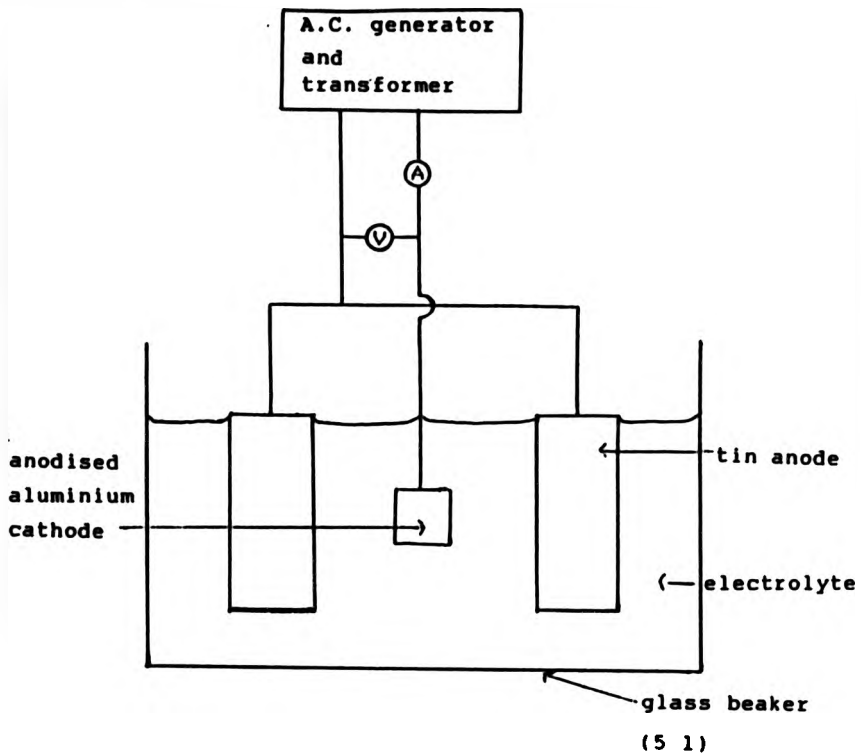


Fig. 25

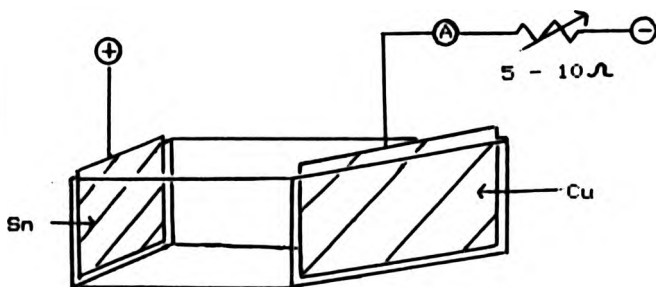


Fig. 26

0.5A/dm². The depth of colour was determined by the amount of metal deposited, i.e. the colouring time, and not the thickness of the oxide film. Colours ranged from 'champagne' for 15sec to black for 15min. Standard colouring was carried out at ambient temperature. Elevated colouring temperatures were achieved by heating the solution on a hot plate. Depressed temperatures were achieved by surrounding the bath with ice and water. Fig.25 is a diagram of the colouring bath.

Other colouring experiments were carried out in which an addition agent 'Tribrite' was added to the basic colouring solution, together with formaldehyde, sodium normal octyl-sulphate and phenol sulphonic acid, which altered the way in which the tin was deposited in the pores.

3.3.3 Hull Cell Test

The Hull Cell Test was used to estimate the covering power of the tin in the various colouring solutions. 267millilitres (ml) of the solution were put into the Hull Cell as in Fig.26. The anode was tin and the cathode was a piece of copper foil measuring 100mm x 63mm. A current of 0.5A was used for 5min. Tin was deposited onto the copper and its appearance indicated the covering power of the solution. A loose deposit of single outward growing crystals indicated poor covering power, while a smooth shiny deposit indicated good covering power. During the test hydrogen gas was evolved at the cathode. More current from the anode tends to concentrate on the near end of the

cathode, therefore the c.d. falls from the near end to the far end. The resistance is bigger between the anode and the far end.

The activity of the addition agents used in some experiments was monitored by the Hull Cell Test. Increased or decreased activity was evaluated from the appearance of the deposited tin.

3.4 Sealing

Panels were sealed by immersing them in hot solutions. Table 14 lists the solutions and conditions. They were kept at a temperature of $>98^{\circ}\text{C}$ and the panels were held over the steam for 15sec. This allowed them to warm up and not experience the 'thermal shock' that caused crazing of the oxide film when cold panels were immersed into boiling solutions. Using sec/ μm or min/ μm sealing times were determined. After sealing, the length of time that panels were stored was taken into consideration when carrying out further experimentation.

Table 14

Solution	Composition
Water	Distilled or deionised, pH 5.5-6.0
Nickel acetate buffered water	5g/l nickel acetate, 5g/l boric acid, pH 5.5-6.0
'Alcoa 482'	4.5g/l nickel acetate, 1g/l sulphuric acid, pH 5.5-6.0
Ammonium acetate	1g/l ammonium acetate, pH 5.5-6.0

3.5 Assessment Tests

Table 15 lists the tests used in this project according to the British Standard Specifications for Anodic Oxidation Coatings on Aluminium (B.S.1615:1987) which refers to Methods of Tests for anodic oxide coatings on aluminium and its alloys (B.S.6161:1981, 1982, 1984, 1985 and 1987) and Methods of Test for Metallic and Related Coatings (B.S.5411:1974). Anodic oxide Coatings on Wrought Aluminium for External Applications (B.S.3987:1974) is also quoted.

3.5.1 Thickness Measurements by the Eddy Current Principle

This method was used as a non-destructive test to measure the thickness of the anodic film. The 'Permascope' instrument (Fischer Instrumentation Ltd.) has a search coil through which a high frequency current is passed. The strength of the reading is dependent upon the distance between the coil and the conducting surface i.e. the aluminium base metal. Five readings were made on each side of the panel and an average taken. The measurements were made after the anodised panels had been rinsed but were not allowed to dry out.

3.5.2 Gravimetric Method for Thickness Determination by Stripping

This was used as a destructive test to measure the thickness of the anodic film, known as the 'strip and weigh' method. This employed a boiling solution containing

20g/l chromic acid and 35ml/l ortho phosphoric acid (density=1.75g/dm³) made up to 1 litre with deionised water. The panel was weighed before and after the test, and the area noted. The panel was degreased before initial weighing and handled as little as possible at all times. The film thickness was evaluated using the equation

$$t = \frac{W.100}{A.d} \quad (3.5)$$

where t is thickness (µm)

W is weight loss (g)

A is area (cm²)

d is density (2.4g/cm³ for unsealed coatings; the density may vary for sealed coatings from 2.6g/cm³ to 2.7g/cm³).

3.5.3 Admittance Measurements

The instrument used was an 'Anotest' meter which operates at a frequency of 1KHz. By employing an alternating current under specific conditions the admittance, inverse of impedance, of an anodised surface could be measured. The admittance was measured in µS and was designated Y(25°C). To account for films of different thicknesses, the product of admittance and thickness, corrected to 25°C, was used and was designated as Yt(25°C) (Sm x 10⁻¹²). The quality of the sealed film could be evaluated.

The panel was degreased and an adhesive annular rubber ring (13mm internal diameter) was fixed to it. Areas were chosen which were unblemished i.e. not scratched. The ring acted as a cell into which an appropriate conducting electrolyte was put. The standard solution used was 35g/l potassium sulphate. Other experiments were performed using various concentrations of nitric acid. A screw clamp was attached to a remote point on the panel. This was screwed tightly in order to break the oxide coating and make electrical contact with the basis metal. A small metal electrode was immersed in the electrolyte, completing the circuit, and a reading taken. Readings were made after 1min to allow the meter to equilibrate. However readings were taken at intervals over a period of time when drifting occurred. British Standard 1615:1987 requires a value of less than $500/t \mu S$ where t is the thickness of the anodic coating in micrometres at 25°C.

The following equation was used to evaluate a correction factor F for any given temperature:

$$F = \frac{\theta}{50} + 0.5 \quad (3.6)$$

where θ is the given temperature and $F=1$ at 25 °C.

At other temperatures Yt was divided by F .

Theory of Admittance of Electrocoloured Anodic Films

The anodic oxide film can be considered to be a parallel plate condenser, the capacitance of which is:

$$C = \frac{KA}{4d} \quad (3.7)$$

where K is the dielectric constant of the film,
 A is the area of the plates,
 d is the distance of separation.

In order to measure the admittance, an annular rubber ring was placed on the surface into which is put the electrolyte. The standard cell size used was 13mm,

$$A = \pi (1.3/2)^2 \quad (3.8)$$

If the anodic film thickness is 25μ ,

$$C = \frac{K\pi(1.3/2)^2}{4\pi 25}$$

$$= 42.25 \text{ esu}$$

Since $8.9 \times 10^{11} \text{ esu} = 1 \text{ farad}$

$$C = 4.7 \times 10^{-11} \text{ farads}$$

At a frequency H , the admittance is

$$Y = 2\pi HC \quad (3.9)$$

The 'Anotest' used $H = 1 \times 10^8$ Hz, hence

$$Y = 2\pi f C \quad (S)$$
$$= 2.95 \times 10^{-1} K \quad (\mu S)$$

If it is assumed K is 10 for a hydrothermally sealed film

$$Y = 2.95 \quad (\mu S)$$

Hence the admittance \times thickness is

$$Yt = 3 \times 25 \quad (3.10)$$
$$= 75 \quad (Sm \times 10^{-12})$$

This is the theoretical calculation. British Standard 1615:1987 requires a value of less than $500Sm \times 10^{-12}$. In practice, values for new well hydrothermally sealed films are $150 (Sm \times 10^{-12})$ or greater. Aged films can give lower values.

An electrocoloured anodic oxide film can be described in terms of the capacitance. The deposited metallic tin can be regarded as a conductor with infinite dielectric constant. If a plate of thickness d' (i.e. the tin) is placed between the capacitor plates (i.e. the metal/oxide interface and the surface of the oxide), the effective separation becomes $d - d'$ (thickness decreases) and capacitance rises to:

$$C' = \frac{KA}{4\pi(d-d')} \quad (3.11)$$

Suppose the metal in the tin layer behaves as a metal plate of uniform thickness, t_m . If the anodic film is well sealed and of total thickness t , the effective dielectric thickness is reduced to:

$$t' = t - t_m \quad (3.12)$$

For a well sealed uncoloured aged film $Yt(25^\circ C)$ is 200, however, for a well sealed electrocoloured film the value is very large, $Yt(25^\circ C)$ is x . If it is assumed that

$$Yt'(25^\circ C) = 200 \quad (3.13)$$

then for the electrocoloured film,

$$\frac{t'}{t} = \frac{200}{x} \quad (3.14)$$

and,

$$t' = \frac{200t}{x}$$

where t' is the thickness of the effective dielectric constant and t_m , the thickness of the tin, can be deduced.

3.5.4 Dye Spot Test

This is a quick and simple test for assessing the degree of sealing. An annular rubber ring was attached to the degreased panel. At room temperature a drop of solution 'A' was put into the ring for 1min exactly. The ring was rinsed and dried with tissues. A drop of solution 'B' was applied to the same ring for 1min exactly, rinsed, the ring removed and the spot rubbed with a dry tissue.

Solution 'A': 25ml H_2SO_4 + 10g KF per litre,

Solution 'B': 1% Aluminium Fast Red G3LW in water

The residual colour intensity was compared to a standard chart. If the coating is fully sealed, no residual colour remains. The colour intensity increases with increasingly poor sealing. However, as with the admittance test, only one specific area is tested and variations over the remainder of the panel are not known. Dark coloured panels obscure the test results.

3.5.5 Phosphoric-Chromic Acid Test

This is a destructive test for assessing the sealing quality of an anodic film. Any surface bloom was removed by rubbing with a dry tissue and the specimen was degreased. A panel of known area was immersed in the test solution which was heated to between 37-39°C for 15min. The solution temperature was maintained by stirring.

Test solution: 20g/l chromic acid + 35ml/l ortho phosphoric acid (density=1.75g/cm³) made up to 1 litre with deionised water.

The panel was rinsed, dried and reweighed. The mass loss in g/m² was calculated. Unsatisfactory sealing is indicated by a value greater than 3g/m². The test solution was reused, but discarded after 10dm² of anodised surface have been treated per litre of solution.

3.5.6 Acidified Sulphite Test

This is a similar acid immersion test to 3.5.5 which assesses the sealing quality by the mass loss in g/m². Any surface bloom was removed as in section 3.5.5. The panel was immersed, at room temperature, in a 50% by volume solution of nitric acid for 10min, the 'predip'. It was rinsed and immersed in the acidified sulphite solution for 20min at a temperature of between 90-92°C. The maximum mass loss allowable is 2g/m².

Test solution: 10g/l sodium sulphite (anhydrous) made up to 1 litre with deionised water to which glacial acetic acid (20ml/l to 40ml/l) has been added to give pH 3.6-3.8 followed by addition of 5N sulphuric acid (10ml/l to 15ml/l) to give pH 2.5. Fresh solution was made for each test.

3.5.7 Bleach Test

This is based on the same principle as the Dye

Spot Test, but was used for coloured panels. The same procedure was followed but different solutions were used:

Solution 'A': 25ml H_2SO_4 + 10g KF per litre, applied 2min

Solution 'C': $NaClO_2$, applied 5min

and

Solution 'D': 50% by vol HNO_3 , applied 5min

Solution 'C': $NaClO_2$, applied 5min

3.5.8 Total Reflectance

The total reflectance is important in defining the depth of colour of diffuse surfaces for colour matching purposes. The colour and shade of the panels were assessed by means of a Sheen Colorimeter. The reflectance of the instrument was calibrated against black velvet (0% reflectance) and a block of white magnesium carbonate (100%). The reflectance was measured at six wavelengths; using six CIE colour filters 600 μ m (red), 610 μ m (orange), 570 μ m (yellow), 520 μ m (green), 480 μ m (blue), 450 μ m (violet), and the instrument was calibrated after each reading. Measurements were made both along and across die-lines for extrusions and rolling directions for sheets. An average of two readings were taken in each direction. Graphs of percentage reflectance against wavelength were plotted (spectral reflectivity curves). The shade and colour was thus characterised by numerical values, the CIE chromaticity co-ordinates and can be described in terms of the CIE colour triangle, Fig.16.

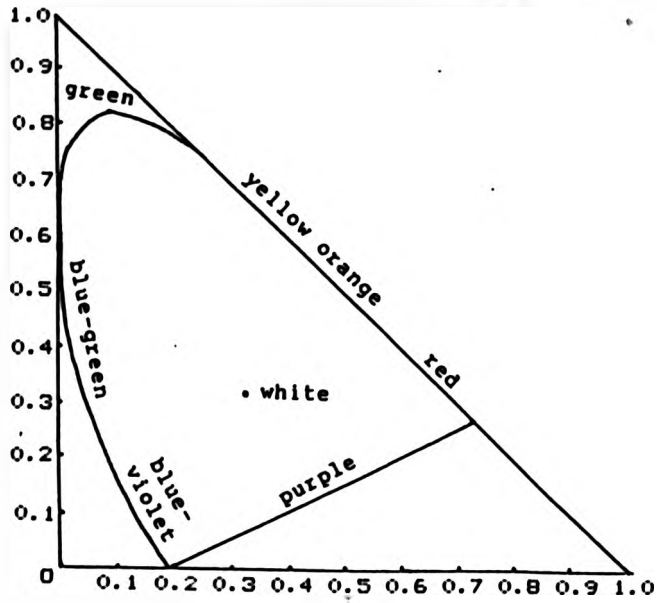


Fig. 16 (68)

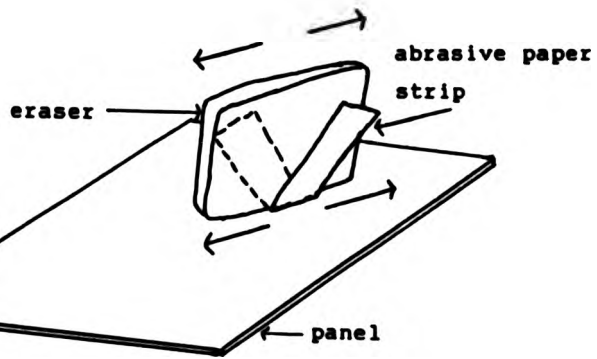


Fig. 27

The chromaticity co-ordinates were evaluated from the equations:

$$x = \frac{X}{X + Y + Z} \quad (3.15)$$

$$y = \frac{Y}{X + Y + Z} \quad (3.16)$$

where x and y are the chromaticity co-ordinates

X is the percentage reflectance at 660µm

Y " " " " 520µm

Z " " " " " 480µm

The luminance (R_{520x}) of a panel is the percentage reflectance value at 520µm (green).

3.5.9 Abrasion Resistance

Two methods were used to assess the abrasion resistance of anodic oxide films: the 'Three Paper Test' and the Abrasive Wheel Test.

Three Paper Test

This is a simple abrasion test which uses glass, garnet and silicon carbide abrasive papers. The particle size of the abrasives used were:

Glass: 'Flour' grade
Garnet: 220 mesh grit
Silicon carbide: 320 mesh grit

(English Abrasives Ltd.)

Strips (12mm wide) of each type of abrasive paper, starting with the glass paper, were wrapped around an eraser (6mm wide) in turn, Fig.27. This edge was rubbed for 10 double strokes against the panel to be tested. The strip of paper was moved so that a fresh area was ready for the next test. The test is based on the principle that one material is only scratched by another which is harder. This is Mohs' principle.

Abrasive Wheel Test

The abrasive wheel used a load of 400 gramme force (gf) (3.92N) and 400 double strokes (ds). The apparatus used was manufactured by the Suga Instrument Company and used a silicon carbide abrasive band of width 12mm, (English Abrasives Ltd. P320A mesh grit). The abrasive band was fixed to the wheel so that it rotated by 0.9° after each double stroke (one forwards and one backwards movement) under the preselected load. Each double stroke therefore used fresh paper and the band was changed after 400 double strokes. The abrasive strip was bonded or mechanically clamped into position, but so that the ends did not overlap. Abrasion detritus was continuously removed by blowing or wiping with a fine brush.

The film thickness loss (or weight loss) from the

abraded area as a function of the number of double strokes used is the measure of the degree of abrasion. This can be quoted in terms of wear resistance, the number of double strokes per micron of wear ($ds/\mu m$); or the abrasion resistance, the thickness loss per n number of double strokes (μm loss/ n ds). A convenient unit of measurement is the wear index which is given by the following equation:

Wear index (mass or thickness) =

$$\frac{\text{loss (mass or thickness) of sample}}{\text{loss (mass or thickness) of standard } 20^{\circ}\text{C H}_2\text{SO}_4 \text{ film}} \quad (2.8)$$

(The wear index is a ratio and is dimensionless).

The thickness loss found for a standard $20^{\circ}\text{C H}_2\text{SO}_4$ film was $-7.43\mu m$ for 400 ds at 400 gf. A thickness wear index of 1 or less indicates a 'hard' film, i.e. this indicates a lower degree of wear than that on the standard specimen. The wear resistance can be found from the gradient of the line of the graph of thickness loss against number of double stroke cycles. This gradient can be found by:

1. The linear regression of the graph. The value is multiplied by 20 and gives a value which takes into account the scatter of all the points on the curve. It is useful if the graph is non-linear.
2. The actual thickness loss found at 400ds.
3. The thickness loss found at 100ds or 200ds and multiplied by a factor of 4 or 2 respectively.
4. By taking an individual point on the graph and

calculating the thickness loss at 400ds by:

$$\frac{\text{thickness loss (y) x 400ds}}{\text{number of ds (x)}} \quad (3.17)$$

3.5.10 Abrasive Wheel Test Apparatus Used as a Microtome

The film was abraded by a set number of double strokes (one cycle) using a 400gf load. After each cycle the admittance and thickness were measured. The admittance x thickness product $Yt(25^{\circ}\text{C})$ was calculated and a graph of $Yt(25^{\circ}\text{C})$ against thickness was plotted; a $Yt-\delta$ profile. Alternatively, a $Y-\delta$ profile could be plotted. This is referred to as a depth survey of the anodic oxide coating.

3.6 Sulphur Dioxide Experiments

3.6.1 Sulphur Dioxide Test

Anodised aluminium panels were exposed for various times and at different temperatures to sulphur dioxide gas. Ambient temperature experiments were conducted in a 30.5l closed glass vessel, Fig.28. Elevated temperature experiments were performed in a 4.94l closed perspex box, Fig.29, which was placed in a thermostatically controlled oven. Careful monitoring of the temperature was observed. Panels were suspended by terylene thread from plastic supports in the vessels. A strip of PVC tape was placed across the panel to mask a control area. Any cut edges were similarly covered. The lid of the glass vessel

lid sealed with 'Vaseline'

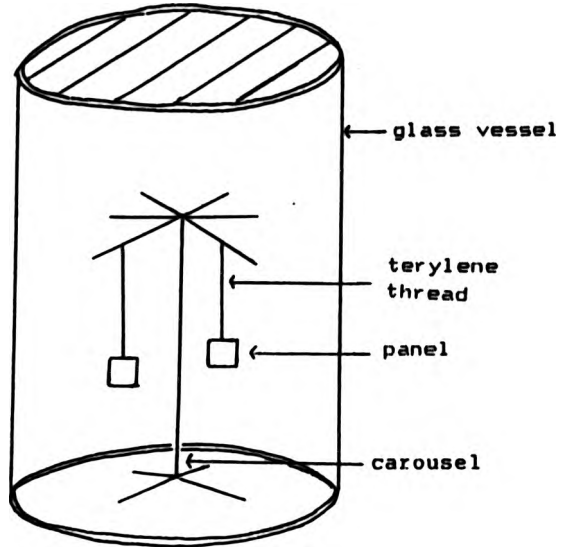


Fig. 28

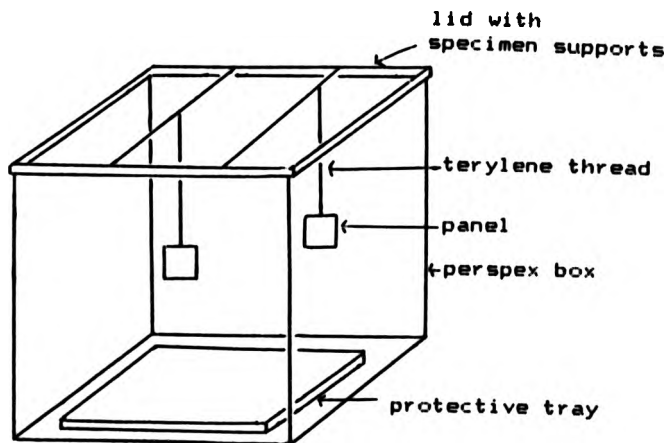


Fig. 29

was made air tight with 'Vaseline'. The perspex box had a fitted lid. The protecting tray in the bottom of the perspex box prevented the effervescence of the reacting solutions from spraying onto the panels. All apparatus, panels and solutions were preheated in the oven before elevated temperature experiments so that condensation was kept to a minimum. The gas was generated by mixing 8% sodium thiosulphate and 8N sulphuric acid immediately prior to sealing the vessel. The volume of solutions used was:

$$V = x \quad (3.18)$$

40

where V is the total volume of the vessel (cm^3)

x is the total volume of solutions used (cm^3)

Thus:

$$\text{H}_2\text{SO}_4 = \frac{1x}{5} = v_1 \quad (3.19)$$

$$\text{Na}_2\text{S}_2\text{O}_3 = \frac{4x}{5} = v_2 \quad (3.20)$$

where v_1 is volume of H_2SO_4 (cm^3)

v_2 is volume of $\text{Na}_2\text{S}_2\text{O}_3$ (cm^3)

3.6.2 Quantitative Analysis of Sulphur Dioxide Gas During Ambient Temperature Experiments

These experiments were performed using a 5l closed glass vessel, Fig.30., and carried out at ambient temperatures for 24 hours. Gas was drawn off from an outlet on the vessel and the percentage evaluated using iodine titrations. The percentage was found from the equation:

$$c = \frac{56x}{x} \quad (3.21)$$

where c is the concentration of the sulphur dioxide

x is the volume of gas needed to reduce the iodine in the titration (cm³).

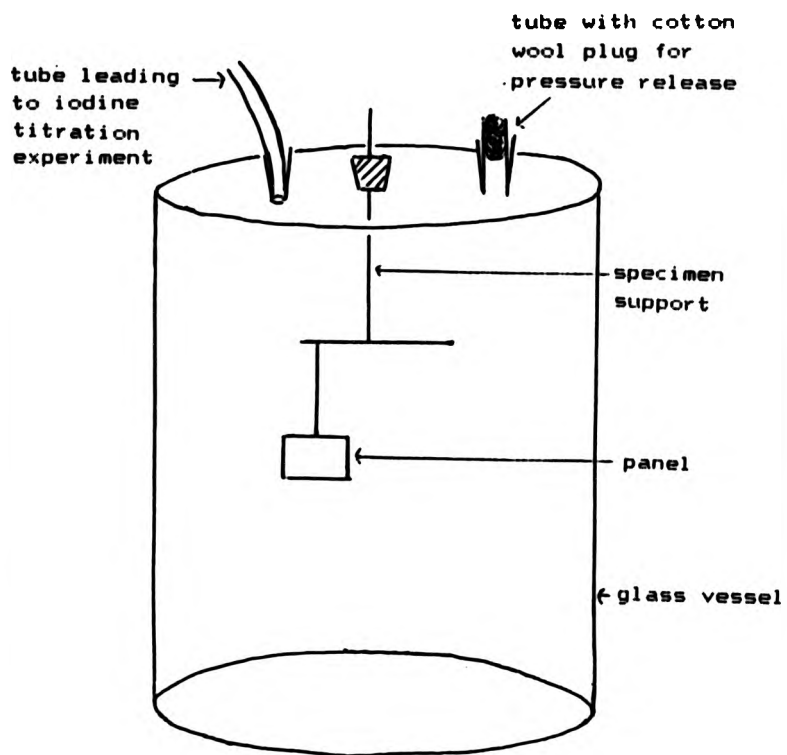


Fig. 30

CHAPTER 4

RESULTS

4.1 The Admittance Drift Test

Concentrated nitric acid and Solution 'A' of the Dye Spot Test (section 3.5.4) were used as alternative test solutions to potassium sulphate (3.5% by wt) for the admittance test. Each was used in an Anotest cell and the change of admittance was measured over a known period of time. The 'admittance drift', \dot{Y} , was evaluated by the following equations:

$$\dot{Y}(25^{\circ}\text{C}) = \frac{Y'' - Y'}{T'' - T'} \quad (\text{S} \times 10^{-6}/\text{min}) \quad (4.1)$$

and the admittance x thickness product drift:

$$\dot{Yt}(25^{\circ}\text{C}) = \frac{Yt'' - Yt'}{T'' - T'} \quad (\text{Sm} \times 10^{-12}/\text{min}) \quad (4.2)$$

where Y'' is the final admittance reading, using HNO_3 (conc) or solution 'A' in a cell 13mm in diameter.

Y' is the initial admittance reading,

Yt'' is the final admittance x thickness product,

Yt' is the initial admittance x thickness product,

$T'' - T'$ is the time (min) over which admittance is measured.

The admittance reading (or admittance x thickness product) at the initial time was subtracted from the reading at the final time and this was divided by the total test time, which was usually 10 min.

Results for panels sealed in deionised water for 1, 2 and 3 min/ μm (panels 494, 495 and 496 respectively), are given in Table 16.

Table 16

Panel	Yt(25°C) K ₂ SO ₄ (Sm x 10 ⁻¹²)	Ȳt(25°C) HNO ₃ (Sm x 10 ⁻¹² /min)	Ȳt(25°C) Solution 'A' (Sm x 10 ⁻¹² /min)
494	318	-0.3 (266)	1.2 (312)
495	224	-0.3 (183)	1.2 (243)
496	194	-0.6 (227)	0.9 (195)

N.B. Figures in parentheses refer to the Yt(25°C) values obtained using the alternative electrolyte to K₂SO₄.

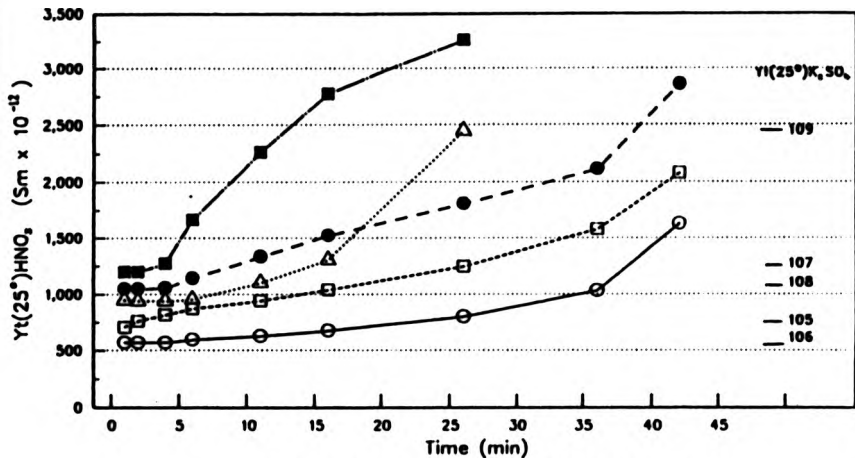
Yt(25°C) decreased as sealing time increased for the electrolytes potassium sulphate and Solution 'A', but panel 495 had a lower Yt(25°C) value than 496 for concentrated nitric acid. The negative values for Ȳt(25°C) using nitric acid showed that the admittance values decreased over 10 min. Those for Solution 'A' showed a positive 'drift' in admittance with time. A Three Paper

Abrasive Test showed that all three panels were scratched by Garnet.

Panels which had been subjected to a period of weathering of 82 weeks (see Results section 4.9) had admittance measured using concentrated nitric acid and $\dot{Y}_t(25^\circ\text{C})$ and $\dot{Y}(25^\circ\text{C})$ evaluated, on exposed faces only. Graphs 1a, 1b, and 1c show how $\dot{Y}_t(25^\circ\text{C})$ varied with admittance test time, using concentrated nitric acid as the electrolyte. $\dot{Y}_t(25^\circ\text{C})$ measured using potassium sulphate is indicated on the graphs. Graph 1a showed how $\dot{Y}_t(25^\circ\text{C})$ increased with time for unsealed panels. Partially sealed panels 112 and 113 showed an increase while 110, 111 and 114 remained parallel to the x axis. A similar pattern was found in Graph 1c where panel 119 alone increased in $\dot{Y}_t(25^\circ\text{C})$ over 60 min. $\dot{Y}_t(25^\circ\text{C})$ and $\dot{Y}(25^\circ\text{C})$, front of panels, can be related to the shape of the graphs. Lines parallel to the x axis gave values of 42.0 for $\dot{Y}_t(25^\circ\text{C})$ and 0.1 for $\dot{Y}(25^\circ\text{C})$.

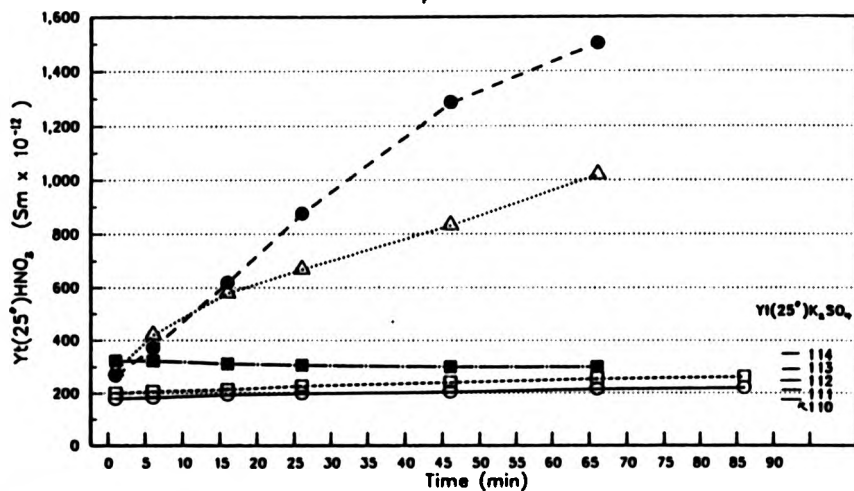
The Admittance Drift Test was performed on aged coloured panels, anodised under standard conditions, Table 17. Panels 439, 440 and 441 were coloured in a standard tin solution while 442, 443 and 444 were coloured in a solution containing Tribrite (see Results section 4.15 Graph 32, Experiments 164 and 166). 439 to 444 were aged for 23 weeks. 'Cow Gum' was used to seal the Anotest rings to the panels 439 to 444, and to prevent the electrolyte from creeping under the ring. ('Cow Gum' is a solution of unvulcanised rubber in an aromatic solvent.) If the electrolyte does creep under the cell wall, this creates a

Graph of $Y_I(25^\circ)HNO_2$, against Time for Unsealed Panels
Graph 1a



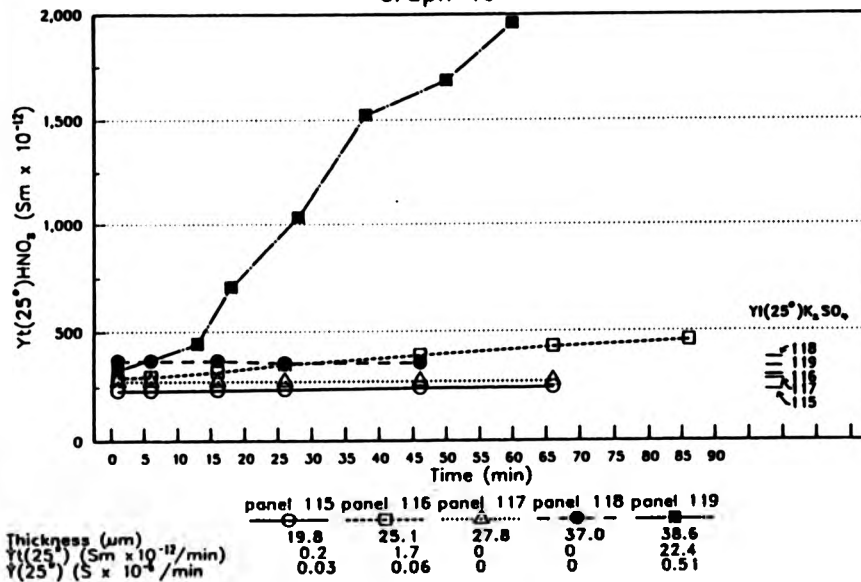
	panel 105	panel 106	panel 107	panel 108	panel 109
Thickness (μm)	19.6	24.8	30.2	34.2	39.0
$\dot{Y}_I(25^\circ)$ ($Sm \times 10^{-12}/min$)	7.2	22.1	23.9	31.7	105.1
$\dot{Y}(25^\circ)$ ($S \times 10^{-4}/min$)	0.3	0.8	0.73	0.83	2.42

Graph of $Y_I(25^\circ)HNO_2$, against Time for Partially Sealed Panels
Graph 1b

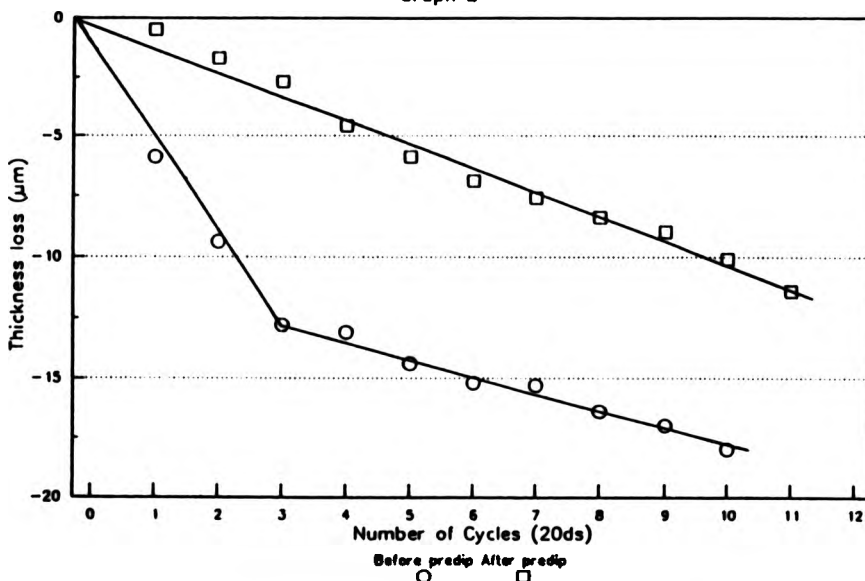


	panel 110	panel 111	panel 112	panel 113	panel 114
Thickness (μm)	19.8	25.5	28.0	36.0	38.6
$\dot{Y}_I(25^\circ)$ ($Sm \times 10^{-12}/min$)	1.1	0.9	17.3	25	-0.7
$\dot{Y}(25^\circ)$ ($S \times 10^{-4}/min$)	0.05	0.03	0.53	0.16	-0.02

Graph of $\gamma(25^\circ)\text{HNO}_3$ against Time for Fully Sealed Panels
 Graph 1c



Graph of Film Thickness Loss against Number of
 20ds Cycles: Panel 528
 Graph 2



positive error in the admittance drift. The $Y_t(25^\circ\text{C})$ values are those measured using potassium sulphate, when the panels were processed, and those in parentheses are the $Y_t(25^\circ\text{C})$ values after ageing. All values decreased after the ageing period. $\dot{Y}_t(25^\circ\text{C})$ and $\dot{Y}(25^\circ\text{C})$ after ageing, gave consistent results for panels 439 to 444. Panels 441 and 444 gave results less than 2.0 and 0.1 for $\dot{Y}_t(25^\circ\text{C})$ and $\dot{Y}(25^\circ\text{C})$ respectively.

Table 17

Panel	Colouring Time (min)	$Y_t(25^\circ\text{C})$ ($\text{Sm} \times 10^{-12}$)	$\dot{Y}_t(25^\circ\text{C})$ HNO_3 ($\text{Sm} \times 10^{-12}/\text{min}$)	$\dot{Y}(25^\circ\text{C})$ HNO_3 ($\text{Sm} \times 10^{-6}/\text{min}$)
439	15	21048 (12272)	339	18
440	8	5269 (3782)	93	4.8
441	3	446 (275)	1.9	0.1
442	15	4957 (2612)	88	3.8
443	8	1769 (1040)	5.3	0.24
444	3	345 (237)	0.9	0.04

Oversealed panels (sealing times 5, 6 and 7 min/ μm) which had aged for 3 months showed negligible admittance drift.

The value of $\dot{Y}(25^\circ\text{C})$ for aged panels, which had been anodised and soaked in sulphuric acid at elevated temperatures was measured using concentrated nitric acid,

Table 18

Panel	Anodising Temperature (°C)	Soaking Temperature (°C)	Thickness Loss (µm)	Thickness	Thickness Wear Index (L.R.)
519	26	-	0.6	aged 80 days	2.05
520	31	-	7.3		
522	31	37	10.6		
526	29.5	26	6.7		
546	15	26	0.8	aged 49 days	1.05
548	15	36.5	0		
550	15	30	0.8		
552	15	18.5	1.2		

Table 20

Panel	Thickness Wear Index (L.R.)		Predip Weight Loss (g/m ²)
	Original	After Predip	
479	1.1	1.0	0.42
480	0.7	0.6	0.41
513	1.7	1.6	0.62
528	2.8 whole film	2.9 whole film	11.02
	9.3 outer film		
	1.9 inner film		

L.R. indicates value was found by linear regression.

Table 18. 'Cow gum' was used to seal the Anotest rings to the panels. The admittance drift was negligible for panels 519, 546, 548, 550 and 552; and -0.1, -0.1 and -0.05 for panels 520, 522 and 526 respectively. Table 18 shows the conditions under which the panels were processed. Panels were soaked for 8 min. The thickness loss refers to the reduction in film thickness on the admittance test area after immersion in the concentrated nitric acid. Significant losses were recorded for panels 520, 522 and 526. The thickness wear indices, found by the linear regression method, measured immediately after the panels were produced showed they carried very soft films.

Subsequent experiments have been performed in which the technique for measuring admittance drift has been refined. The results for new tests performed on the panels mentioned above and on others, are given in section 4.3.

4.2 The Nitric Acid Predip

Panels were immersed in 33% nitric acid for 10 min at room temperature. The weight loss and/or abrasion resistance were found. The thickness wear indices were evaluated from the following equation:

$$\text{Wear Index} = \frac{\text{thickness loss equivalent to 400ds at 400gf (2.8)}}{-7.43}$$

Table 19 gives the histories of the panels tested.

Table 19

Expt/Panel	Histories
171/479	Anodised at 15°C, soaked at 38°C,
171/480	Anodised at 15°C,
183/513	Anodised at 24.5°C, coloured at 22.5°C,
183/517	Anodised at 26°C, coloured at 38°C,
183/518	Anodised at 26°C, soaked at 37.5°C,
183/528	Anodised at 30°C, soaked at 30°C,
193/553	Anodised at 25°C, sulphur dioxide test for 6 hours at 50°C.

Table 20 gives the thickness wear indices found by the linear regression method (section 3.5.9) and the predip weight loss in g/m². The thickness wear indices for panels 479, 480 and 513 were not changed by the predip and weight losses were small. Panel 528 revealed a slightly harder film after the predip and suffered a substantial weight loss. Graph 2 shows how two distinct layers existed before the predip, but only one afterwards.

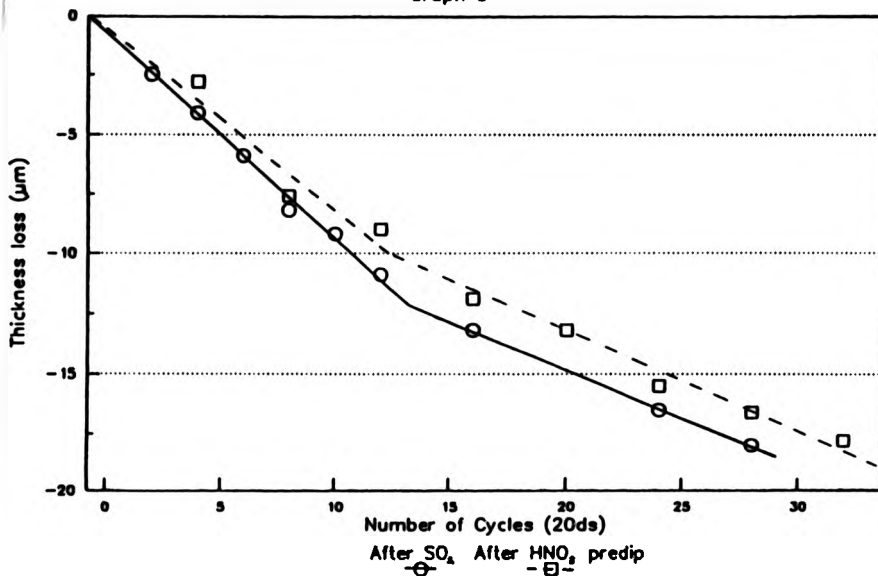
Table 21 gives the thickness wear indices for another set of panels before the predip. Panel 528 had already been subjected to the test as in Table 20.

Table 21 gives the thickness wear indices and weight losses for panels 517, 518, 528 and 553 after the predip. Panels 517 and 518 showed a substantial weight loss and the thickness wear indices revealed the films remained

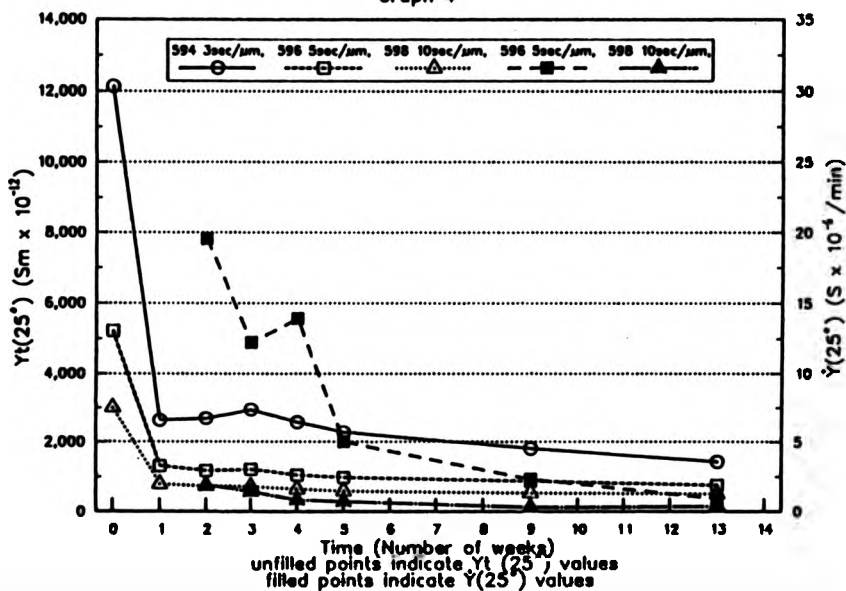
Table 21

Panel	Thickness Wear Index (L.R.)	Thickness Wear Index After Predip (L.R.)	Predip Weight Loss (g/m ²)
517	4.0	3.0	7.5
518	3.3	3.4	4.2
528	2.8 whole film 9.3 outer film 1.9 inner film 2.9 after predip	3.0	0.5
553	1.8 whole film 2.3 outer film 1.1 inner film	1.5 whole film 2.1 outer film 1.0 inner film	1.5

Graph of Film Thickness Loss against Number of
20ds Cycles : Panel 553
Graph 3



Graph of $\dot{Y}_t(25^\circ)$ and $\dot{Y}(25^\circ)$ against Time:
Panels 594, 596 and 598
Graph 4



soft. There was only a small weight loss for panel 528 after the second nitric acid predip but the film remained soft. The thickness wear indices for panel 553 after the sulphur dioxide test, but before the predip, showed that there was a slightly soft film as a whole, but there was a harder underlying film above which a softer film was present. There were no significant changes for the values for the outer and inner layers, although the thickness wear index indicated a slightly harder film as a whole. Some weight loss was observed. Graph 3 shows how these values were represented as thickness loss against number of 20 ds cycles.

Further experiments have been performed to observe any thickness loss caused by nitric acid dissolution and to calculate the abrasion resistance on panels subjected to varying periods of immersion in nitric acid. The results are given in section 4.3.

4.3 Improved Admittance Drift Test

Concentrated nitric acid in the cell tended to undermine the film at the ring edges and creep. This enlarged the test area and added a false drift to any real one. Attempts to use a circle of absorbent paper with a waxed circle and a stainless steel 13mm cylinder were better, but there was still creep. A method was devised to avoid creep of the nitric acid as follows:

Potassium sulphate was used in the normal manner for measuring the original admittance of the film for the

modified technique. A reading was taken at 1 min intervals for a period of 5 min. The solution was washed off and the cell dried with tissue paper. A solution of 33% nitric acid was introduced into the same cell (13mm) and left for a period of 10 min. At the end of this period it was washed off, the cell removed, and the panel dried. A fresh cell was placed on exactly the same area, potassium sulphate solution introduced and the admittance measured at 1 min intervals for a period of 5 min.

Admittance drift:

$$\dot{Y}(25^{\circ}\text{C}) = \frac{Y'' - Y'}{10} \quad (\text{S} \times 10^{-6}/\text{min}) \quad (4.1)$$

Admittance x thickness product drift:

$$\dot{Y}_t(25^{\circ}\text{C}) = \frac{Y_t'' - Y_t'}{10} \quad (\text{Sm} \times 10^{-12}/\text{min}) \quad (4.2)$$

where Y' is the admittance using 3.5% K_2SO_4 at 1 min after introducing the solution,

Y'' is the admittance using a fresh cell, applied to the area exposed for 10min to 33% HNO_3 , using 3.5% K_2SO_4 with the conditions as for Y' .

Y_t is the admittance x thickness product.

The $Y_t(25^{\circ}\text{C})$ values of panels 439 to 444 aged 2 years and 1 week (Table 22) can be compared to those of Table 17, where the $Y_t(25^{\circ}\text{C})$ values are for the fresh film

Table 22

Panel	Yt(25°C) (Sm x 10 ⁻¹²)	Ageing Period	ȳ(25°C) (S x 10 ⁻⁶ /min)	Thickness Wear Index (L.R.)
439	7744	2 years 1 week	48.9	-
440	2635		4.7	-
441	178		0.13	-
442	2738		6.6	-
443	1230		1.2	-
444	166		0.1	-
546	139(293)	1 year	0.13	1.02
548	169(356)	7 months	0.09	1.32
519	170(307)	1 year	0.19	2.37
520	295(581)	8 months	0.25	4.63
526	363(655)		0.21	6.3

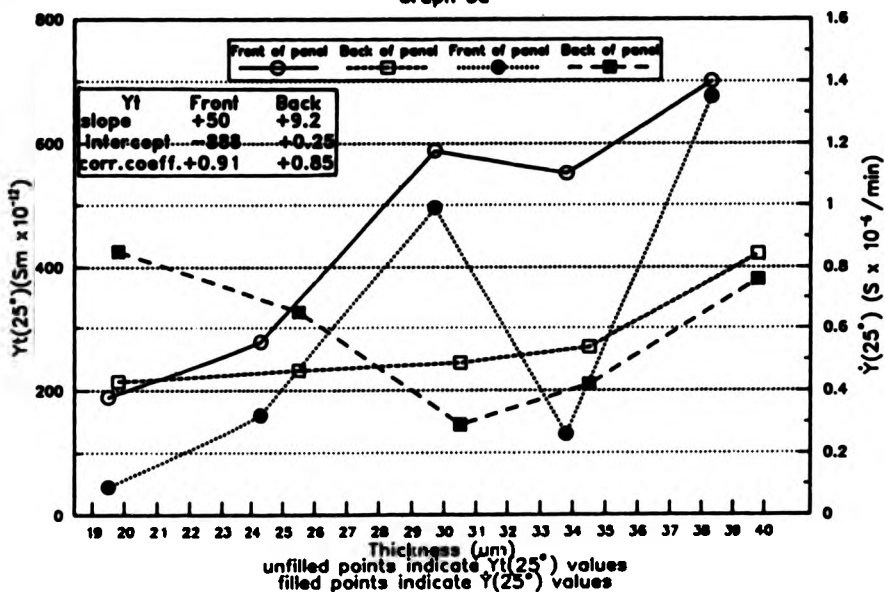
N.B. Yt(25°C) values in parentheses are those after ageing periods as in Table 18: Panels 546 and 548 aged 49 days, panels 519, 520 and 526 aged 80 days.

and after an ageing period of 23 weeks. $Y_t(25^\circ\text{C})$ had decreased for all the panels except 442 and 443 which had increased slightly during the period 23 weeks to 2 years and 1 week. The new admittance drift test gave results comparable to the old method, $\dot{Y}(25^\circ\text{C})$ Table 17. Panels 441 and 444 passed the $Y_t(25^\circ\text{C}) < 500$ criterion. The remaining panels in Table 22 (process conditions as in Table 18) were placed in order of the thickness wear indices. The thickness wear indices had been measured immediately after anodising. The admittance drift values roughly followed this pattern. The old method gave negligible and small negative values. The values of $Y_t(25^\circ\text{C})$ halved during the ageing periods of 49 days to 1 year and 7 months (panels 546 and 548), and 80 days to 1 year and 8 months (panels 519, 520 and 526).

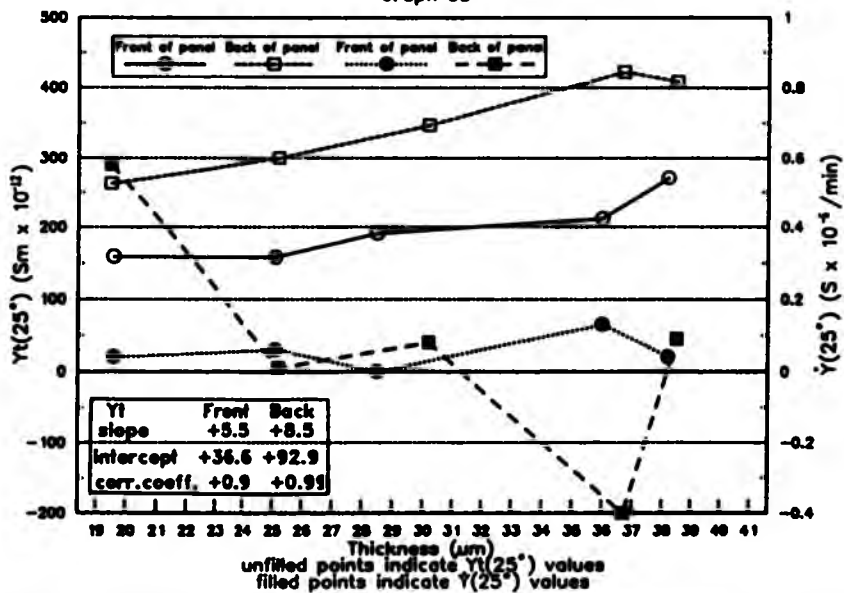
Graph 4 shows the change in $Y_t(25^\circ\text{C})$ and admittance drift with time for panels sealed in 'Alcoa 482' for 3, 5, 10 sec/ μm (panels 594, 596 and 598 respectively). Both measurements decreased with time.

The admittance drift, $\dot{Y}(25^\circ\text{C})$, results for the Weathering Experiment panels (section 4.9) are compared to $Y_t(25^\circ\text{C})$ in Graphs 5a, 5b and 5c, where the abscissa is in microns. The panels had been exposed for 3 years and 7 months. The unsealed panels (Graph 5a) showed erratic changes for the admittance drift. Both lines lay above the value of 0.1. The line for $Y_t(25^\circ\text{C})$ for the front of these panels did not lie below $500/t \mu\text{S}$. The front of the partially sealed panels (Graph 5b) showed a steady line^{for \dot{Y}} , while that of the back showed an overall decrease. Both

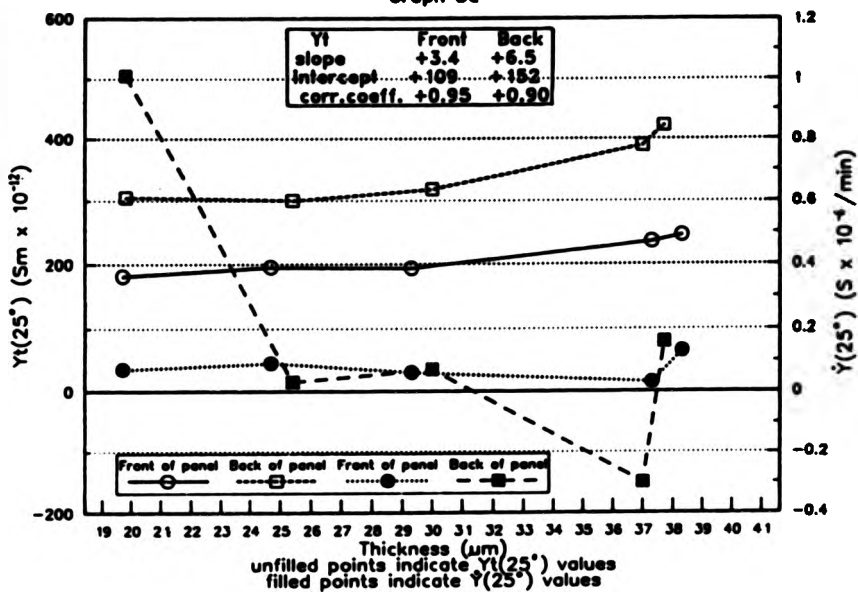
Graph of $\gamma_t(25^\circ)$ and $\dot{\gamma}(25^\circ)$ against Thickness:
Unsealed Panels
Graph 5a



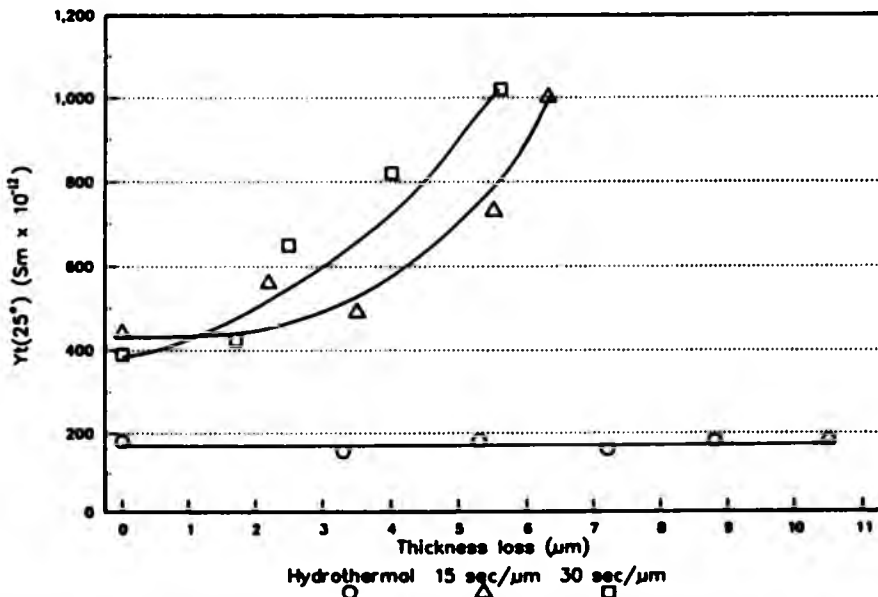
Graph of $\gamma_t(25^\circ)$ and $\dot{\gamma}(25^\circ)$ against Thickness:
Partially Sealed Panels
Graph 5b



Graph of $Y_t(25^\circ)$ and $\dot{Y}(25^\circ)$ against Thickness:
Fully Sealed Panels
Graph 5c



Graph of $Y_t(25^\circ)$ against Film Thickness Loss
Graph 6



lines lie below the $\dot{Y}(25^{\circ}\text{C})$ value of 0.1, except for a single point. The admittance drift for the front of the fully sealed panels (Graph 5c) gave a line parallel to the abscissa, with values below 0.1. $\dot{Y}(25^{\circ}\text{C})$ for the back of the panels gave varying values for the thinnest and thickest films.

4.4 Thickness and Weight Loss Due to Nitric Acid Immersion

Table 23 gives the thickness wear indices in increasing order. The 33% HNO_3 predip weight loss (Tables 20 and 21) was included in order to compare with the thickness lost after 33% nitric acid was put in a cell for 10 min and then washed off. Significant thickness loss was observed for panels 520 and 527. Panels 517, 518 and 528, having similar large thickness wear indices to the latter panels, also showed large predip weight losses.

Panels anodised under standard conditions were sealed for varying periods of time and all were immersed in 33% nitric acid for increasing lengths of time. This was done to see whether HNO_3 itself had a role in softening films as distinct from dissolving films already softened by other agents. The thickness wear indices after the acid soak averaged 0.48. The only significant effect of nitric acid immersion was that the poorly sealed film soaked for 16 hours and the well sealed film not soaked showed some softening, although the hardness remained acceptable. The alloy used was NS4. The panel sealed for 5 min/ μm and soaked for 4 hours was tested a second time revealing a

Table 23

Panel	Thickness Wear Index (L.R.)	Pre-dip Weight Loss (g/dm ²)	Thickness Loss (µm)
480	0.7	0.42	-
477	0.8	-	1.4
479	1.1	0.41	-
476	1.6	-	2.2
513	1.7	0.62	-
514	1.7	-	0.6
528	2.8	11.02	-
520	2.9	-	6.8
518	3.3	4.2	-
527	3.8	-	7.9
517	4.0	7.5	-

value more in line with the others than the first.

4.5 Sealing with 'Alcoa 482'

Panels were sealed for various times in a proprietary solution 'Alcoa 482', the composition of which was 4.5g/l nickel acetate and 1g/l sulphuric acid made up to a pH of 5.5 to 6.0. Admittance was measured and a Phosphoric Acid/Chromic Acid Test (PCA) was performed on the sealed films.

Initially the panels were dried before sealing, but this gave rise to very variable $Y_t(25^\circ\text{C})$ values, and a sealing time of 75 sec/ μm did not pass the test. The PCA test also gave variable results. PCA values of 3.0g/m² and 3.1g/m² were achieved for sealing times of 10 and 35 sec/ μm respectively. However, a sealing time of 25 sec/ μm gave a range of values, the lowest being 2.06g/m² and the highest 5.15g/m².

Further experiments were done where the panels were not dried before sealing. A sealing time of 60 sec/ μm passed the PCA test at 2.9g/m². $Y_t(25^\circ\text{C})$ was not passed for this time, ($1279\text{Sm} \times 10^{-12}$). A subsequent experiment was performed using the 'Alcoa 482' solution at ten times the concentration. $Y_t(25^\circ\text{C})$ was not passed, but PCA values of 2.4 and 2.6g/m² were achieved for 15 sec/ μm .

Subsequent experiments have been carried out to show how the PCA test and $Y_t(25^\circ\text{C})$ can be passed at very short sealing times, as follows:

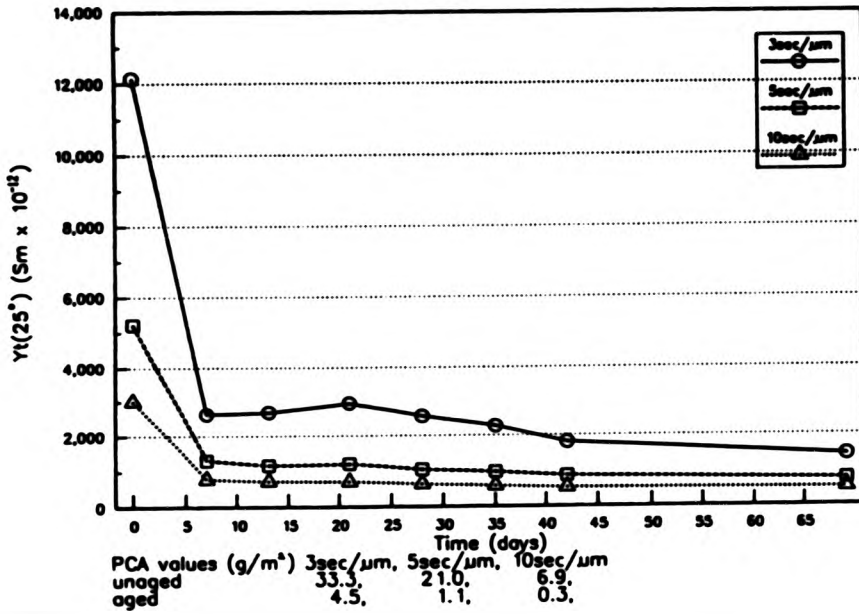
It was found that if panels sealed in 'Alcoa 482' were left to 'age', then both Yt(25°C) and PCA test were eventually passed. Table 24 gives the results of Experiment 3A where panels were aged for 14 days.

Table 24

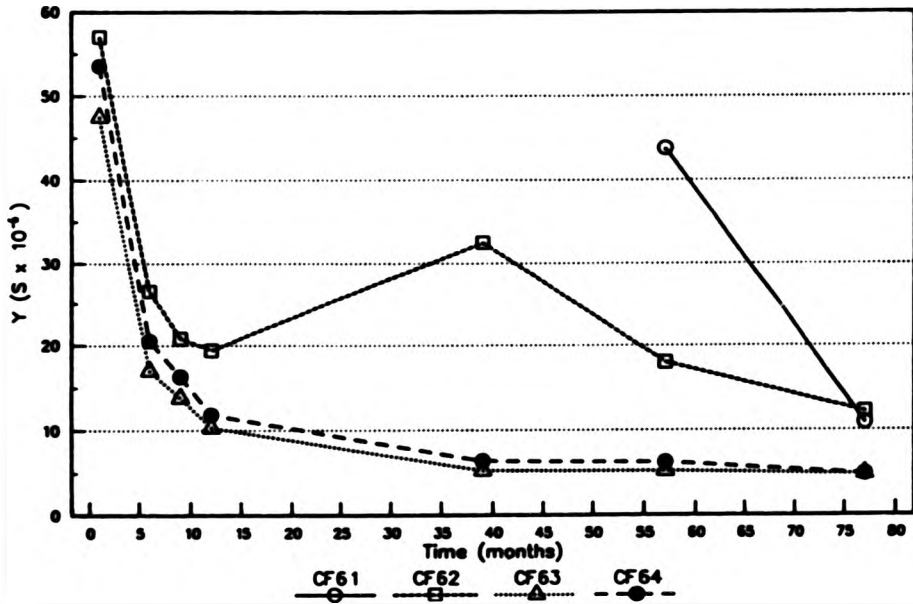
Sealing Time (sec/μm)	'Unaged' Yt(25°C) (Sm x 10 ⁻¹²)	PCA (g/m ²)	'Aged' Yt(25°C) (Sm x 10 ⁻¹²)	PCA (g/m ²)
5	7295	25.7	864	5.1
15	3056	6.5	523	2.6
30	1129	1.4	412	1.2

The PCA test was passed after 14 days for the panel sealed for 15 sec/μm, and although the PCA test was passed on the same day as anodising for the sealing time of 30 sec/μm, Yt(25°C) criterion was not reached until the film had aged. Graph 6 shows Yt(25°C) versus abrasion loss (section 3.5.10) for sealing times of 15 and 30 sec/μm, panels 590 and 592 respectively. This analysis was carried out on the panels after they had had the PCA test. The x axis shows the thickness removed by the abrasive wheel after every 100 double strokes. An hydrothermally sealed panel, [933.2], was included as a comparison. However, this had not had a PCA test. This gave a line horizontal to the x axis, while the 'Alcoa 482' sealed panels showed increase in Yt(25°C) as thickness was removed. The thickness wear indices as found by linear regression of thickness loss versus the

Graph of $Y_t(25^\circ)$ against Time
Graph 7



Graph of $Y(25^\circ)$ against Time
Graph 8



number of double strokes for panels 590 and 592 were 0.85 and 0.64 respectively. That of panel [933.2] was 0.99. Panel 588, sealed for 5 sec/ μm , was analysed by the abrasive wheel method, but it was found that the $Y_t(25^\circ\text{C})$ value was of the order of 10^6 . No graph was drawn.

Panels were aged for 63 days (Expt.7A), but sealed for shorter times than Expt. 3A. A sealing time of 5 sec/ μm passed the PCA test after the ageing period, and $Y_t(25^\circ\text{C})$ was borderline to passing for 10 sec/ μm . Graph 7 shows the decrease of $Y_t(25^\circ\text{C})$ with ageing.

4.6 Long Term Cold Sealing

Anodic oxide films 25 μm in thickness were formed by anodising for 33min at 2.4A/dm² and at a temperature of 12°C. They were not sealed but immersed on 8/9/81 as follows:

1. CF61 and CF62 in deionised water,
2. CF63 and CF64 in 5g/l nickel acetate and 5g/l boric acid.

The present investigation made various tests on these panels at 39, 57 and 77 months after immersion. Previous data is included with these results.

The admittance value $Y(25^\circ\text{C})$ was recorded over 77 months, Graph B. The values decreased with time. Panel CF61 gave readings of $>300\mu\text{S}$ until the two final readings:

57 months	43.75 μS
77 months	10.9 μS

During the period 0 to 12 months there was a slow increase in mass; about +0.08g in water and +0.14g in nickel solution. During the period 39 to 57 months there was a slight decrease in mass; about -0.05g in water and -0.02g in nickel solution. After 12 months the panels were cut in half and half was used for destructive sealing tests (failed). The remaining panel was cut in half again after 57 months and a phosphoric acid/chromic acid test conducted on one half of each panel, PCA Test, Table 25. The panels immersed in water failed the test while those immersed in the nickel solution were borderline failures. The thickness wear indices were measured at 57 months which showed the films sealed in nickel acetate to be harder than those sealed in water. All the films have acceptable hardness values, Table 25. The Dye Spot Test showed that CF63 and CF64 passed the test, but the test solutions discoloured the films of CF61 and CF62. This result could not be compared to the standard test chart. At 57 and 77 months an Anotest cell containing concentrated nitric acid was placed on the panels for 40 min and 10 min respectively. The change in thickness was recorded, Table 25. There was a small thickness loss for panels CF61 and CF62 at 57 and 77 months. Panels CF63 and CF64 showed a very small loss at 57 months but a negligible thickness gain at 77 months.

Table 25

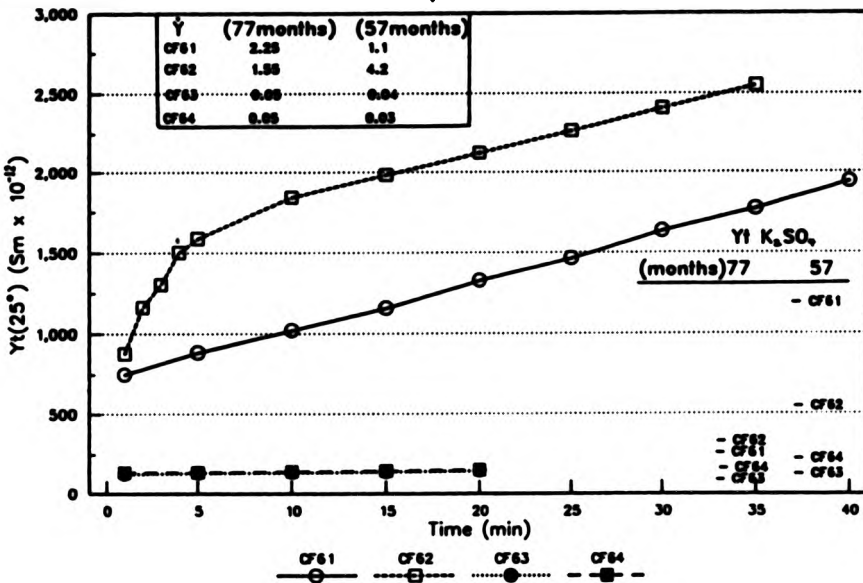
Panel	PCA Test Loss g/m ²	Thickness Wear Index	Dye Spot Test	Thickness change (g)	
				57m	77m
CF61	8.06	0.94	white mark	-1.9	-1.15
CF62	14.36	1.09	white mark	-1.9	-1.0
CF63	4.43	0.32	1	-1.0	+0.4
CF64	4.34	0.42	1	-0.6	+0.1

Graph 9 shows the $Y_t(25^\circ\text{C})$ values using concentrated nitric acid against time. The panels sealed in the nickel solution have constant $Y_t(25^\circ\text{C})$ values while those sealed in water are much higher and increase over time. The admittance drift values recorded after 77 months showed high values for the panels sealed in water but small values for those sealed in the nickel solution. Graph 10 is the abrasion profile of 50 double strokes at 300gf against thickness loss. Panels CF61 and CF62 showed an underlying film which was harder than the surface film. The other panels showed the films to have the same hardnesses throughout.

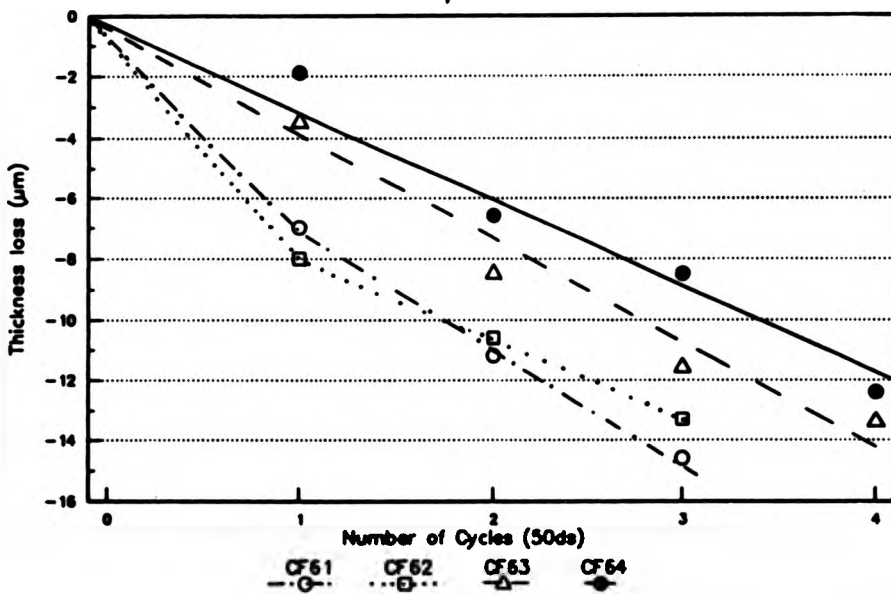
4.7 Sulphur Dioxide Test

Experiments were performed using combinations of 0.5% and 0.5N, 1% and 1N, 2% and 2N, and 4% and 4N sodium thiosulphate and sulphuric acid respectively in both the 30 litre and 5 litre vessels as described in section 3.6.1.

Graph of $\gamma_t(25^\circ)$ [conc. HNO_3] against Time:
57 months, front of panels
Graph 9



Graph of Film Thickness Loss against Number of
50ds Cycles:3000gf
Graph 10



Panels were sealed for 0.25min/ μm and 3min/ μm in deionised water and others were left unsealed. Sulphur dioxide gas was analysed as described in section 3.6.2 and the percentage was found to be between 0.32% and 0.6% for the 8% and BN combination.

The appearance of the panels after the tests was recorded and compared to the length of sealing time. Generally it was found that unsealed panels were very badly corroded while panels sealed for 0.25min/ μm , although corroded, did not show such heavy corrosion. Those panels sealed for 3min/ μm gave results which varied from no corrosion to quite heavy corrosion products. It was subsequently observed that the anodic oxide on the sealed panels experienced 'thermal shock' when the cold panels were immersed directly in the boiling sealing solution. This caused the anodic oxide film to crack (craze), leaving the aluminium prone to corrosion at the discontinuities. Initially, the appearance of 'blisters', glassy films, dried yellow crystalline deposits and white powder were believed to indicate the formation of corrosion products, but when panels were cleaned, removing the surface deposits, a bloom or iridescence was seen to be present on the oxide film beneath. The surface deposits, although more voluminous on badly corroded panels, were in fact the result of spray from the sulphuric acid and sodium thiosulphate. The effervescence produced products which collected and dried on the panels. This false indication of corrosion was avoided by positioning the panels further away from the reacting solutions. The optimum

concentrations were found to be 8% sodium thiosulphate and 8N sulphuric acid. The method of assessing the corroded panels was as follows : a light was shone obliquely onto the surface of the panels, which were viewed against a dark background perpendicular to their plane. The panels were viewed at eye level. A panel was deemed to pass the test and to be well sealed if no bloom nor iridescence was visible after cleaning

Table 26 gives the results of sulphur dioxide tests on panels sealed in a buffered nickel acetate solution. However, these results and those of Tables 27 and 28 must be interpreted with caution since the panels had been allowed to dry after anodising and before being sealed. The oxide film on panels in Tables 27 and 28 were found to be cracked to varying degrees, which influenced the results. $Y_t(25^\circ\text{C})$ values, before the sulphur dioxide test, for panels in groups '62' and '64' are comparable, while those of group '63' are higher. This was probably because the latter panels were sealed 4 days after anodising. The values of $Y_t(25^\circ\text{C})$ measured after the sulphur dioxide tests show that, for the test conducted at room temp (group '62') there was a decrease. Values obtained after a test at 38°C were generally higher than the initial ones. Values found after the room temperature sulphur dioxide test carried out on panels sealed 4 days after anodising, show both increases and decreases.

In the high temperature sulphur dioxide test, all the panels failed with severe corrosion. The panels sealed 4 days after anodising also failed. However group '62'

Table 26

Panel	Sealing Time (min/ μ m)	Notes/Sulphur Dioxide Test Conditions	Appearance after Sulphur Dioxide Test	Yt(25°C)	
				(8m x 10 ⁻¹²)	
				Before	After
62/1	0.33	Room temp. 21.5 hours	Slight bloom	10978	4254
62/2	0.5	"	A little bloom	5844	2992
62/3	0.7	"	around	2565	1936
62/4	0.83	"	identification mark	1170	1712
63/1	0.33	Sealed after 4 days/ Room temp. 22 hours	Bloom	17928	12422
63/2	0.5	"	Patchy bloom	11620	10067
63/3	0.7	"	"	6754	7661
63/4	0.83	"	"	3412	3715
64/1	0.33	38°C, 22 hours	Heavy bloom	11766	8309
64/2	0.5	"	"	4368	6752
64/3	0.7	"	"	3789	13500
64/4	0.83	"	Bloom	1452	8249
67/2*	0.7	38°C 24 hours	Bloom	596	525
67/4*	0.75	"	"	530	343
68/2*	0.83	"	"	480	322

Table 27

(Sulphur Dioxide Test Conditions were 38°C for 24 hours)

Panel	Sealing Time (min/ μ m)	Appearance after Sulphur Dioxide Test	Yt(25°C) ($8\mu \times 10^{-12}$)	
			Before	After
65/1	1	Bloom	2649	-
65/2	8	"	234	-
69/2	2	Slight bloom	225	282
69/3	8	Irridescence	149	686
70/1	2	Bloom	280	1676
70/2	3	"	237	1757
70/3	4	"	201	1185
70/4	5	"	187	2745

Table 28

Panel	Sealing Time (min/ μ m)	Notes/Sulphur Dioxide Test Conditions	Appearance after Sulphur Dioxide Test	Yt (25°C)	
				(Sm x 10 ⁻¹²)	
				Before	After
98/1	0.17	Room temp. 6 hours	Slight bloom	2248	-
98/2	0.75	"	No bloom	607	-
98/3	1.5	"	"	396	-
98/4	5.35	"	Slight bloom	230	-
72/1	1	40°C, 24 hours	Slight bloom	477	1075
72/3	3	"	Speckled bloom	231	1266
72/2	1	40°C, 6 hours	Slight bloom	421	380
72/4	3	"	"	230	236
71/4	"	"	No bloom	220	235
97/1	0.17	40°C, 6 hours	"	2658	-
97/2	0.75	"	"	515	-
97/3	1.5	"	"	390	-
97/4	5.35	"	"	234	-
99/1	0.17	50°C, 6 hours	Heavy bloom	2571	-
99/2	0.75	"	Bloom	597	-
99/3	1.5	"	"	390	-
99/4	5.35	"	"	228	-

Table 28 continued

Panel	Sealing Time (min/ μ m)	Thickness/ Sulphur Dioxide Test Conditions	Appearance after Sulphur Dioxide Test	Yt(25°C) ($8m \times 10^{-12}$) Before
142/1	5	9 μ m/ 50°C, 6 hours	Speckled	548
142/2	10	"	Slightly speckled	359
143/1	5	25 μ m/ 50°C, 6 hours	No bloom	215
143/2	10.4	"	Bloom	174

Table 29

Expt/ Panel	Dye Spot Test	Sulphur Dioxide Test Conditions	Appearance after Sulphur Dioxide Test	Yt(25°C) ($8m \times 10^{-12}$) Before
43/ 5 μ 0m	1	50°C, 6 hrs	Heavy bloom	3547
5 μ 3m	2	"	No bloom	110
25 μ 0m	5	"	Heavy bloom	19954
25 μ 3m	2	"	No bloom	136
56/ 5 μ 0m	3	50°C, 4 hrs	Heavy bloom	>7224
5 μ 3m	0	"	No bloom	91
25 μ 0m	5	"	Heavy bloom	>34776
25 μ 3m	1	"	No bloom	108

failed with only slight corrosion. Panels marked with an asterisk (67/2, 67/4, 68/2) had had a room temperature, 24 hour sulphur dioxide test before the (second) test in Table 26. The appearance of the panels after the first test showed very slight spotting. $Y_t(25^\circ\text{C})$ values decreased marginally after the first test to the figures in the 'before' column of Table 26. After the second test a more pronounced bloom was observed, and again the $Y_t(25^\circ\text{C})$ values decreased slightly. The values of $Y_t(25^\circ\text{C})$ for panels 67/2, 67/4 and 68/2 were much lower than those of the other panels.

The results of a sulphur dioxide test and corresponding values of $Y_t(25^\circ\text{C})$ are given in Table 27 for panels sealed in deionised water. The surfaces were washed and rinsed in deionised water after the sulphur dioxide test. Panels 65/1 and 65/2 showed very erratic values of $Y_t(25^\circ\text{C})$ after the test indicating that the oxide films were severely cracked, also indicated by a bloom on each. Panels 69/2 and 69/3 failed but the corrosion was slight, and only iridescence was observed on 69/3, which had been sealed for 8min/ μm . Group '70' all failed the test. The values of $Y_t(25^\circ\text{C})$ fell within a narrow range, and all had increased after the test.

Other panels, sealed in deionised water, were subjected to various sulphur dioxide tests, Table 28. The oxide films were allowed to warm up in the steam above the sealing bath before immersion so that crazing was avoided. Only the oxides on panels 72/3 and 72/1 were cracked. Groups '97', '98' and '99' had average oxide thicknesses of

11 μ m. The sulphur dioxide tests were performed either in a 5 litre glass vessel, or in a 4.94 litre 'perspex' box. Panels exposed to SO₂ at 40°C, for 24 hours developed only slight bloom but high Yt(25°C) values, after the test, showing that the oxides were cracked. Panels 72/2, 72/4 and 71/4 carried uncracked films, whose value of Yt(25°C) did not increase after the test. For them the 40°C, 6 hour test gave more satisfactory results. In the room temperature, 6 hour test both the poorly sealed and over-sealed films failed. Groups '97' and '99' tested at 40°C and 50°C respectively all failed. The oxide films on groups '97', '98' and '99' were not cracked, and had consistent values of Yt(25°C) for each range of sealing conditions. Panels 142/1, 142/2, 143/1 and 143/2 were sealed for long times. Those films sealed for 10min/ μ m or more failed by bloom formation caused by 'over-sealing'. For sealing times of 5 min/ μ m, the thinner film failed, but the 25 μ m film passed. The values of Yt(25°C) before the sulphur dioxide test were higher for the thinner films than for the 25 μ m films.

Other panels were sealed in 'Alcoa 482' solution for 1, 1.3, 1.7, and 2 min/ μ m. The sealed films passed both room temperature and 38°C sulphur dioxide tests, conducted for 6 hours. Only one panel, whose film had been sealed for 2 min/ μ m, passed Yt(25°C) before the SO₂ test. After the room temperature SO₂ test, the values of Yt(25°C) decreased slightly, so that a second film sealed for 2 min/ μ m passed. These films passed both the Dye Spot test and the phosphoric acid/chromic acid test prior to the SO₂ test.

Samples produced by Alcan Laboratories were also given various sulphur dioxide tests, Table 29. The panel notation gives the thickness, and sealing time in min/ μm , e.g. '5 μm 0m' means 5 μm sealed for 0min/ μm . In these tests the unsealed films failed both the sulphur dioxide tests and Yt(25°C), while those sealed for 3min/ μm passed all the tests. The '5 μm 0m' oxide films appeared to pass the Dye Spot test, but this was a false result caused by solution 'A' of the test (section 3.5.4) dissolving most of the surface oxide (removing 2-3 μm). There was so little film left to absorb the dye solution ('B'), that a false negative result was obtained. An SO₂ test carried out at 50°C for 2 hours made on a set of panels similar to those in Table 29, failed to distinguish between the sealed and unsealed samples.

4.8 Sealing Bloom

Films were not dried after anodising and were not cracked. Panels sealed for 1, 2, 3, 5, 6 and 7 min/ μm in ammonium acetate were tested in sulphur dioxide at the optimum conditions of 50°C and 6 hours. All panels passed Yt(25°C) except those sealed for 1 min/ μm which were borderline failures.

A set of panels was sealed for 1, 2 and 3 min/ μm . Only the oxide sealed for 1 min/ μm developed a bloom after the sulphur dioxide test. A strip of masking tape was placed across the surface of the panels to leave an area unattacked by the sulphur dioxide for comparison. For oxide films sealed for 2 and 3 min/ μm there was a noticeable

difference between the masked and unmasked areas (the masked area was darker than the unmasked area), but no bloom was observed. A three paper abrasion test (section 3.5.9), was carried out after the sulphur dioxide humidity test. Garnet paper carried a white powder residue after two applications of double strokes to the same area for all the panels. With glass paper the first ten strokes left a residue of white powder, but a further ten on the same area did not. A thin soft layer of a sealing bloom was detected by the sulphur dioxide and by the latter abrasion tests. These panels were anodised during December when the anodising electrolyte temperature was between 12°C and 14°C. Additional tests were performed during May when the anodising temperature was between 18 and 20°C. A set of panels was sealed for 1, 2 and 3 min/ μm and given a three paper abrasion test before the sulphur dioxide test. Garnet paper abraded the oxide on all three panels in two successive applications of ten double strokes. Glass paper did not abrade the oxides sealed for 1 min/ μm but gave a slight white powder residue for the first ten strokes, but not for a further ten strokes, with the other panels. No SO_2 bloom was found. The oxide film on another set of panels was sealed for 5, 6 and 7 min/ μm during May. No bloom developed when these oxides were tested in sulphur dioxide. The abrasion test (before SO_2) showed that garnet abraded all the films after two successive applications of ten strokes. Glass paper also gave slight white powder residues for two successive lots of ten strokes.

Two panels were anodised at a temperature of 25°C

(cross ref: Table 33, experiment 193). One oxide film was sealed for 2.3 min/ μm (panel 553) and the other for 6 min/ μm (panel 554). An overall bloom was formed on both oxide films after the sulphur dioxide test. Thickness wear indices equivalent to 400 ds at 400 gf were calculated from the linear regression of thickness loss against number of 20 ds cycles, Graph 23, for abrasive wheel tests made after the sulphur dioxide test. Both panels carried a soft outer film. Other panels anodised at elevated temperatures (experiment 195, panels 521 and 524) also investigated using the abrasive wheel tests, were found to have very soft outer layers of oxide. The underlying oxides although harder, were still unacceptably soft for architectural service conditions (cross ref: Table 34).

Samples designated 'A, B, C and D', anodised at 20°C, from another laboratory were also tested for the presence of a sealing bloom. Panels had been sealed for 60, 30, 15, and 5 min in the order B, C, A and D. 'D' did not pass Yt(25°C). They were subjected to a 50°C sulphur dioxide test for 6 hours. All developed a bloom and the order from best to worst was C, B, A and D. After the films had been exposed to SO_2 and were cleaned with water and acetone, they were given the following series of tests:

1. Abrasive Paper Test

All were abraded by garnet paper. Glass paper abraded A and D during the first ten strokes, but no white powder residues were observed after a further ten strokes on the same area.

2. Nitric Acid Predip Test

The specimens were immersed for half their length in 50/50 nitric acid for 10 min. There was a difference in appearance between the two halves.

3. Dye Spot Test

The oxide films on B and C gave the result 0, but a white mark remained on both halves after testing the films on A and D.

4. SO₂ Test (50°C for 6hours)

The order of increasing bloom was C, B, A and D after the second SO₂ test.

5. Colorimetry

There was no difference between that half of each panel which had been immersed in HNO₃ before or after the second sulphur dioxide test.

Other Alcan samples similar to those in Table 29 were tested with abrasive papers before and after a sulphur dioxide test, Table 30. White powder residues were observed after ten strokes with glass paper on both of the panels sealed for 3 min/ μ m but not for those unsealed, before the SO₂ test. A grey coloured powder residue on the garnet paper used on the 5 μ m films showed that this paper had cut through to the metal. The unsealed 25 μ m oxide film was not abraded by garnet as expected. After the sulphur dioxide

Table 30

Expt/ Panel	3 Paper Test before SO ₂	3 Paper Test after SO ₂	Dye Spot Test	Appearance after SO ₂ Test
142/ 5μ0m	G1:-(10) Gt:grey(20)	G1:white(10) grey(10) Gt:white(10)	1	Bloom
5μ3m	G1:white(10) Gt:grey(10)	G1:-(20) Gt:grey(10)	0	No bloom
25μ0m	G1:-(10) Gt:-(20)	G1:white(20) Gt:white(10)	1	Slight bloom
25μ3m	G1:white(10) Gt:white(10)	G1:white(20) Gt:white(10)	0	Slight bloom

Note: G1 is glass, Gt is garnet, and the numbers in parentheses refer to the number of double strokes taken to abrade the surface.

test, the unsealed films had been attacked. The 'slight bloom' found on the sealed 25 μ m oxide film was also detected by glass paper, while the 5 μ m film was not abraded by glass paper. Hence, if the anodising temperatures were high (20°C) then oxide films anodised to a thickness of 25 μ m would have been exposed to sulphuric acid at relatively high temperatures than those anodised to a thickness of only 5 μ m, thus causing a sealing bloom. This was revealed by powder formation in the three paper test made before the sulphur dioxide test, and as a surface bloom after it. The Dye Spot test solution 'A' had dissolved the 5 μ m film, giving a false negative result, while the 25 μ m film was shown to have 'self-sealed' at least on the surface. All panels had been half immersed in 33% nitric acid before the sulphur dioxide test but the SO₂ results were not affected by the immersion. Hence the nitric acid did not remove the softer outer layer which caused the sealing bloom. Colorimetry detected no difference before and after the sulphur dioxide test.

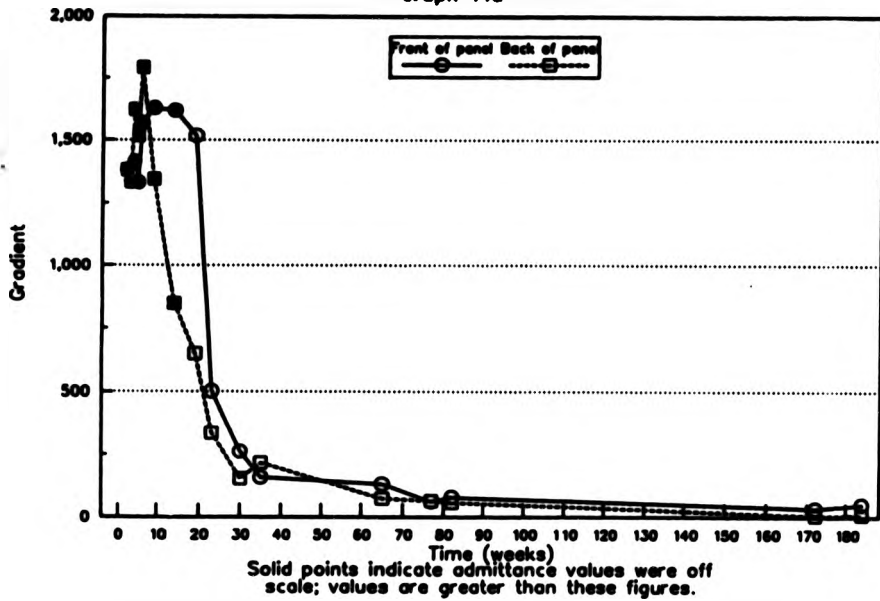
4.9 The Weathering of Unsealed, Partially Sealed and Fully Sealed Anodised Panels.

Panels were anodised to give average film thicknesses of 20, 25, 30, 35 and 40 μ m. The sealing solution was deionised water at a pH of 5.5 to 6.0. The set of panels 105 to 109 were not sealed. Panels 110 to 114 were sealed for 16.5 min. The final set 115 to 119 were sealed for 75 min. Each set comprised five panels of

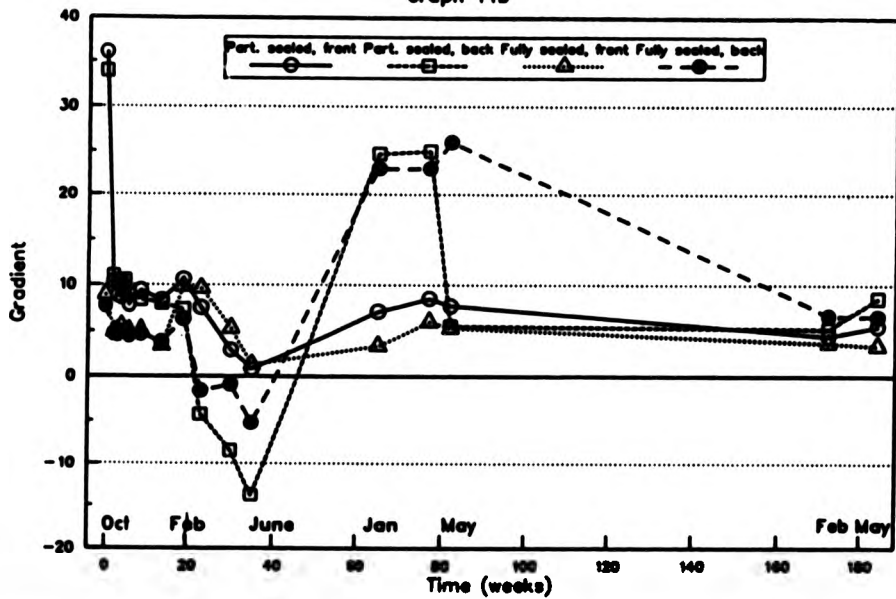
different thicknesses, and the sealing time was based on the 30 μm thickness. The admittance was measured after sealing and $Y_t(25^\circ\text{C})$ was calculated. The panels were exposed on the roof of Central House, London, E1, at an angle of 45° , facing south. The admittance was measured at intervals, over a total period of exposure of 3 years 7 months. The panels were allowed to dry in the laboratory for 24 hours before the tests were made. The panels were cleaned under running tap water with tissues and then rinsed with deionised water each time they were withdrawn to measure the admittance up to week 82. The panels tested at week 172 were cleaned under running tap water with a nylon brush, rinsed in distilled water, and rubbed with a cloth soaked in acetone. For the final measurement at week 184, the panels were cleaned with soap and water using a nylon brush, and rinsed in distilled water. The admittance was measured on areas which were, as far as possible, free from crazing.

Graphs of $Y_t(25^\circ\text{C})$ against thickness were plotted for each series of admittance tests. (Readings for the first few weeks were off scale.) Graphs for the unsealed panels, front and back showed a decrease of the linear regression gradient with time. However, only after exposure of 172 and 184 weeks did the back of the panels reach a gradient of less than $+10$. These lines were below the pass criterion, while those for the front of the panels straddled the pass criterion, with gradients not less than $+10$. Graph 11a shows how the gradient varied with exposure time for unsealed panels. Ignoring the solid points,

Graph of the Gradient against Time :
Unsealed Panels
Graph 11a



Graph of the Gradient against Time : Partially
and Fully Sealed Panels
Graph 11b



(which indicate that the reading was off the highest scale of the admittance meter) the gradient dropped very sharply after 23 weeks for the front, which continued to decrease until it leveled out after 82 weeks. The gradient for the back of the panel decreased sharply between 19 and 30 weeks. It continued to decrease, reaching a steady value after 172 weeks.

The graph for partially sealed panels, front only, showed the lines were, from top to bottom, generally in the order of the number of weeks exposure, except for weeks 19, 23 and 30 which were positioned above weeks 2, 3, 4, 5, 6, 9 and 14. Notably, the admittance values for weeks 19 and 23 lay above the pass criterion. Graph 11b shows the gradient against the number of weeks exposure for the partially and fully sealed panels. The line corresponding to the front of the partially sealed panels showed an initial large decrease which steadied temporarily until another significant decrease in the period from 19 to 35 weeks. The gradient increased again at 65 and 77 weeks, and finally levelled out. All the gradients except for week 0 were less than or fractionally above +10.

The graph for partially sealed panels, back only, did not give such a uniform sequence of changes in the positions of the lines with time. However, the gradients could be classified into groups, as shown by Graph 11b. Initially, the gradient decreased smoothly from 2 to 19 weeks. A very large decrease followed in the period from 19 to 35 weeks, which was followed by a very large increase from weeks 65 to 77. The gradients became fairly steady at

weeks 82, 172 and 184. Gradients from 2 to 14 weeks were +10 plus or minus 1.6. Gradients from 65 to 77 weeks varied widely, while those of 82, 172 and 184 weeks were well below +10. The lines for weeks 19, 23, 30 and 35 were above the sealing pass criterion.

The lines for fully sealed panels, front surfaces were close together and all lying below the pass criterion. The closeness of the lines masked the order. However, weeks 19, 23 and 30 were found above all the other weeks, and 172 and 184 were below any of the others. All gradients were less than +10. They decreased smoothly to week 14 and rose at week 19. There was another decrease to week 35 followed by a small increase and finally a levelling out of the line. The back surfaces of fully sealed panels behaved more erratically, in a manner similar to that of partially sealed back surfaces. Referring to Graph 11 b, there was a smooth decrease to week 14, where gradients were all well below +10, and then a rise at week 19. There was then a sharp decrease to week 35 followed by a very large increase to week 65, the gradients being negative for the former and very large for the latter. The line showed a decrease again at week 172 and 184, where the gradients fell to +6.6 and +6.5 respectively. Graph of fully sealed panels, back only showed that in weeks 30 and 35 the values lay above the pass criterion, while at weeks 65, 77 and 82 they straddled it.

The group of unsealed panels showed identical behaviour for both front and back, which was very different from that of the partially and fully sealed panels. These

latter groups showed very similar trends to one another for both front and back. The difference between graphs of partially and fully sealed panels, front and back, was the relative position of the sealing pass criterion with respect to the lines. Graph 11 b shows all four lines follow a similar pattern. If the appropriate months were assigned to the x axis then it is found that all lines decreased from October to February where a small increase was observed (except for partially sealed, back coatings). There was another decrease from February to June, which had the lowest gradients in each case, but thereafter there were significant increases in the following January. The gradients were steady until the following May, when all decreased (except fully sealed, back, which subsequently decreased in the next February). The gradients remained stable through to the next May. It was shown that the back of both groups of panels gave wider fluctuations in the gradients than did the front.

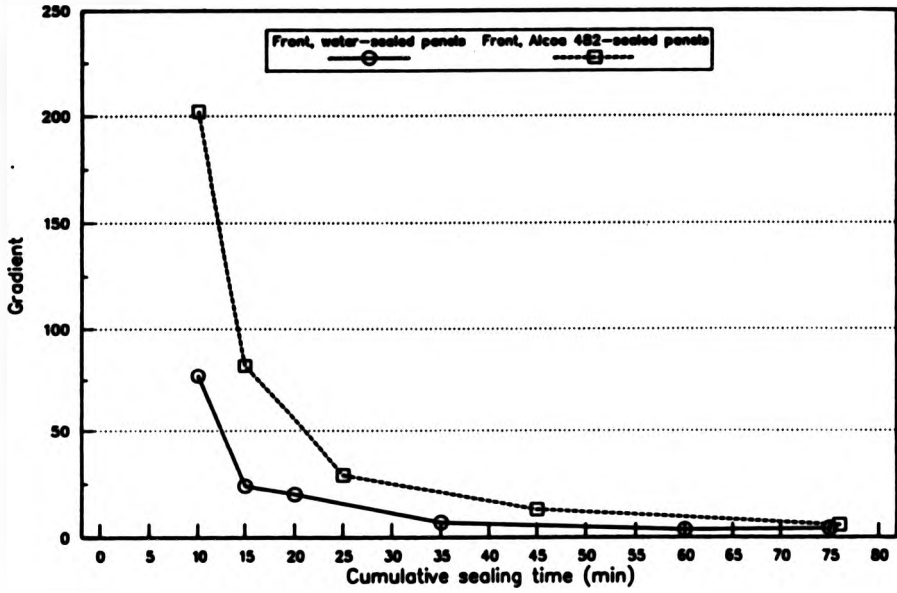
Thicknesses did not change significantly after 172 weeks exposure when they were remeasured. Loose dirt had accumulated on the front sides which was removed with a nylon brush and water. Thick tenacious dirt on the undersides was removed by rubbing with a cloth soaked in acetone. Bloom was worse on the front sides than on the undersides. The bloom on the fully sealed panels was much lighter in colour than that on the unsealed and partially sealed panels.

4.10 Linear Regression of $Y_t(25^\circ\text{C})$ Against Thickness for Natural Panels

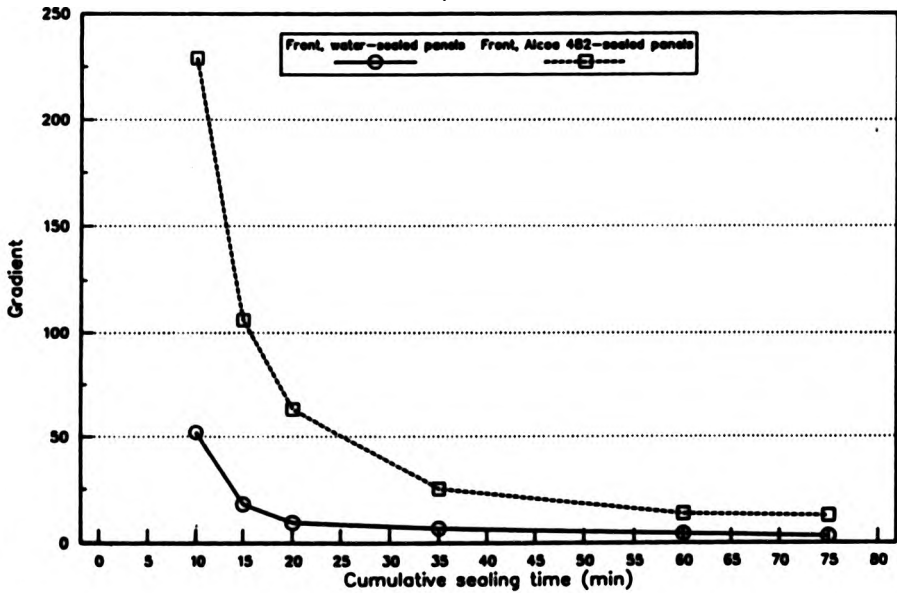
Anodic film thicknesses of 18, 24, 26, 33 and $36\mu\text{m}$ were formed by anodising at a constant time of 55 min and at current densities of 1.47, 1.76, 2.05, 2.35, and $2.64\text{A}/\text{dm}^2$ respectively. One series of panels was sealed in deionised water 24 hours after anodising, and the other set, sealed in 'Alcoa 482', was sealed 48 hours after anodising. The $Y_t(25^\circ\text{C})$ values are not representative of panels which are usually sealed immediately after anodising without being dried. Each range of thicknesses was sealed for cumulative times as indicated on the Graph 12. The $Y_t(25^\circ\text{C})$ value for each thickness was recorded after each sealing period. The gradient corresponding to each sealing period was calculated together with the ordinate intercept and the coefficient of correlation of the points on the curves. The gradients decreased for both the sealing solutions as sealing time was increased. The gradient fell below +10 after a total sealing time of 35 mins for water and after 76 mins for 'Alcoa 482'.

Further experiments were performed in which thicknesses of 18 to $36\mu\text{m}$ were formed by anodising at a constant current density of $1.8\text{A}/\text{dm}^2$ and varying the times. One range of thicknesses was sealed in deionised water and the other sealed in 'Alcoa 482', both 24 hours after anodising. Once again the $Y_t(25^\circ\text{C})$ values must be interpreted with caution. Each range of thicknesses was sealed for cumulative times as indicated on the Graph 13.

Graph of Gradient against Cumulative Sealing Time: Anodised at Constant Time
Graph 12



Graph of Gradient against Cumulative Sealing Time: Anodised at Constant Current Density
Graph 13



The gradients decreased as sealing time was increased for both sealing solutions. The gradient fell to +10 or less after a total sealing time of 20 min for water, but the 'Alcoa 482' panels failed to achieve a gradient of +10 or less despite a total sealing time of 75 mins, Graph 13.

4.11 Linear Regression of $Y_t(25^\circ\text{C})$ Against Thickness for Coloured Panels

The lines of linear regression of $Y_t(25^\circ\text{C})$ on thickness were plotted for panels coloured with and without Tribrite. One set of panels was coloured for 6 min at a current density of $0.5\text{A}/\text{dm}^2$, and a second set was coloured for 1.5 min at a current density of $0.5\text{A}/\text{dm}^2$, Graphs 14a and 15a respectively show the gradient against cumulative sealing time.

The first experiment, experiment 181: anodising temperature 17°C and colouring temperature 20°C , used a solution made up of 20g/l sulphuric acid, 20g/l stannous sulphate, 20g/l phenol sulphonic acid and 13.5ml/l SNDS. This solution was divided into two 2 litre amounts and one was used without Tribrite and the other with a total addition of 4ml Tribrite, dissolved in a small amount of dilute sulphuric acid. No formaldehyde was added. HCTs were done as follows:

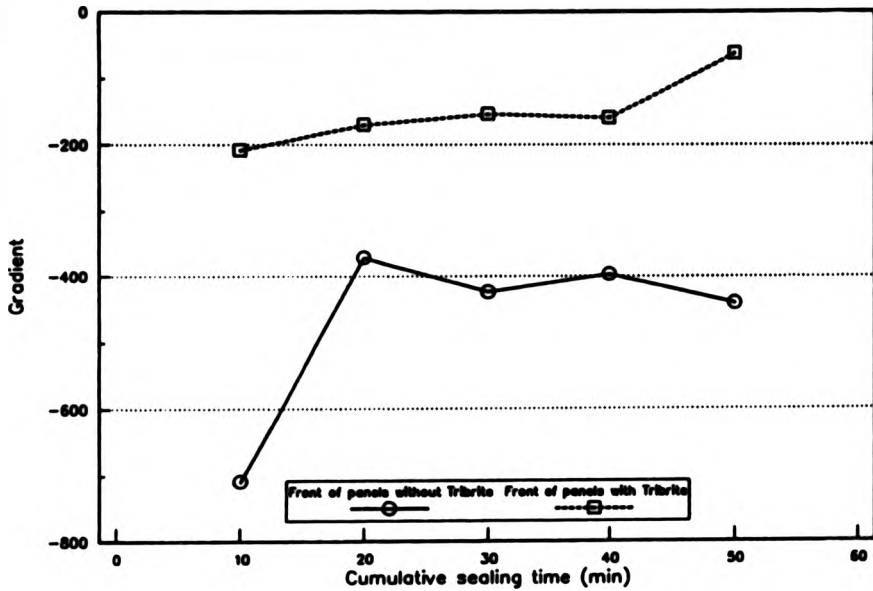
Table 31

HCT	Tribrite Addition (ml)	Appearance of Tin Deposit
72	-	Loose
73	2	Good cover, dull.
74	1	"
75	1	"
76	as above + 27ml SNOS	Good cover, not bright but metallic finish (Table 35), gas streaked.

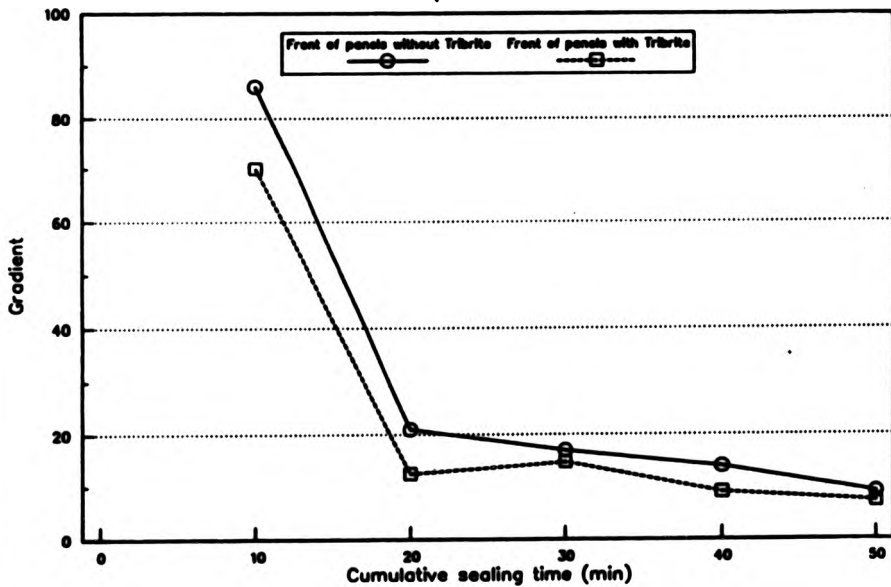
Panels were anodised in pairs to various thicknesses. One of each pair was coloured in the solution not containing Tribrite and the other in the Tribrite solution. Both panels were sealed for consecutive intervals of 10 min in ammonium acetate buffered water (pH 5.9 - 6.0). After each 10 min sealing period $Y_t(25^\circ\text{C})$ was measured on the front of the panels. All panels were sealed for a total of 50 min. Graph 14a shows that there was a significant decrease in the gradient (i.e a more positive number) for the solution containing Tribrite compared to that without. However, the slopes were still very large and negative. It was noticeable that there was a marked decrease in the gradient for the 20 min sealing time compared to the 10 min value. The gradients for 20, 30, 40 and 50 min sealing times generally decreased but with fluctuations.

In the second experiment films were anodised at

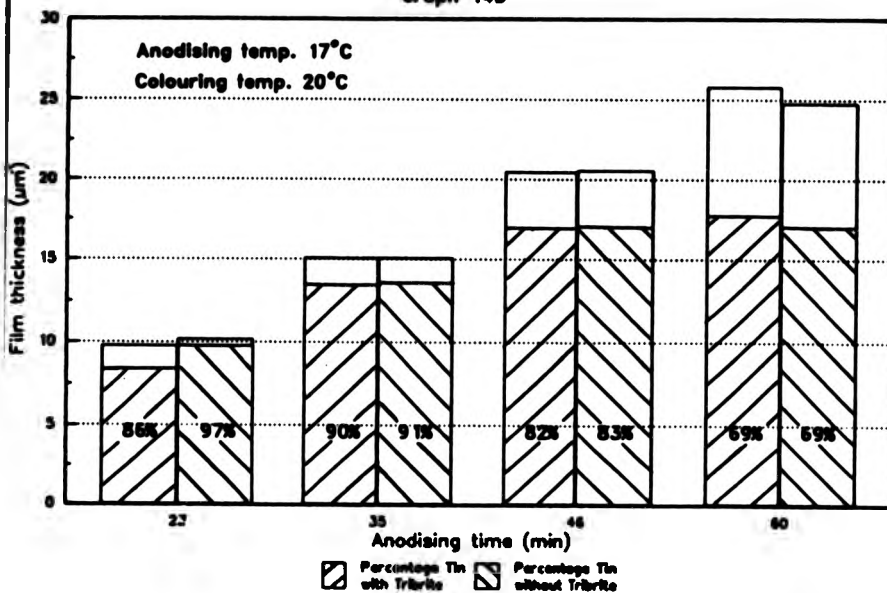
Graph of Gradient against Cumulative Sealing Time: Colouring Time 6 minutes
Graph 14a



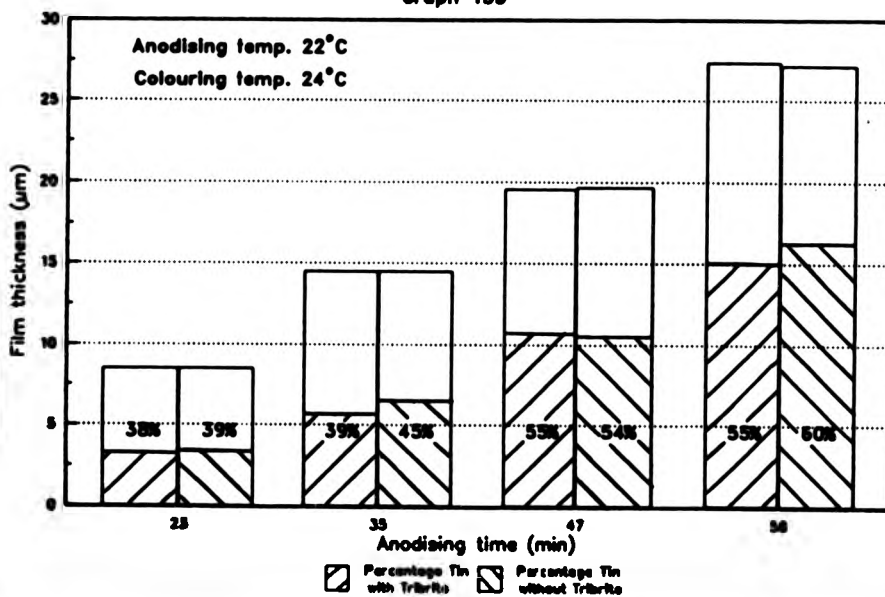
Graph of Gradient against Cumulative Sealing Time: Colouring Time 1.5 minutes
Graph 15a



Graph of Tin Content against Anodising Time:
Colouring Time 6 min
Graph 14b



Graph of Tin Content against Anodising Time:
Colouring Time 1.5 min
Graph 15b



a temperature of 22°C and coloured at a temperature of 24°C. Films were coloured for 1.5 min. This experiment was done 43 days after Experiment 181 using the same solution. HCT 78 was made 42 days after experiment 181. This showed a loose tin deposit. An extra 1 ml of Tribrite was added before the start of this experiment. The subsequent HCT 79 was found to have better cover but it was dull.

In this experiment, Graph 15a, all the gradients were positive, and decreased (i.e. became less positive). There was no distinction in the gradients between the solution containing Tribrite and that without. The gradients for the 10 min sealing times were greater than those for 20, 30, 40 and 50 min sealing times. The gradients for these latter times decreased smoothly. Only the 40 and 50 min sealing time points (except the panel sealed for 40 min and coloured without Tribrite) had gradients of +10 or less.

Graphs 14b (colouring time 6min) and Graph 15b (colouring time 1.5min) show the percentage of tin in the films as calculated from the equations:

$$t' = t - t_m \quad (3.12)$$

and

$$t' = \frac{200t}{x} \quad (3.14)$$

x

$$\text{if } Yt' = 200 S_m \times 10^{-12} \quad (3.13)$$

where the values of $Yt(25^\circ\text{C})$ measured at a total cumulative

time of 50min, are used to represent the well sealed film, i.e. for the 24.8 μ m film coloured without Tribrite, $Y_t(25^\circ\text{C})$ at a sealing time of 50min is $650 \text{ Sm} \times 10^{-12}$:

$$t' = \frac{200 \times 24.8}{650}$$

$$t' = 7.6\mu\text{m}$$

therefore,

$$t' = t - t_m$$

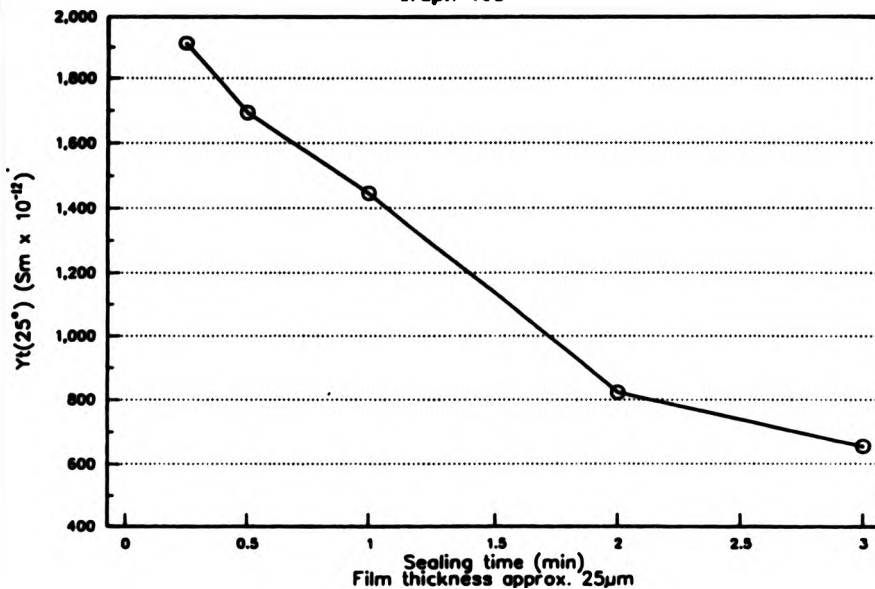
$$7.6 = 24.8 - t_m$$

$$t_m = 17.2\mu\text{m}$$

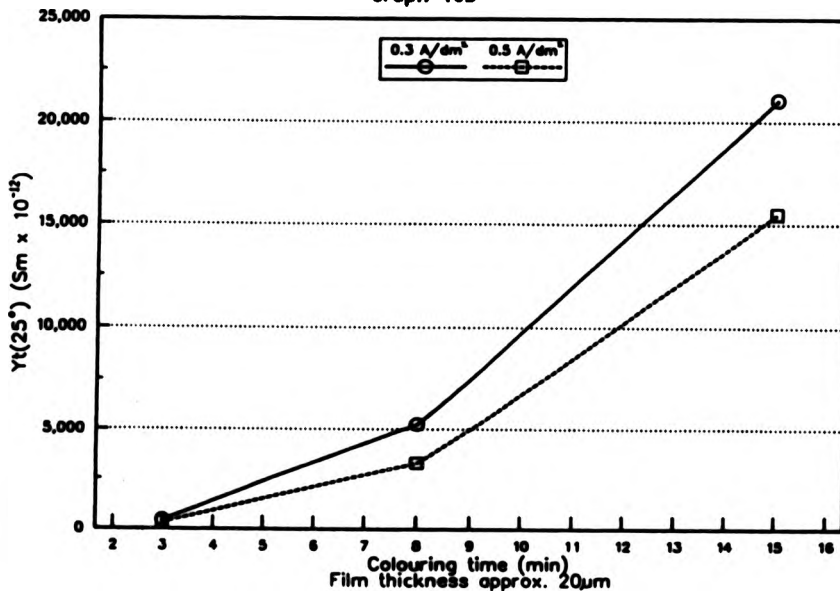
4.12 Results Using Standard Colouring Solution

The standard colouring solution used was 20g/l sulphuric acid, 20g/l stannous sulphate and 20g/l phenol sulphonic acid. Graphs 16a and 16b gives some typical values of $Y_t(25^\circ\text{C})$ for a range of colouring and sealing times. All panels were anodised at room temperature and sealed in 1g/l ammonium acetate buffered water. $Y_t(25^\circ\text{C})$ values decreased as panels coloured for 3 min were sealed for increasing times. Values of $Y_t(25^\circ\text{C})$ increased as panels sealed for 2min/ μm were coloured for increasing times. It was found that for extended colouring times (greater than 10min), a current density of $0.8\text{A}/\text{dm}^2$ caused spalling of the anodic film. Very long colouring times at

Graph of $Y_t(25^\circ)$ against Sealing Time:
 Colouring Time 3 minutes, c.d. 0.8 A/dm^2
 Graph 16a



Graph of $Y_t(25^\circ)$ against Colouring Time:
 Sealing Time $2\text{min}/\mu\text{m}$
 Graph 16b



low current densities, produced a patchy grey colour on the black films when spalling did not occur. The current densities of 0.3, 0.5 and 0.8A/dm² were accompanied by voltages of 11.0, 12.7 and 14.7V respectively.

The thickness of the anodic film does not affect the colour produced by equivalent short colouring times. There is some variation in chromaticity co-ordinates for equivalent colouring times, but the R_{200x} values are within a narrow range.

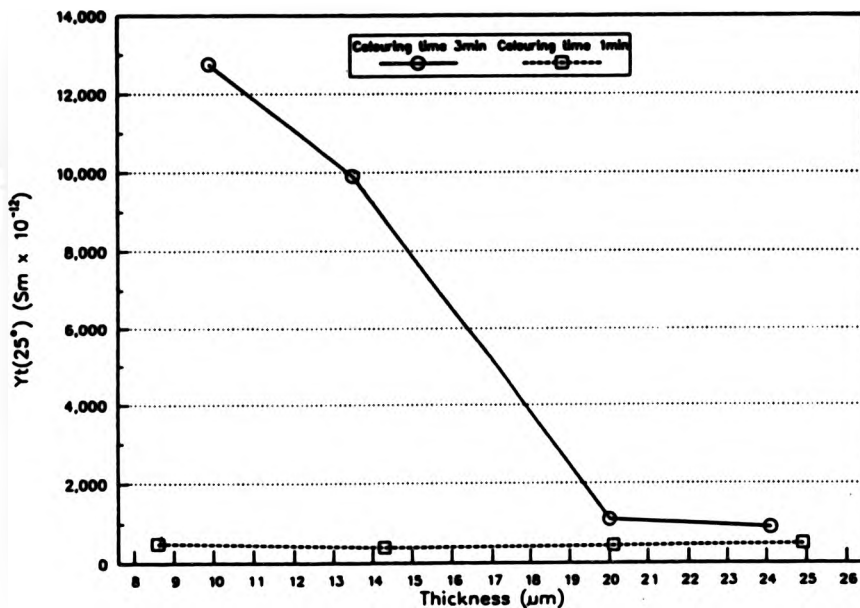
Graph 17 gives the effect of thickness on $Y_t(25^\circ C)$ values for identical sealing times. For 3 minutes colouring time the thinner the film, the higher the $Y_t(25^\circ C)$ value. However for 1 minute colouring time, the Y_t values show no such trend. In fact the values are totally random. Colouring did not alter the thickness of the oxide films.

Graph 18, the CIE chromaticity diagram, shows all films coloured for any length of time and uncoloured, to be clustered around one area. Films coloured red, yellow, blue and violet are included for comparison. Graph 19 is semi-logarithmic and shows the position of films coloured for different times and those uncoloured.

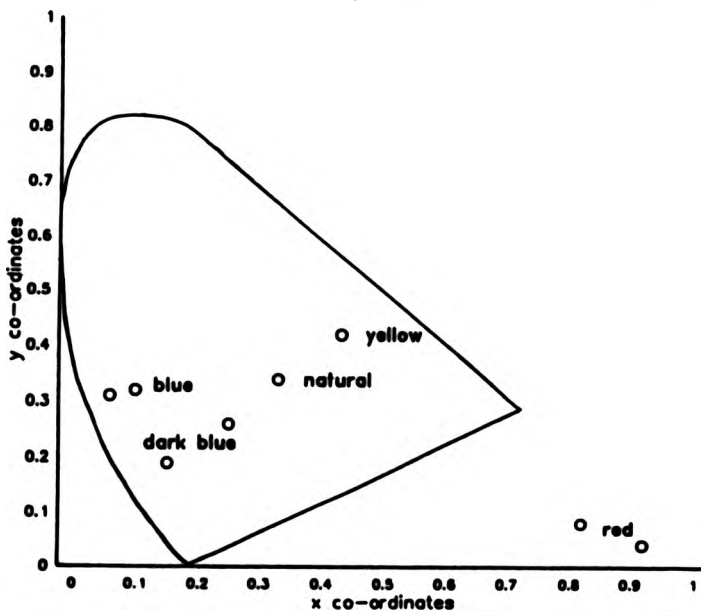
Graph 20 shows the L values against colouring time. The L values for the colouring current densities of 0.5 and 0.8A/dm² decrease with colouring time at approximately the same rate. The order of the current densities for decreasing luminance is 0.33, 0.5, and 0.8A/dm². This order is reversed at long colouring times.

The chromaticity co-ordinates show no distinction

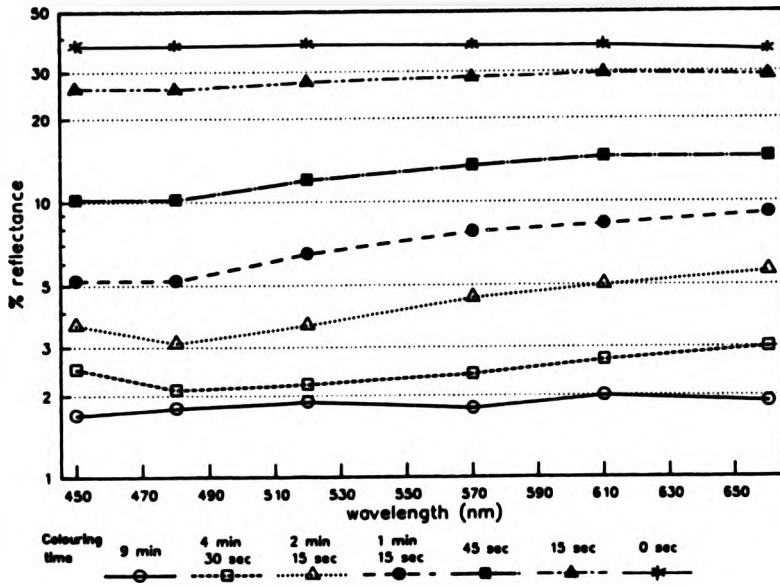
Graph of $Y_i(25^\circ)$ against Thickness
Graph 17



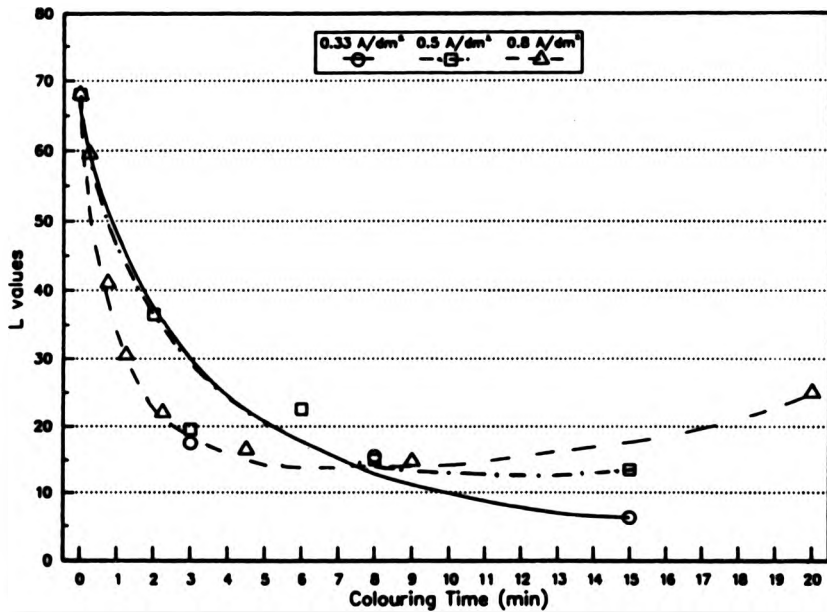
CIE Chromaticity Diagram
Graph 18



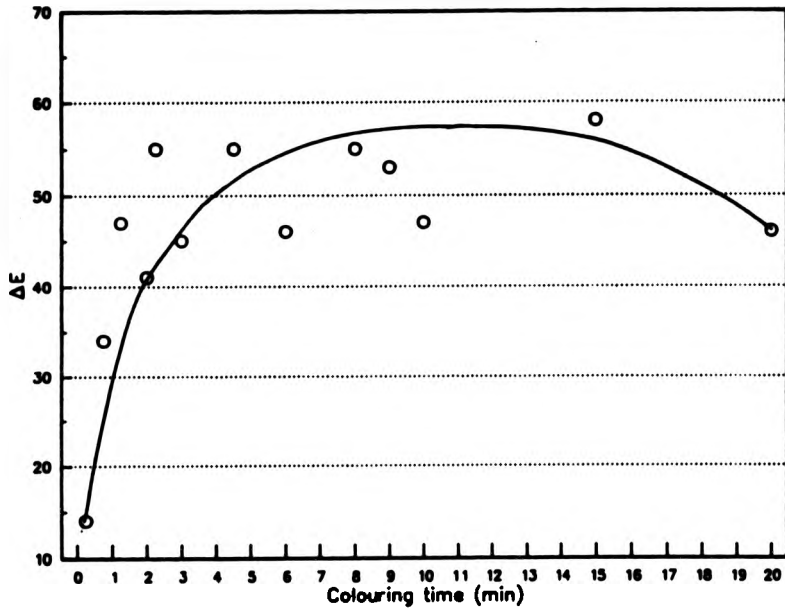
Graph of Percentage Reflectance against Wavelength
Graph 19



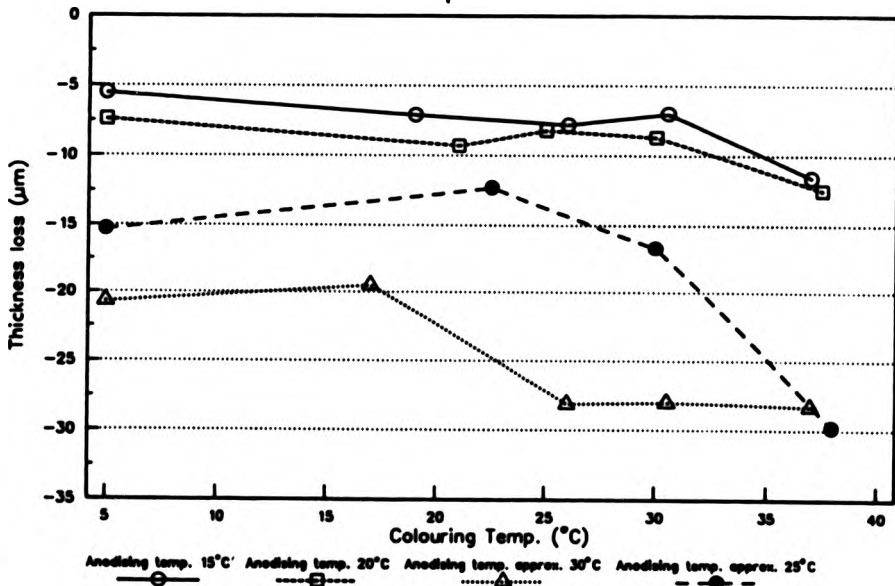
Graph of L values against Colouring Time
Graph 20



Graph of ΔE Values against Colouring Time
Graph 21



Graph of Film Thickness Loss against Colouring Temperature
Graph 22



between colouring times for different current densities.

Graph 21 shows the ΔE values against colouring time for all current densities. The curve of the graph is the mirror-image of that on the graph of L on colouring time.

4.13 Analysis of Tin

Both the abrasive wheel test and the glass paper test gave a black powder trace on the first application for a $20\mu\text{m}$ film coloured for 15min.

$25\mu\text{m}$ films were coloured for 3 and 6min. They were left unsealed, dried and weighed. The anodic oxide film was stripped from the aluminium using a solution of 35ml/l H_2PO_4 and 20g/l CrO_3 . The stripped aluminium had a grey/black powder remaining which was the tin. The panels were dried, reweighed and the tin removed. They were weighed again and the weight of the tin calculated. The film thickness as estimated from the 'strip and weigh' method was found to be approximately $25\mu\text{m}$, which was in agreement with that found with the eddy current method. $14\text{mg}/\text{dm}^2$ of tin was found for both colouring times.

4.13.1 X-Ray Diffraction Analysis

X-ray diffraction analysis showed that the d-spacings for pure aluminium correlated very well with the theoretical values. The values for pure tin found by experiment also correlated very well with the theoretical values for tetragonal tin. Tin deposited in the oxide film

was analysed and the experimental d-spacings were found to be 0.01 to 0.02 units higher than the theoretical values for pure tin.

4.13.2 Powder Diffraction Analysis

Two methods for removing the anodic oxide film containing tin were used:

1. Film was scraped from the aluminium.
2. Film was removed with HgCl_2 .

The experimental d-spacings correlated fairly well with the theoretical values for tetragonal tin by the first method, and very well by the second method.

4.14 The Effect of Elevated Temperatures During Anodising, Soaking and Colouring.

In this section all panels were sealed in ammonium acetate buffered water. Thickness wear indices were derived from the value for thickness loss found by the abrasive wheel test using 400ds and 400 gf and were calculated from the gradient of the linear regression graph of thickness loss against number of cycles.

Panels soaked for varying lengths of time in 20g/l sulphuric acid at 30°C but not sealed, showed no loss in abrasion resistance. Coloured films which had been soaked after sealing showed reduced abrasion resistance. A film soaked for over 2 hours had almost dissolved

completely, Table 32, Expt. 113.

Colouring or soaking at elevated temperatures in the basic colouring solution, (20g/l sulphuric acid, 20g/l stannous sulphate and 20g/l phenol sulphonc acid), prior to sealing, also revealed a decrease in the abrasion resistance Table 32, Expt.170. The thickness wear indices however were still within acceptable limits despite the noted effects of colouring and soaking prior to sealing. Colouring gave marginally larger thickness wear indices than soaking. The panels not soaked nor coloured gave the lowest thickness wear indices.

A subsequent experiment showed no reduction in abrasion resistance after long colouring times.

A series of experiments was performed to observe the effects of a range of anodising, colouring and soaking temperatures on the abrasion resistance of anodic oxide films. Graph 22 shows the effects of raising the anodising temperature. Within each anodising temperature the colouring temperature was increased (colouring time 8min). Raising both temperatures brought about a decrease in abrasion resistance. The first point of each line on the graph is a reference point showing the thickness loss for a panel anodised at the appropriate temperature, but not coloured. Similarly, an almost identical trend is shown for soaking at elevated temperatures (soaking time 8min). All thickness losses were derived by the linear regression method.

The effect of over sealing was investigated. Sealing for 2min/ μ m is sufficient to pass the sealing

Table 32

Expt/ Panel	Colouring (min)	Soaking (min)	Sealing (min/ μ m)	Three Paper Test	Thickness Wear Index (L.R.)
113/326	3	unsoaked	2	garnet	0.74
113/327	room	20	2	glass	1.81
113/328	temp	2hr28	2	glass	1-2 μ m rem.
170/475	uncoloured	8 30.5°C	1	garnet	1.2
170/476	8 30°C	unsoaked	1	garnet	1.6
170/477	uncoloured	unsoaked	1	garnet	0.8
170/478	8 38°C	unsoaked	1	garnet	1.4
170/479	uncoloured	8 38°C	2	garnet	1.1
170/480	uncoloured	unsoaked	2	garnet	0.7

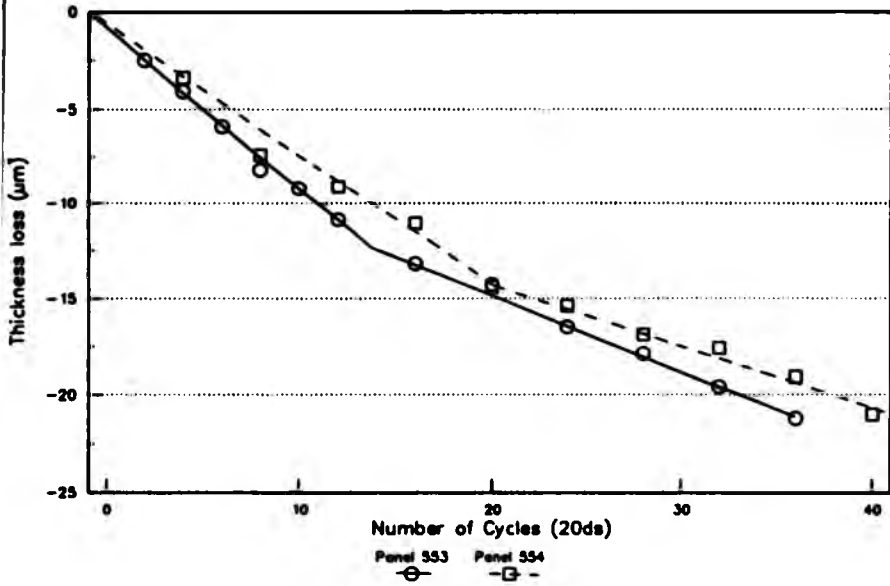
rem. means remaining

Table 33

Expt/ Panel	Soaking/ Colouring (min)	Sealing Conditions (min/ μ m)	Thickness Wear Index (L.R.)	SO ₂ Test
193/553	unsoaked uncoloured	2.27	1.8 whole film 2.3 outer film 1.1 inner film	uniform
193/554	unsoaked uncoloured	6	1.7 whole film 1.7 outer film 0.9 inner film	bloom

L.R. indicates values were found by linear regression.

Graph of Film Thickness Loss against Number of 20ds Cycles: An Abrasion Profile
Graph 23



Graph of Film Thickness Loss against Number of 20ds Cycles: An Abrasion Profile
Graph 24

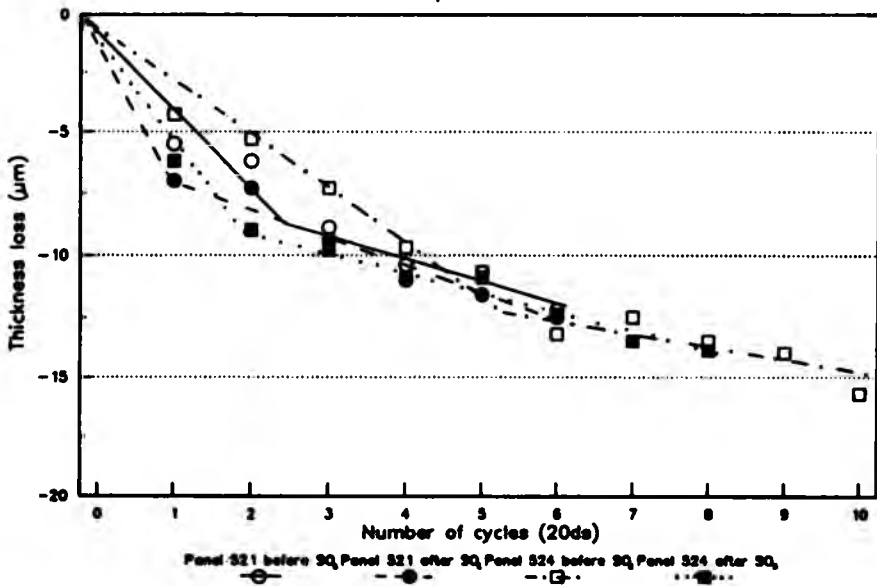


Table 34

Expt/ Panel	Anodising Conditions	Soaking/ Colouring (min)	Thickness Wear Index (L.R.)	SO ₂ Test
195/521	31°C	coloured 8 37°C	before SO ₂ 3.4 whole film 4.8 outer film 2.7 inner film after SO ₂ 16.7 outer film 3.4 inner film	very heavy bloom
195/524	29°C	soaked 8 15°C	before SO ₂ 3.8 whole film 4.7 outer film 1.7 inner film after SO ₂ 12.1 outer film 2.3 inner film	very heavy bloom

tests. Times longer than this are unnecessary. Films anodised at 20°C showed no reduction in abrasion resistance when panels were oversealed. A graph confirmed this, although a sealing bloom was apparent as indicated by the three paper test. The panels were unaffected by the sulphur dioxide test. Anodising at 25°C, Table 33, Expt.193, showed that the elevated anodising temperature had a softening effect on the film, while the length of sealing time was irrelevant. The sulphur dioxide test and the subsequent abrasion profile, Graph 23, showed a soft outer layer and a slightly harder inner layer.

The final experiment showed the effects of elevated anodising temperatures with respect to the sulphur dioxide test and abrasion resistance, Table 34, Expt. 195. The abrasion resistance was greatly reduced and a very heavy bloom resulted in the sulphur dioxide test. The detrimental effect of the sulphur dioxide was shown by the subsequent thickness wear indices for the inner and outer layers. The inner layer, although 'harder' was still unacceptably soft, Graph 24.

The appearance of a grey or black streak during the abrasive wheel test, and the thickness loss at which this occurred, was noted. From the known total film thickness, the metal thickness can be calculated from the equation:

$$t_m = t - t'$$

(3.12)

where t_m is the tin metal thickness,

t is the total film thickness,

t' is the metal-free section of the film.

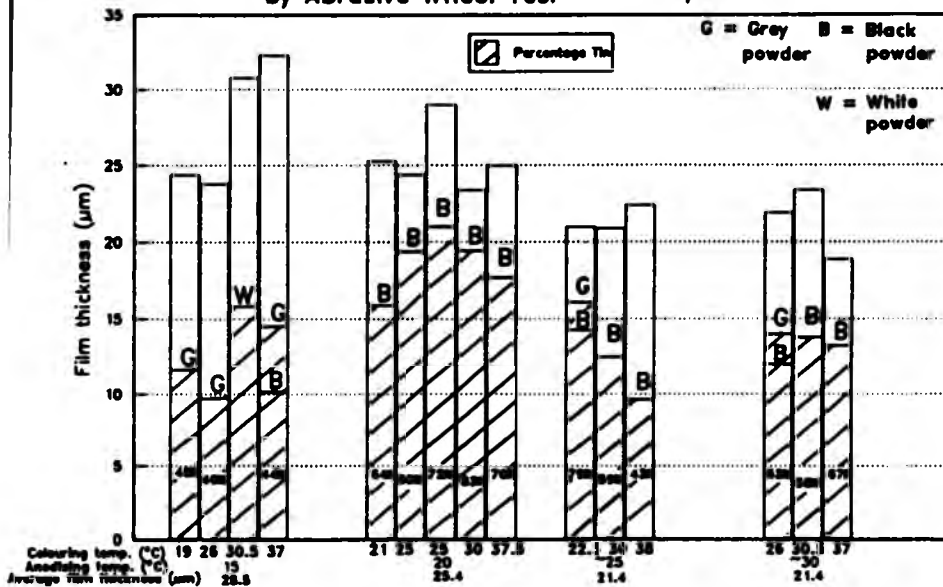
The results are given in Graph 25. The results show that generally, films anodised at 15°C have less tin in the pores than films anodised above 15°C. Within each anodising temperature range, the colouring temperature does not have a clear trend with respect to the amount of tin present. The average film thickness decreased as anodising temperature increased.

After 40 cycles of the abrasive wheel test, the film anodised at 15°C and coloured at 30.5°C showed only white powder residues. This indicates that when the film was abraded down to 16.3µm tin had not appeared, i.e. due to the very good abrasion resistance of this film, the depth at which tin was deposited was not reached.

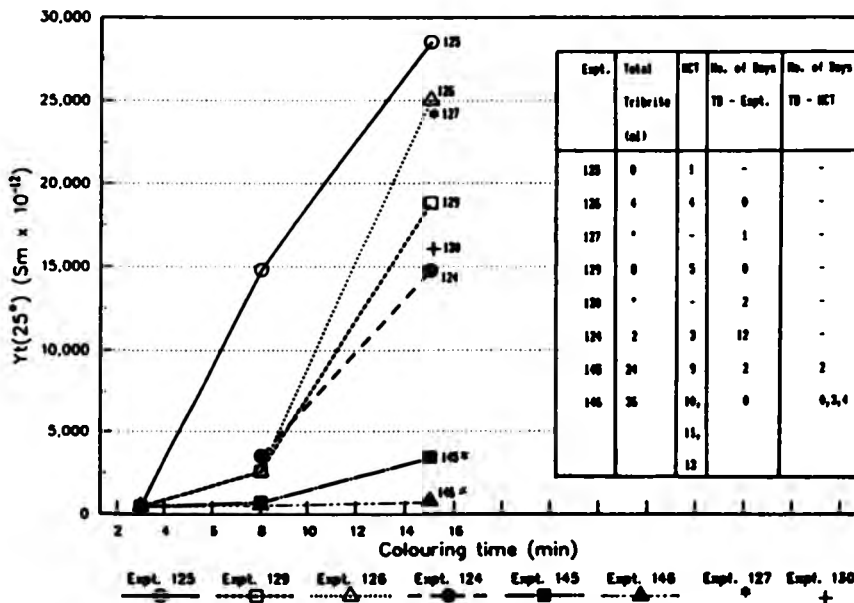
4.15 The Effects of Using 'Tribrite' in the Tin Colouring Solution

Experiments were performed to investigate the effects of 'Tribrite', an electroplating bath brightening addition agent, on the deposition of tin in the pores of the anodic oxide film. Throughout the experiments the sealing solution used was water buffered with 1g/l ammonium acetate and all coatings were sealed for 2min/µm. In the

Graph of Tin Content against Anodising Temperature and Colouring Temperature as Found by Abrasive Wheel Test
Graph 25



Graph of $Y_t(25^\circ)$ against Colouring Time
Graph 26



Graph 26, the column headed 'No. of Days, TB-Expt' means the number of days between adding the Tribrite and the use of the colouring bath. The column headed 'No. of Days, TB-HCT' means the number of days between adding Tribrite and the Hull Cell Test on the solution. 'HCT' always means the latter, and a column headed thus gives the reference number of the HCT.

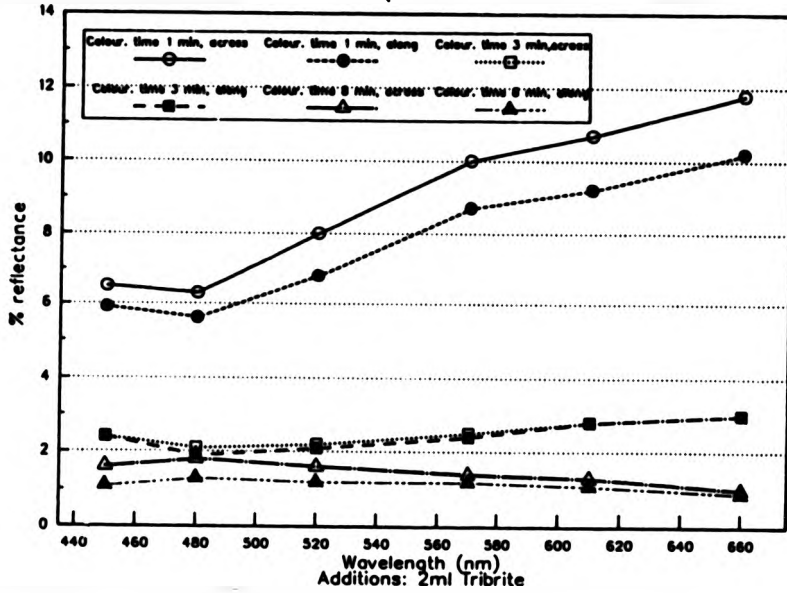
The solution used for experiments 124 to 130 had a volume of 4 litres, and contained 20g/l sulphuric acid, 20g/l stannous sulphate, 20g/l phenol sulphonic acid, 18ml/l sodium normal octyl sulphate solution (27%), (SNOS), plus various amounts of formaldehyde and Tribrite. Formaldehyde (40% solution) was added in the same volumes as the Tribrite solution, (see 'Total Tribrite' column). For all the experiments in Graph 26 the HCT was made 6 days after the addition of Tribrite. The colouring current density used was $0.5A/dm^2$ and the film thickness was approximately $24\mu m$.

The general trend of $Y_t(25^\circ C)$ is that as more Tribrite was added, the values decreased. Although the decrease was consistent for 3min colouring time, the values for 8min colouring time remained constant for 4ml and 8ml Tribrite additions. For the 15min colouring time $Y_t(25^\circ C)$ rose for experiment 126 but decreased after the addition of a further 4ml of Tribrite. It was found that the Tribrite did not dissolve completely in the tin solution until the following day. For this reason the 15min colouring time was repeated with no further Tribrite additions. HCT 1 gave a very loose tin deposit. There was a slight improvement for

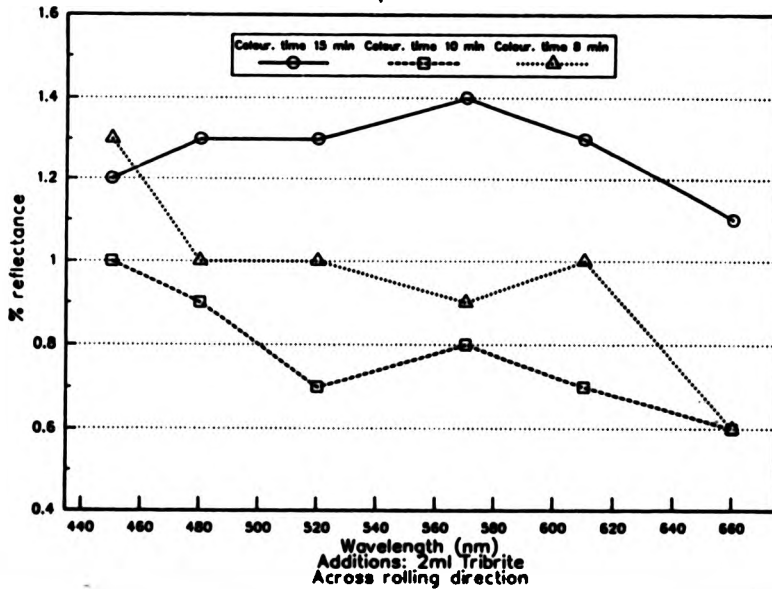
HCT 3, 4 and 5, but the deposit did not adhere well to the copper surface of the Hull Cell cathodes.

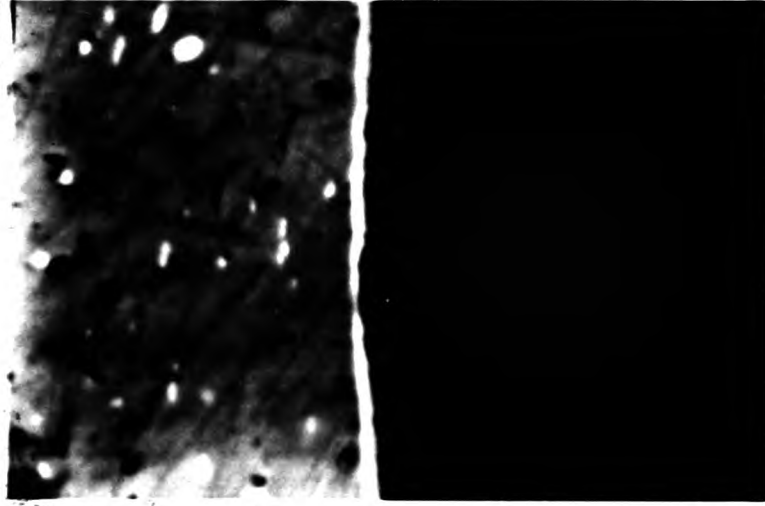
To show the affect of colouring time within the anodic oxide film graphs of percentage spectral reflectance against wavelength were plotted and Scanning Electron Micrograph (SEM) pictures taken. Graph 27a shows colouring times of 1, 3 and 8min, and Graph 27b shows 8, 10 and 15 min colouring time. Figures 31 to 36 are the respective SEM pictures. It can be seen that the graphs for 8, 10 and 15 min colouring times were very similar. Colouring times of 3 and 1 min showed an increase in percentage reflectance towards the red end of the spectrum. The SEM pictures showed a noticeable increase in amount of tin in the pores from 1 to 8 min colouring times. Those of 8 and 10 min were similar, while that of 15 min showed the tin to extend slightly further towards the oxide surface, reaching the surface in places. The composition of the solution used was 20g/l sulphuric acid, 20g/l stannous sulphate, 20g/l phenol sulphonic acid, 18ml/l SNOS, 2ml formaldehyde and 2ml Tribrite. The effect of Tribrite on the deposition of tin could not be observed in the SEM pictures, Figures 37 to 42. Those figures without Tribrite correspond to Experiment 125 and those with Tribrite correspond to Experiment 129, Graph 26. Spectral curves for 15 and 8 min colouring times, with and without Tribrite showed no distinction between them. However, 3 min colouring time did show changes for varying amounts of Tribrite, Graph 28 which shows the amounts of Tribrite corresponding to Experiments 125, 126 and 129 (Graph 26). Finally, Figure 43 shows an oxide film

Graph of Percentage Reflectance against Wavelength
Graph 27a



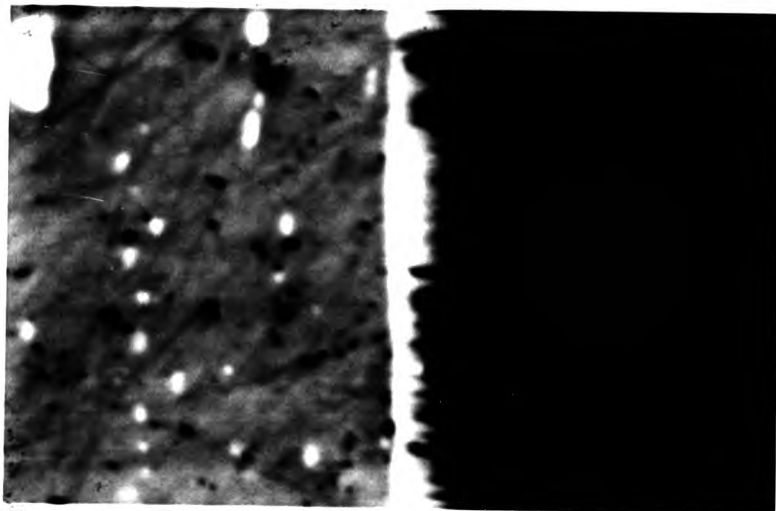
Graph of Percentage Reflectance against Wavelength
Graph 27b





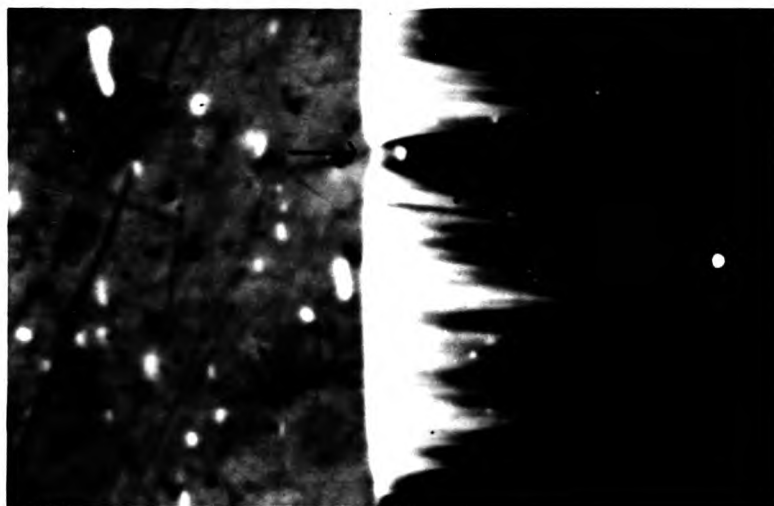
Colouring time 1 min

Fig. 31



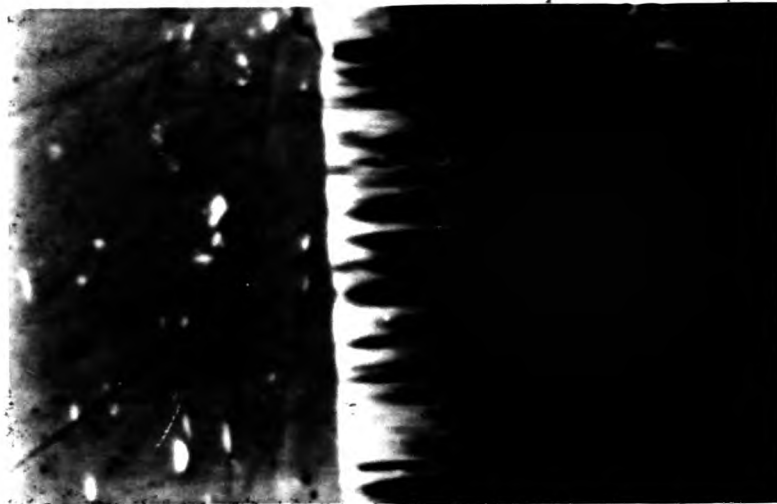
Colouring time 3 min

Fig. 32



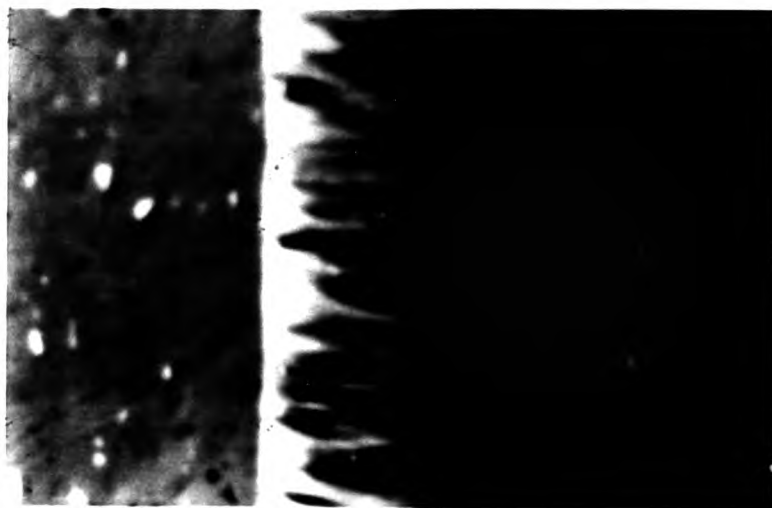
Colouring time 8 min

Fig. 33



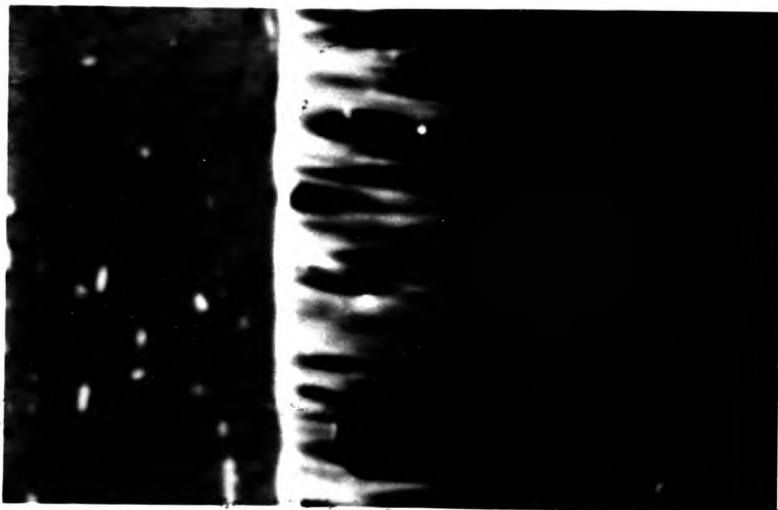
Colouring time 8 min

Fig. 34



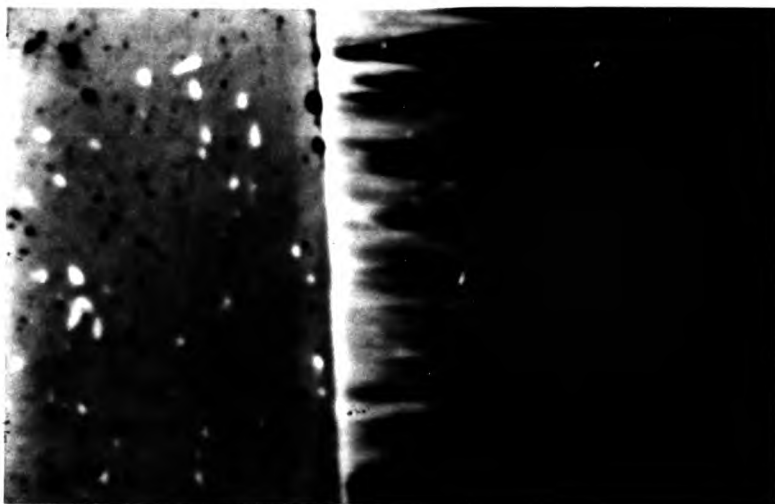
Colouring time 10 min

Fig. 35



Colouring time 15 min

Fig. 36



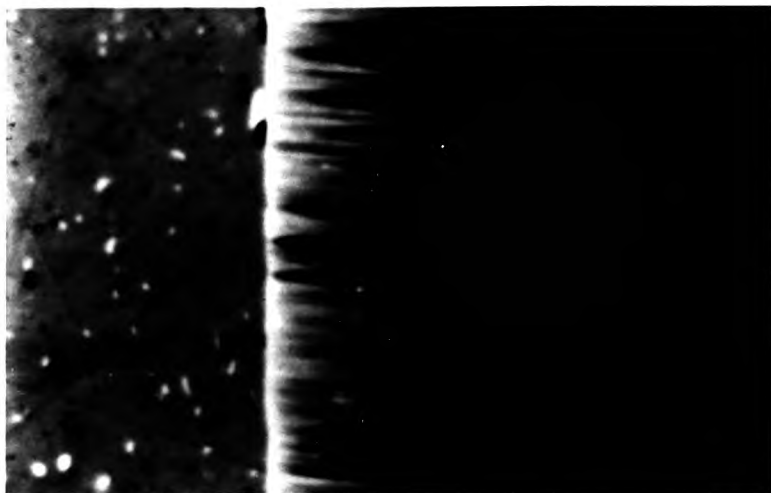
Colouring time 15 min without 'Tribrite'

Fig. 37



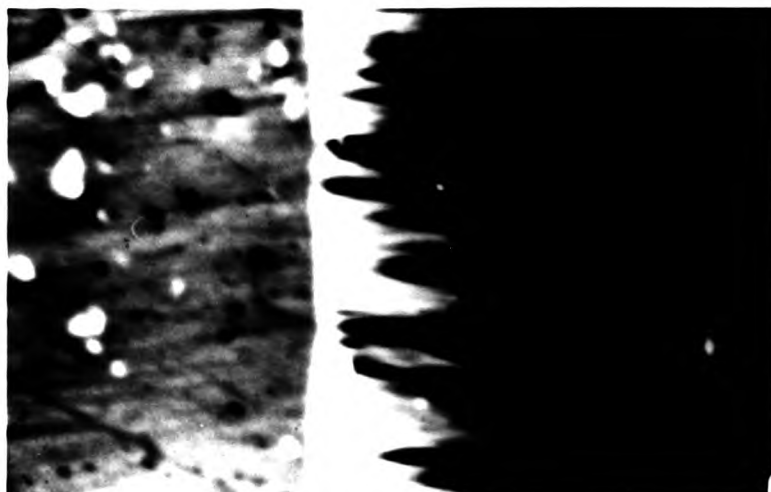
Colouring time 15 min with 'Tribrite'

Fig. 38



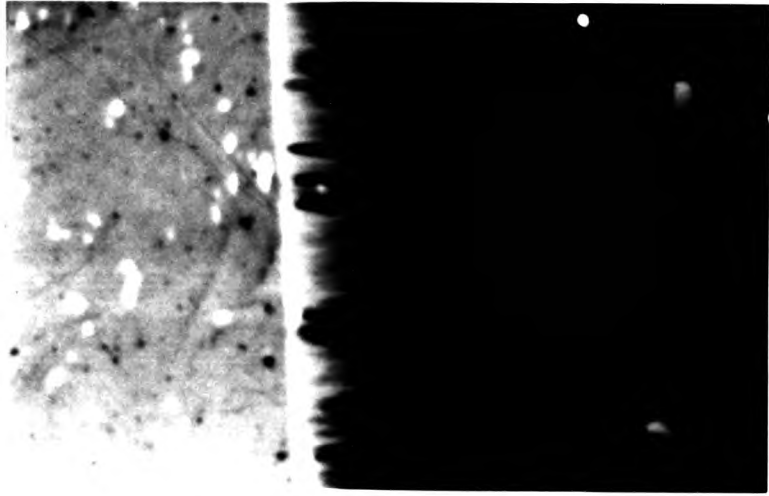
Colouring time 8 min without 'Tribrite'

Fig. 39



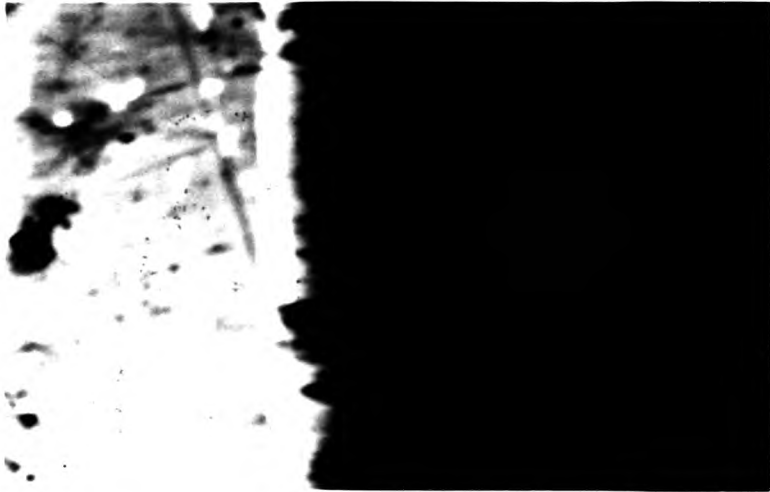
Colouring time 8 min with 'Tribrite'

Fig. 40



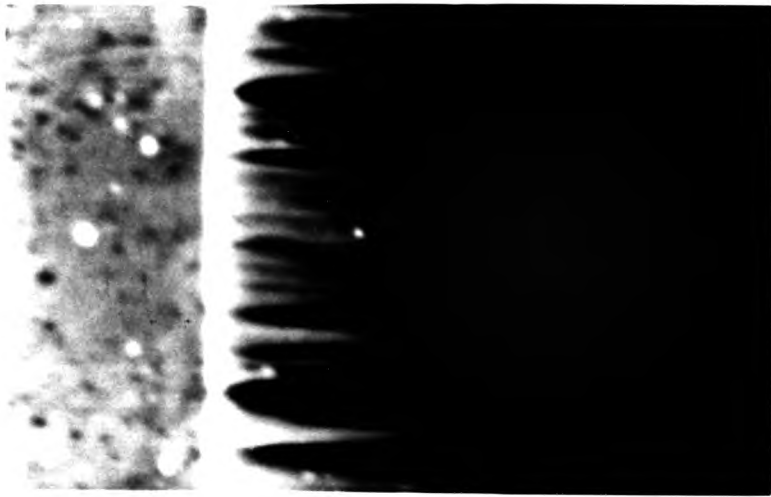
Colouring time 3 min without 'Tribrite'

Fig. 41



Colouring time 3 min with 'Tribrite'

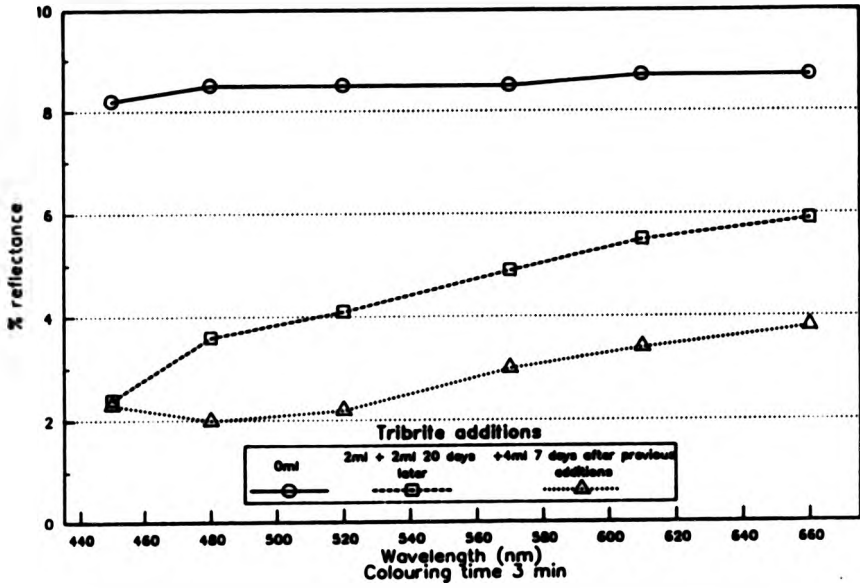
Fig. 42



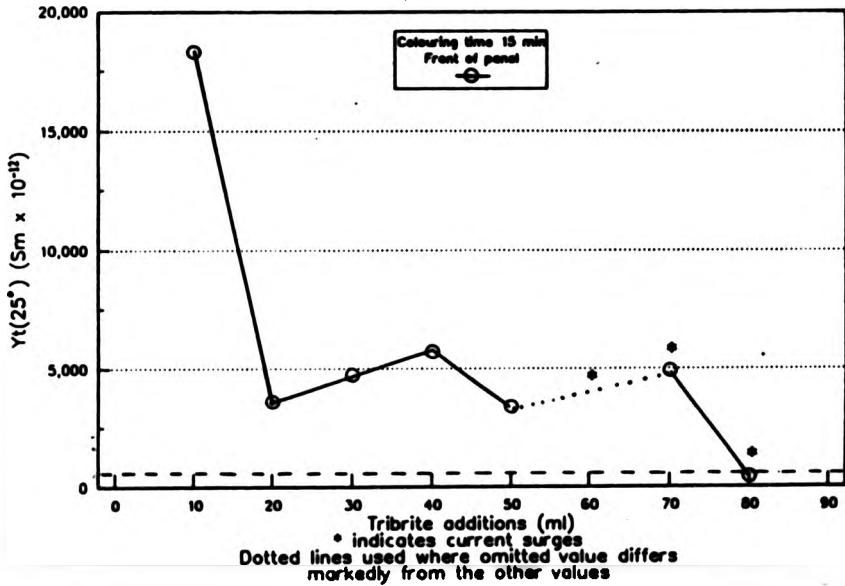
Colouring time 20 min without 'Tribrite'

Fig. 43

Graph of Percentage Reflectance against Wavelength
Graph 28



Graph of $Y_t(25^\circ)$ against Tribrite Additions
Stannous Sulphate 60 g/l
Graph 29a



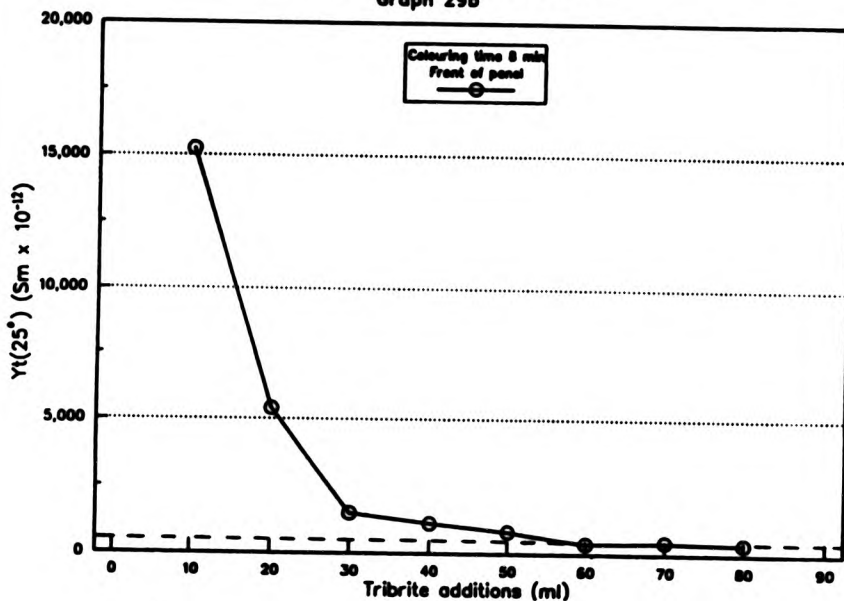
coloured for 20 min in a solution containing no Tribrite. The tin is seen to extend out to the surface of the film.

Experiments 145 and 146 used the same colouring solution as in the last set, 124 to 130, Graph 26. Further additions of Tribrite and formaldehyde were made as in the column headed 'Total Tribrite', where formaldehyde was added in the same volumes as the Tribrite. The further addition of 4ml Tribrite and 4ml formaldehyde in experiment 131 was made 6 days after the addition in experiment 129. Colouring current density was $0.5A/dm^2$ and film thickness was approximately $25\mu m$.

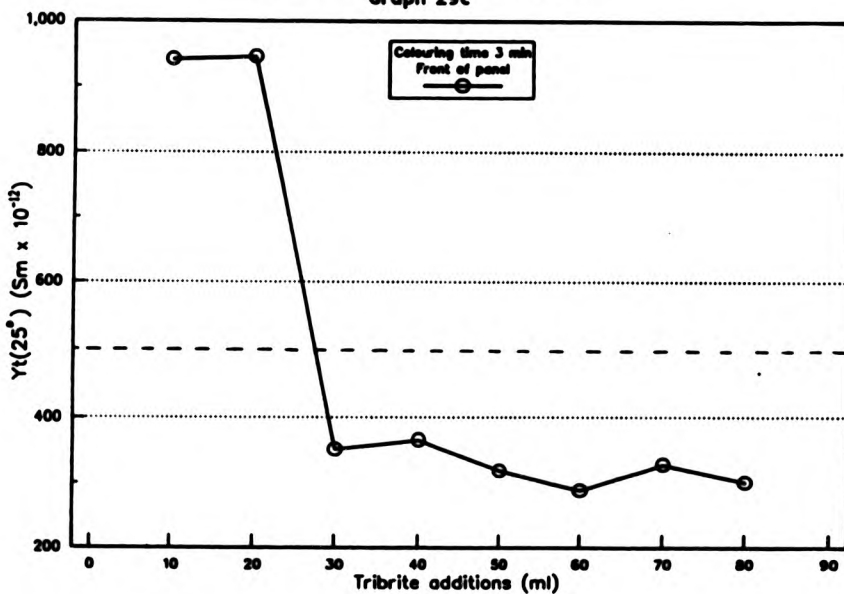
In experiment 131 the film was detached during the 8 and 15min colouring times, while for a colouring time of 3 min the colour was a very pale gold. $Y_t(25^\circ C)$ was not measured for these panels. The cathode for HCT 6 showed better covering than HCT 7 or 8, but the deposit did not adhere. HCT 8 showed poor cover 46 days after the Tribrite addition. The next addition of 12ml Tribrite in experiment 145 was made 79 days after that made for experiment 131. HCT 9 was made 2 days thereafter and showed a marked improvement in cover. The next addition (experiment 146) was made 3 days after that of experiment 145. HCT 10 was made the same day as this latter addition which showed a further improvement in cover. HCT 11, done 3 days later, showed a slightly further improvement. $Y_t(25^\circ C)$ decreased markedly from those found in experiment 129, and the decrease continued from experiment 145 to 146. The asterisk against the 15min colouring times indicates that 'popping' noises were heard during the later stages of colouring.

Experiments were performed using a volume of 4l colouring solution containing 60g/l sulphuric acid, 60g/l stannous sulphate, 60g/l phenol sulphonic acid and 54ml/l SNOS. Successive additions of 10ml Tribrite together with 10ml formaldehyde were made. The colouring current was $0.5A/dm^2$. Panels were coloured the day after the additions, except where a weekend intervened, in which case 3 days elapsed. The HCT was made on the same day as colouring. $Y_t(25^\circ C)$ was measured on the day after colouring, except at weekends. Because it became increasingly difficult to dissolve the Tribrite solely by agitation the additions of 50, 60, 70, and 80ml Tribrite were dissolved in the minimum amount of dilute sulphuric acid. 'Popping' noises were heard during the colouring of the final 3 panels in the series coloured for 15 min, accompanied by current surges. Small rings had appeared on the film surfaces and in some places bare aluminium was exposed. When panels were sealed, further sections of the film were detached. Graphs 29a, 29b and 29c show the relationship between $Y_t(25^\circ C)$ and the amount of Tribrite added. Generally, as Tribrite concentration was increased, $Y_t(25^\circ C)$ decreased. There was a significantly large decrease between 10 and 20ml additions for colouring times of 15 and 8min, (Graphs 29a and 29b). A further large decrease occurred between additions of 20 to 30ml, for 8 and 3min colouring times, (Graphs 29b and 29c). After these large decreases, the rate of decrease fell. The pass criterion for $Y_t(25^\circ C)$ is shown by the dotted line. Admittances decreased slightly during the 2min monitoring period for panels coloured for 15 and

Graph of $Y_t(25^\circ)$ against Tribrite Additions
 Stannous Sulphate 60 g/l
 Graph 29b



Graph of $Y_t(25^\circ)$ against Tribrite Additions
 Stannous Sulphate 60 g/l
 Graph 29c



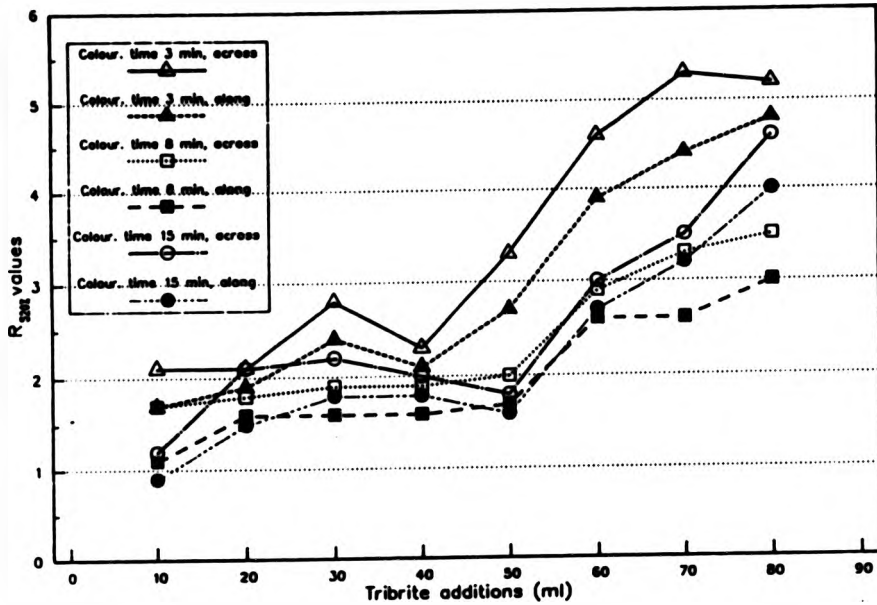
8min in baths with 20ml Tribrite.

Graph 30 shows the relationship between the luminance and the amount of Tribrite added. All colouring times show increases in the graphs corresponding to the first three 10 ml additions. Colouring times of 8 and 15min show a slight decrease with a further two 10ml additions, while a colouring time of 3min shows a decrease for another 10ml addition. All luminance values increase thereafter.

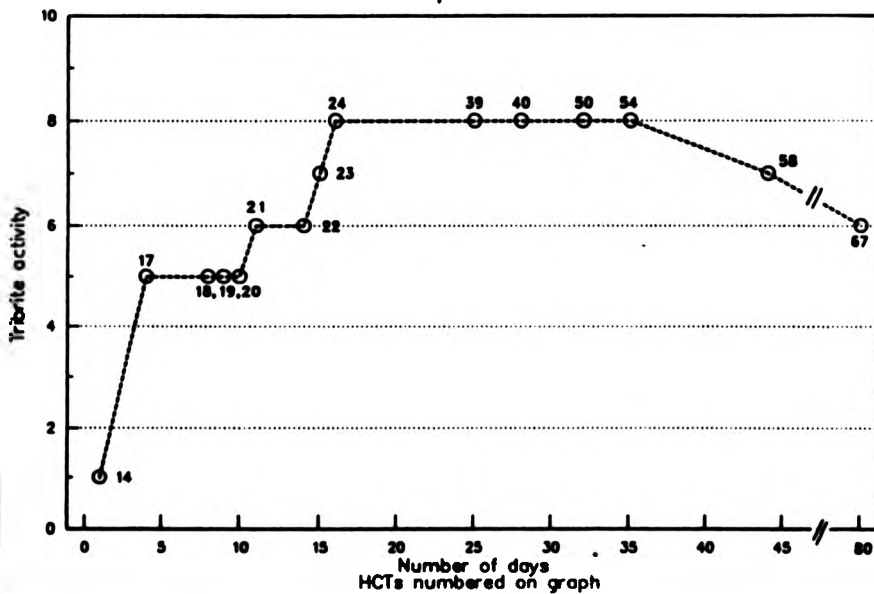
Finally a graph showing the relationship between colour differences ΔE , and the amount of Tribrite is similar to graph 30. The 3min colouring time shows a smooth increase. The 8 min colouring time shows a slightly less smooth increase, while the line for 15min colouring time shows a smooth increase from 50ml Tribrite onwards but below this the graph is erratic.

The HCT for 10ml Tribrite (HCT 17) gave the best cover. HCT 18 to 23, for the corresponding 10ml additions, gave increasingly roughened cover, especially at the high current density end, and large mirrored areas were observed on the back of the copper plate. HCT 23 was blackened and discoloured. Table 35 assigns values to the appearance of the tin deposit under various conditions. These values are represented in graphical form against the number of days between HCTs. Graph 31 is such a graph. HCT 24 corresponds to the final 10ml additions. No further additions were made and subsequent HCT cathodes showed the activity of the Tribrite with respect to tin cover on the cathodes. HCTs 24, 39, 40, 50, and 54 showed extremely blackened and roughened surfaces. HCT 58 showed a marked improvement.

Graph of R_{220} Values against Tribrite Additions
Graph 30



Graph of Tribrite Activity against Number of Days: Stannous Sulphate 60 g/l
Graph 31



4.15.1 Experiments Using Optimum Amounts of 'Tribrite'

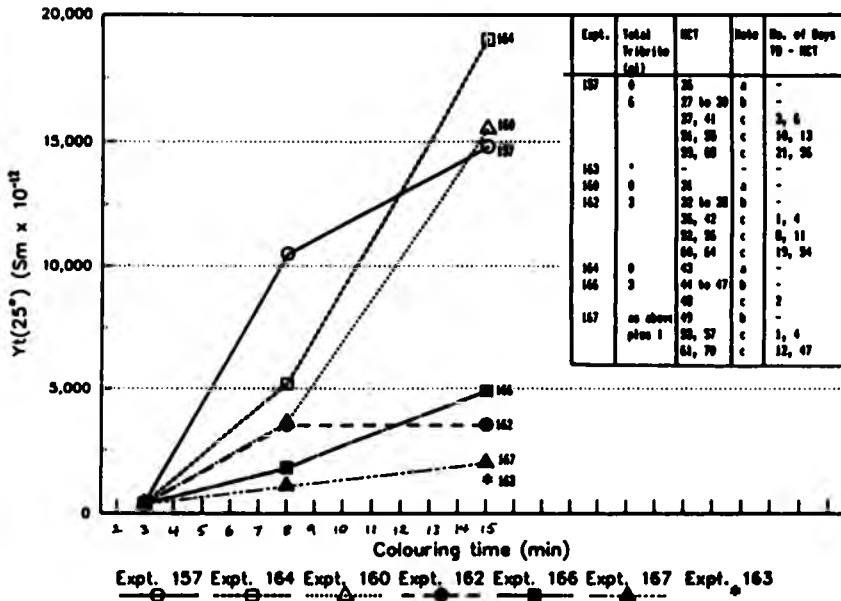
In the final set of experiments in this section, a 1 litre bath was made up of 20g/l sulphuric acid, 20g/l stannous sulphate and 20g/l phenol sulphonic acid. Film thicknesses were approximately 20 μ m. The first experiment was 157, Graph 32.

[Notes on Graph 32 :

- a) Hull Cell Test was made when no Tribrite was present.
- b) Hull Cell Test was made after each addition. The first addition was SNOS, the second was formaldehyde plus the first addition of Tribrite and subsequent additions were equal amounts of Tribrite.
- c) Hull Cell Test was made at selected intervals after the experiment. Number of days from the addition of Tribrite until the Hull Cell Test is given in the final column.]

Colouring current density used was 0.5A/dm². Three panels were coloured in this standard solution for 15, 8 and 3min colouring time. 18ml/l SNOS was added to the solution separately and HCT 27 made. Tribrite was added to this solution in equal amounts. 2ml formaldehyde was added at the same time as the first addition of 2ml Tribrite. After each addition of Tribrite, a HCT was made until an optimum concentration of Tribrite was reached, Graph 32, note b. The Tribrite was dissolved in 4ml dilute sulphuric acid before addition to the solution. Panels were coloured for 15, 8 and 3min in this 'new' solution, on the same day as

Graph of $Y_I(25^\circ)$ against Colouring Time
Graph 32



Graph of Tribrite Activity against Number of Days
(Expt 157)
Graph 33

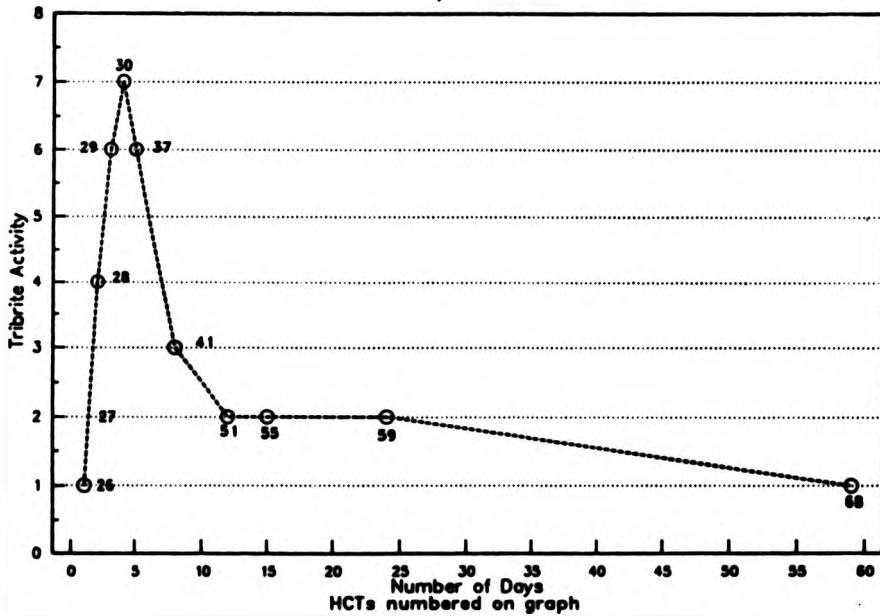


Table 35

Table of Hull Cell Test Appearance

<p>Tribrite not present.</p>	<p>1. Very loose tin deposit. Outward growth of crystals. Areas of copper plate still exposed.</p>
<p>Tribrite insufficient.</p>	<p>2. Bright area shrinks. When it is less than two thirds of the plate, addition is necessary.</p> <p>3. High current density end dull/grey, dull streaks may stand above brighter background. Brighter areas may be at low current density end. No mirrored surface on back of plate.</p>
<p>Correct amount of Tribrite activity restored.</p>	<p>4. Mirrored surface over most of plate. Some gas streaking at high current density end,</p> <p>5. Also small mirrored band on back of plate.</p> <p>6. Very bright at high current density end, where bright streaks stand above dull area, but less mirrored at low current density end. Large mirrored band on back, which may start to blacken.</p>

Table 35 continued

<p>Tribrite in excess/ working-in period not complete.</p>	<p>7.And/or blackened streaking or roughness at high current density end, sometimes extending over whole of plate.</p>
<p>Time delay after Tribrite addition/ working-in period complete.</p>	<p>8.Excessive amounts of Tribrite indicated by blackened surface on back of plate as well as front. Uneven areas of copper appear.</p> <p>7.After a period of time the mirrored surface reappears at high current density end, but blackening may still be at low current density end.</p>

the additions had been made. $Y_t(25^\circ\text{C})$ was measured for panels coloured in the standard solution and for those coloured in the solution containing Tribrite. Graph 32, Expt 157, shows the $Y_t(25^\circ\text{C})$ values for panels coloured without Tribrite. However, upon colouring after a total addition of 6ml, the film was detached and no admittance could be measured. Inspection of the HCT cathodes showed that HCT 28 had the optimum cover. HCT 29 and 30 showed roughening and a mirrored back. Subsequent HCT cathodes showed varying degrees of cover, as shown by Graph 33. Significantly, the curve reached a peak for HCT 30, then declined as sharply as it increased until HCT 51 after which the decline was gradual.

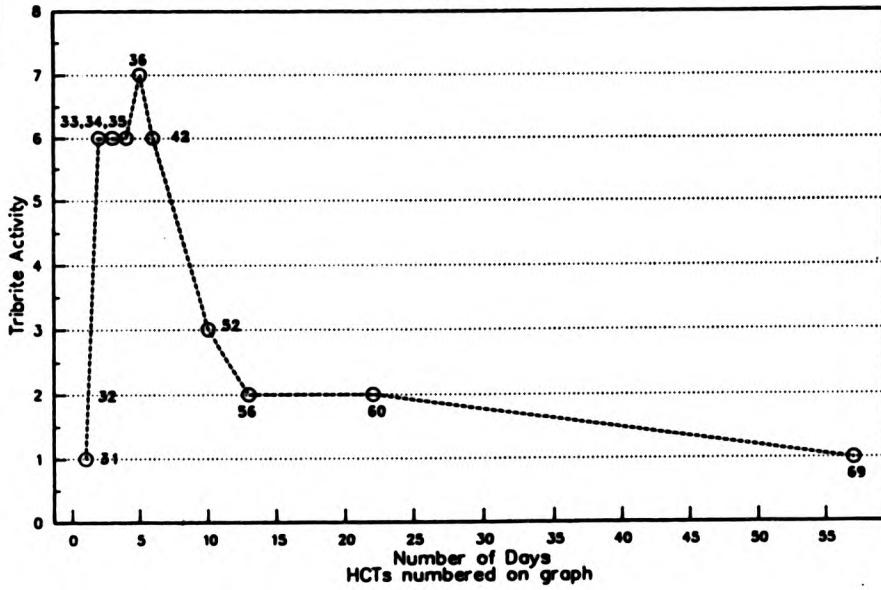
This solution was used in another experiment, 163, 4 days after the Tribrite addition, to determine if the colouring current density had been too high. Panels were coloured for 15min at various current densities. The current density during which no 'popping' noises were heard was taken as the best. This was found to be $0.33\text{A}/\text{dm}^2$. $Y_t(25^\circ\text{C})$ was recorded for this panel.

The next experiments, 160 and 162, used a solution made to the same formula as that used above. The current density used was $0.5\text{A}/\text{dm}^2$. 1ml Tribrite was added separately dissolved in 2ml dilute sulphuric acid. 2ml formaldehyde was added with the first addition. The experiment was performed as in experiment 157. $Y_t(25^\circ\text{C})$ values in Graph 32 for colouring with and without Tribrite, decreased when coloured with the Tribrite solution, except for the 3min colouring time. 'Popping' noises were heard

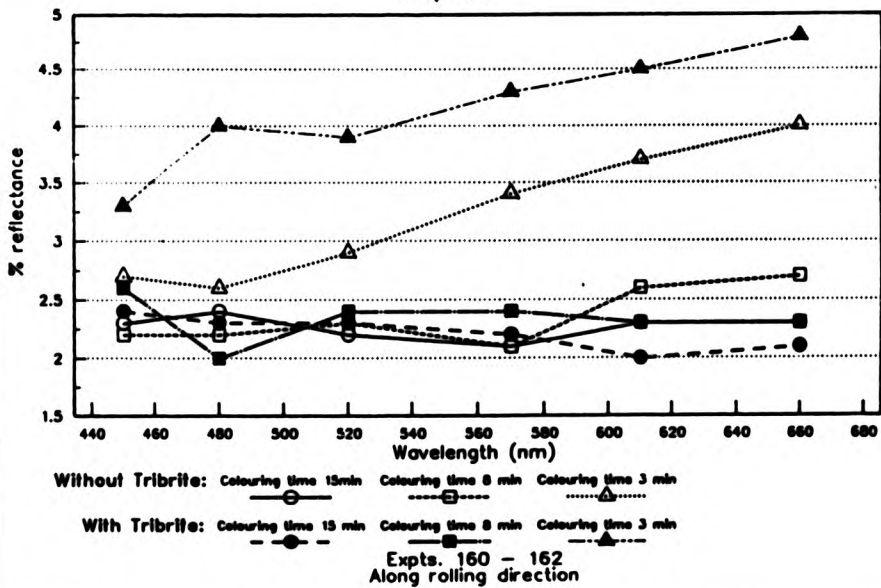
during the 15min colouring time. HCT 35 gave the optimum tin cover. The subsequent HCT cathodes showed varying degrees of cover, as shown by Graph 34. The shape of this graph is similar to Graph 33, except that there is a plateau between HCT 33 to 35. Graph 35 shows the percentage spectral reflectance against wavelength for the panel in experiments 160 and 162. The 3min colouring time resulted in higher reflectances at all wavelengths for colouring with Tribrite than for colouring without, but for 8 and 15min colouring times, the reflectances with and without Tribrite are inseparable.

The final set of experiments, 164, 166 and 167 used a solution again made to the same formula but using a colouring current density of $0.33A/dm^2$. The additions of formaldehyde and Tribrite were the same as in the last experiment, and the experiments were performed as above. The $Y_t(25^\circ C)$ values decreased with the addition of the Tribrite. No 'popping' noises were heard. The optimum tin cover was given by HCT 47, Graph 36. A small plateau was observed between HCT 45 and 46. HCT 48 was not as good as HCT 47. A further 1ml Tribrite was added 2 days later to this solution, experiment 167. Graph 32 shows even lower $Y_t(25^\circ C)$ values. However, 'popping' was heard for a 15min colouring time. HCT 49 showed good cover, but severe gas streaking was noted at the high current density end of the copper cathode. Subsequent HCT cathodes showed varying degrees of cover. A sharp peak was noted for HCT 49 which declined as rapidly as it rose until HCT 57 after which the decline was very gradual. Graph 37 shows that the curve for

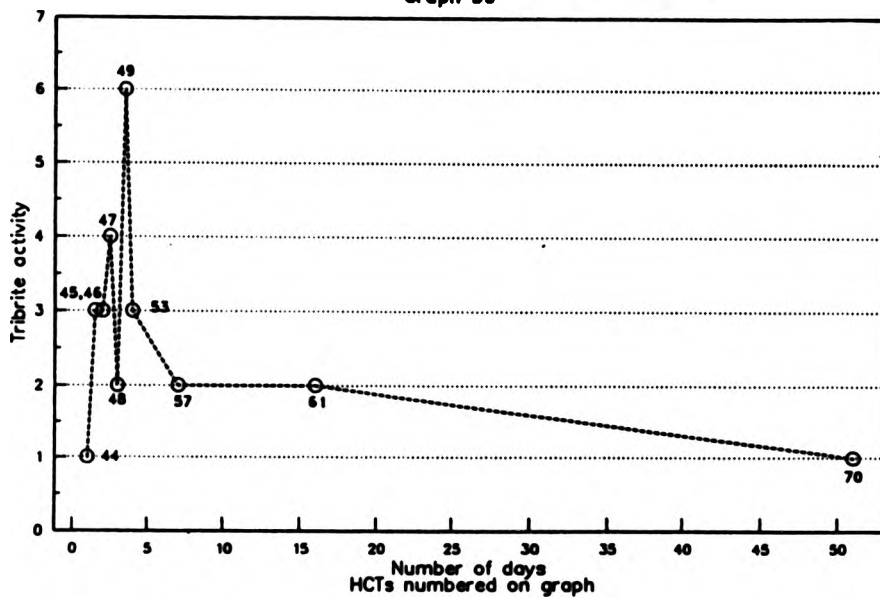
Graph of Tribrite Activity against Number of Days
Days (Expt 162)
Graph 34



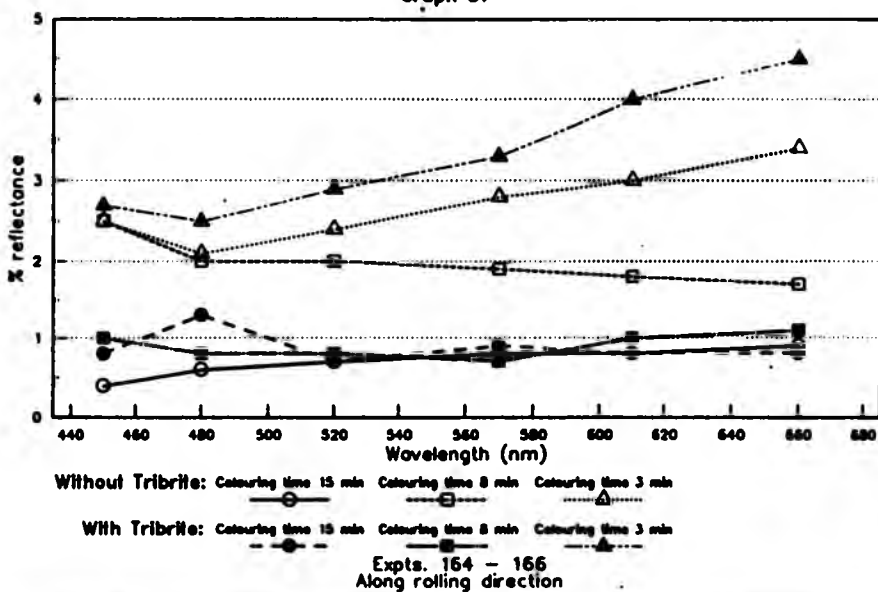
Graph of Percentage Reflectance against Wavelength
Graph 35



Graph of Tribrite Activity against Number of Days (Expts 164, 166, 167)
Graph 36



Graph of Percentage Reflectance against Wavelength
Graph 37



a 3min colouring time with Tribrite resulted in higher reflectance at all wavelengths than that without Tribrite. However, the colouring time of 8min shows the two curves reversed, while at 15min colouring time the curves are inseparable.

4.15.2 Colorimetry

Variations in the luminance values at the lower end of the percentage reflectance scale are insignificant because the films are black and very little light is reflected. A variation of 1 to 5% between values is acceptable. Small amounts of Tribrite did not affect the colour significantly and this was not detected by the colorimeter.

4.15.3 Stannous Tin Content of the Colouring Baths

The stannous tin content was measured by titration with 0.1N iodate-iodide solution using starch as the indicator. To a 5ml sample of solution, 20ml 20% hydrochloric acid was added before titration. All tin solutions were stored in air-tight bottles containing a piece of tin metal. Solutions were analysed which had been made between 2 years 6 months and 2 years 10 months, and had not been exposed to the air during the period of storage. Some of these solutions had various amounts of the Tribrite solution. Fresh standard colouring solutions were made (not containing Tribrite) and the tin content was analysed at intervals. The results show that the stored

solutions (with and without Tribrite) contained 2.3g/l to 5g/l of tin. The freshly prepared solutions had 5.5g/l to 6g/l of tin. There was no change in the stannous tin content for the fresh solutions over a period of 62 days.

If the assumption is made that 20mg/dm² of tin is deposited during one colouring period, the amount of tin removed from each of the old solutions can be calculated. This was found to be between 0.2g/l and 0.7g/l. One solution which had been used for a total colouring time of 300min may have lost 1.47g/l of tin.

CHAPTER 5

DISCUSSION OF RESULTS

5.1 The Nitric Acid Predip

The effect of the 33% HNO_3 predip was investigated on films of various degrees of hardness. If films had already been softened by agents such as warm anodising electrolytes (as revealed by a thickness wear index of greater than 1) then both substantial thickness and weight loss occurred during the predip. If films had not been previously softened, then it was found that the acid had no softening effect on the hard films. A very slightly softer film remained after the predip for a poorly sealed film soaked for 16 hours in the acid. An unsoaked well sealed film (5 min/ μm) showed a hardness similar to that of the latter film. As sealing time increased the surface and intermediate layers increased in thickness. The pore filling material increased in density. The overlying layers thus protected the porous layer from attack. After a sealing time of 0.5 min/ μm (approximately 12.5 min) the intermediate layer would be sufficiently thick so as not to be dissolved by the acid (102). The intermediate layer is protected in turn by the surface layer to a small extent. However, due to the nature of the surface layer it is 'porous' and does not offer much protection to the intermediate layer. At very long acid immersion times the intermediate layer may be slightly attacked. At very long sealing times (5 min/ μm approximately 125 min) the surface

layer reaches its limiting thickness. Due to the formation of primary and secondary groups of platelets, which the acid dislodges, some surface layer is lost. A higher wear index is obtained because of the removal of the soft outer layer, while the hard underlying layer is retained. This is confirmed by an unsoaked well sealed film having a slightly softer film due to the presence of these sheets. This layer is approximately $0.5 \mu\text{m}$ in thickness and once removed, the underlying well sealed film is unaffected by the acid.

Soft films which have lost some of the outer layer by dissolution do not lose any further film after subsequent additional predips; the thickness wear index remains constant and no weight loss is observed, despite the film being inherently soft. Prior to the predip, an abrasion profile of thickness loss against the number of cycles of 20 double strokes showed two distinct layers. The outer was softer than the inner. The total film thickness wear index was an average of the two separate layers. After the predip the two layers no longer existed, but the total film thickness wear index was the same as before the predip.

If there is no thickness wear index data, then a substantial weight loss after the predip would indicate a soft film, part of which would be lost during the predip. Inherently soft films which were adequately sealed were attacked by the 33% HNO_3 . The alumina, when hydrated, failed to form well defined crystalline boehmite. It is proposed that a different type of intermediate layer formed in soft films since they exhibit two distinct layers. This

intermediate layer is attacked by the acid and removed. During anodising at elevated temperatures the dissolution effect of the electrolyte is more pronounced. This promotes a more porous layer. Subsequent sealing may not take place efficiently due to the reduced microcrystallite content. It was suggested that the cell wall roughens during sealing, resembling a parallel stacking of platelets (76). This was thought to be a dissolution pattern on the cell wall and that sealing enhanced rather than caused the platelet stacking. If the cell wall is a more open structure, platelet stacking would not be so concentrated and it is likely the anhydrous cell walls themselves become hydrated. This may account for the soft outer layer.

5.2 33% Nitric Acid Admittance Drift Test

The usefulness of the 33% HNO_3 drift test to indicate the quality of sealing of an anodic film can be assessed by applying the mechanisms involved in the predip.

Hard, well sealed, aged films gave a positive \dot{Y} drift of 0.1 to 0.2 and $\dot{Y}t$ of 1 to 2. The small drift was due to the removal of some of the surface layer (saut). The consolidation throughout of a well sealed film has been shown by the $Y-\xi$ profile method. Softer, well sealed, aged films had larger positive drifts. This was due to the dissolution of the soft outer layers, and not due to inadequate sealing.

The drifts can thus be explained: if the film is inadequately sealed then the drift is large and positive

and is due to the dissolution of the pore filling material and is given by the equation:

$$\dot{Y}(25^{\circ}\text{C}) = \frac{Y'' - Y'}{10} \quad (\text{S} \times 10^{-6} / \text{min}) \quad (4.1)$$

where Y' is the first admittance reading,

Y'' is the final admittance reading, after 10 min.

Similarly, \dot{Y}_t will also be large and positive. If a soft, well sealed film gave a positive \dot{Y} drift larger than 0.2 then the drift would be due to thickness loss and is given by the equation:

$$\dot{Y}(25^{\circ}\text{C}) = \frac{k}{10} \left(\frac{l - l'}{t' - t} \right) \quad (5.1)$$

where k is a constant (i.e. $Y_t(25^{\circ}\text{C}) = 200$ for a well sealed film),

t is the initial thickness,

t' is the final thickness.

For an inadequately sealed hard film the drift will be due solely to the dissolution of the pore filling material, thus:

$$\dot{Y} = \frac{Y'' - Y'}{10} \neq k \left(\frac{1 - 1}{10(t' - t)} \right) \quad \text{since}$$

$$k \left(\frac{1 - 1}{10(t' - t)} \right) = 0$$

An inadequately sealed soft film would give a very large positive drift due to the combination of the two factors.

Negative drifts occur under certain circumstances. If the admittance decreases during the 33% nitric acid application this implies that either there is a change in the conductivity of the pore filling material, or that the thickness has actually increased. Negative drifts were recorded for two thick weathered films (see discussion on Weathering section 5.6). The admittance decreased due to the collapse of the cell walls. These drifts were recorded on the shielded faces. The shielded sides of thin films showed large positive drifts confirming the observations of Faller (126). All things being equal, corrosion is higher on the undersides than on the exposed sides, and thinner films suffer more than thicker films.

It is the contribution of the intermediate layer to the sealing quality which determines the type of drift. The surface layer contributes little to the overall values.

The drift test showed how consolidation within the pores occurred over a period of weeks in films sealed in 'Alcoa 482' (see discussion on Proposed Mechanism for Sealing in Nickel Acetate Solutions section 5.4). These films do not attain the same drift values as hydrothermal

films after 13 weeks but a steady low value would be expected to be reached eventually.

Only films coloured for short times attain the low drift values. Films coloured with Tribrite attain lower values than those coloured without Tribrite (see discussion on Tribrite section 5.11).

5.3 Concentrated Nitric Acid Admittance Drift Test

The drawback of this method was that the conductivity of the acid was greater than that of 33% nitric acid. Freshly prepared films showed negative drifts. The drift found by using solution 'A' of the Dye Spot test as an alternative electrolyte to the acid gave positive drifts, and the admittance values were comparable to those found with potassium sulphate electrolyte. This indicated that the concentrated acid reacted with the pore filling material. In freshly prepared films this material would be the gel which had not yet crystallised.

The admittance drift found for the sky-ward faces of the weathered films which had been exposed for 82 weeks compared very well with those found at an exposure time of 172 weeks and measured using 33% nitric acid. However, for the thick unsealed, partially sealed and well sealed films the concentrated acid drift values were larger than those found with 33% acid. This indicated that the concentrated acid had a larger dissolving effect on the more porous thick films. At 82 weeks exposure the gradients (of the graph of admittance against time) had begun to decline

again suggesting cracks were healing. The very small negative drift found for the thickest partially sealed film showed that the collapse of the cell walls just outweighed any dissolution effects, i.e. some redistribution of material and debris balanced any dissolution effects. The large positive drift for the thick well sealed film showed that the film was defective (see discussion on Weathering section 5.6).

Oversealed films gave negligible drifts showing complete consolidation of the film.

Films anodised and soaked, in sulphuric acid, at elevated temperatures (>26°C) gave soft films. Those anodised at 26°C and not soaked at high temperatures, or anodised at 15°C and soaked at high temperatures gave only marginally softer films than those produced under ideal conditions. The thickness loss for the soft films was greater than that for the hard films. This gave larger positive values for the equation

$$\dot{Y} = \frac{k}{10} \left(\frac{1 - 1}{t' - t} \right) \quad (5.1)$$

\dot{Y} found from the drift in admittance gave small negative values. This indicates that the soft outer layers are not only dissolved but there is a redistribution of material causing the pores to become blocked. This gave a false impression of increased sealing quality. It is postulated that it is the surface layer which is dissolved and the intermediate layer which is redistributed.

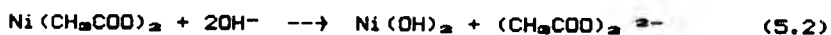
Aged coloured films gave comparable drift values to those found with 33% nitric acid. This showed how well-sealed films are unaffected by any concentration of acid.

5.4 A Proposed Mechanism for Sealing in Nickel Acetate Solutions

The products of the hydrothermal sealing reaction are combinations of aluminium hydroxide gel, pseudoboehmite and crystalline boehmite, or compounds similar to these but containing more water than the stoichiometric compounds. Different amounts of each type of hydration product occur at different stages throughout the sealing reaction, which proceeds throughout the length of the pore. As sealing proceeds local pH changes occur within and around the pore influencing the progression of the sealing reaction. This mechanism has been proposed by Thompson and Wood (79).

When sealing is carried out in a boiling nickel acetate solution such as 'Alcoa 482', the mechanisms involve not only those associated with the hydrothermal reaction but a pore blocking mechanism also. During the initial stages of sealing a poorly developed crystalline form of pseudoboehmite precipitates within the pores as water, at relatively high pH, meets the acidic Al^{3+} ions diffusing out of the pores. At about the same time dissolution of the macroscopic film surface occurs causing formation of a surface layer. This layer appears to be crystalline boehmite. Some Al^{3+} ions may diffuse from within the pores to contribute to the formation of this

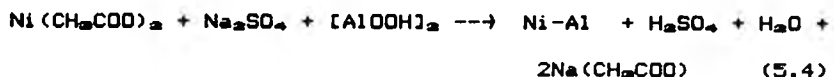
surface layer by a precipitation-dissolution mechanism. Groups of platelets form at nucleation sites increasing the thickness of this layer. As these hydrothermal reactions proceed the presence of a green surface bloom confirms the presence of nickel hydroxide which is deposited as $\text{Ni}(\text{OH})_2 \cdot 0.25\text{H}_2\text{O}$ (101). This reaction is also favoured by relatively high pH according to the reaction



For pore filling or surface product to occur it is necessary for local solution conditions to be favourable for precipitation rather than dissolution. In the neutral pH range 4-8 aluminium has a very low solubility. But as the pore blocking material increases, the Al^{3+} ion concentration within the pore increases. The 'Alcoa 482' solution is slightly acidic since 1 g/l sulphuric acid is contained within the solution while sodium hydroxide is used to achieve a pH of between 5.5-6.0.

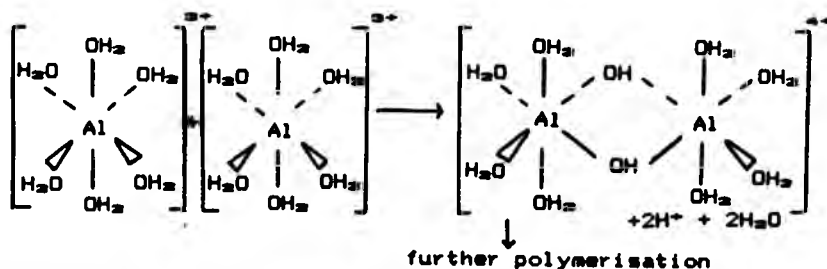


The reaction between nickel acetate, sodium sulphate and pseudoboehmite is as follows



Nickel acetate does not react significantly with

crystalline boehmite since attempts to seal a film for 3min/ μm after drying failed to attain an admittance value below 500/t (μS). The 'active sites' have become blocked. The reaction therefore involves pseudoboehmite. The pore filling material undergoes an 'ageing' process, whereby it polymerizes in a condensation reaction, releasing water as proposed by Baker (78). The crystalline boehmite is stable, while less stable pseudoboehmite and gels require a reduction in free energy in order to attain stability. The removal and access of molecular water is limited by the pore filling material and consequently the hydroxyl ion concentration increases. This probably occurs on the microcrystallites surfaces of the pore walls at 'active sites' and by formation of poorly hydrated alumina. However there is net uptake of water even though some is released during this polymerization reaction. This net uptake of water controls the pore filling process and intermediate layer formation by diffusion. However, at very short sealing times the intermediate layer would be extremely thin and its formation during nickel salt sealing has not been reported, although its formation is thought to occur early on during hydrothermal sealing (102). The condensation reaction has been proposed by Baker (78) as follows:



Aluminium and nickel both form hydrated ions in which the spatial arrangement of water molecules is octahedral. As well as the hydroxide, nickel is known to form the hexaaquanickel (II) ion $[\text{Ni}(\text{H}_2\text{O})_6]^{2+}$. It is likely that this ion combines with $[\text{Al}(\text{H}_2\text{O})_6]^{3+}$ in a condensation reaction similar to that proposed above with the elimination of water. At pH 5 as much as 90% of aluminium is in the form of polymers and at a high degree of hydrolysis the main ion has been found to be $[\text{Al}_{12}\text{O}_4(\text{OH})_{24}(\text{H}_2\text{O})_{12}]^{7-}$ (121). Successive condensation reactions would eliminate water leaving ill-defined forms of the hydrated product. It is well known that pseudoboehmite has a small crystal size with the majority of its hydroxyl ions spatially arranged in much the same manner as boehmite but with excess hydroxyl ions which are not in a boehmite arrangement. Since nickel is also found in highly hydrated forms it too would be involved in such complicated reactions and the result would be a complex crystalline matrix of aluminium and nickel ions as stated in the above reaction equation. As polymerisation proceeds during the ageing process the density and crystallinity of this pore blocking material increases and diffusion pathways become blocked. It has been suggested that water may diffuse through the anhydrous cell walls releasing SO_4^{2-} ions into the bulk solution. A volume expansion of the cell wall material may be associated with intermediate layer formation (102). Polymerisation and ageing are promoted by low acidity, high temperatures and high Al^{3+} ion levels. The latter levels are maintained by the

increasing density of the pore blocking material. The fact that very short sealing times give very low weight losses in the phosphoric acid/chromic acid test while high admittance values are found indicates that it is the outer most layers which are the most impermeable to the acid solution. The nickel is confined to the outer layers of the anodic oxide film. This is partly due to the rapid formation of the gel which restricts fresh solution entry. It must also be borne in mind that the presence of nickel itself would create unfavourable concentrations gradients for further uptake. This is confirmed since sealing in more concentrated solutions is less rapid than in dilute solutions (101). The extremely rapid crystallisation can be explained partially due to the ability of nickel to prevent the detrimental effects of silicates and phosphates, allowing the 'active sites' of the pore walls to promote the hydroxyl concentration. This maintains a low acid level which enhances the ageing reaction. As the pore filling material becomes more crystalline this promotes intermediate layer formation, although its presence may be very small at very short sealing times as stated previously. Assuming that there is some intermediate layer formation, water diffusion controls its formation. As it advances towards the metal/film interface it encounters the increasing Al^{3+} ion concentration. However, if bound SO_4^{2-} ions are released from the cell walls, the pH would become locally favourable. The increasing hydroxyl ion concentration would also favour intermediate layer formation. The participation of the acid anion incorporated

in the porous oxide film from the anodising acid may influence these reactions. Hydrolysis sites are considered to be the initiators of the reactions and these anions may have an effect on the development of colloidal alumina, its polymerisation and precipitation. It is also likely that the above mechanism proceeds in combination with that proposed by Wefers (76). The formation of a nickel-hydroxo sulphate salt similar to that proposed for aluminium, $[\text{Al}(\text{OH})(\text{SO}_4)\text{H}_2\text{O}]$, may be an unstable intermediate in the series of complex reaction mechanisms.

When films were dried before being sealed, it was found that 'Alcoa 4B2' was not as efficient as water at subsequently sealing the films. This showed that the hydration of the alumina which takes place when unsealed films are dried, causes sufficient blocking of the pores so as not to allow precipitation of Ni-Al compounds. It can be assumed that nickel acetate does not react with crystalline boehmite. The subsequent sealing in water probably occurred by diffusion of water from the bulk electrolyte.

5.5 A Proposed Mechanism for Long Term Cold Sealing

It has been shown that long term cold immersion in water and nickel acetate solution caused anodic oxide films to seal, but by different mechanisms. Water-sealed films showed a softening of the outer layer and the pore blocking material was not crystalline boehmite. Nickel acetate-sealed films showed no softening and the films were properly sealed and not blocked, as found with the boiling

solution.

The films immersed in water can be compared to those sealed in boiling water; they can be regarded as partially sealed. The solution was at room temperature and the precipitation/dissolution mechanism was very slow. The bloom observed upon removal from the solution during the period of immersion was possibly due to the precipitation/dissolution mechanism creating a surface layer. Competition between dissolution and precipitation varies during the immersion time and this accounted for variations in thickness recorded at intervals. The surface layer may have reached a limiting value after a period of time. This layer may have become undermined and dislodged in a mechanism similar to weathering due to continual electrolyte contact. After the total immersion period both films showed a surface bloom which was approximately $0.5\mu\text{m}$. At the pore bases continual dissolution would give Al^{3+} ions and the hydroxyl ion content would be mobile due to the presence of the electrolyte, but diffusion of both species would be slow. The formation of the intermediate layer is also promoted by precipitation/dissolution and this forms to some extent due to the continual diffusion of water from the bulk electrolyte which controls its production. This intermediate layer may contribute to the soft outer layer. Subsequent work (122) involving the Y- δ profile method has shown that for poorly sealed films there is increasingly less, or ill-defined boehmite as the pore depths are reached. The admittance drift test is a useful tool in this case. Some polymerisation of the

pseudoboehmite takes place. This is promoted by low acidity, high temperature and high Al^{3+} ion levels. The latter levels are maintained by the continuing dissolution of the pore bases. The continual contact with the electrolyte keeps the acidity relatively low due to fresh supplies of hydroxyl ions. This promotes the ageing reaction, but because the temperature is low, it occurs extremely slowly. The hydroxyl ion concentration also favours intermediate layer formation.

Long term cold immersion in nickel acetate solution seals the film by a mechanism similar to that occurring during hot nickel acetate sealing. It is assumed that the mechanisms occurring in cold water immersion also occur in the present case. The nickel also contributes to the sealing. It is assumed that the ageing reaction, which was shown by the Y- δ profile to occur in hot nickel acetate sealing, occurs in this case, but at a slower rate. At the same time as the surface layer is formed, nickel hydroxide is deposited as a surface bloom. The formation of Ni-Al complexes proceeds in a manner similar to that found in hot sealing. The polymerisation of the crystalline material occurs quite quickly, compared to cold water sealing, despite the low temperatures. The increased density tends to block the diffusion pathways, thus polymerisation is promoted by low acidity and high Al^{3+} ion levels. The continual presence of the electrolyte offers a continued hydroxyl ion concentration which is promoted at 'active sites'. These do not become inhibited due to the presence of the nickel. It is questionable as to whether an

intermediate layer forms during cold nickel acetate sealing since no soft outer layer was observed. It has been noted (97) that anti-smut additives do not form an intermediate layer. The presence of nickel hydroxide in the surface layer also showed how it hindered the formation of a soft outer layer. The solution 'A' of the Dye Spot test did not have a dissolving effect on the surface, while for the water-sealed film it gave a reaction showing some dissolution.

If the results of the admittance drift test and the $Y-\delta$ profile method are compared for nickel acetate-sealed films, it can be shown that the consolidation of the crystalline material increases with time. That most of the nickel is confined to the outer layers does not appear to lessen the extent of the underlying crystallinity. Minute quantities of nickel in this region appear to be sufficient for polymerisation. It appears from the $Y-\delta$ profiles that it is not the depth of penetration that influences the ageing process, but the concentration of the nickel. This concentration appears to be critical in the ageing process. After 48 days ageing the film sealed for the shorter time showed a lower admittance than that sealed for longer time. Measurements were made at the same film depth as for those performed on the freshly prepared film. It is concluded that the nickel content affects the dielectric constant of the sealed film. This varies throughout the whole film, and at any one point is determined by the amount of nickel present and the resulting crystallinity.

Earlier work performed on the same films (123) upholds these proposed mechanisms. Fisher showed that there were 3 sealing stages for both water and nickel acetate.

1. A rapid $Y_t(25^\circ\text{C})$ decrease due to hydration accompanied by a decrease in the pore length and diameter.
2. Irregular behaviour of $Y_t(25^\circ\text{C})$ due to formation of a pore mouth plug.
3. Subsequent slow rate of sealing due to diffusion of sealant through plugged pore mouth.

There was three times more weight increase for nickel acetate than for water during the first 5 to 7 days of immersion. This weight increase is now accounted for by the incorporation of the heavier Ni-Al material and this shows the rapidity with which it formed. The graph of $Y_t(25^\circ\text{C})$ against time showed that the superficial mechanisms of early pore blocking/sealing are quite different in the two electrolytes.

The admittance drift distinguished between films sealed by cold immersion in water and those in nickel acetate. The admittance drift for films sealed in water was large and positive as found by the equation:

$$\dot{Y}(25^\circ\text{C}) = \frac{Y'' - Y'}{T'' - T'} \quad (4.1)$$

There was a small drift due to thickness loss as found from the following equation, but this was small:

$$\dot{Y}(25^\circ\text{C}) = k \left(\frac{1}{t'} - \frac{1}{t} \right) \quad (5.1)$$

These results show that the pore blocking material was dissolved, i.e. the film was not 'sealed'.

Films immersed in nickel acetate showed that a negligible amount of pore blocking material was dissolved as indicated by a very small drift found by equation 4.1. The negligible negative drift found from equation 5.1 arose due to instrument error and is assumed to be zero. This implies there was no drift due to thickness loss. Thus, for water sealed films the actual thickness loss outweighed any contribution from instrument error, whereas for films sealed in nickel solutions, instrument error alone was recorded, since there was no change in thickness.

5.5.1 The Y- δ Profile Method on Films Sealed in Boiling 'Alcoa 482'

There is a change in the amount of Ni-Al complex throughout the pore length. The ageing of such films was observed by admittance measurements. Measurements made immediately after sealing showed very high values indicating little crystallisation of the gel. As ageing proceeded the admittance values decreased showing increased crystallisation. A Y- δ profile made on a properly hydrothermally sealed film showed the admittance to be constant throughout the length of the pore. A poorly sealed film which had been aged showed that the admittance rose as the film was abraded away. This was also observed for films sealed for 5sec/ μm in 'Alcoa 482'. If 'Alcoa 482' films,

sealed for longer times, were also regarded as poorly sealed, like the poorly sealed hydrothermal films, then the $Y-\delta$ profiles for aged films might be expected to be similar. However, after ageing for 48 days the 'Alcoa 482' films attained a line horizontal to the x axis, while the poorly sealed hydrothermal films, aged for number of years, showed the admittance rose within the pore depths. This supports the proposition that it is the intermediate layer which has a significant bearing on the hydrothermal reaction.

The mechanism of ageing can be proposed. For poorly sealed hydrothermal films the extent of formation of pseudoboehmite by dissolution of the pore walls is limited, particularly at the pore bases. Subsequent polymerisation once the film is removed from the solution is restricted since the temperature is low, the Al^{3+} ion concentration decreases, and the hydroxyl ion concentration decreases as the condensation slowly stops. The sealing product eventually reaches a stable state leaving a more 'open' matrix at the pore base than at the mouth. The rate of ageing is dependent upon the OH^- ion concentration (76). Thus short sealing times only allow limited formation of hydroxyl ions at the active sites. This 'open' matrix lends support to the proposition that the intermediate layer plays a role in the agglomeration of the gel, since it has been shown (79) that dissolution and precipitation occur throughout the length of the pore. The formation of this layer is controlled by diffusion of water from the bulk electrolyte. The presence of the intermediate layer

therefore promotes polymerisation. It is unlikely that continuing condensation reactions contribute enough water to be of any significance to the overall hydroxyl ion content.

Films sealed in 'Alcoa 482' show very different sealing mechanisms. Assuming that there is a contribution to sealing from an accompanying hydrothermal reaction (although at very short times) then the following ageing mechanism can be proposed:

1. The presence of nickel allows 'active sites' to remain unhindered and consequently more hydroxyl ions are present.
2. The Ni-Al complexes are very much larger than the boehmite molecules creating greater consolidation.
3. It is the concentration of nickel that influences the admittance.

5.6 Weathering

The theory of long term cold immersion can be loosely applied to films which are unsealed and subjected to long term outdoor exposure.

The admittance for unsealed films decreased with time. The first few weeks of exposure showed no adequate sealing but after a while sealing proceeded rapidly, followed by a more gradual rate. The shielded sides showed adequate sealing and some thickness increase while exposed sides were not adequately sealed and there was some thickness reduction. This 'sealing' was combined with 'weathering' as exposed surfaces had a pronounced bloom,

which was more severe than on the shielded sides. The admittance drift test, however, revealed that the pores were not sealed but blocked. These findings are in agreement with Patrie (124) who found that the admittance values remained overall above 400/t (μS), even though admittance may decrease during the course of exposure. These decreases were not a true indication of sealing. The admittance drift confirmed this. Only the shielded faces attained values less than 500/t (μS) while exposed faces remained above this value. In the work of Patrie it was the 'landward' face which became corroded. My work revealed that for partially sealed films the exposed face gave the worst bloom. However, subsequent admittance drift tests showed the exposed face to be sealed while values for the shielded face indicated inadequate sealing. Bloom and corrosion are different phenomena and the comparison of these results with those of Patrie must be treated with caution.

The pore blocking material was probably poorly formed pseudoboehmite/boehmite as found with long term cold sealing. There was little crystallinity. Due to the presence of a bloom, some form of weathering also took place. It may be that the 'weathering product' blocked the pores to give favourable admittance values, but the admittance drift revealed no true sealing. Weathering also undermined the surface layers and caused sheets of platelets to become dislodged. This would account for the thickness decrease on the exposed surfaces. This 'lateral flaking' has also been suggested by Furneaux et al (97). It

was suggested that the intermediate layer may have a role since it too was a lateral feature.

Shielded faces showed thickness increases and this may be because conditions were favourable for the precipitation/dissolution mechanism to form surface layers.

Some polymerisation takes place although it would be very slow. During wet periods this may proceed due to favourable conditions, although the temperature would not be high. However, the temperature can vary by as much as 25°C, and damp warm periods would promote crystallisation. The metal would heat up quite considerably in the sun. The films were first exposed during October and during the damp winter months polymerisation would have been enhanced. This was shown by a sharp decline in the graph of gradient (found from the linear regression of admittance against thickness) against time from October to June of the first year. It can only be conjectured that if the films had been exposed during the summer months, and the weather had not been damp, then the gradients may not have decreased as rapidly. Subsequent periods of electrolyte contact did not have such an effect on polymerisation as the diffusion pathways would have become blocked. However, crazing may have opened up other pathways. Renewed precipitation/dissolution may ultimately heal these cracks. The effects of dry periods may be rectified by subsequent wet periods. Additionally, wet periods also increase the effects of weathering. Environmental humidity cycling was mentioned by Furneaux (37) confirming this theory. Furneaux found that very many samples produced under a

variety of conditions exhibited light bloom or matting. This is in agreement with my findings that well sealed films exhibited a bloom. The mechanisms of long term cold immersion and weathering of unsealed films are akin to one another.

Partially and fully sealed films which were subjected to outdoor exposure were subject to mechanisms similar to those of unsealed films. The extent of further sealing was limited because the alumina had already been hydrated either partially or completely. Similar trends for the gradients were observed for partially and fully sealed films. The pattern for the exposed faces were almost identical while that for the shielded faces showed the partially sealed films to have larger maxima and minima. Less adequate sealing on the shielded faces had been reported previously (125). Further polymerisation was shown by continued decrease in gradients despite the blocked diffusion pathways. This indicates that diffusion of water may take place through the anhydrous cell wall and this may be enhanced by the presence of microcracks. This effect was less pronounced on fully sealed films. The occurrence of all the gradients increasing during the summer/autumn period suggests polymerisation has slowed and that microcracks are not healed over. The admittance was shown to improve on purposely cracked films (125) confirming these ideas. Final thicknesses were found to be the same as for unsealed films except that for the exposed faces 60% of fully sealed films showed thickness reduction and 40% thickness increase. This result shows the competition

between the precipitation/dissolution mechanism and weathering. Weathering may occur during dry periods due to surface layers drying out and then subsequent ingress of water between lateral flakes. I found that bloom formation was worse on exposed faces than shielded faces, and worse on the partially sealed films than on the fully sealed films.

The admittance drift test after exposure showed the well sealed film to give consistently low values for all thicknesses. This showed that, although weathering had produced a bloom, it had not undermined the well sealed film.

Unsealed films were shown by the drift test not to be sealed but blocked by pore filling material which was not boehmite. The values varied widely for different thicknesses and did not consistently attain low values.

Partially sealed films showed that the exposed faces gave consistently low values while the shielded faces gave widely varying values. Despite a bloom on both faces, that on the exposed face was superficial and confined to the surface layers while that on the shielded face included weathering product inherent in the anodic film. These results show the need for maintenance of shielded areas which may be subject to increasing dirt accumulation and moisture retention as discussed by Sheasby (116).

Negative admittance drifts were recorded for thick partially and fully sealed films. This showed (as with the results found for conc. HNO_3 drift tests on thick films) that the film collapses during the measurements,

blocking the pores. If the thickness decreased and/or the pore filling material was dissolved then the drift would be positive. The negative drifts indicate that the thick films have softer outer layers. The cell walls of these soft films collapse and this effect outweighs any dissolution, which would be small. Only small positive drifts are recorded for other similar films.

Concentrated HNO_3 , as an electrolyte for the admittance drift test, has a larger dissolving effect than 33% HNO_3 . Well sealed films showed no drift with the former electrolyte, but very thick films showed some drift. Thick partially sealed films were not as well sealed as thinner films. Films having very high thicknesses ($40\mu\text{m}$) showed small negative drifts and the thickness was reduced after measurement. One panel carrying a thick, well sealed film gave a large positive drift. The film was not soft and any thickness reduction did not account for such a large drift. It was concluded that the film was defective in some way, perhaps crazed. Sheasby (116) reported that film thickness was the single most important factor for crazing of thick films.

5.7 Sulphur Dioxide Tests

Sulphur dioxide tests are accelerated corrosion tests. They were intended to represent outdoor exposure at an accelerated rate. The optimum test conditions were found to be for 6 hours and at a temperature of 40°C . Perfectly sealed films $25\mu\text{m}$ in thickness passed the test, which was

indicated by no attack of the film surface. The admittance measured before and after the test gave small variations. An oversealed 25 μm film failed after a test performed for 24 hours at 38°C. The admittance after the test was greater than before and there was an iridescent surface bloom. Films less than 25 μm in thickness failed the test, even those which had been oversealed. Crazeing of the anodic film was observed to cause a bloom and the admittance increased after the sulphur dioxide test. Uncrazed films which failed the test gave a slight bloom and the admittance decreased. This result was also found by Fisher (123). Although pores become blocked due to attack by the sulphur dioxide, the inadequate sealing allows corrosion within the film. My work showed that subsequent tests on failed films, which had been cleaned, continued to show a bloom but the admittance decreased. Fisher (123) suggests that subsequent tests block the pores.

Poorly or oversealed films are attacked by the sulphur dioxide gas during the test. The reaction of sodium thiosulphate and sulphuric acid is complex. A variety of compounds are produced (115). The initial reactions are:



The sulphurous acid is partitioned between the gas space of the test chamber as SO_2 and water vapour and the solution in which it probably exists as H^+ and HSO_3^- . By slow

decomposition and reformation reactions other polythionic acids decompose to give the final products SO_2 , H_2SO_4 and sulphur. Very little H_2S is formed since the equilibrium reaction



lies far to the right hand side. In a room temperature test lasting 24 hours the SO_2 concentration rises during the first 2 to 3 hours and the ratio of water vapour to SO_2 decreases sharply. The water content remains constant. Prior to elevated temperature tests, all solutions and equipment were preheated so as to avoid excessive condensation in the test chamber. Excessive aluminium sulphate may be produced if condensation is present during this critical period. The appearance of a wet surface film on the specimens indicates that sulphate, probably as sulphuric acid, is present. These wet films form deposits of crystalline sulphates obscuring the true test result. These deposits were also recorded by Fisher (123) during a test performed at 60°C for 2 hours. In this test the H_2SO_4 concentration was low and $\text{Na}_2\text{S}_2\text{O}_3$ concentration was high. The reduced acid content and high temperature lead to an increase in humidity. At high temperatures H_2SO_4 does not form but the species exist as SO_2 and H_2O . The sulphurous acid attacks the film; SO_2 and H_2O separately do not dissolve alumina. The high temperature has a sealing effect on the film, thus giving false positive results. The best test temperature was 40°C , as the temperature stability

of the oven was poor.

Unsealed films in which the alumina has not been hydrated were subject to corrosion. The sulphurous acid dissolved the alumina. Partially sealed films also showed attack. In both cases the attack was within the porous layer. The bloom was possibly partly aluminium sulphate.

Oversealed films were also subject to bloom formation, although this appeared as iridescence. This form of attack was similar to that encountered during the weathering of thick films, and is a consequence of lateral flaking of the surface and intermediate layers (97).

Films sealed for short times in 'Alcoa 482' and aged for 24 hours showed no bloom formation during room temperature or 38°C tests conducted for 6 hours. This showed that the pore filling material was resistant to the sulphurous acid. Only well sealed (2 min/ μm) films gave an admittance of less than 500/t (μS) after the tests. This showed there was some redistribution of the surface layers.

5.7.1 Sealing Bloom

It has been shown that oversealed films had a sealing smut which was detected by the sulphur dioxide test. However, this investigation has also shown that a sealing bloom formed on films sealed for other times may not be revealed by this test. The appearance of white powder residues on the abrasive papers of the Three Paper test, before the sulphur dioxide test, reveals the sealing bloom of well sealed films. Short sealing times did not

give any residues. This indicates that the bloom is associated with the surface and/or intermediate layers. Analysis of the Three Paper test results and the Sulphur Dioxide test results showed the following: well sealed films which gave no sulphur dioxide bloom were abraded by garnet paper to give white powder residues after each application of 10 double strokes. The first 10 double strokes with glass paper gave a residue, but a further 10 double strokes did not abrade the surface. This showed that there was a very thin soft outer layer. Poorly sealed films which gave an SO₂ bloom were abraded by both glass and garnet paper after the test. If a Three Paper test was performed before the sulphur dioxide test, no abrasion occurred. Well sealed films, anodised at 20°C, were abraded by the glass paper revealing the sealing bloom, but a subsequent sulphur dioxide test gave no bloom. This showed that the Three Paper test is an alternative method of revealing the extent of sealing. It can also separate thick and thin films which were anodised at 20°C.

Film softening caused by anodising at elevated temperatures was revealed by an abrasion profile and sulphur dioxide test. An abrasion profile (thickness loss against number of double strokes) showed there to be two distinct layers after the sulphur dioxide test. After immersing this film in 33% nitric acid a subsequent abrasion profile revealed that both layers had been softened further; the outer layer to a greater extent than the inner. The overall thickness wear index of the whole film was slightly lower after the predip than before. The

predip does not remove the sulphur dioxide bloom, but accentuates it. A soft film which exhibited two distinct layers but did not have a sulphur dioxide test, was given a predip. A subsequent abrasion profile showed only one layer. The overall thickness wear index was unchanged. This showed the predip had removed the softest outer layer although the whole film was inherently soft.

5.8 Analysis of the Gradients of $Y_t(25^\circ\text{C})$ Against Thickness Found by Linear Regression for Natural Coloured Films

The anodic oxide film should be at least $25\mu\text{m}$ thick for external architectural use in Britain. In commercial production it has been found that film thicknesses of a batch may have a wide range of thicknesses. A standard sealing time of $2\text{min}/\mu\text{m}$ for a nominal film thickness of $25\mu\text{m}$ should give an admittance of less than $500/t$ (μS) (25°C) to be of acceptable sealing quality. If the sealing time was fixed at 50min, based on a nominal batch film thickness of $25\mu\text{m}$, then thinner films would be sealed for longer than $2\text{min}/\mu\text{m}$ and thicker films sealed for less. Variation in thickness during production is to be expected. The technological use of linear regression to find the gradients during inspection of commercial products was the origin of the experimental investigation. Over a limited range of thicknesses the points on the graph of $Y_t(25^\circ\text{C})$ against thickness were treated by linear regression to obtain an equivalent linear gradient. A batch of thicknesses was deemed

acceptable if the gradient was $\leq +10$, which allowed for some thickness variation. It has been shown that a total sealing time of 50 min, in water, gave a gradient of $< +10$ for a thickness range of between $19\mu\text{m}$ and $36\mu\text{m}$. The method of measurement of $Y_t(25^\circ\text{C})$ required each film to be dried after each 10min sealing period. Therefore the stated sealing time included periods during which the films experienced some ageing. This was not exactly representative of commercial production control. The application of the linear regression to find the gradient does show however, a useful connection with the question of the degree of sealing of batches having a range of thicknesses but a common sealing time. The selected, carefully measured points generally seem to confirm that the linear relation is a reasonable assumption. Films which were anodised under constant time and increasing current density to achieve various thicknesses attained a gradient of $+10$ or less after a longer total sealing time than those films anodised to various thicknesses by increasing the anodising time. This showed that for the thicker films the pores were larger and hence required longer sealing time to close the pores. Both graphs gave good coefficients of correlation.

Films sealed in 'Alcoa 482' gave good coefficients of correlation for the graph of $Y_t(25^\circ\text{C})$ against thickness when anodised at varying current densities. Films produced by anodising at varying times showed the points to fit almost perfectly (coefficient of correlation was $+1$). Both sets had been dried prior to

sealing. The results indicate that, despite gradients not decreasing below +10, all films were sealed at the same rate. Ageing sealed the pores which were ultimately blocked by the nickel compounds; the sealing time was irrelevant.

5.9 Electrolytic Colouring (Electrocolouring)

The amount of tin deposited during electrocolouring was in agreement with that found elsewhere, typically 5 - 20mg/dm² (127). Gohausen (128) referred to the metallic nature of the deposits. In this investigation the d-spacings found by X-ray analysis were slightly higher than those of pure tin. Powder diffraction analysis gave d-spacings which correlated very well with those of pure tin. This suggests that the tin was in a slightly distorted tetragonal form.

It was found that the current density affected the admittance values of the anodic oxide films. High current densities caused 'spalling', a local flaking of the film from the substrate metal. During long colouring times at high current densities 'popping' noises were heard which were accompanied by surges in current. There was a break down of the oxide film allowing electrical conduction of current through the aluminium. Spalling has been explained by two theories. The first (129) is evolution of hydrogen gas at the pore bases mechanically separates the film from the metal. During alternating current a large proportion of flaws are activated in the barrier layer. This allows a large proportion of pores to fill with metal. Flaws are

caused by 'puncturing' of the barrier layer and this is caused partly by thermally enhanced field assisted dissolution. An alternative explanation (60) is that after pigmentation, re-anodising beneath the original barrier layer creates a less mechanically sound film.

Deposition of tin is not favoured by bulk conduction of electrons but by the presence of the flaws within the residual barrier layer. During the initial recovery period where barrier layer thinning occurs (when colouring voltage is less than anodising voltage) hydrogen gas is evolved in preference to tin deposition. It is postulated that the trapped electrons, which reduce the H^+ ions may play a role in flaw generation. At long colouring times at high current densities the puncturing may cease due to the physical impossibility of creating more flaws. The final reanodising stage may exacerbate the mechanical weakness of the new barrier layer, above which the old barrier layer can no longer support flaw formation. Thus spalling may be a combined effect of hydrogen gas at the new barrier layer/old barrier layer interface.

As colouring time increased, the colours became darker (in appearance). At extended colouring times the tin was shown by a number of methods to extend to the pore mouths. The variations in the chromaticity co-ordinates for films coloured under identical conditions were due to variations in the surface topography. This was particularly noticeable along and across the rolling directions of the aluminium. This macroscopic effect was detectable at low percentage reflectance, although the differences were

small. All colours are a comprise^{ed} of a variety of reflectances at all the visible wavelengths of light. The chromaticity co-ordinates show the ratio of one specific wavelength to the sum of two others and that specific one. Subtle variations in one of these three reflectances gives different co-ordinates. These variations are not detectable by the eye. The measurement of colour is dependent upon not only the reflectance at selected wavelengths, but also the physical features of the surface. The luminance is a more useful variable by which to compare colours. Similarly, the L values of the L, a, b, ΔE system give useful information as to the degree of colouring. Topographical effects still cause variations in measurement. At low percentage reflectances the topographical effects affect the luminance value less. Graphs of the luminance values against colouring time showed that higher current densities produced colours with lower luminances, i.e. the colours were darker. This indicated there was more tin within the pores. The colours were produced by light scattering. This correlated with the higher admittance values. At long colouring times the colours became lighter. The luminance values were high for low colouring current densities ($0.3A/dm^2$) at short colouring times (up to 5min). At long colouring times the luminance values were lower at low current densities than the high current densities. The influence of the colouring voltages play an important role with respect to the colouring time (130). At short times the voltage range may be from 8 to 20V, but only 10 to 16V for long colouring times (15min) above which the colour

lightens again (58). The lower current density (and voltage) produces the darker colours for longer colouring times, while at high current densities (and voltages) the limiting values are approached and spalling occurs or the colour lightens. At low current densities spalling did not occur because the preferential reaction was tin deposition. Both high current densities, and long colouring times at low current densities, gave high admittance values.

At very short colouring times (1min) the admittance values were low but irregular. This was because during the first minute of colouring the current rose rapidly due to the rectifying action of the anodic film. The same two theories that were postulated for tin deposition can be applied once again. An alternative theory is that the pH rises and this enhances tin deposition. Thus the time taken for rectification to cease determines the initial tin deposition. The variations in the admittance values reflect the variations in cessation of rectification. Electrons must play a part either in H^+ reduction or the activation of flaws. It may be that semi-conduction occurs through the flaws. It has been proposed (60) that current probably passes through the flaws and deposition of tin occurs at the original pores, while new tiny incipient pores form during the recovery stage. It is these new pores which cause barrier layer thinning by their nucleation and growth (58). The re-anodised layer does not contain electrolyte acid anions due to the difficulty of solution species diffusing past the deposits.

The graph of ΔE against colouring time was the mirror-image of the graph of the luminance value against the colouring time. Although there was a certain amount of scatter in the former graph, the general trend showed that the curve increased rapidly at short colouring times; it levelled out at long colouring times. The scatter was due to topographical effects of the film surface and instrument error. ΔE is the difference between the reference colour (a natural film) and the selected colour. The graph showed that ΔE changed more rapidly due to increasing amounts of tin up to a certain amount. The differences at long colouring times were not as great because the optimum amount of tin had been achieved. 'Over-filling' the pores with tin can be avoided by observing the shape of this graph.

The admittance is proportionally related to the capacitance of a parallel plate capacitor which is the anodic oxide film. The theoretical admittance value was calculated as $3\mu S$ for an uncoloured well sealed film. In practice the figure is usually about 6 to $10\mu S$, although aged films may approach the theoretical value. Admittance of electrocoloured films was shown to be greater than that of natural films, although very short colouring times varied little from natural films. The high values were accounted for by the presence of the tin within the pores. Theoretical calculations showed the amount of tin deposited for films of different thicknesses but the same colouring time. This showed that, for equivalent colouring times, thin films contained proportionally more tin than

the thick films. The bar charts (Graphs 14b and 15b) showed that the position of the tin appeared to be influenced by the thickness of the oxide film. For long colouring times (6min) the percentage of tin decreased as the thickness increased, while for short colouring times (1.5min) the percentage of tin increased as the thickness increased.

It was proposed that deposition occurred preferentially in shorter pores, suggesting a significant solution resistance within the pores (131). This was confirmed by the calculated t_m values for a colouring time of 6min. The effect of solution resistance was not as pronounced for short colouring times. The proportion of different pore lengths within a film must be taken into account, although evaluation was not possible. The proportions of short and long pores may vary due to different thinning rates of the barrier film in thick and thin films. During the recovery period of electrocolouring, field assisted dissolution proceeded by the nucleation of 3 or 4 incipient pores at the base of each original pore (60). Favoured pores increased in length and diameter once the barrier layer had thinned. At the new voltage the steady state population density of pores indicated that at least 100 incipient pores were nucleated from every original pore. The alternating current activated flaws and pigmentation occurred at different rates in different length pores. It is proposed that because thicker films had larger pores, there was a smaller flaw population and so less tin was deposited.

The calculated tin content was based upon the assumption that for an uncoloured well sealed film $Y_t(25^\circ\text{C})$ was $200\text{S}\Omega \times 10^{-12}$, and that $Y_t'(25^\circ\text{C})$ also equaled $200\text{S}\Omega \times 10^{-12}$ (where t' was the metal-free section of the film i.e. $t'=t-t_m$) then if t' equals $2\mu\text{m}$ in a $25\mu\text{m}$ electrocoloured film, Y must be 100. When films consisting of a range of thicknesses were sealed for a common sealing time, then thin uncoloured films had small admittance values and thick films had large values. When thin films were coloured for long times the admittances were large, indicating the contribution made by the tin. The calculated tin content ($t'=t-t_m$) for these films confirmed the proposed theory of admittance of electrocoloured films.

The large tin content in thin films indicated that the optimum colouring time had been exceeded; they were 'over-coloured'. For the same colouring time, thicker films had just reached the optimum amount of tin. Proportionately less tin was deposited in the thicker films than in the thinner films due to the increased surface area of the larger pores. At short colouring times the percentage of tin increased as thickness increased because the ratio of internal pore surface area to colouring time was smaller than for long colouring times. Thin films are therefore more sensitive to colouring time and this is reflected in the admittance values. This situation is analogous to thick films coloured for extended periods. These results are at variance with those of Sheasby (54) who claimed that colour was independent of the anodic film thickness. This allowed a full range of colours to be

produced on relatively thin films, 5 to 10 μ m in thickness. The colouring time of less than 10min was used but I have shown that this would exceed the optimum colouring time for thin films. It can be said that colour is independent of film thickness up to a point, but film quality of coloured films is dependent upon film thickness and colouring time. This is in agreement with Gohausen (128). However, Gohausen showed that both tin and cobalt deposits extended to the same distances through the film. Others (57) have disputed this; but comparisons cannot be made since the latter authors do not give colouring times.

5.2.1 Theory of the Gradient Found by Linear Regression of Admittance Against Thickness for Electrocoloured Films.

Theory suggests that as the metal comes further up the pores, the gradient for each thickness becomes more negative. This is a non-linear relation (given that $Yt(25^{\circ}C)$ for the sealed metal-free section of the pore is a constant). By treating the points (on the graph of admittance against thickness) by linear regression an equivalent average linear gradient is obtained. It can be assumed that $Yt(25^{\circ}C) = a + bt$ [where $Yt(25^{\circ}C)$ is the admittance x thickness, t is the thickness and a and b are constants], and $Yt(25^{\circ}C)$ varies with the degree of sealing. Over a range of t , b gives information as to the degree of sealing.

When the thickness covers a range of values in a batch, the assumption is made that the metal thickness t_m

is fixed. The remaining film t' is well sealed so that $Yt'(25^\circ\text{C})$ is a constant, 'A' for a freshly prepared film.

$$t' = t - t_m \quad (3.12)$$

so, $t' = t - \text{constant}$

$$\text{hence, } Yt(25^\circ\text{C}) = \frac{A}{t'} \times t = \frac{At}{(t-t_m)} \quad (5.8)$$

the admittance x thickness of the whole film.

The gradient of a set of well sealed films of various thickness is given by

$$\frac{d(Yt)}{dt} = \frac{d}{dt} \left(\frac{At}{t-t_m} \right) \quad (5.9)$$

$$= A \left(\frac{1}{(t-t_m)} - \frac{t}{(t-t_m)^2} \right)$$

$$\text{therefore, } b = \frac{-At_m}{(t-t_m)^2} \quad (5.10)$$

where $A = Y(t-t_m)(25^\circ\text{C}) = Yt'(25^\circ\text{C})$

However, b is a non-linear function of t . The gradient is negative and becomes numerically greater the higher the metal comes up the pores. The assumption is made that $A = 400S\mu \times 10^{-12}$ for a well sealed, fresh film. (A is a constant even when the effective dielectric thickness t' is

very small. Ageing causes A to decrease. Oversealing may cause A to reach a limiting value.) As the film thickness increases the gradient decreases (assuming A and t_m remain constant). The change in film thickness is accounted for in $(t-t_m)^2$ in the above equations. Over a limited range of t, the theoretical points could be treated by linear regression to get an average linear gradient; an average value of the form $Yt(25^\circ\text{C}) = a + bt$. This average gradient, found by experiment, was compared to the empirical value obtained by linear regression of $Yt(25^\circ\text{C})$ data for commercial tin electrocoloured blacks in a similar t range. Hence the gradient can be calculated for each thickness assuming $A = 4005\text{m} \times 10^{-12}$. Linear regression will give an average value of a gradient over the whole range. The comparison of experimentally produced ranges and commercial ranges suggests the theory is not too simple to give reasonable results if the assumption is made that the tin fills 22 to 23 μm of a 25 to 30 μm film. Coefficients of correlation are good indicating a good fit of the points.

Using the linear regression on films coloured for 6min the gradient became more negative as the thickness decreased when the calculated values for metal thickness were used in the equation

$$b = \frac{-At_m}{(t-t_m)^2} \quad (5.10)$$

However, the value of A must vary as t' varies for a common sealing time for a range of thicknesses i.e. for a sealing

time of 10min :

$t' = 0.3, 1.3, 3.5, 7.7$ (μm) corresponds to
 $\text{min}/\mu\text{m} = 33.3, 7.7, 2.9, 1.3$

and so Yt' must increase as t' decreases. In depth sealing has not been found to occur (58). The assumption that $A=400 \text{ Sm} \times 10^{-12}$ is incorrect, as shown by the bar charts (Graph 25). The metal thickness was not a constant when a range of thicknesses were coloured for a common time. Therefore if t_m changes as thickness increases for a colouring time of 6min, the individual gradients for each thickness found from the equation

$$b = \frac{-At_m}{(t-t_m)^2} \quad (5.10)$$

decrease (become less negative). This is non-linear as theory suggests. The gradients are spread more evenly than if calculated with t_m as a constant. Also if A has varying values then the graph of gradient against total film thickness approaches a semi-logarithmic relationship. If linear regression is applied to the range of thicknesses, the average linear gradient is found to be a reasonable one.

For very short colouring times (1.5min) the gradients found by experiment were positive. A gradient of less than +10 was achieved after a total sealing time of

40min. It can be assumed that the metal thickness was not significant and that the effective dielectric thickness was approximately equal to that of the total oxide thickness. In this case a linear relationship was assumed and the electrocolour admittance theory did not apply. Graph 15b showed the percentage of tin within the pores for a range of thicknesses as calculated from $t' = t - t_m$ and $t' = 200t/Yt'$. This showed that if the pores were filled to half their length then the metal did not have a bearing on the admittance values of well sealed films. This was confirmed since the gradients were also positive for poorly sealed films.

5.9.2 Flaws and Defects

Due to the presence of Silicon in the SiC alloy, flaws originating from these inclusions are proposed in electrocoloured films. Others (132) have found such flaws in barrier layer films although these thin films were analysed by STEM which has higher resolution than SEM. If it is assumed that the flaws originated from Si inclusion, then my results may be interpreted by this model. Only relatively coarse particles were analysed and their positions were different from those of the barrier layer films due to the film being porous. The photograph of panel 344 (Fig. 33) showed the presence of a ridge in the barrier layer and above this no tin was present. If it was assumed that this was due to an inclusion in that region then either there was a void above the particle or, assuming it

to be silicon, it had been oxidised to some extent to form an amorphous material. During anodic oxidation of porous films any ridges at the oxide surface were flattened. The massive particle in the photograph of panel 352 (Fig. 38) corresponds to a similar particle also observed by Shimizu, Thompson and Wood (132). It was assumed that the particle was separated from the metal by the barrier layer but this was not observed due to the poor resolution. The photographs of panels 349 and 351 (Figs. 34 and 36) did not reveal the presence of any particles, but it was assumed the resolution was not sufficient to detect them. Not all gaps in tin deposition can be accounted for by particle inclusion.

5.10 Elevated Anodising, Soaking and Colouring Temperatures

The amount of tin in the pores of films anodised and coloured at different temperatures was assessed by means of the abrasive wheel test (see section 3.5.10). The original purpose of this test was to determine the abrasion resistance of a film. By measuring the thickness at which the residue powder turned from white to grey or black, the position of the highest tin in the pores was found. This was converted into the percentage of tin which filled the pores (Graph 25). The general trend showed that there was less tin in the films when anodised at 15°C than when anodised above this temperature. This indicated that pores were enlarged when films were anodised at elevated temperatures allowing a large surface area for tin to be

deposited. Elsewhere (131) it has been proposed that the amount of deposition depends upon film porosity. Therefore the thinner pores appear to restrict the tin to the pore depths. This contradicts my earlier results in which thinner films had larger tin deposits than thicker films; although 'thicker' films do not necessarily imply greater porosity; i.e. larger pores. This indicates that the physical geometry of the pore plays a role in how tin is deposited. The calculated values for t_m (Graph 14 b) appear to be overestimated compared to the tin content found by the abrasive wheel method (for colouring time of 8min). This overestimation was due to the assumption that $Yt' = 200S_m \times 10^{-12}$ the equation

$$t' = \frac{Yt' \times t}{Yt} \quad (5.11)$$

If Yt' (A) changed as t' changed i.e. Yt' increased as t' decreased, then the tin content, calculated from $t' = t - t_m$ may have been similar to those found by the abrasive wheel method, i.e. less tin in the thicker films. The $Y-\xi$ profile would be useful tool to use with the abrasive wheel method. The abrasive wheel method was not used on films of thicknesses less than $20\mu m$.

Soaking a coloured film in sulphuric acid for extended periods after it had been sealed, completely dissolved the film. It was found that soaking films in sulphuric acid before sealing had a detrimental effect on the anodic oxide film. Colouring and soaking films in H_2SO_4

at elevated temperatures before sealing reduced the abrasion resistance. Colouring had a marginally greater effect than soaking. Colouring for any length of time at room temperature did not have a detectable softening effect. Soaking or colouring unsealed films did not reduce the abrasion resistance, and the pore bases were not softened, as was found by the abrasion profile graph. The process of sealing, once the film has been coloured or soaked, softens the film. It is well known that unsealed films are very abrasion resistant. It has been proposed that unsealed films may have a relatively soft outer layer and a harder inner layer (133). Sealing balances this difference to some extent. It has been shown in the present work that both colouring and soaking at elevated temperatures soften the film. If anodising was performed at high temperatures then the softening effect was exacerbated. Anodising below 20°C only slightly reduced the abrasion resistance when films were subsequently coloured or soaked at elevated temperatures. The acceptable thickness loss for an anodic oxide film is 7 - 8µm (400gf, 400ds). Agreement (108) is near on an International Specification for the abrasive wheel test (ISO DP8251). The abrasive wheel test will be included in the next revision of BS1615. Only when films were anodised at 20°C or less and soaked or coloured at very high temperatures (37°C) was this optimum exceeded. Gohausen (133) showed that for anodising at 18 - 19°C, 2.5µm were abraded when coloured at a temperature of 17°C, and 7.5µm at 30°C; a three-fold increase. My results (anodised at 15 and 20°C gave

thickness losses of 11.5 and 12.5 μ m for colouring at 18.5 and 37°C) did not show such a large difference between two colouring temperatures. Agreement was found however that at low anodising and colouring temperatures there was no difference in the thickness loss between coloured and uncoloured films. When anodising at 25 and 30°C the uncoloured film lost more film thickness than the coloured film. Also, the critical anodising temperature was found to be 20°C. If close temperature control of the anodising bath cannot be ensured then a temperature of 18-19°C allows for any small rise which may occur. When a film was anodised at a temperature of 30°C, the abrasion resistance was greater than that of a film anodised at a temperature of 25°C, when the colouring temperature was 37°C. This effect has been reported elsewhere (133). Gohausen showed that for a colouring temperature of 18°C, a film anodised at 27°C gave a greater thickness loss than a film anodised at 30°C. Gohausen stated that the ability of sulphuric acid of a specific concentration to dissolve unsealed alumina increases rapidly above a temperature which is dependent upon the concentration. This accounts for differences in the two sets of results. Discrepancies also arise because Gohausen anodised for a fixed time while I anodised for various times. However, the contribution played by the temperature of the colouring electrolyte is an important one. Soaking may have a different 'critical temperature', (where the combination of anodising and soaking temperatures cause differences in abrasion resistance), to that of colouring.

My investigations showed agreement with those of Gohausen; the electrolytic colouring treatment did not detrimentally affect abrasion resistance if films had been anodised under standard conditions. If inherently soft films existed then the abrasion resistance was reduced for uncoloured films and further reduced upon electrolytic colouring treatment. It was not the alternating current colouring treatment at elevated temperatures which caused the reduction in abrasion resistance, but the temperature. This was confirmed by experiments in which the films were soaked in the colouring electrolyte. An almost identical trend in thickness loss was observed. This was also shown by the abrasion profile graph. Thus factors which influence the redissolving process influence the abrasion resistance.

Two distinct layers were observed in films anodised at high temperatures; a soft outer layer and a comparatively harder inner layer. This latter layer did not give a thickness wear index of less than 1, however. For coloured films the ratio of outer to inner layer was 1:2 while for soaked films it was 1:1. The inner layer of the coloured film was softer than that of the soaked film; the outer layers gave the same abrasion resistance. The combination of acid electrolyte and the bulk high temperature, and possibly higher local temperatures, caused the anodic film to soften after a period of time. The outer layers were exposed to these factors for longer than the newer inner layers. The marginally greater dissolving effect of the colouring process was noted. It is not coincidence that the thickness at which the inner layer

occurs corresponds to the appearance of tin in the abrasive wheel test.

The exclusion of the thickness lost during the first 100 double strokes of the abrasive wheel test may be required to eliminate any roughness on the surface, eliminating topographical high points. For soft films the roughened surface is a distinct feature which influences other properties of the film. The first 100 double strokes may give an indication of this surface phenomenon and in this case cannot be excluded. The load used and the number of double strokes in a cycle are important in this respect. The three paper test is unaffected by rough surfaces.

Oversealing alone does not reduce the abrasion resistance, but a sealing bloom was shown by the three paper test (section 5.7.1). If a film was anodised above 20°C then the surface layers were softened, irrespective of sealing time. A subsequent sulphur dioxide test (38°C for 6 hours) carried out on these films gave a uniform bloom. This showed an already soft film was softened more by the sulphur dioxide. Graph 24 showed how both inner and outer layers were softened, but the outer layer to a greater extent. The outer layers were not as thick as they were before the test. The softening of the inner layers showed how the sulphur dioxide undermined the whole film.

Anodising at elevated temperatures caused the pores to widen. Dissolution of the pore walls occurred and this effectively weakened the matrix of as-anodised material (131). This was shown by the reduced abrasion resistance. Chemical dissolution is also known to 'open up'

the cell wall structure. If the cell wall material had a low apparent density, sealing may have been adversely affected. Softening occurs irrespective of sealing time. Even at short sealing times the softening process has begun and is irreversible. Complete closure of the pores cannot harden the film. The detrimental effect of the sulphur dioxide gas was exacerbated when films were anodised at high temperatures.

5.11 The Role of 'Tribrite' in Electrolytic Colouring

The composition of the Tribrite solution is not certain. When used in a stannous sulphate plating bath it causes bright deposition which is not explained as a phenomenon as yet. It promotes high throwing power i.e. the ability to give even deposit thickness on cathodes of uneven shape. On copper cathodes the effect of adding it to a stannous sulphate solution was to suppress outward growth of tin (whiskers), and promote sideways growth and very small grain size. If the poor distribution of tin in the anodic pores was caused by using tin baths which would plate only loose whiskery deposits, use of a bright solution should favour a compact pore deposit at the pore base; a form of lateral growth.

The application of Tribrite in a plating bath has been discussed (134). Its use in electrolytic colouring will be explained in the light of this present knowledge. A substantial proportion of the brightener was found to be incorporated in the bright deposit plated onto a copper

cathode. This was 3 or 4 times as hard as tin and was compressively stressed. It was the addition of the brightener which gave a throwing efficiency of $>+100\%$, and the unusual potentiostatic polarization curve. The brightener caused more tin deposition on the far cathode than on the near cathode. Thus more recessed areas distant from the anode were analogous with the base of the pores, and it can be assumed that more tin was deposited in this region, in preference to the pore mouths. Excessive amount of brightener gave a throwing efficiency of $>+100\%$, while normal additions gave below $+100\%$. This phenomenon occurred at low average cathode current density. Co-deposition of H_2 gas occurred as the current density was raised, and throwing efficiency was $<+100\%$. Gas evolution was also observed during electrocolouring. The potentiostatic polarization curve showed that at a specific potential, polarization of the cathode occurred. This only happened with the addition of brightener. With the other ingredients polarization was low up to a limiting current density. This cathode passivity was where the cathode reaction of tin deposition stopped. In electrocolouring the deposition of tin and evolution of hydrogen gas ceased. The potentiostatic polarization curve showed the 'active' and 'passive' regions of the cathode potential. At about $-0.25V$ (nhe) brightener adsorbed very strongly onto the tin to form a layer through which stannous ions passed with difficulty. Thus the heavy incorporation of the non-metallic matter immobilized the tin atoms; but at normal plating temperatures they were particularly mobile.

Therefore the two mechanisms were in competition. Deposition of tin occurred over the whole potential range -0.2 to -0.7V; it was the brightener which gave the unusual potentiostatic curve. It should be possible to find conditions where the near cathodes (pore mouths) are polarized while the far cathodes (pore bases) are on the 'active' part of the potentiostatic polarization curve, which would receive a higher current. Due to the 'oscillating polarization' found by galvanostatic polarization curves, the upper part of the pore was in the 'active' state for a short time, allowing some deposition to occur here. If the pore bases spent more of the time in the 'active' state, then the majority of deposition would occur here. The proposition that tin is deposited preferentially in short pores (131) does not follow from this active-passive pore theory. The total cell current was low because it was made up of the small near cathode current and the larger far cathode current. Additions of brightener increased the polarization for H_2 discharge on the tin cathode; such polarization is in any case high on tin. The gas evolution eventually stopped due to the polarization. Applying this to electrocolouring, it was shown the brightener favoured deposition over the other cathodic reaction. Tests of samples of the stannous solution containing the brightener in a Hull Cell Test showed a sharp demarcation between bright and dull areas. The equation $i = [1035 - 524 \log x] I$ was only applicable when polarization was negligible. The brightener was incorporated into the bright area, at the high current

density end of the Hull Cell Test cathode, which was where polarization was negligible. However, if tin deposited on the low current density end of the cathode, then polarization occurred and the equation was not applicable. Coarse dull deposits were formed on the Haring-Blum cathode at lower (more negative) potentials, even when brightener was present. Thus the cathode potential of the anodised aluminium determined what type of tin was deposited i.e. bright in the active region or dull near the passive region. The amount of brightener had a direct bearing on this deposition.

Admittance decreased with increasing Tribrite because tin was suppressed down the pores. A greater fraction of the total thickness acts as a dielectric and hence the admittance is less than for electrocoloured films from baths not having Tribrite added. At long colouring times suppression of tin reached a limiting point and when coloured for excessive periods evolution of hydrogen gas became the predominant reaction, causing the film to spall. The admittance reached a limit for small additions of the brightener to a concentrated tin solution, and further additions did not cause admittance to decrease any further.

Increased amounts of Tribrite caused spalling to occur at shorter colouring times than in solutions without the brightener. Lower current densities prevented spalling. The presence of Tribrite may promote either a greater flaw production, more reanodising beneath the original barrier layer or greater hydrogen gas evolution, or a combination of all three factors. It is thought the gas evolution plays

a significant role.

The Hull Cell Test cathodes showed how well the tin solutions plated onto the copper. Small quantities of Tribrite gave good cover but as the amounts increased the smoothness and brightness of the cover deteriorated. The Hull Cell Test cathodes showed no correlation with either the admittance or the luminance. These latter measurements indicated better performance than the corresponding cathode cover would suggest. The admittance was influenced by small initial quantities, rather than excessive amounts. This showed the immediate impact of the Tribrite. Occasionally the cover on the cathodes did not change after further additions of brightener. This was because it may not have dissolved completely. Another factor was that if additions were made within a short period then the activity of the brightener would not have been increased since a 'working-in' period was required before full activity was reached. In the concentrated tin solution plating on the copper cathode occurred at the high current density end only. For less concentrated solutions polarization forced the tin round the back of the cathode. Resistance was small between the anode and near end because when current density is high, the potential tends to zero i.e. non-polarizable. The equation $i = [1035-524\log x]I$ is used only if polarization is negligible i.e. the concentrated solution where plating occurred at the high current density end.

The activity of the Tribrite diminished with time. Optimum amounts reached a peak of activity which declined rapidly but then maintained a low level of

activity for a period of time. This indicates that the Tribrite complexes with the tin solution and excessive amounts simply saturate it. The activity cannot be increased beyond a limiting value.

5.11.1 Colorimetry

Gold and light bronze colours had a high percentage reflectance at the red end of the spectrum. The percentage reflectance, at all wavelengths, became fairly equal as the colour tended towards black. Very little light was reflected from dark colours, but even the gold colour only reflected small amounts overall (approximately 12 %). At long colouring times the colour becomes grey, this was confirmed by the SEM photographs. Tribrite decreased the percentage reflectance at all wavelengths, but there was a slightly greater percentage reflectance at the red end of the spectrum than at the blue end, for short colouring times. This showed Tribrite altered the light scattering centres of the deposits. For concentrated tin solutions, increasing amounts of Tribrite caused the colours to become lighter for all colouring times. This indicated that Tribrite altered the way in which the tin was deposited. Tribrite may cause preferential formation of β -tin, as is found in the pure metal.

A standard 20g/l stannous sulphate solution should contained 10g/l Sn^{2+} , but analysis showed that only 5g/l Sn^{2+} was in solution. The tin was lost during preparation of the solution due to oxidation to stannic sulphate. Of the 5g/l Sn^{2+} in solution, up to half was lost

due to oxidation depending upon the frequency of use and slow oxidation over time. However, Sheasby (54) stated that this loss occurred whether the bath was used or not. Presumably the solutions were left open to the air. In my investigations, the solutions were bottled when not in use and this limited the amount of oxidation.

5.11.2 The Effects of 'Tribrite' on the Gradients of Admittance Against Thickness Found by Linear Regression

The negative gradients for the colouring time of 6min showed irregular behaviour for colouring with and without Tribrite as sealing time increased. Overall, the gradients were lower when films were coloured with the addition of Tribrite. A similar trend was also observed for the positive gradients for short colouring times, although the effect was not as pronounced. Graphs 14b and 15b, which showed the calculated tin content, indicated that there was less distinction between the amount of tin found with or without Tribrite present. Tribrite appears to have a greater influence at short sealing times. At short sealing times, and particularly for fresh films, the pore blocking material was gelatinous. The contribution made by the tin to the admittance value may have been greater in this case and hence any effect of Tribrite may have been detected more readily. The gradients calculated from the equation

$$b = \frac{-At_m}{(t-t_m)^2} \quad (5.10)$$

were smaller when Tribrite was used, particularly for the thin films. If a small negative gradient found by linear regression was to be achieved then the elimination of the thinnest films would have been necessary.

CHAPTER 6
CONCLUSIONS

6.1 Nitric Acid Predip

Films already softened by other agents, such as high anodising electrolyte temperature, suffered substantial weight and thickness loss, while hard films did not. It is the surface/intermediate layer which is lost when two layers exist. It may be the intermediate layer which is the much softer outer layer in inherently soft films, and this may be accounted for by the more 'porous' anhydrous cell walls which occur in soft films. The cell walls may themselves become hydrated. Oversealed films lost some of the soft outer layer to reveal an underlying hard film.

6.2 33% Nitric Acid Admittance Drift Test

It appeared to be the intermediate layer which influenced the drift test. Well sealed films gave small positive drifts while inadequately sealed films gave large positive drifts. The $Y-\delta$ profile showed how well sealed films were consolidated throughout while partially sealed films were not. Soft films exhibited a drift, but this was due to the removal of the soft outer layer, decreasing the thickness, and not due to inferior sealing quality. It was found that well sealed hard films gave a positive \dot{Y} of 0.1 to 0.2 and $\dot{Y}t$ of 1 to 2.

The drift method showed how the pore filling material of films sealed in 'Alcoa 482' increased in consolidation as ageing proceeded. However, the drifts did not attain the low values characteristic of hydrothermally sealed films.

The concentrated nitric acid drift of freshly prepared films could not be measured because the pore filling gel required consolidation before a value could be measured.

Negative drift values indicated that soft outer layers were not dissolved but that some redistribution of material caused the pores to become blocked. It is postulated that it is the surface layer which is dissolved and part of the intermediate layer which is redistributed. This redistribution may just outweigh the dissolution effects. If dissolution is greater, this would result in a positive drift.

6.3 Nickel Acetate Sealing

When anti-smut agents are present in the sealing solution it is thought that no intermediate layer is formed. However, due to the competing hydrothermal reaction some form of boehmite may be present. The possible combination of the hexaaquanickel (II) ion with the $[Al(H_2O)_6]^{3+}$ ion may form an insoluble complex which blocked the pores. The ageing of this complex may proceed by a polymerisation reaction causing the density and crystallinity to increase, and blocking the diffusion

pathways. The outer regions of the pores were the most impermeable since rapid initial gel formation occurred here. The presence of nickel allowed the 'active sites' to remain unhindered by contaminants, so that the hydroxyl ion concentration continued to be promoted at these sites. As the quantity of pore blocking material increased, a higher Al^{3+} ion concentration was promoted, and the low acidity due to the increase in hydroxyl ion concentration, and high solution temperature, favoured the ageing process. A net uptake of water may control the pore filling process. It was found that water seals unsealed films, which have been dried, to a greater extent than 'Alcoa 482', supporting the view that once the pores became partially blocked by boehmite, the nickel was hindered from entering and forming the complex to any great extent.

The admittance-abrasion profile ($Y-\xi$) of a well sealed hydrothermal film showed a constant ^{value of $Y(25)$} ~~admittance~~ throughout the length of the sealed pores. Both fresh and aged poorly sealed hydrothermal films showed ^{a rise in $Y(25)$} ~~the admittance~~ ~~to rise~~ as the film was abraded, as occurs also with freshly prepared poorly sealed 'Alcoa 482' films. However an aged 'poorly' sealed 'Alcoa 482' film attained a line horizontal to the x-axis. This showed that consolidation increased with ageing throughout the length of the pore.

6.4 Long Term Cold Immersion

The sealing mechanism for films sealed in plain water differed from that for films sealed in nickel

acetate. The superficial mechanisms of early pore blocking/sealing were quite different.

Water sealed films can be compared to partially hydrothermally sealed films. Admittance measurements appeared to show the films were sealed, but the admittance drift test showed that the pores were only blocked with material soluble in nitric acid. These films were similar to those partially sealed by exposure to the environment where there was a competition between sealing and weathering.

Films immersed in a nickel acetate solution were sealed by a mechanism similar to that which occurs during hot nickel acetate sealing. The formation of a nickel-aluminium complex blocked the pores by solidification of the complex, as shown by the admittance drift values. The consolidation of the material increased with time and changed the dielectric constant of the material. The concentration of the nickel rather than the depth of penetration appeared to affect the ageing process.

6.5 Outdoor Exposure of Anodised Films

Exposed faces of unsealed films which were not adequately sealed, had a severe bloom and there had been some thickness reduction. The shielded faces appeared to be sealed by the criterion of an admittance test, but the admittance drift test revealed the sealing was inferior. There was a bloom and some thickness increase. These results are similar to those of unsealed films immersed for

long periods in water.

The admittance drift on partially sealed films showed the exposed faces to be sealed while the shielded faces were inadequately sealed. However, exposed faces carried a worse bloom. Weathering products may block the pores, giving a low admittance value, but in the admittance drift test, this loose, pore blocking material dissolves. The decrease in thickness was due to the surface layer being undermined and removed by the weather. The intermediate layer may also experience the same phenomena. Thickness increases were due to favourable conditions for the precipitation/dissolution mechanism.

Microcracks and crazing may have influenced the admittance values at different times of the year causing admittance to rise after hot, dry periods and renewed precipitation/dissolution may have healed these defects after wet periods. However, wet periods would also promote 'weathering' of the film. Thus there was a competition between weathering and sealing, the effects of either one predominating during specific environmental patterns.

The continued decrease in the gradients of partially and fully sealed films indicated that, although diffusion pathways may be blocked, further sealing occurred since some diffusion of water may take place through the anhydrous cell walls, and this may be enhanced by microcracks. Variations in thickness on exposed faces of fully sealed films showed the competition between the precipitation/dissolution mechanism and weathering. The admittance drift of well sealed films was small indicating

that exposure had not undermined the film. Very thick films were prone to crazing even when well sealed.

6.6 Sulphur Dioxide Test

The optimum conditions for a sulphur dioxide test were 6 hours at a temperature of 40°C. Well sealed hydrothermal 25µm films passed the test. Films sealed for other times and having other thicknesses failed the test. Crazed, well sealed films also failed. The pores of inadequately sealed films became blocked due to the presence of corrosion products, which undermined the film as shown by an inherent bloom. The sulphur dioxide gas softened films which exhibited an outer soft layer and an inner harder layer. The presence of condensation during the first 2 to 3 hours of the test caused the formation of sulphate. Oversealed films showed iridescence due to the lateral flaking of surface and intermediate layers.

Films sealed in 'Alcoa 482' were not attacked by the sulphurous acid indicating the impermeable nature of the pore filling material.

6.7 Sealing Bloom

White powder residues on the glass paper of the three paper test showed a sealing bloom to be present on well sealed 25µm films, while the sulphur dioxide test gave no bloom. Short sealing times did not give a sealing bloom, but a sulphur dioxide bloom formed. The three paper

abrasion test can distinguish between poorly and well sealed films, before a sulphur dioxide test is performed. It can also discriminate between thick and thin films which were anodised at electrolyte temperatures above 20°C. Thick films were subjected to the dissolution effects of the acid and showed soft outer layers while thin films did not.

Anodising films at elevated temperatures and subjecting them to a sulphur dioxide test gave two distinct layers in the film, the outer layer being softer than the inner layer, which was also unacceptably soft. After a predip in 33% nitric acid both layers were softened further showing that the nitric acid predip does not remove the sulphur dioxide bloom/soft layers but accentuates them. This bloom is inherent within the film. A soft film having two layers and subjected to a predip alone carried only one layer after the predip. The predip had removed the soft outer layer. It can be concluded that the intermediate layer plays a significant role in the soft outer layer and when this layer is attacked by the sulphurous acid its form changes so that it becomes insoluble in 33% nitric acid.

6.8 The Significance of the Gradients of the Graph of $Y_t(25^\circ\text{C})$ Against Thickness as found by the Linear Regression Method

Over a limited range of deliberate thickness variations of anodic oxide films it was found that if the points on the graph of $Y_t(25^\circ\text{C})$ against thickness were treated by linear regression to obtain an equivalent linear

gradient, the batch was deemed acceptable if the gradient was less than +10. This approach showed a useful connection with the question of the degree of sealing of batches having a range of thicknesses but a common sealing time. The linear relationship is a reasonable assumption.

6.9 Electrocoloured Oxide Films

It is possible that the electrolytically deposited tin is in a distorted tetragonal form. The influence of colouring current densities played an important role with respect to colouring time. The lower current densities produced the darker colours for long colouring times, while at high current densities the limiting values were approached quickly and spalling occurred. This may have been due to a combined effect of hydrogen gas evolution and the new/old barrier layer interface. An alternative explanation is that a rise in pH enhances tin deposition. Electrons must play a part in either a reduction reaction or activation of flaws, and semi-conduction may occur through these flaws. As colouring time increased the colours became darker as shown by colorimetry, and at extended colouring times tin was shown by various means to extend to the mouths of the pores. Variations in the chromaticity co-ordinates for films coloured under identical conditions were due to variations in surface topography. The luminance value was found to be more useful measurement than the co-ordinates and together with the L, a, b, ΔE system, gave quantitative evaluations

of colour. By observing the shapes of the graphs of ΔE against colouring time, and the luminance against colouring time (which are mirror-images), the 'overfilling' of pores with tin may be avoided. Both curves of these graphs increased rapidly at short colouring times, but at long colouring times produced little variation. This showed the increase in the amount of tin deposited occurred very quickly reaching an 'optimum' value. Increasing the tin beyond this optimum value was detrimental to the film.

At short colouring times the amount of tin appears to be irregular for identical colouring times. During the first minute of colouring the current rose rapidly due to the rectifying action of the anodic film. The time taken for the rectification to decrease may determine when tin deposition begins.

The admittance of electrocoloured films was greater than that of natural coloured films. Film thickness was independent of colouring time up to a point but film quality was dependent upon the film thickness. Theoretical calculations showed the thickness of the film influenced the amount of tin deposited for identical colouring times. Long colouring times showed the percentage of tin decreased as thickness increased, while for short colouring times the percentage increased as thickness increased. It was suggested that deposition occurred preferentially in shorter pores which appeared to be confirmed by the calculations of tin thickness. It was possible that the thicker films had a larger pores creating a smaller flaw population and less deposition of tin (but see sections 6.10 and 6.11).

The gradients of the graph of $Yt(25^\circ\text{C})$ against film thickness for well-sealed films were large and negative due to the presence of tin in the pores. As film thickness increased, the gradient found from the equation

$$b = \frac{-At}{(t-t_m)^2}$$

decreased, assuming that A and t_m remained constant. The points on the graph of $Yt(25^\circ\text{C})$ against thickness over a limited thickness range can be treated by linear regression to give an equivalent linear gradient; an average value of the form $Yt(25^\circ\text{C}) = a + bt$, over the whole thickness range. The comparison of experimentally produced ranges with commercial ranges suggested the theory was not too simple to give reasonable results, if the assumption was made that the tin fills 22 to $23\mu\text{m}$ of a 25 to $30\mu\text{m}$ film. However, A must vary as t' varies for a common sealing time for a range of thicknesses. Thus A and t_m did not remain constant. (A increased as t' decreased.) The graph of the gradient against total film thickness then approached a semi-logarithmic relationship. If the linear regression method was applied to a range of thicknesses the average linear gradient was found to be more reasonable.

For short colouring times the tin metal thickness was not significant and the effective dielectric thickness was approximately equal to that of the total oxide thickness. The gradients were positive and achieved a value of +10, so the electrocolour admittance theory did not

apply as negative gradients were only found with dark colours.

6.10 The Effects of Anodising, Soaking and Colouring at Elevated Temperatures

The abrasive wheel test was useful for assessing the thickness at which tin was present in the film. The general trend showed that there was less tin in the pores when films were anodised at 15°C than when anodised above this temperature. This indicated that the pores were enlarged at elevated anodising temperatures. The thinner pores appeared to restrict the tin to the pore depths. This result was at variance with the thickness of tin found by theoretical calculations for films of different thicknesses coloured for identical times, in which the larger pores carried less tin (but see section 6.9). However, the morphological changes which occurred to the porous structure during elevated temperature anodising were greater than any changes to pore dimensions which may occur simply due to chemical dissolution. This fact together with the evidence of tin thickness found from the abrasive wheel test suggests the experimental evidence is reasonable. The tin content found by the theoretical calculations appeared to be overestimated compared to those found by the abrasive wheel method. This overestimation was due to the assumption that A was a constant [$Yt'(25^\circ\text{C}) = 200 \text{ Sm} \times 10^{-12}$], and if A increased as t' decreased, then the tin content may have been more in line with that found from the abrasive wheel

test. However, the abrasive wheel method was not used on films less than $20\mu\text{m}$ in thickness. The contribution made by the elevated temperatures to the size of the pores was significant and the apparent contradictory results may be genuine due to geometrical factors.

Colouring and soaking films in sulphuric acid at elevated temperatures before sealing reduced the abrasion resistance. Colouring at room temperature did not have a detectable softening effect. Colouring had a marginally greater effect than soaking. It was not the alternating current colouring treatment at elevated temperatures which caused the reduction in abrasion resistance, but the temperature of the solution. Factors which influenced the redissolving processes affected the abrasion resistance. Two distinct layers were observed in films anodised and coloured or soaked at high temperatures. The inner layer of coloured films was softer than that of the soaked films and the thickness at which the inner layer occurred corresponded to the appearance of the tin during the abrasive wheel test. Inherently soft films which were coloured at elevated temperatures had a thicker, softer inner layer than soaked films, showing the slightly greater detrimental effect of colouring. It seems that soaking soft films exacerbated the softness of the two layers, while colouring influenced the relative positions of these layers.

Anodising at elevated temperatures caused pore widening. Dissolution of the pore walls weakened the matrix of the as-anodised material. Colouring and soaking at

elevated temperatures compounded this effect. If the pore wall had low apparent density, subsequent sealing may have undermined the cell wall structure causing greater softening since the hydrothermal reaction is known to soften the film.

6.11 The Effects of Using 'Tribrite' in the Electrolytic Colouring Solution

When Tribite was used in the tin sulphate colouring bath it was shown, by various analytical techniques that it caused some degree of suppression of the outward growth of tin in the pores of the anodic oxide film. This occurred in a manner similar to that which occurred during tin plating on copper cathodes. If the pore base was likened to the far cathode in the Hull Cell Test, then this would account for the preferential tin deposition in this area. Two mechanisms were in competition with one another: (i) tin atoms were immobilised by the incorporation of the non-metallic matter, and (ii) at normal plating temperatures the tin atoms were particularly mobile. It may be possible to find conditions where the near cathodes (pore mouths) were polarised while the far cathodes (pore bases) were on the 'active' part of the potentiostatic polarisation curve. The proposition that tin deposited preferentially in short pores is not supported by this active-passive pore theory (see section 6.9).

Additions of the brightener increased the polarisation for hydrogen gas discharge on the tin

cathodes, and gas evolution eventually ceased due to this polarisation. The brightener was incorporated into the bright area of the Hull Cell Test cathode, at the high current density end, where polarisation was negligible. The cathode potential of the anodised aluminium determined what type of tin was deposited, i.e. bright tin in the active region or dull tin in the passive region. At long colouring times suppression of tin reached a limiting value and hydrogen evolution became the predominant reaction, causing the film to spall. An optimum brightener concentration was found by means of the Hull Cell Test cathodes. Spalling occurred at high current densities for long colouring times due to the increased polarisation for hydrogen discharge. This may have increased the flaw production, or stimulated reanodising beneath the original barrier layer, but it is thought that the evolution of hydrogen gas played a significant role.

Hull Cell Tests showed how well tin solutions plated onto copper cathodes, although the cathodes showed no correlation as to the type or degree of tin deposition as indicated by the admittance and luminance values. These latter measurements gave a better indication of tin suppression.

A 'working-in' period was required for the Tribrite to exhibit any activity. An optimum activity was assessed by the Hull Cell Test cathode cover. Activity diminished with time, but was maintained at a low level for a considerable time. The activity could not be increased beyond a limiting value. The equation $i = [1035 - 524 \log x]I$

was only applicable when polarization was negligible, i.e. when plating occurred at the high current density end.

The negative gradients of the graph of admittance against thickness as found by the linear regression method were lower when films were coloured with Tribrite than when coloured without Tribrite. At short colouring times (positive gradients) the effect was not as pronounced. Tribrite appeared to affect the admittance more at short sealing times due to the freshly formed boehmite. If smaller negative gradients were to be obtained, the exclusion of the thinnest films would be necessary in a range of thicknesses.

CHAPTER 7

FUTURE WORK

7.1 The Admittance Drift Test (Y)

The admittance drift test may be applied as a rapid, non-destructive test to monitor ageing/weathering of anodic oxide film which have been sealed in boiling solutions other than water, where the admittance value is anomalously low.

Similarly, to discover whether impregnated (cold-sealed) films have been correctly processed.

The use of the drift test to supplement negative gradients of tin blacks and dark bronzes for which the admittance values are anomalously high needs further investigation.

7.2 The Admittance - Abrasion (Y - I) Profile

This test may be used to confirm non-destructive test results from admittance values on impregnated films and on metal growth up pores from electrocolouring. The combination of the admittance drift test used at different depths during the Y-I profile may give useful information on these films.

The effects of the sulphur dioxide test could be investigated further by the admittance drift test and Y-I profile. Similarly, information on the effects of ageing before and after the sulphur dioxide test may be found.

The competing mechanisms of weathering and sealing may be followed more closely by these tests, revealing the contribution of the intermediate and surface layers.

7.3 The Abrasive Wheel Test

Detailed depth analysis using this test may throw light on the effects of elevated temperatures of the process solutions. A destructive test may be found by combining the abrasive wheel test and the nitric acid predip, which may give information on the participation of the different layers in soft films.

7.1 The Use of Additions Agents During Electrolytic Colouring of Anodic Oxide Films.

Further testing and modifications of the metal-in-pore distribution by use of appropriate addition agents is required. 'Tribrite' shows there is an effect, but this may not be the best agent.

Additional spectroscopic analysis and colorimetry together with the admittance tests and abrasive wheel test may indicate the contribution addition agents make to tin suppression.

The effects of contaminants, pH and temperature of the electrolytic colouring solution on the addition agents, and the concentrations, activity, working-in period and age of the agents require a systematic programme of

research.

Addition agents may be beneficial to electrocoloured films which are subject to outdoor exposure and sulphur dioxide tests, since the addition agent 'Tribrite' is known to act as a corrosion inhibitor.

The use of the addition agents in electrocolouring solutions containing mixtures of metallic salts, such as tin-nickel solutions, requires investigation.

During interference colouring not all pores give interference colours, but some produce normal electrolytic colouring effects. This is shown by the bronze overtones and the effect is enhanced as colouring proceeds. Addition agents may prevent these bronze overtones.

REFERENCES

- (1) G.D. Bengough & J.M. Stuart, Brit. Pat. 223,994 (1923)
- (2) S. Setoh & A. Miyata, Proceedings of World Engineering Congress, Tokyo, 1929, 727.
References (1) and (2) from J.M. Kape, Product Finish., 1982, **35**, Part 7, 33-36.
- (3) V. Caboni, Italian Pat. 339,232 (1936)
Reference (3) taken from reference (53).
- (4) V. E. Carter, Trans. Inst. Metal. Finish., 1977, **55**, 9.
- (5) S. Wernick and R. Pinner, "The Surface Treatment and Finishing of Aluminium and Its Alloys", 4th edition, Robert Draper, Teddington, 1972, Vol. 1, 45.
Vol. 1, 45.
- (6) E. Survila, Trans. Inst. Metal. Finish., 1984, **62** (2), 45-47.
- (7) J. M. Kape, Trans. Inst. Metal. Finish., 1984, **62**, (2) 41-45.
- (8) V. F. Henley, "Anodic Oxidation of Aluminium and Its Alloys", Pergamon Press, London, 1982, 24.
- (9) D. J. Arrowsmith, Trans. Inst. Metal. Finish., 1986, **64**, Part 1, 6.
- (10) G. E. Thompson & G. C. Wood, "Anodic Films on Aluminium" in "Corrosion: Aqueous Processes and Passive Films", ed. J. C. Scully, Academic Press, 1983, Vol. 23, 208.

- (11) S. Wernick, R. Finner & P. G. Sheasby, "The Surface Treatment and Finishing of Aluminium and Its Alloys", 5th edition, Finishing Publications Ltd., London, 1987, 292-293.
- (12) H. S. Kim, G. E. Thompson, G. C. Wood, I. G. Wright & R. E. Marringer, Trans. Inst. Metal. Finish., 1984, **62**, (2), 49-54.
- (12a) S. Wernick, R. Finner & P. G. Sheasby, "The Surface Treatment and Finishing of Aluminium and Its Alloys", 5th edition, Finishing Publications Ltd., London, 1987, 8.
- (13) G. C. Wood, "Oxide and Oxide Films" in "Anodic Behaviour of Metals and Semiconductor Series", 1st edition, ed. John W. Diggle, Dekker, New York, 1973, Vol. 2, 171.
- (14) G. E. Thompson & G. C. Wood, "Anodic Films on Aluminium" in Corrosion: Aqueous Processes and Films, Passive Films", ed. J. C. Scully, Academic Press, 1983, Vol. 23, 254.
- (15) J. P. O'Sullivan & G. C. Wood, Proc. R. Soc. Lond. 1970, **317A**, 511-543.
- (16) S. Wernick, R. Finner & P. G. Sheasby, "The Surface Treatment and Finishing of Aluminium and Its Alloys", 5th edition, Finishing Publications Ltd., London, 1987, 309.
- (17) R. W. Franklin, The Aluminium Development Association, Conference on Anodising Aluminium, Nottingham, 1961, No. 7, Proceedings, 96-100.

- (18) G. E. Thompson & G. C. Wood, "Anodic Films on Aluminium" in "Corrosion: Aqueous Processes and Passive Films", ed. J. C. Scully, Academic Press, 1983 Vol. 23, 235.
- (19) F. Keller, M. S. Hunter & D. L. Robinson, J. Electrochem. Soc., 1953, 100, No. 9, 411-419.
- (20) T. P. Hoar & N. F. Mott, Physics Chem. Solids., 1959, 9, 97-99.
- (21) V. P. Parkhutik, Corros. Sci., 1986, 105, 295-310.
- (22) G. C. Wood & J. F. O'Sullivan, Electrochim. Acta, 1970, 15, 1865-1876.
- (23) P. Csokan, "Advances in Corrosion Science and Technology", 1st edition, Plenum Press, ed. Mars G. Fontana & Roger W. Staehle, New York, 1980, Vol. 7, 245-247.
- (24) J. F. Murphy & C. E. Michelson, The Aluminium Development Association, Conference on Anodising Aluminium, Nottingham, 1961, No. 6, Proceedings, 83-95.
- (25) G. C. Wood, "Oxide and Oxide Films" in "Anodic Behaviour of Metals and Semiconductor Series", 1st edition, ed. John W. Diggle, Dekker, New York, 1973, Vol. 2, 240.
- (26) H. Ginsberg & K. Wefers, Metall, 1963, 17, Part 3, 202-209.
- (27) J. Siejka & C. Ortega, J. Electrochem. Soc., Solid - State Science and Technology, 1977, 124, No. 6, 883-890.

- (28) G. E. Thompson, R. C. Furneaux, G. C. Wood,
J. A. Richardson & J. S. Goode, *Nature*, 1978, **272**,
433-435.
- (29) R. C. Plumb, *J. Electrochem. Soc.*, 1958, **105**, No. 9,
498-501.
- (30) D. R. Gabe & J. H. Dowty, *Surface and Coatings
Technology*, 1987, **30**, Part 3, 309-316.
- (31) J. P. O'Sullivan J. A. Hockey & G. C. Wood, *Trans.
Faraday Soc.*, 1969, **65**, 535-541.
- (32) Y. Xu, G. E. Thompson & G. C. Wood, *Electrochim.
Acta*, 1982, **27**, No. 11, 1623-1625.
- (33) J. S. L. Leach & P. Neufeld, *Corros. Sci.* 1969, **9**,
413-421.
- (34) P. Csokan, *Trans. Inst. Metal. Finish.*, 1973, **51**,
6-10.
- (35) K. V. Heber, *Electrochim. Acta*, 1978, **23**, 127-133.
- (36) J. A. Treverton & N. C. Davies, *Electrochim. Acta*,
1980, **25**, 1571-1576.
- (37) J. M. Kape, *trans. Inst. Metal. Finish.*, 1977, **55**,
25-30.
- (38) J. A. Kneeshaw & D. R. Gabe, *Trans. Inst. Metal.
Finish.*, 1984, **62**, (2), 59-63.
- (39) S. Wernick & R. Pinner, "The Surface Treatment and
Finishing of Aluminium and Its Alloys", 4th edition,
Robert Draper, Teddington, 1971, Vol. 1, 552.
- (40) S. Wernick & R. Pinner, *op. cit.* 651.
- (41) S. Wernick & R. Pinner, *op. cit.* 648.
- (42) J. M. Kape, *Conference of the Institute of Metal
Finishing*, 1959, 364.

- (43) S. Wernick & R. Pinner, "The Surface Treatment and Finishing of Aluminium and Its Alloys", 4th edition, Robert Draper, Teddington, 1971, Vol. 1, 624.
- (44) C. Th. Speiser, Aluminium Finishing Seminar, Technical papers, 1982, Vol.1, 123-144.
- (45) S. Wernick & R. Pinner, "The Surface Treatment and Finishing of Aluminium and Its Alloys", 4th edition, Robert Draper, Teddington, 1971, Vol. 1, 508.
- (46) S. Wernick & R. Pinner, op. cit. 513.
- (47) G. C. Wood, "Oxide and Oxide Films" in "Anodic Behaviour of Metals and Semiconductor Series", 1st edition, ed. John W. Diggle, Dekker, New York, 1973, Vol. 2, 177.
- (48) G. C. Wood, op. cit. 174.
- (49) J. M. Kape, The Aluminium Federation, Symposium on Anodising Aluminium, Aston, 1967, No. 10, Proceedings, 123.
- (50) P. G. Sheasby, Metal Finish., 1974,
- (51) G. C. Wood, "Oxide and Oxide Films" in "Anodic Behaviour of Metals and Semiconductor Series", 1st edition, ed. John W. Diggle, Dekker, New York, 1973, Vol. 2, 180.
- (52) S. Tajima, N. Baba, T. Mori, & M. Shimura, The Aluminium Federation, Symposium on Anodising Aluminium, Aston, 1967, No. 4, Proceedings, 43.
- (53) P. G. Sheasby & W. E. Cooke, Trans. Inst. Metal. Finish., 1974, 52, 103.
- (54) Private Communication.

- (55) S. Wernick & R. Pinner, "The Surface Treatment and Finishing of Aluminium and Its Alloys", 4th edition, Robert Draper, Teddington, 1971, Vol. 1, 546.
- (56) H. J. Gohausen & H. Puderbach, *Aluminium*, 1983, **59**, No. 9, E295-297.
- (57) M. P. Amor & R. C. Furneaux, *Aluminium*, Reprint from 1985, **61**, No. 2, E111-113.
- (58) R. C. Furneaux, *Trans. Inst. Metal. Finish.*, 1983, **61**, 35-40.
- (59) H. J. Gohausen & G. C. Shoener, *Plat. & Surf. Finish.* 1984, **71**, Part 2, 56-63.
- (60) A. S. Doughty, G. E. Thompson, J. A. Richardson & G. C. Wood, *Trans. Inst. Metal. Finish.* 1975, **53**, 33-39.
- (61) K. Tachihara, Y. Itoi, & E. Sato, *Electrochim. Acta*, 1981, **26**, No. 9, 1299-1302.
- (62) V. Balasubramanian & B. A. Shenoi, *Metal Finish.* **80**, Part 3, 61-65.
- (63) P. G. Sheasby, J. Patrie, M. Badia & G. Cheetham, *Trans. Inst. Metal. Finish.*, 1980, **58**, 41-47.
- (64) P. G. Sheasby, E. P. Short, & G. Cheetham, *Metals Australasia*, 1985, **17**, Part 3, 10-12.
- (65) C. Th. Speiser, *Trans. Inst. Metal. Finish.*, 1980, **58**, 121-127.
- (66) S. Wernick & R. Pinner, "The Surface Treatment and Finishing of Aluminium and Its Alloys", 4th edition, Robert Draper, Teddington, 1971, Vol.1, 548.
- (67) R. S. Hunter, "The Measurement of Appearance", John Wiley and Sons Inc., 1975.

- (68) S. Wernick & R. Pinner, "The Surface Treatment and Finishing of Aluminium and Its Alloys", 4th edition, Robert Draper, Teddington, 1971, Vol. 2, 943-971.
- (69) W. J. Bernard & J. J. Randall Jnr., J. Electrochem. Soc. 1961, **108**, No. 9, 822-825.
- (70) H. Ginsberg & K. Wefers, Aluminium, 1961, **37**, No. 1, 19-28.
- (71) S. Wernick, R. Pinner & P. G. Sheasby, "The Surface Treatment and Finishing of Aluminium and Its Alloys" 5th edition, Finishing Publications Ltd., 1987, Vol. 2, 775.
- (72) S. Wernick, R. Pinner & P. G. Sheasby, op. cit. 777.
- (73) J. P. O'Sullivan, J. H. Hockey & G. C. Wood, Trans. Faraday Soc., 1969, **65**, 535-541.
- (74) J. P. O'Sullivan & G. C. Wood, Trans. Inst. Metal. Finish., 1969, **47**, 142-144.
- (75) S. Wernick, R. Pinner & P. G. Sheasby, "The Surface Treatment and Finishing of Aluminium and ITS Alloys" 5th edition, Finishing Publications Ltd., 1987, Vol. 2, 780.
- (76) K. Wefers, Aluminium, 1973, **49**, No. 8, 553-561.
- (77) G. C. Wood, "Oxide and Oxide Films" in "Anodic Behaviour of Metals and Semiconductor Series", 1st edition, ed. John W. Diggle, Dekker, New York, 1973, Vol. 2, 222.
- (78) B. R. Baker, Aluminium Finishing Seminar, 1982, Vol. 1 180-183.

- (79) G. E. Thompson & G. C. Wood, "Anodic Films on Aluminium" in "Corrosion: Aqueous Processes and Passive Films", ed. J. C. Scully, Academic Press, 1983, Vol. 23, 312-313.
- (80) V. F. Henley, "Anodic Oxidation of Aluminium and Its Alloys", Pergamon Press, London, 1982, 92.
- (81) S. Wernick, R. Pinner & P. G. Sheasby, "The Surface Treatment and Finishing of Aluminium and Its Alloys" 5th edition, Finishing Publications Ltd., 1987, Vol. 2, 792.
- (82) "Advances in Corrosion Science and Technology", Plenum Press, 1970, Vol. 1, 331.
- (83) S. Wernick, R. Pinner & P. G. Sheasby, "The Surface Treatment and Finishing of Aluminium and Its Alloys" 5th edition, Finishing Publications Ltd., 1987, Vol. 2, 796.
- (84) S. Wernick, R. Pinner & P. G. Sheasby, op. cit. 798.
- (85) S. Wernick, R. Pinner & P. G. Sheasby, op. cit. 799.
- (86) H. J. Gohausen & G. C. Shoener, Aluminium Finishing Seminar, 1982, 163-175.
- (87) S. Wernick, R. Pinner & P. G. Sheasby, "The Surface Treatment and Finishing of Aluminium and Its Alloys" 5th edition, Finishing Publications Ltd., 1987, Vol. 2, 800.
- (88) T. P. Hoar & G. C. Wood, Aluminium Development Association, Conference on Anodising Aluminium, Nottingham, 1961, No. 15, Proceedings, 186-200.
- (89) B. R. Baker, Aluminium Finishing Seminar, Missouri, 1982, 185.

- (90) S. Wernick, R. Pinner & P. G. Sheasby, "The Surface Treatment and Finishing of Aluminium and Its Alloys" 5th edition, Finishing Publications Ltd., 1987, Vol. 2, 801.
- (91) S. Wernick, R. Pinner & P. G. Sheasby, op. cit. 802.
- (92) V. F. Henley, "Anodic Oxidation of Aluminium and Its Alloys", Pergamon Press, London, 1982, 95.
- (93) S. Wernick, R. Pinner & P. G. Sheasby, "The Surface Treatment and Finishing of Aluminium and Its Alloys" 5th edition, Finishing Publications Ltd., 1987, Vol. 2, 804.
- (94) S. Wernick, R. Pinner & P. G. Sheasby, op. cit. 811.
- (95) F. Saachi, Ossidare, 1984, March-April, 45-48.
- (96) S. Wernick, R. Pinner & P. G. Sheasby, "The Surface Treatment and Finishing of Aluminium and Its Alloys" 5th edition, Finishing Publications Ltd., 1987, Vol. 2, 828.
- (97) R. C. Furneaux, W. R. Rigby & B. G. Carter, Proc. Interfinish '84, Israel, 1984, 376-384.
- (98) S. Wernick, R. Pinner & P. G. Sheasby, "The Surface Treatment and Finishing of Aluminium and Its Alloys" 5th edition, Finishing Publications Ltd., 1987, Vol. 2, 914.
- (99) S. Wernick, R. Pinner & P. G. Sheasby, op. cit. 833.
- (100) S. Wernick, R. Pinner & P. G. Sheasby, op. cit. 915.
- (101) G. C. Wood & V. J. J. Marron, Trans. Inst. Metal. Finish., 1967, 45, Part I, 17-25 and Part II 107-113.

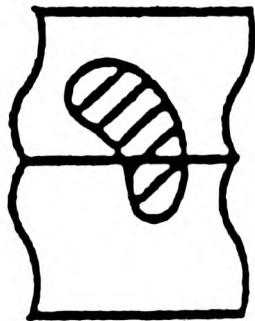
- (102) R. C. Furneaux & G. C. Wood, *Trans. Inst. Metal. Finish.*, 1982, **60**, 14-24.
- (103) T. P. Hoar & G. C. Wood, *Trans. Inst. Metal. Finish.* 1960, **37**, 7-10.
- (104) J.M. Kape, *Electroplg Metal Finish.*, 1975, **28**, (8), 26-31.
- (105) P. G. Sheasby, *Aluminium Industry*, 1983, **2**, No. 1, 9-15.
- (106) S. Wernick, R. Pinner & P. G. Sheasby, "The Surface Treatment and Finishing of Aluminium and Its Alloys" 5th edition, *Finishing Publications Ltd.*, 1987, Vol. 2, 832.
- (107) S. Wernick, R. Pinner & P. G. Sheasby, *op. cit.* 891-893.
- (108) M. Clarke, *Trans. Inst. Metal. Finish.*, 1985, **62**, 70-73.
- (109) Private Communication.
- (110) S. Wernick, R. Pinner & P. G. Sheasby, "The Surface Treatment and Finishing of Aluminium and Its Alloys" 5th edition, *Finishing Publications Ltd.*, 1987, Vol. 2, 885.
- (111) H. J. Gohausen, *Aluminium*, 1979, **55**, No. 8, 515-521.
- (112) S. Wernick, R. Pinner & P. G. Sheasby, "The Surface Treatment and Finishing of Aluminium and Its Alloys" 5th edition, *Finishing Publications Ltd.*, 1987, Vol. 2, 921-926.
- (113) E. Strazzi, *Alluminio*, January 1984, 85-87.

- (114) S. Wernick, R. Pinner & P. G. Sheasby, "The Surface Treatment and Finishing of Aluminium and Its Alloys" 5th edition, Finishing Publications Ltd., 1987, Vol. 2, 932.
- (115) M. Clarke & J. M. Leeds, Trans. Inst. Metal. Finish. 1968, **46**, 81-86.
- (116) P. G. Sheasby, The Aluminium Federation, Symposium on Anodising Aluminium, Aston, 1967, No. 11, Proceedings, 133-144.
- (117) C. A. Witt & S. Jahnke, Aluminium, February 1986, **62**, No. 2, 119.
- (118) S. Wernick, R. Pinner & P. G. Sheasby, "The Surface Treatment and Finishing of Aluminium and Its Alloys" 5th edition, Finishing Publications Ltd., 1987, Vol. 2, 912.
- (119) F. Saachi & G. Garuti, Ossidare, 1984, September-October, 21, 24, 25.
- (120) Private Communication.
- (121) F. A. Cotton & G. Wilkinson, "Advanced Inorganic Chemistry", 4th edition, John Wiley & Sons, 1980, 333.
- (122) Unpublished work.
- (123) C. A. Fisher, M. Sc. Thesis, "The Sealing and Corrosion Aspects of Aluminium Anodised to Architectural Quality", 1982.
- (124) J. Patrie, Trans. Inst. Metal. Finish., 1975, **53**, 28-32.

- (125) M. Aslam, M. Sc. Thesis, "The Behaviour of Discontinuities in Thick Anodic Films on Aluminium", 1978.
- (126) F. E. Faller, Aluminium, 1987, **58**, Part 3, E23-25.
- (127) S. Wernick, R. Pinner & P. G. Sheasby, "The Surface Treatment and Finishing of Aluminium and Its Alloys" 5th edition, Finishing Publications Ltd., 1987, Vol. 2, 628.
- (128) H. J. Gohausen, Trans. Inst. Metal. Finish., 1982, **60**, 74-80.
- (129) G. E. Thompson & G. C. Wood, "Anodic Films on Aluminium" in "Corrosion: Aqueous Processes and Passive Films", ed. J. C. Scully, 1983, Vol. 23, 308-309.
- (130) S. Wernick, R. Pinner & P. G. Sheasby, "The Surface Treatment and Finishing of Aluminium and Its Alloys" 5th edition, Finishing Publications Ltd., 1987, Vol. 2, 607.
- (131) R. C. Furneaux, Aluminium Finishing Seminar, 1982, 107-120.
- (132) K. Shimizu, G. E. Thompson & G. C. Wood, Electrochim Acta, 1982, **27**, No. 2, 245-250.
- (133) H. J. Gohausen, Trans. Inst. Metal. Finish., 1978, **56**, 57-64.
- (134) M. Clarke & J. A. Bernie, Electrochim. Acta, 1967, **2**, 205-212.

[Abbreviations from the World List of Scientific Periodicals.]

BEST COPY
AVAILABLE



THE BRITISH LIBRARY DOCUMENT SUPPLY CENTRE

TITLE

THE COLOURING, SEALING AND ABRASION RESISTANCE
OF ANODIC OXIDE COATINGS

AUTHOR

MARILYN SMITH

**INSTITUTION
and DATE**

City of London Polytechnic
CNA 1990

Attention is drawn to the fact that the copyright of this thesis rests with its author.

This copy of the thesis has been supplied on condition that anyone who consults it is understood to recognise that its copyright rests with its author and that no information derived from it may be published without the author's prior written consent.



**THE BRITISH LIBRARY
DOCUMENT SUPPLY CENTRE**
Boston Spa, Wetherby
West Yorkshire
United Kingdom

20

REDUCTION X

8

DX

91543